Wind Power Integration on Power System Reliability and Operating Reserve Capacity

A thesis submitted for the degree of

Doctor of Philosophy

At the University of Strathclyde

By

Su Wang

Supervisor: Professor K. L. Lo

Power System Research Group

Department of Electronic and Electrical Engineering

University of Strathclyde

2020

Declaration of Author's Right

This thesis is the result of the author's original research. It has been composed by the author and has not been previously submitted for examination which has led to the award of a degree.

Signed: Su Wang

Date:

Acknowledgements

I would like to express my sincere appreciation to my supervisor, Professor K. L. Lo, Head of the Power System Research Group (PSRG), for his supervision and support throughout my research work. The completion of this thesis would not have been possible without his constant encouragement and patient guidance.

I also wish to thank my colleagues at PSRG for providing a positive and supportive environment. Special thanks to Gao Gao, Zhonglei Shao and Jiajun Ma for their care and support for my study and life. I would also like to thank my friend Yijun Yan for accompanying me through a happy and intense doctoral life.

Most importantly, thanks to my dear parents Lianglan Xu and Shoulin Wang, and my Uncle Hui Xu, for their material and spiritual support during my study, to provide me with comprehensive support and care in both physically and spiritually during my studies.

Abstract

This thesis proposes a WP-HPS cooperation method which utilizes Hydro Pumped Storage (HPS) to cooperate with wind power in order to reduce the impact of wind power characteristics on system reliability, smooth output fluctuation of conventional generation units and maintain system reliability at a required level. Based on the output characteristics of each power generation unit, two control strategies for wind power and pumped storage power stations are proposed.

In addition, the traditional reliability evaluation methods are not applicable to the proposed power system containing HPS and wind power. Therefore, the probability-based reliability assessmentmethod and the reliability cost-benefit analysis method are improved based on the operating characteristics of the proposed power system. These two assessment methods are used to analyze and verify the validity of the two control strategies in improving the reliability of a wind-powered system.

The proposed strategy 2 is applied to three different test systems, and comprehensive analysis in terms of long-term planning and daily operation of the power system at different wind penetration levels is conducted. Simulation experimental results in Chapter 5 show that strategy 2 is more effective than strategy 1 in improving power system reliability. The results in Chapter 6 proved that the WP-HPS cooperation (strategy 2) method can improve the reliability of the power system with a wind penetration level not exceeding 40% to the original level. The proposed method was finally applied to the actual power system to analyze the proposed method for

improving the reliability of the existing system. The evaluation results show that the proposed method not only can meet the requirements of system reliability but also can reduce the wind curtailment rate to the level required by the system.

Content

Figure

Table

Glossary of Terms

PSD	Power System Dispatch
CGU	Conventional Generation Units
MC	Markov Chain
ARMA	Autoregressive Moving Average
MCS	Monte Carlo Simulation
HPS	Hydro Pumped Storage
OR	Operating Reserve
ISO	Independent System Operator
PJM	Pennsylvania-New Jersey-Maryland
WIMPG	Western Inner Mongolia Power Grid
GWEC	Global Wind Energy Council
WTG	Wind Turbine Generator
SCIG	Squirrel Cage Induction Generator
WRIG	Wound Rotor Induction Generator
DFIG	Doubly Fed Induction Generator
$AP_{wi}[t]$	the available output of i^{th} WTG.

v_{ci}	cut-in wind speed of the wind turbine
$v_{r,}$	rated wind speed of the wind turbine
v_{co}	cut-out wind speed of the wind turbine
$v[t]$	the wind speed at time t
c	the scale parameter of Weibull distribution
k	the shape parameter of Weibull distribution
P_{rate}	the rated power output of the wind turbine
ESS	Energy Storage System
FOR	Forced Outage Rate
LOLP	Loss of Load Probability
LOLE	Loss of Load Expectation
LOEE	Loss of Energy Expectation
LOLF	Loss of Load Frequency
LOLD	Loss of Load duration
MTTF	Mean Time to Failure
MTTR	Mean Time to Repair
MTBF	Mean Time before Failure

IP	Individual Probability
CCP	Complementary Cumulative Probability
COPT	Capacity Outage Probability Table
NMCS	Non-sequential Monte Carlo Simulation
SMCS	Sequential Monte Carlo Simulation
CIC	the Customer Interruption Cost
PPS	Pure Pumped Storage
$E_{hps}[t]$	the energy stored by the HPS at time t
E_{rate}	the maximum amount of energy that the HPS can store
$P_h[t]$	the generation output of the HPS at time t
$P_p[t]$	the pumping output of the HPS at time t
P_{h_rate}	the power rating of the HPS during the generating period
P_{p_rate}	the power rating of the HPS during the pumping period
η_h	HPS efficiency during generating period
η_p	HPS efficiency during pumping period
$\mathrm{LD}_{total}[\mathrm{t}]$	the total load demand at time t
$P_{total}[t]$	the total power at time t

$P_{cgu}[t]$	the power supplied by CGU at time t
$P_w[t]$	the wind power directly absorbed by power system at time t
LD[t]	the power required by the load at time t
$P_{w\_ab}[t]$	the amount of wasted wind power at time t
X%	the wind dispatch ratio
$P_{w\_limit}[t]$	the dispatch limit of wind power in time t
EENU	Expected Energy Not Used
B_{EENU}	The annualized reliability worth from reducing the coal cost
r_{fuel}	the fuel price
B_{CIC}	The annualized reliability worth from reducing the CIC
r_{cic}	the LOLE cost rate
RB	the reliability benefit
C_{cap}	The annualized capital cost of HPS
C_{IOM}	The annualized maintenance cost of HPS
C_P	the cost rate associated with installing power capacity
C_E	the cost rate associated with installing reservoir capacity
r_F	the cost rates for the fixed cost

r_V	the cost rates for the variable cost
α	the yearly discount rate
RC	the reliability cost
TB	the total benefit of adding an HPS system
$AP_{cgu}[t]$	the available output of CGU in time t
$P_{cgu\_limit}[t]$	The dispatch limit of CGU in time t

Chapter 1.Introduction

1.1 Motivation

Nowadays, many countries with an energy structure dominated by conventional fossil fuel energy face increasingly severe supply shortages and marketing conflicts [1]. Additionally, the atmospheric and environmental pollution caused by the utilization of fossil fuel energy is also becoming progressively serious [2]. Wind power generation will be the largest renewable energy, accounting for 34% of global renewable energy, followed by hydropower, accounting for 30% in 2030 [3]. The integration of wind power into the power grid will alleviate the energy crisis and environmental pollution, but it will also have a negative impact on the power system reliability.

The power system is a complex operational system, by which power is supplied to the load through a transmission and distribution network powered by different power plants [4]. The System Operator (ISO) directs, supervises and manages the operation of power generation. ISO aims to provide users with uninterrupted power and runs the power system reliably and economically. The power system includes departments responsible for power generation, transmission, substation management, power distribution and load demand.For the power system to operate reliably, the balance between power generation and load must be maintained

throughout.In conventional power systems, the power generation units are mainly composed of large, controllable generator units (thermal power and hydropower). These units could adjust their output based on the change of load demand, so that the power generation and load demand in the system are balanced. However, the output characteristics of wind power are very different from those of conventional generation units (CGUs). The inherent characteristics of wind cause the output power of wind power plant to be random, volatile and intermittent. Therefore, considering the output characteristics of wind power in current researches on the operation and planning of power systems is necessary, as the wind power output characteristics affect the power system.

Wind power output data is known to be a dynamic series on the time scale. Therefore, the time-domain analysis method is the most commonly used method for wind power output characteristic analysis, including the analytical function method based on probability density function and time series analysis method. The probability density function provides the analytical expression of the wind power output distribution characteristics. Common probability distribution models include the Weibull distribution, Rayleigh distribution, Normal distribution, and lognormal distribution [5]. Measured data show that the wind power output data does not satisfy the most probability distributions, while the wind speed satisfies the Weibull distribution [6]. Therefore, in [7], Weibull distribution is utilized to fit

the measured wind speed data of the wind farm, and then the probability distribution characteristics of the wind power are obtained from the relationship curve between the wind speed and the output power of the wind turbine. The time series analysis method emphasizes the simulation of wind speed time correlation, and mainly includes Markov Chain (MC) model and Autoregressive Moving Average (ARMA) model. In [8], the Markov chain model is used to simulate wind speed. It not only considers the wind speed probability but also considers the frequency and duration of the wind speed. [9] used the ARMA model to simulate wind speed, analyzed wind power prediction error, and obtained the variation of prediction error with time. The time series analysis method reduces the randomness and volatility of wind power output through the simulation of the time correlation of wind speed data.

The effect of wind power output characteristics in power system reliability is usually studied by Monte Carlo Simulation (MCS) [10]. The probability density function or time series analysis method model is used to simulate the wind power output to generate various wind power output scenarios to analyze the impact of wind power grid connection on power system [11]–[13]. The inherent characteristics of wind power output necessitate adjusting the active power dispatching strategy of the wind-powered system due to the low controllability of wind power output [14].

According to the influence of the wind power output characteristics in power system, the large-scale integration of wind power brings a challenge to the reliable operation of power system due to following three key reasons: first, the volatility of wind power makes the total available power generation capacity of the system unstable and reduces the reliability of the system [15]. Secondly, in order to accept wind power, conventional generating units need to adjust their output frequently according to the output of wind power, which may reduce the service life of the equipment and increases the cost of power generation [4]. Thirdly, with the increasing installed capacity of wind power in the system, the wind power industry has the characteristics of large scale and high concentration [16]. Due to the limited operating reserve capacity of the power system, the increase in wind power penetration level will make curtailment of wind power more serious [17].

The main methods to ensure the reliable operation of the power system after wind power integrated can be divided into two aspects: one is to strengthen the interconnection between each power grids, improve the power transmission capacity and achieve wind power consumption in a wider range [18]; the other one is to build large-scale energy storage capacity in the power grid, increase the capacity of Operating Reserve (OR) and improve the operation of the system, and achieve peak shaving and valley filling of wind power [19]. [20] analyzed the relationship between the transmission capacity of the connecting lines between the

various regions of the power grid and the wind power curtailed energy. The results show that strengthening the interconnection between each power grids improves the overall wind power consumption. [21] summarizes major issues such as wind power development and transportation, pointing out the large investment cost of power grid construction, a long construction period and a low utilization of wind power, with little economic benefits posing a cost recovery problem. For the study of the use of energy storage system to solve the problem of wind power integration, [22] summarizes the technical characteristics of different energy storage systems and their application in power systems in various countries. The paper mentions that compressed air, Hydro Pumped Storage (HPS) and some chemical batteries can realize large-scale energy storage and solve the problem of wind power integration. This paper also suggests HPS as the only viable large-scale energy storage method for power systems due to its technology maturity and economy.

As the best provider of OR, HPS can not only balance the load fluctuations, but also set the system load forecast error, the unexpected failure of the generation and transmission equipment and the system load demand [23]. This suggestion is to build HPS to increase the OR capacity of the system to cope with the impact of large-scale wind power grid integration into the system.

Consider a power system that includes three -types of generation, i.e., wind turbines, HPS and CGUs, as shown in Figure 1.1 [24]. Generally, CGUs are

usually powered by non-renewable energy sources, including coal, oil and gas. Conventional power generation equipment has a long start/stop timespan. Conversely, although wind power is clean and does not consume fuel, it has poor stability and reversed peak regulation with local load curves, so a large portion of wind power is often wasted, due to the demand for system reliability, reverse peak regulation and its impact on the system will be discussed in detail in section 2.6. [17]. An HPS system is an auxiliary system that pumps water to store energywhen there is excess; it is then used to generate power as required. The start/stop timespan of HPS power generation equipment is very short, and its output can adjust quickly. Specific HPS operating conditions can be determined by the supply and demand relationship of the power system.

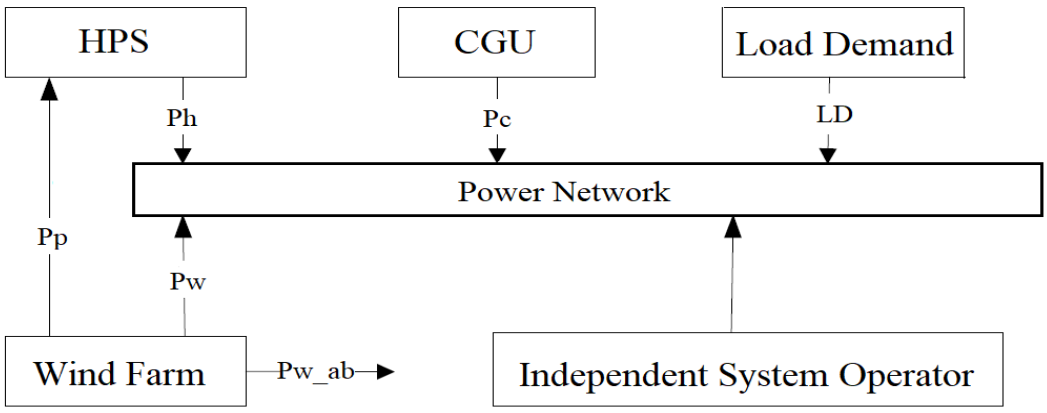

Figure 1.1: Structure of the proposed power system [24]

The proposedpower system consists of HPS, wind power, CGUs and load, there should be a suitable dispatch scheme. The ISO controls the operation of the entire system and is the core of the entire proposed power system. The dispatching

scheme formulated by ISO influence the wind power curtailmentand overall system reliability, with a good dispatch scheme greatly reducing the capacity of HPS and wind power curtailment. The optimal cordinatedoperation of the wind power, HPS, and CGU components is the key to maximizing the advantages of the proposed power system; it is thereby of considerable importance in the efficient functioning of the entire proposed power system.

Because the operating cost of wind power is almost zero, the greater the proportion of energy provided by wind power, the higher the economic of the system power without affecting the reliability and power quality of the system. This indicates that different dispatch schemes have different effects, and the capacity and cooperation method of the HPS system is a key aspect of optimized dispatch. Control of the power supplied by wind power and CGUs, over time, is also important, and these aspects taken together are the focus of proposed power systems dispatch research.

If the wind farm cooperates with HPS, the utilization of wind power can be enhanced, thereby improving the system reliability. Presently, the research on the wind power and HPS cooperation system has been discussed in many published papers. The analysis of wind power output characteristics in [25] showed that the wind power fluctuations and the regulation ability of HPS are complementary. The coordinated operation of HPS and wind power can effectively solve the adverse

impact of wind power output instability and random fluctuations on the power grid, and ensure the power quality and safe operation of the power grid. [26] proposed a cooperative strategy for wind power and HPS for the purpose of balancing the impact of wind power forecast errors on the Estonian power system. The simulation was performed using real-time data from the power grid, and the results were proved that the cooperation between HPS and wind power can effectively alleviate the uncertainty of wind power output prediction. Considering wind curtailment due to wind power output reverse peak regulation and the transmission congestion, [27] took the minimization of wind power curtailment and low transmission reinforcement costs as optimization goals. A multi-objective optimization model was established to evaluate the positive effect of wind power and HPS coordination on reducing wind curtailment and transmission reinforcement costs. [28] considered the worst scenario of wind power output in the unit commitment schedule model and utilized robust optimization approach to obtain the day-ahead output schedule of each unit in the power system. It is found that HPS can effectively reduce operating costs of wind power grid-connected systems. [29] optimized the benefits of the wind power and HPS cooperation system in consideration of the peak-to-valley electricity price difference and grid transmission restrictions. The experimental results clarify the economic feasibility of the coordination system. Based on characteristics of the wind power and HPS, [30] aimed at the maximizing the economic benefits of wind power-HPS

cooperation system, and utilized a new adaptive genetic algorithm to solve the optimal capacity of wind power and HPS. [31] established a cooperation optimization model of wind power and HPS for the purpose of maximizing the social benefit to study the optimal capacity of wind power and HPS in power system, and used the scenario reduction algorithm for optimization simulation analysis. Simulation results showed that the reasonable coordination of wind power and HPS can promote the development of wind power and achieve a significant increase in social benefits.

In general, the current research on wind power and HPS cooperation system focuses on three directions: one is to cordinate wind power and HPS to make the total output of wind power and HPS smooth, the second is to reduce the curtailment of wind power, and the third is to maximize the economic benefits of the cooperation system. However, there are few studies about wind power and HPS cooperation system capacity planning based on system reliability requirements. Owing to the high cost of HPS, its optimal capacity requires further studies under the premise of meeting system reliability requirements and cooperating with wind power. The methods for determining OR capacity based on reliability are mainly divided into three types: the traditional determination methods (details in Subsection 3.3), the probability based reliability assessment methods (details in

Subsection 3.4), and the Reliability Cost-Benefit Analysis (RCBA) determination (details in Subsection 3.5) methods.

The commonly used traditional determination methods are the percentage reserve margin method and the rule of thumb method [32]. Although the traditional determination methods are simple and easy to use, they may lead to insufficient or excess OR capacity without considering the impact of wind power uncertainty on the system, which makes it difficult to determine the exact OR capacity and it is not conducive for the reliable and economical operation of the system.

The reliability-based probabilistic methods analyze the various risk factors that affect the reliability of the system and determines the system OR capacity by setting the reliability indicators (details in Subsection 3.2.4) that the system needs to meet. The earliest reliability-based probabilistic method was the Pennsylvania-New Jersey-Maryland (PJM) method proposed in [33]. On this basis, Billiton associates OR capacity with system reliability indicators through the risk assessment [34]. However, it is impossible to directly determine the OR capacity based on the reliability indicators because there is no clear functional relationship between the reliability indicators and the unit operating status and OR capacity. Therefore, [35] adopts the idea of step-by-step research to determine the optimal OR capacity of the system by repeatedly iteratively correcting the OR under the given conditions. In [36], the reliability requirement is added to the constraint

condition for determining OR capacity of the system. By seeking the relationship between reliability and OR capacity, the optimal OR capacity of the system is determined in the process of unit commitment optimization.

With wind power integration, many scholars regard wind power as one of the risk factors affecting OR capacity within the power system. The determination of OR is to fully consider the impact of uncertainty on wind power. [37] considers the forced outage rate, prediction error of load and wind power output to determine the OR capacity according to the system's one-year operation and maintains system reliability at the same level, but does not consider the economic impact of system reliable operation. [38], [39] and [40] used the PJM method to calculate the probability table of generating capacity including the uncertainty of wind power. Under the premise of satisfying a given reliability level, the OR capacity of the system is determined, but the analytical formula is complicated and its practical application is difficult.

The RCBA method does not set a standard of the system reliability level that must be met, but instead finds the equilibrium point between the OR cost and the benefit, so as to determine the OR capacity, and translates the system's reliability into economic indicators [41]. For determining the OR capacity of the system after wind power integration, many studies used RCBA. [42] compares the traditional determination methods and the RCBA determination methods, and the results

show that a method based on RCBA can take into account errors in wind power generation and load forecasting, so it is more comprehensive and is significantly advantageous. In [43], the minimum cost of OR is taken as the goal, taking the requirements of system reliability as a constraint, and establishing a mathematical model to determine the optimal OR capacity of the system, using MCS and genetic algorithms to find the optimal capacity. Given the uncertainty of wind power, [44] based on the uncertain factors such as the forced outage rate of the power generating unit and the forecast errors of the load and the wind power output, used the RCBA method find the optimal OR capacity of the wind farm.

Since the capacity planning of wind power and HPS cooperation systems based on system reliability requirements has not been fully studied, this thesis will develop the WP-HPS cooperation method (details in Subsection 5.2) from the perspective of the reliability of the combined system, and study the impact of the proposed method on the reliability and related economics benefits of power system with large-scale wind power integrated.

Due to the inherent characteristics of wind, wind power output has great fluctuations. Large-scale wind power integration may affect the safety and reliability of the entire power system. The potential problems are summarized as follows:

Generation level: The power system needs to balance power generation and load demand, and sudden changes in wind power output may cause the total available output of the generation system could not meet the load demand. In addition, in order to absorb wind power, fluctuations in wind power may lead to the frequent adjustment of the output of CGUs, which may reduce the service life of CGUs.

Transmission level: the high wind power penetration levels may cause the voltage magnitude of some nodes in the system to fail to meet system requirements, and may also increase the energy transmission losses.

In detail, the WP-HPS cooperation method proposed in this thesis mainly include:

1. Determine the control strategy of wind power and HPS to mitigate the impact of wind power integrated into the power system

2. Improve existing system reliability assessment methods to evaluate the improvement of reliability of power systems by the proposed WP-HPS cooperation method

3. Improve the existing RCBA determination method to provide criteria for determining the optimal capacity of HPS.

The increasing wind penetration level has brought new challenges to the reliability of power systems. The proposed WP-HPS cooperation method provides a possible solution to this problem and helps the power system maintain the required level of reliability while increasing the wind penetration level, and provides a measurement for grid planning and operation.

The IEEE 30 bus system, IEEE 118 bus system and the Western Inner Mongolia Power Grid are used to validate the proposed WP-HPS cooperation method by computer simulation. The well-proven software tools MATLAB and MATPOWER are used for the simulation study.

1.2 Objectives

The main objectives of this thesis are summarized as follows:

- To propose a new reliability-based cooperation method between wind power and HPS. The operating state of HPS can be determined according to the power generation of each power generation unit and load demand in the system, aimed at not only smoothing the volatility of wind power but also alleviating the peaking adjustment of CGUs and reducing the wind power curtailment.

- To investigate two possible control strategies of wind power and HPS. When the wind power is in short supply, HPS can be used to provide electrical energy and fill the shortage. When the CGUs cannot meet the load demand, whether using HPS or both HPS and wind power to provide the electrical energy depends on the reliability improvement that two operation strategies can provide to the power system with wind power.

- To improve the probability-based simulation reliability assessment method of evaluating the reliability of the proposedpower system containing wind power and HPS. The operating characteristics of wind power and HPS are different from those of CGUs, and the methods of reliability evaluation need to be modified according to these operating characteristics.

- To improve RCBA method for determing the optimal capacity of HPS, which can quantify the improvement of power system reliability of HPS into economic indicators, and can be used to draw a comparison with the costs of HPS in order to provide a basis for determining the optimal capacity of HPS.

- To investigate the voltage magnitude of each node in the power system according to different wind power output and load demand, and determine whether the capacity scenario of HPS can meet the requirements of reliable operation of the system.

- To investigate the network losses in original power system, the power system with wind power and power system with WP-HPS cooperation method, and determine whether the proposed cooperation between HPS and wind power can alleviate the impact of wind power integration on network loss.

1.3 Original contributions

The main original contributions of this thesis are summarized as follows:

- **Contribution 1**: Considering the characteristics of wind power and HPS, the Sequential Monte Carlo Simulation (SMCS) method is used to evaluate the reliability of the power system with wind power. The wind speed fluctuations make it difficult to fully utilize wind power. Therefore, unlike the CGUs, the available power output needs to be changed according to the wind speed. Besides that, HPS is a load in the pumping state and is a generator in the hydro state. It is also necessary to improve the reliability evaluation for HPS-specific characteristics.

- **Contribution 2**: A new wind-power and HPS cooperative strategy based on system reliability is proposed to reduce the impact of wind power integration into the system. The characteristic of wind power will reduce the reliability of the system and increase the output adjustment of CGUs, which is not

productive to the utilization of wind power. The dispatch ratio is introduced to limit the output of wind power and CGUs. The wind power directly absorbed by the system is limited to a certain proportion of the load, and other loads are provided by CGUs. The HPS can store the surplus wind power when the available wind power output is larger than the dispatch limitation, and supply energy to the system when the system is insufficiently powered. This does not only improve system reliability but also improves the utilization of wind power.

- **Contribution 3**: Using cost-benefit analysis to quantify the improvement in system reliability of HPS as economic indicators. There are many capacity scenarios for HPS that can meet system reliability requirements, so the cost and benefit from system reliability improvement requires analyzing. It is difficult to estimate the social and economic benefit generated by HPS under a certain power supply reliability level. Therefore, the reliability benefit in this thesis uses indirect assessment method: the reduction in customer interruption cost. In order to better evaluate the benefits of HPS to system reliability, the proposed method considers the reduction of fuel cost in addition to the reduction of customer interruption cost compared with the traditional RCBA. Because of the higher utilization of wind power after the addition of HPS, the cost of generating electricy has reduced.

1.4 Outline of the thesis

This thesis consists of eight chapters and is organized as follows:

Chapter 2 outlines the development of wind energy and related issues. This chapter introduces the development of wind power and related policies to promote the development of wind power. It also reviews the increasingly alarming rate of curtailment of wind power output when it was rapid industrialized. Next, the wind power generation technology, including the typical wind power system structures, the wind speed model, the wind turbine output model and ways to utilize wind power are discussed in detail. The characteristics of wind power generation and the impact of the system after wind power integration are also introduced. Finally,HPS are briefly introduced.

Chapter 3 summarizes the important literature on the method of determining OR capacity of the system. First, the basic concepts and indicators of power system reliability are introduced, and then the commonly used OR capacity determination methods are described in detail. There are three methods for determining OR capacity: the traditional determination method, the reliability-based probability method and the RCBA method. Finally, the WP-HPS cooperation method is proposed to reduce the impact of wind power characteristic on the system aimed at ensuring system reliability.

Chapter 4 utilizes SMCS to evaluate the reliability of power systems containing wind power. First, the method of artificially generating wind speed by Weibull distribution is analyzed in detail. Then it describes the wind turbine output model and reliability model. Finally, the modified IEEE 30 Bus Test System was used to test the proposed method and evaluate the impact of wind power integration on system reliability.

Chapter 5 analyses the proposed WP-HPS cooperation method in detail through the theory, the mathematical model and the flow chart of the entire simulation process. Then, the two possible control strategies of wind power and HPS are compared by the modified IEEE 30 Bus Test System, and the ability of the proposed WP-HPS cooperation method to mitigate the effect of wind power on power system reliability is analysed and the optimal strategy obtained.

Chapter 6 applies the WP-HPS cooperation (strategy 2) method in the modified IEEE 118 Bus Test System and analyzes the simulation results. The simulation is divided into two parts: long-term system reliability planning and daily system operation planning. Six different wind penetration levels are analyzed in detail. The evaluation results show that the WP-HPS cooperation (strategy 2) method can effectively alleviate the negative impact brought by wind power grid integration, not only ensuring the reliable operation of the system in long-term planning but also effectively reducing the network loss in daily operation.

Chapter 7 applies the WP-HPS cooperation (strategy 2) method to the actual power system, Western Inner Mongolia Power Grid (WIMPG), to solve the actual system reliability planning problem. First, the status of wind power and HPS in WIMPG is briefly introduced. Then, the reliability evaluation of the WIMPG in three different years are carried out. The evaluation results prove that the WP-HPS cooperation (strategy 2) method is an effective means to solve the rapid development of wind power in WIMPG, which not only maintains the reliability of the system but also reduces the curtailment of wind power.

Chapter 8 summarizes the conclusions of this thesis and discusses possible improvements in future work.

1.5 Publications

According to the results of the research reported in this thesis, the following papers have been published:

- S Wang, S Shi, K Lo, J Lu. "An Approach to Calculate the Capacity of Pump-Hydro Combined Energy Storage with Wind Power Integration". *World J Eng Technol*. 2016.

- S Wang, K Lo, J Lu. “Calculating Size of Pump-Hydro Combined Energy Storage System in Wind-Diesel Systems Based on PHCES Dynamic Model”. *Energy Power Eng*. 2017.

- S Wang, K Lo. “Optimization of the Capacity of a Hydro Pumped Storage System to Enhance the Reliability and Cost Efficiency of the Associated Power System”. IET journal paper (Under preparation)

Chapter 2. Wind Energy and associated Issues of Wind Energy Integration

2.1 Introduction

Rapid industrialisation has led to an energy crisis in many countries where the increasing power load demand continues to be met using coal-based thermal power, resulting in high costs of power generation and high environmental pollution. Efficiently utilized renewable energy is considered to be the best solution to this crisis. Nowadays, the installed capacity of wind power generation is taking a larger and larger proportion in the power grid, which has become one of the most mature and realistic clean energy power generations. According to the prediction from the International Energy Agency (IEA) [3], wind power generation will be the largest renewable source of installed energy, accounting for 34% of renewable energy in 2030. Although in the sense of energy-saving and emission reduction, large-scale wind power integration improves the power supply structure, it brings new problems to the power system.

The power system must have sufficient generating capacity to meet the load demand at every moment and have enough operating reserve to handle emergencies. Unlike traditional power generation, wind power has the characteristics of volatility, uncertainty and reverse peak regulation. Due to these characteristics of wind power, integrating wind power into power grids on a large scale could cause large power

fluctuations, which have a certain impact on the operation of a power system [45]. Particularly, if the proportion of wind power generation capacity in the total power generation capacity is too large,, serious consequences can not be ignored [46]. Current energy storage technologies can provide a power system with energy storage, the balance of supply, and operating reserve. Adding an energy storage system to a power system with integrated wind generation can reduce the fluctuations of power output caused by wind power, smoothing the generation system output, effectively improving the imbalance between supply and demand, and improving the reliability of the power generation system.

This chapter provides an introductory background to the wind power and related issues of wind power integration. The global wind development situation is described in section 2.2. Section 2.3 presents the policies taken by several countries to encourage wind power. The state of wind power curtailment is reviewed in section 2.4. Section 2.5 introduces wind turbine technology and ways to utilize wind power. Finally, the associated effects of wind power integration and a review of pumped hydro storage station are explained in Section 2.6.

2.2 Global installed capacity of wind power development

According to the Global Wind Report Annual Market Update 2018 released by the Global Wind Energy Council (GWEC) [47], wind power utilization in the world grew rapidly in the 10 years prior to 2018, as shown in Figure 2.1. By the end of 2018, the global cumulative installed capacity of wind power had reached 591.550 GW, up 10% from 2016 and nearly 25 times higher than the value of 23.9 GW in 2001.

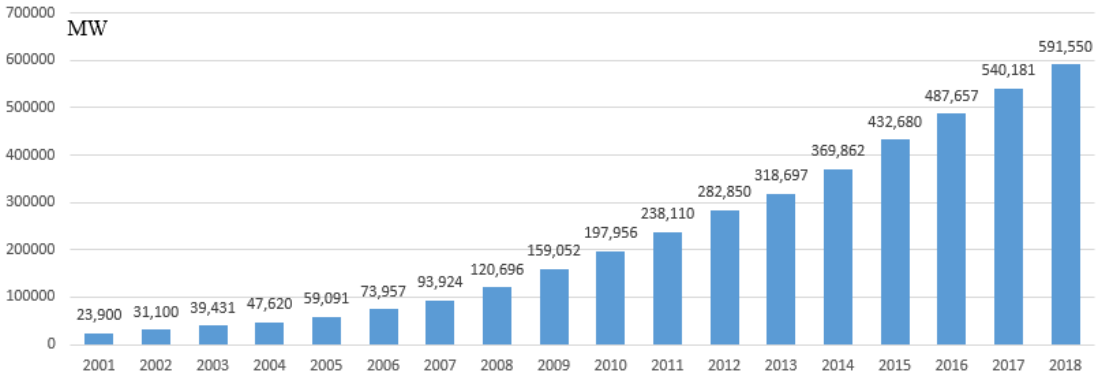

Figure 2.1: Global cumulative installed wind capacity from 2001 to 2018 [47]

It continued to maintain rapid growth, as can be seen from Figure 2.2, which shows that the annual installed wind capacity increased every year from 2001 to 2012. Due to economic reasons, the annual installed wind capacity declined in 2013, reaching a lower value than the annual installed capacity in 2009. However, one year later, the strong growth rate resumed, and a record high of 51.675 GW was attained. The global emphasis on wind power continued into 2015, which had the first increase of more

than 60 GW, once again ushering in a new record of global annual installed wind capacity. Although the installed capacity values in 2016, 2017 and 2018 were lower than the value in 2015, they were still larger than 50 GW. In summary, the global annual installed wind capacity data indicate that the global wind power industry has maintained a steady and rapid development trend.

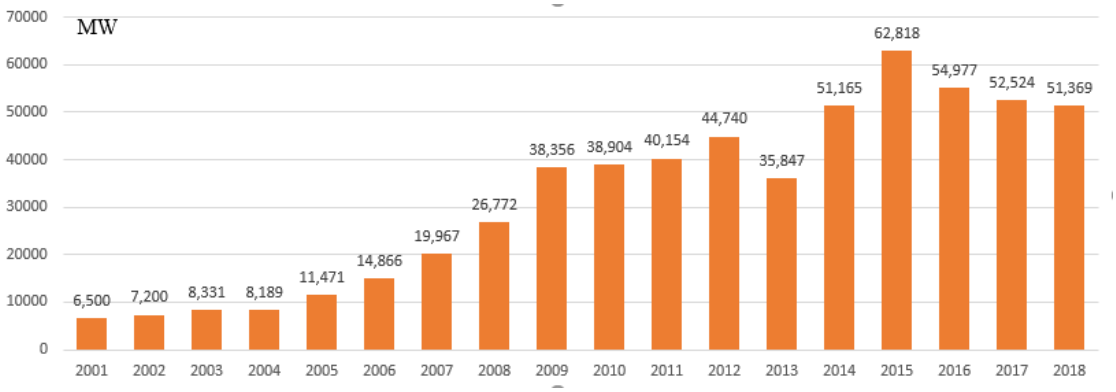

Figure 2.2: Global annual installed wind capacity from 2001 to 2018 [47]

As shown in Figure 2.3, the top ten countries in the world in annual installed wind capacity in 2018 were China, United States, Germany, United Kingdom, India, Brazil, France, Turkey, Mexico, and Belgium, accounting for 37%, 13%, 13%, 8%, 8%, 4%, 3%, 1%, 1%, and 1% of the total, respectively. These top ten countries have accumulated 89% of the total new installed capacity. The wind power new installed capacity in China in 2018 was 21.2 GW, far more than that of other countries. In addition, Figure 2.4 shows that the top ten countries in the world according to cumulative wind power capacity in 2018 were China, United States, Germany, India, Spain, United Kingdom, France, Brazil, Canada, and Italy, respectively. These top ten

countries accounted for 85% of the global cumulative wind power installed capacity, while the cumulative installed wind power capacity in China reached 206,804 GW, accounting for one-third of the global cumulative wind capacity. In the context of the global economic slowdown in 2015, the new installed capacity of wind power in China, Europe, and the United States still created an rapiddevelopment trend. At the same time, Canada, Brazil, Mexico, and other emerging markets have also continued a rapid development trend of wind power.

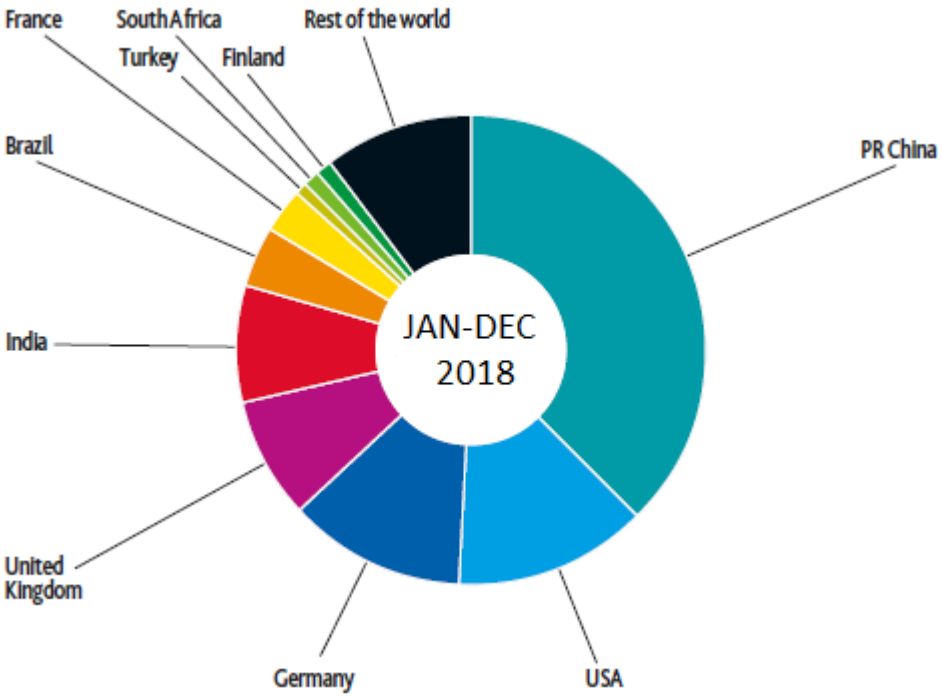

Figure 2.3: Top 10 countries in new installed capacity from January to December 2018 [47]

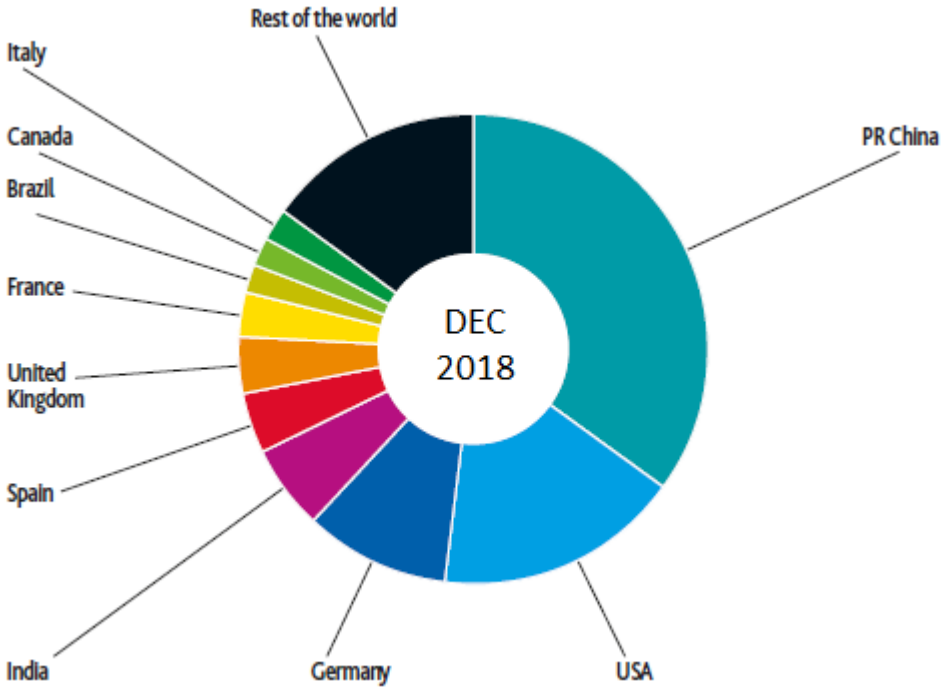

Figure 2.4: Top 10 countries in cumulative capacity in December 2018 [47]

The GWEC has predicted the development of the wind power market worldwide from 2018 to 2023. As shown in Figure 2.5, The development prospects of wind power in the next five years are still optimistic: by 2023, the annual new installed capacity will be larger than 2018 and will remain above 58GW.

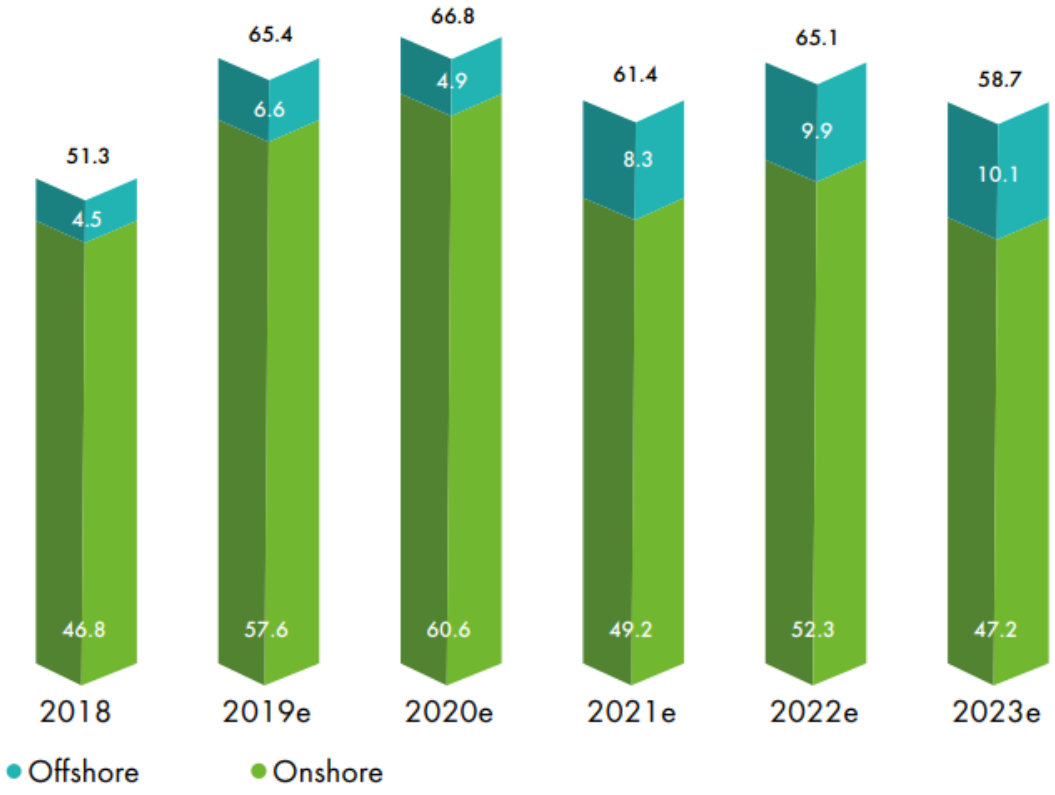

Figure 2.5: New installed capacity of wind power market forecast for 2018–2023 [47]

2.3 Policies to encourage wind power development

Wind energy has prominent advantages in terms of optimizing energy structure, easing energy tension, and reducing environmental damage [48]. Therefore, promoting the healthy and rapid development of wind energy, increasing the proportion of wind energy in energy consumption, and improving the efficiency of wind power development and utilization have become important goals for each country for formulating wind power policies. Germany, Spain, Denmark, and the United Kingdom, with strong wind power, prioritize the development of wind power [49], which

depends to a large extent on guarantees by policies and regulations, financial support, and vigorous promotion of technological research and development. Although each country has different policies and regulations, they all promote the development of wind power by combining "driving force" and "guidance force".

2.3.1 Germany

Germany attaches great importance to the guiding role of policies and regulations on the development of wind power and makes timely adjustments according to the actual development [50]. In 1990, Germany enacted the *Mandatory Electricity Purchase Law*, which required power companies to access wind power into the grid and acquire the power at a fixed price. It also mandated that 90% of the sales price of local power companies would be taken as the grid-connection price of wind power, and the cost difference between the grid-connection price of wind power and conventional power generation technology is undertaken by local power companies. In 1991, the *Feed-in Law* was introduced. It mandated that power companies acquire renewable energy power. The *Renewable Energy Act*, introduced in 2000, which prioritized grid connection of renewable energy, replaced the *Feed-in Law* of 1991. An *Amendment to the Renewable Energy Act*, in which the purchase price and technical requirements of wind turbines were revised, was enacted in 2009. It required that new wind turbine generators meet the requirements of technical specifications for transmission and medium-voltage power networks and those old units that have been connected to the

grid and cannot meet the requirements of the new grid-connection guidelines be modified within a time limit. Since 2000, when Germany's *Renewable Energy Act* was enacted, the power price has been revised three times. A third amendment did not change the basic principles or design principles of the fixed price of power; instead, it adjusted the power price according to the level of technology and resource development. In this way, policy stability, as well as the scientific nature of the power price, was ensured to the greatest extent.

2.3.2 Denmark

The wind power penetration rate of Denmark is 44% of its electricity demand which is the highest in the world, and Denmark was the first country to build wind power stations [51]. The government has established a power conservation fund to subsidize technologies and equipment that improve energy efficiency in 1981. A series of renewable energy policies and regulations in Denmark has provided practical guarantees for the development of wind power [52]. Denmark mandated that wind power be on-grid as early as 1979, with power companies paying a portion of the grid-connection cost. Since 1992, power companies have been required to buy wind power at 85% of the company's net power price, which excludes taxes on production and distribution costs. The Danish government promulgated energy plans successively in 1976, 1981, 1990, 1996, and 2004. Recently, it proposed that wind power would meet about half of the power demand by 2030.

2.3.3 Spain

The rapid development of wind power in Spain is inseparable from the following policies and regulations [53][54]. Since the introduction of *The Energy Law* in 1981, Spain has been seeking to establish a favourable market environment for the development of wind power. The *Electric Power Law*, enforced in 1997, was a milestone in the development of wind power in Spain. In 2010, in the *National Renewable Energy Action Plan*, it was proposed that the renewable energy supply in Spain would meet 22.4% of the energy demand by 2020 of which approximately 40% would be fulfilled by renewable sources. Specific safeguards, including modifying and improving technical specifications related to wind power integration, are also listed in the action plan.

2.3.4 United Kingdom

The United Kingdom is a country with the rapid development of wind power and is a leader in the development of offshore wind power [55][56]. The rapid development of wind power in the United Kingdom benefited from the *Electric Power Law* enacted in 1989, which provided for the non-nationalization of the power industry to the market. Citizens are required to consume non-fossil fuels and the government regulates a surcharge on fossil-fuel consumption, which is levied according to a 10% surcharge on power. To promote the development of wind power, the British government has

formulated policies of encouragement and support from various aspects. The 1990's *Convention on Non-fossil Fuel Obligations* required public power providers to establish non-fossil fuel purchase agents to sign up all non-fossil fuel power through the tendering process. The tender is divided into different technical tender sections to ensure that different renewable energy technologies are involved.

2.4 State of wind power curtailment

With the increasing installed capacity of wind power, attention has been paid to the construction of wind power, but the phenomenon of restricted use of wind power has become progressively more serious. Due to the characteristics of wind power output, curtailment of wind power and limiting the electricity generated has become a common phenomenon in the wind power industry. Taking China as an example, as shown in Table 2.1, the data of power loss due to wind curtailment in China from 2011 to 2016 show that the generation loss due to wind curtailment first increased and then decreased from 2011 to 2014, and the wind power curtailment rate also showed the same change, which is the inevitable result of China's timely introduction of relevant policies and the adjustment of wind power enterprises themselves. However, due to the increase in installed wind power capacity and economic constraints, the amount of electricity lost by wind curtailment also increased significantly in 2015 and 2016, reaching new historical highs of 33900 GWh and 49700 GWh, respectively. Electricity curtailment rates were 15% and 17% in 2015 and 2016, respectively, with Gansu,

Xinjiang, Jilin, and Inner Mongolia being the provinces with the most severe power curtailment losses, as shown in Table 2-2.

Table 2-1: Data statistics of wind power curtailment from 2011 to 2016 [17]

Year	Expected unused wind energy (GWh)	Average wind curtailment rate (%)	Electricity fee loss (m¥)	Standard coal replacement (MT)
2011	12300	16.23	6600	56.65
2012	20800	17.12	11200	94.74
2013	16200	10.74	8800	72.94
2014	12600	8.00	6800	56.62
2015	33900	15.00	18300	152.34
2016	49700	17.1	26800	223.34
Total	145500	14.03	78500	656.63

Table 2-2: Top four provinces with the highest wind power curtailment [17]

Year		Province			
		Gansu	Xinjiang	Jilin	Inner Mongolia
2015	Average wind curtailment rate (%)	39	32	32	32
	Expected unused wind energy (GWh)	8200	7100	2700	9100
2016	Average wind curtailment rate (%)	43	38	30	21
	Expected unused wind energy (GWh)	10400	13700	2900	12400

2.5 Wind turbine technology

After years of development, wind power technology has become relatively mature. Technological innovations based on the principles of wind power have been mastered, and full use of wind energy resources has been achieved through better methods. Wind power is divided into offshore and onshore wind power [57]. Although the working environments are not the same, the operating principles have many similarities.

2.5.1 Principle of wind power generation

Wind turbines have a mechanical combination that converts wind energy into electrical energy [58]. The wind blades, which is the heart of the wind unit, consists of blades and hubs that absorb wind energy and provide a variable and volatile source of mechanical energy for power generation. The blades need to have a good aerodynamic shape. Driven to rotate by airflow, the wind wheel converts the aerodynamic energy into mechanical energy, which causes the gears in the gearbox rotate to pull the generator to convert the mechanical energy into electrical energy [59]. At present, among the non-hydro renewable energy sources used for power generation, wind power generation is the one with the most mature technology, the most large-scale and commercial development conditions, and the best development prospects. It is an important field at present and will continue to be so in the future.

2.5.2 Types of wind turbine

Wind turbines are of a great variety of forms; according to different structures and functions, they could be divided into different types. Based on their blade structure and their position in the airflow, wind turbines could be divided into two categories in general: the horizontal axis wind turbine and the vertical axis wind turbine. Figure 2.6 is the schematic diagram of these two types of wind turbines.

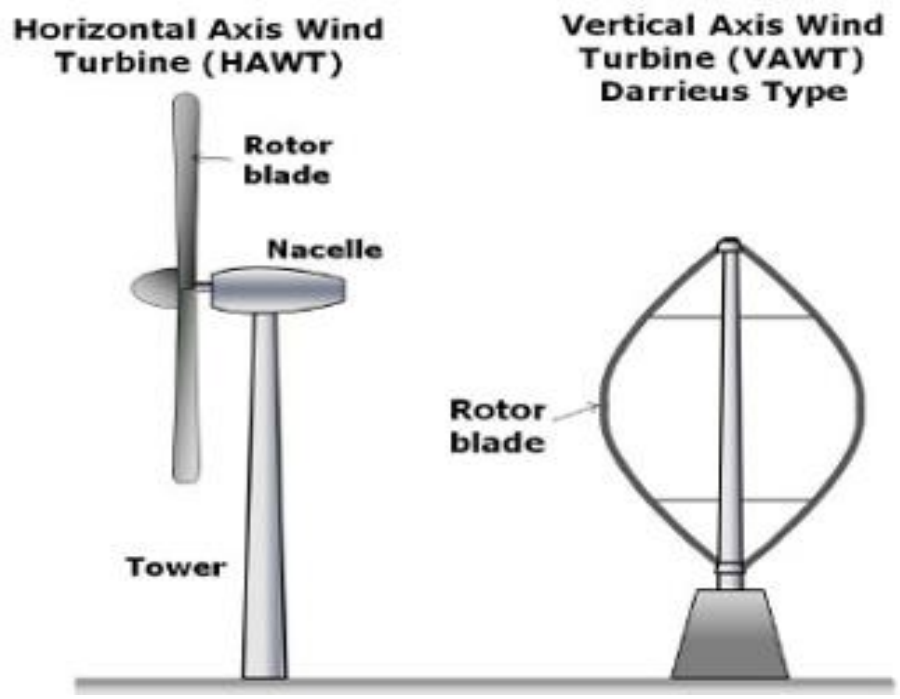

Figure 2.6: The horizontal axis and vertical axis wind turbines [60]

Blades of vertical axis wind turbine rotate around a vertical axis and can receive winds from all directions. Large-scale wind turbine generators are usually horizontal axis wind turbines.The blades of a horizontal axis wind turbine rotate around a horizontal

axis. When working, the plane of rotation of the blades is perpendicular to the wind direction.

There are many ways to classify Wind Turbine Generators (WTGs), according to the types of generator, WTGs can be divided into direct current generators, synchronous generators, asynchronous generators. Direct current generators are often used in small wind turbine; synchronous generators and asynchronous generators are widely applied to large and medium-scale WTGs. Synchronous generators boast self-excitation current; on the other hand, they are of high costs and complex grid-connection methods. When the rotational speed exceeds the synchronous speed, the asynchronous generator works under the power-generation mode and transmits active power to the grid; however, its needs to absorb reactive power from the grid to establish a magnetic field; it is without voltage and reactive power-regulating capacity. Asynchronous generators are of simple structure, low costs and no oscillation; they could be easily connected to the grid. Therefore, WTGs of large-scale wind farms usually employ asynchronous generators. Wind turbines also can be divided into the fixed-speed and variable-speed wind turbines according to its rotor speed. Fixed-speed rotors operate at a constant speed with low wind energy conversion efficiency, while the variable-speed type has the capacity to maximize the capture of wind energy through the continuous adjustments made within the range of the rotation speed.

Several typical wind power system structures are introduced below.

(1) The fixed-speed wind power system with asynchronous generator [61]

A fixed-speed wind power system adopts a Squirrel Cage Induction Generator (SCIG), whose stator is connected directly to the power grid via a transformer, and the structure is shown in Figure 2.7(1). SCIG can only operate at speeds very close to the synchronous speed. Therefore, wind turbines using such generators are called fixed-speed wind turbines. Since SCIG needs to absorb reactive power, in addition to an extra reactive compensation device, a soft starter should also be installed to make the grid connection smoother.

(2) The limited variable speed wind power system with asynchronous generator [62]

Figure 2.7(2) shows a limited variable-speed wind power system adopts a rotor-adjustable resistor and a Wound Rotor Induction Generator (WRIG) to operate at variable speed by changing the rotor resistor via adjustments of the controlled resistor externally connected to the rotor. Due to the restriction of the energy consumption of the external resistor capacity, the maximum speed of generator operates is 10% higher than that of the synchronous speed. Even so, a reactive compensation device and a soft starter are still needed.

(3) The variable-speed wind power system with Doubly Fed Induction Generator (DFIG) [63]

This scheme is essentially a wind power system that is composed of the WRIG of a power converter connected in series in the rotor circuit, and the structure is represented in Figure 2.7(3). The stator of the generator is connected to the power grid directly and the rotor is connected to the power grid via a power converter which controls the generator's operation by controlling the current at the rotor side.

(4) The wind power system with synchronous generator [64]

Synchronous generators applied in large wind turbines mainly adopt full-power converters to connect PMSG, WRIG, or WRSG directly to the transformer without the gearbox, as shown in Figure 2.7(4). The stator of the generator is connected to the power grid via the full-power converter.

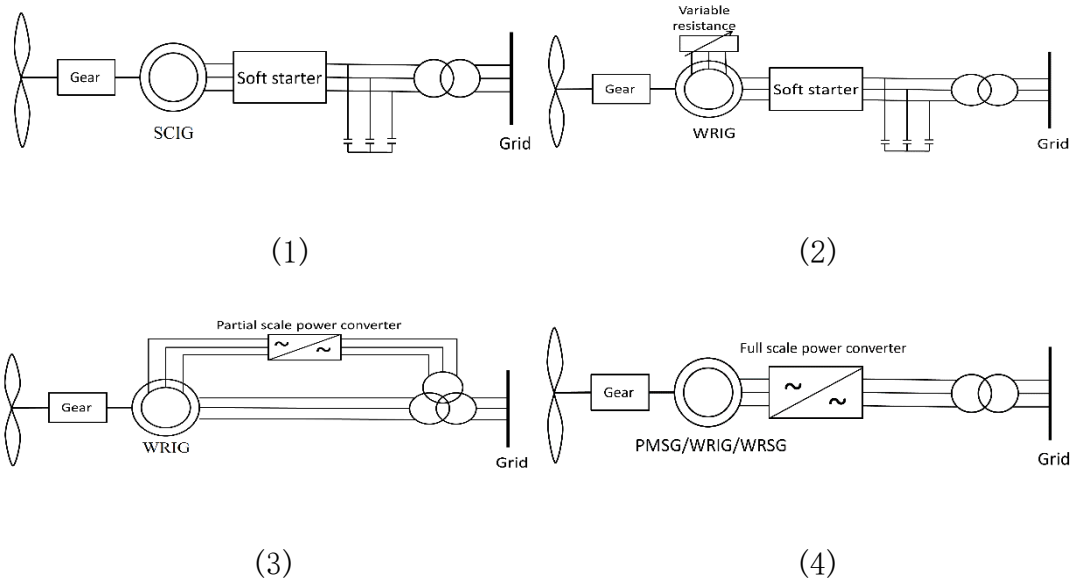

Figure 2.7: Structure of four types of wind power systems

2.5.3 Wind speed model

Wind power is related to the kinetic energy of the airflow and is proportional to the cube of the wind velocity.The wind speed model has great significance to the operation of wind farms and power systems. Wind energy is random and unpredictable, so the wind speed model is used to reflect the change rule of wind speed, which is the basis for overall planning of wind resources and reliability evaluation of wind farms. Common wind speed models can be divided into two types, probability distribution models [65]–[81] and time-series models [82]–[85]. The wind speed probability distribution model is a type of data analysis method that can be used to characterize the distribution characteristics of wind speed probability. The probability distribution of wind speed reflects the probability of the wind speed of the wind farm in each wind speed interval within a certain period of time, which has very important guiding significance for planning the wind farm. Common probability distribution models include the Weibull distribution [65]–[67], Rayleigh distribution [68]–[72], normal distribution [73]–[76], and lognormal distribution [77]–[81] . The time series model is a type of model that can describe the dynamic change process of the wind speed time series. The wind speed series has the characteristics of a probability distribution but also contains dynamic information that changes with time. Common time series models include the Autoregressive (AR) [82], Autoregressive Moving Average

(ARMA) [83][84], and Autoregressive Integrated Moving Average (ARIMA) [85] models.

The following three common wind speed models are commonly used in reliability analysis.

(1) Average wind speed prediction model: This model uses continuous time-series wind speed data from a wind farm anemometer tower or meteorological department to analyze the average wind speed. It determines a very constant wind speed in the research interval that is equivalent to the result of the time series wind speed sequence, ignoring the change of wind speed during the interval and is used mainly for long-term wind resource assessment of a wind farm. The average wind speed is expressed as in Equation 2.1:

$$\bar{v} = \frac{1}{n}\sum_{i=1}^{n} v_i \tag{2.1}$$

where n is the total amount of wind speed data in the study area.

(2) Wind speed probability distribution model: Wind energy is highly random, but the probability model could be utilized to describe statistical characteristics of wind energy. The Weibull distribution is considered a probability model that fits well with the measured wind speed distribution. It has been used widely for evaluating wind

energy resources, calculating power generation, selecting wind turbine models, and long-term planning. The probability density function of the Weibull distribution model is

$$f(v) = (\frac{k}{c}) \times (\frac{v}{c})^{k-1} \times e^{-(\frac{v}{c})^k} \quad (2.2)$$

and the cumulative probability function is

$$F(v) = 1 - e^{-(\frac{v}{c})^k} \quad (2.3)$$

where v is the random wind speed, c is the scale parameter, and k is the shape parameter reflecting the skewness of the Weibull distribution. The Weibull distribution will be utilized in this thesis to generate wind speed, further details will be discussed in Chapter 4.

(3) Wind speed prediction model based on time series regression: The time series simulation method represented by the autoregressive moving average model can better reflect the time-series relationship between current wind speed and historical wind speed. It is used mainly for dynamic simulation of the operation process of a single wind turbine. An introduction of ARMA follows. The smoothed wind speed sequence $\{y_t\}$ can be simulated by the general form of the ARMA(i,j) or AR(i) model, given by the following equations, respectively:

$$y_t = \sum_{i=1}^{n} \theta_i y_{t-i} + \alpha_t - \sum_{j=1}^{m} \theta_j y_{t-j} \quad (2.4)$$

$$y_t = \sum_{i=1}^{n} \theta_i y_{t-i} + \alpha_t \quad (2.5)$$

where θ_i and θ_j are the autoregressive coefficient and moving average coefficient, respectively, and $\{\alpha_t\}$ is a white noise sequence with a mean value of 0 and a variance of σ_a^2. The wind speed sequence v_t can be simulated by the mean value μ_t and standard deviation σ_t of the wind speed samples at time T.

2.5.4 Wind turbine output model

When studying the related problems of wind power generation, the first problem that needs to be determined is the output power of the wind turbine. The output power of the wind turbine mainly depends on the wind speed, and there is an obvious nonlinear relationship between the output of the wind turbine and the wind speed. When the wind speed is less than the cut-in wind speed v_{ci} or higher than the cut-out wind speed v_{co}, the unit output is 0 MW. When the wind speed increases from the v_{ci} component to the rated wind speed v_r, the output of the unit will gradually increase. When the rated wind speed v_r is reached or exceeded, the power remains at the rated power P_{rate}. Most studies describe the relationship between the output power and wind speed of the wind turbine as a linear [86], quadratic [87], and cubic [88] function as shown in Figure 2.8.

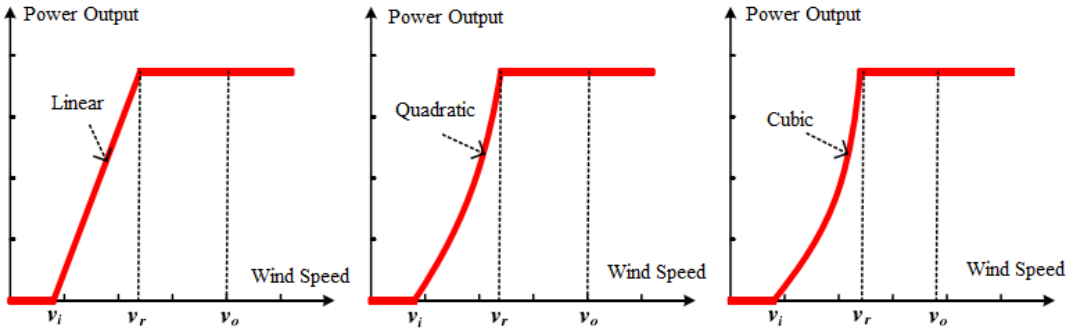

Figure 2.8: Comparison of wind power output characteristic

The function of the linear relationship between wind speed and wind power can be expressed by the following Equation 2.7:

$$AP_{wi}[t] = \begin{cases} 0, \ v[t] \le v_{ci} \ \text{ or } \ v[t] > v_{co}, \\ P_{rate} \times \left(\frac{v[t]-v_{co}}{v[t]-v_i}\right), \ v_{ci} < v[t] \le v_r \\ P_{rate}, \ v_r < v[t] \le v_{co} \end{cases} \tag{2.7}$$

where: $v_{ci}, v_{r,}$ and v_{co} are the designed cut-in speed, rate speed, and cut-out speed of the wind turbine (m/s); $v[t]$ is the wind speed at time t (m/s), P_{rate} is the rated power output of the wind turbine (MW), $AP_w[t]$ is the available output of WTG.

The function of the quadratic relationship between wind speed and wind power can be expressed by the following Equation 2.8:

$$AP_{wi}[t] = \begin{cases} 0, \ v[t] \le v_{ci} \ \text{ or } \ v[t] > v_{co}, \\ (A - B \times v[t] + C \times v^2[t]) \times P_{rate}, v_{ci} < v[t] \le v_r \\ P_{rate}, \ v_r < v[t] \le v_{co} \end{cases} \tag{2.8}$$

where A, B, and C can be calculated using v_{ci}, v_r, and v_{co} [89]:

$$A = \frac{1}{(v_{ci}-v_r)^2}\left[v_{ci}(v_{ci}+v_r) - 4v_{ci}v_{cr}\left(\frac{v_{ci}+v_r}{2v_r}\right)^3\right]$$

$$B = \frac{1}{(v_{ci}-v_r)^2}\left[-(3v_{ci}+v_r) + 4(v_{ci}+v_r)\left(\frac{v_{ci}+v_r}{2v_r}\right)^3\right]$$

$$C = \frac{1}{(v_{ci}-v_r)^2}\left[2 - 4\left(\frac{v_{ci}+v_r}{2v_r}\right)^3\right]$$

The function of the cubic relationship between wind speed and wind power can be expressed by the following Equation 2.9:

$$AP_{wi}[t] = \begin{cases} 0, \ v[t] \le v_{ci} \ \text{ or } \ v[t] > v_{co} \ , \\ \frac{1}{2}\rho A C_p \eta v[t]^3, \ v_{ci} < v[t] \le v_r \\ \frac{1}{2}\rho A C_p \eta {v_r}^3 , \ v_r < v[t] \le v_{co} \end{cases} \tag{2.9}$$

Where: ρ is air density (Kg/m^3), A is the area swept by the blades (m^2), η is wind turbine power conversion factor, C_p is wind rotor power coefficient.

Under the same unit data, the corresponding curve of characteristics of power output could be obtained from different power expressions. When the wind speed is between the cut-in speed and the rated speed, the output power of the turbines calculated from the linear and quadratic expressions was higher and the results of cubic expressions

more conservative. In practice, we should adopt different models according to actual requirements.

2.5.5 Wind power utilization

There are two ways to utilize wind power: on-grid and off-grid [6]. The off-grid system is also known as the isolated power system, which means that wind power directly supplies power to the load and is not integrated into the power grid, and the power generation capacity and load demand are not large. This system is mainly used in remote areas, and these areas have weak power grid and wind turbines are used with Energy Storage System (ESS) [90] or conventional generators [91] to solve the problem of community electricity use in the region. Figure 2.9 shows one of typical wind power and ESS off-grid system.

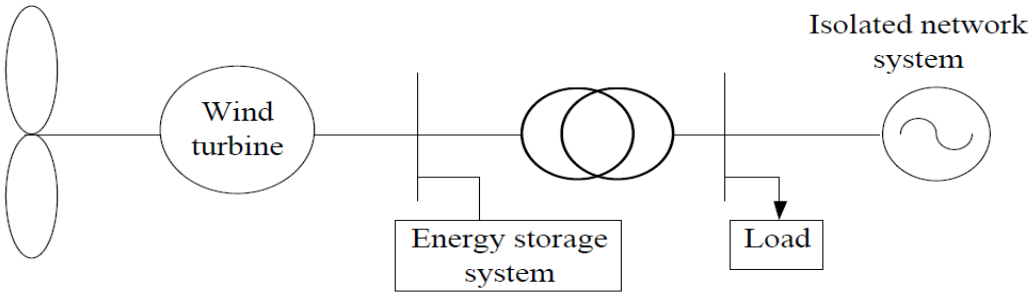

Figure 2.9: Schematic diagram of typical off-grid wind and ESS power system [90]

The on-grid system is integrated wind power to the grid as the power generating source, and it is the most effective way to utilized wind energy and the main trend of wind

power development. The capacity can reach several MW to several hundred MW. It is a wind farm composed of dozens or even hundreds of wind turbines. The main power generation equipment of the wind farm is wind turbines, which is integrated into the grid through transformers, as shown in Figure 2.10 [92].

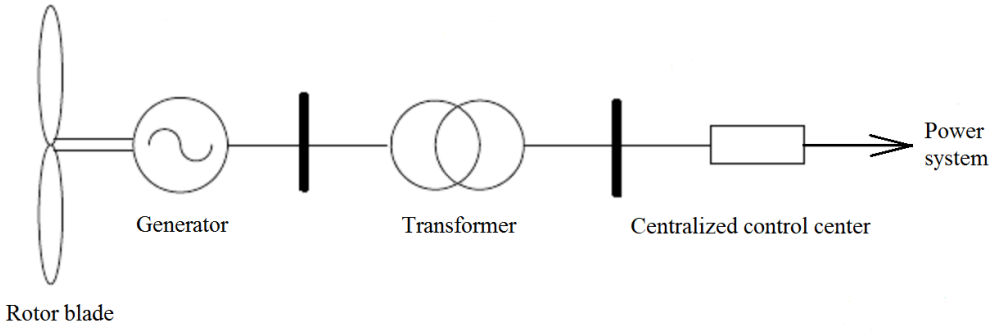

Figure 2.10: Schematic diagram of wind farm integrated into power system [92]

With the increase of wind power installed capacity, especially after many new large-capacity wind turbines are put into use, the installed capacity of wind power accounts for an increasing proportion of the total generating capacity of the power system. Analysis the wind power integrated into the power system is one of the key technologies of wind power development. This thesis will analyze the impact of wind power integration on the power system from the perspective of reliability.

2.6 Impacts of wind power integration on the power system

2.6.1 Characteristics of wind power

The most typical differences between wind power generation and conventional power generation lie in that resources to generate power conventionally, such as coal and water, can be stored and controlled and used to generate power when needed; while wind resources cannot be stored and controlled. Wind power is generated only when there is wind and the wind turbine operation conditions are satisfied. Given the feature that wind power cannot be stored, the wind power output changes as a function of the wind speed and synchronizes with wind speed.

(1) Volatility

Wind fluctuates frequently, so it is the same case with wind power. Figure 2.11 shows the wind-time curve of wind speed data from a wind farm in Inner Mongolia measured from 0:00 to 24:00 on February 11, 2017, with a sampling interval of 15 minutes [93].

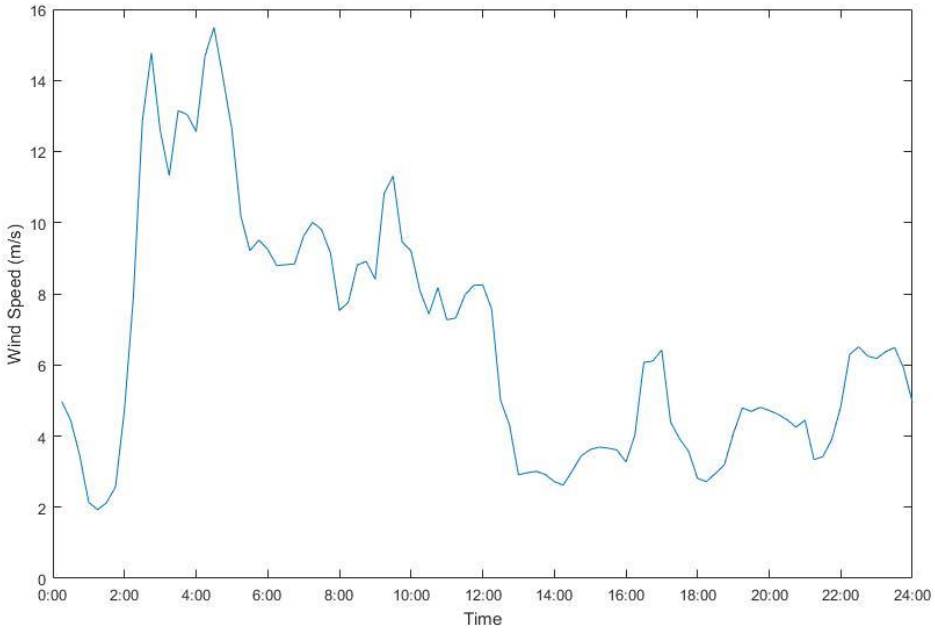

Figure 2.11: Daily wind speed curve of a wind farm [93]

Figure 2.12 shows the output power of a turbine with a rated power of 2MW, cut-in speed, rated speed and cut-out speed of 3, 10 and 22m/s respectively. It can be seen that the output power of the turbine fluctuates greatly.

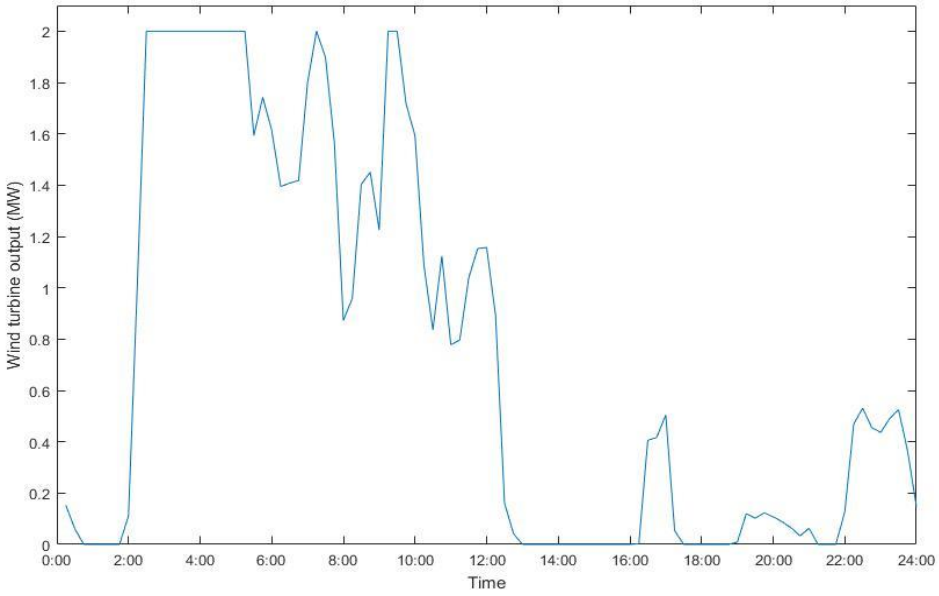

Figure 2.12: Daily output curve of WTG

(2) Uncertainty

Besides the fluctuation of wind power output, the impact of wind power gird connection system to the balance of active power is a result of the uncertainty of wind power output to a greater extent, which is shown in the deviation of prediction of wind power output [94]. If wind speed and wind power can be predicted more correctly, the adverse impact of the wind uncertainty to the system can be reduced. In spite of more and more study on wind power prediction, the deviation is inevitable, usually ranging from 10% to 30% [95]. There are many reasons for such deviation and technically it is relevant to the method, cycle and selection of points of prediction. In reality, it is also influenced by factors such as weather change and outage caused by failure of wind turbines [96].

(3) Reverse peak regulation

If the fluctuation of wind power output is consistent with the fluctuation of system load, the former will benefit the system. However, there is still the opposite situation. As the sun rises and sets, the large probability is that wind is strong at night and weak in the daytime. This characteristic is also reflected in the wind power output where it is high at night (i.e., valley load demand) and low in the daytime (peak load demand) [97]. So the reverse peak regulation of wind power is shown in the Figure 2.13, it shows that the valley of equivalent load (the result of load minus wind power) decreases obviously upon wind power connected to the grid, leading to a greater peak-valley gap [98].

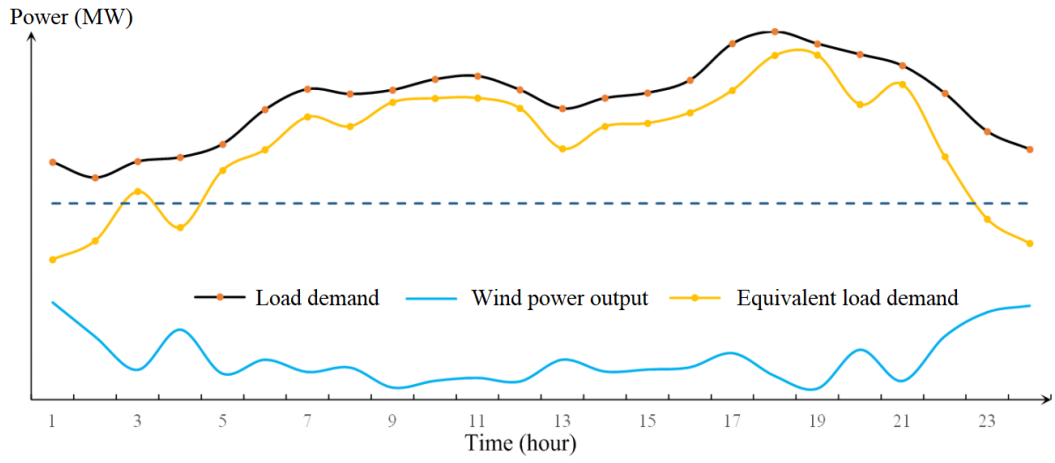

Figure 2.13: A sketch map of reverse peak regulation characteristics of wind power [98]

2.6.2 Issues of large-scale wind power integration

Although the reliability of a wind turbine is poor, the integration of a small amount of wind power is beneficial to the entire power system when the other conditions of the system are unchanged [99]. However, due to the randomness of wind power, replacement of the original conventional generators with large-scale wind power in the long-term planning of a power system will make the system reliability indices worse. Hence, the power system will become more unreliable as wind power penetration increases [100]. The influences of the introduction of large-scale wind power can be summarized in the following three aspects.

Firstly, the fluctuation and uncertainty of wind power output increase the system demand for operating reserve. Because wind power output cannot be controlled, wind power is always regarded as "negative load" in operation [47], due to the fluctuation and uncertainty of wind power, equivalent load has greater fluctuations and is more uncertain than pure power load, so more operating reserve is required to balance wind power output.

Secondly, wind power that replaces traditional power reduces the potential of the traditional power supply as an operating reserve source. The traditional generator unit can be also used as operating reserve to improve the reliability of the system [49]. In a system with a small proportion of wind power integration, the independent system

operator can always reserve power for wind power. However, when wind power assumes a large proportion in a power system, wind power may replace some traditional thermal power generator units with the effect of reducing not only the proportion of thermal power generator units but also the proportion of reserve resource of available thermal power generator units in the power system.

Thirdly, reverse peak regulation of wind power may reduce the reserve capacity of the traditional power supply [50]. reverse peak regulation of wind power may increase the difference between the peak and valley of the active output of conventional generators (the result of power load minus wind power). This causes the generated output of traditional units to approach the upper limit and lower limit of operation, which may reduce the operating reserve capacity of power supply and result in insufficient operating reserve.

In conclusion, the increase in the proportion of wind power integration will result in a reduction in operating reserve, which may weaken the reliability of operation and threaten the safety of the power system. Therefore, it is necessary to overcome the characteristics of wind power by providing additional operating reserve to improve the reliability level of the power system, more details on the operating reserve capacity calculation methods will be analyzed in Chapter 3.

2.6.3 Review of Hydro Pumped Storage

Currently, as the most rapidly developed and proven technology with the widest application, the Hydro Pumped Storage (HPS) station assumes the largest percentage of the total installed ESS capacity. It is widely applied for power grid peak regulation and operating reserve [23]. As HPS is not impacted by water inflow and its operating performance is rarely impacted by wet season, dry season, it is a very good ESS for regulating power generation. With a large storage capacity, HPS can meet the requirements of power supply and demand balance for several days, months, or even longer and is usually used for power dispatching management, including peak cutting and valley filling, operating reserve for peak power, and phase and frequency regulation [101][102]. Meanwhile, due to its low forced outage rate, safe and reliable operation, good stability, and high-power supply quality of water turbines, HPS is widely applied in many countries [103].

The HPS station consists mainly of an upstream reservoir, water conveyance system, plant buildings with generating and pumping units, and a downstream reservoir, as can be seen in Figure 2.14. The hydro-pumped generator is the core part of the HPS in the powerhouse, as this mechanical and electrical equipment must function for both the water pumping and power generation—as well as for auxiliary functions, such as frequency modulation and phase modulation [104].

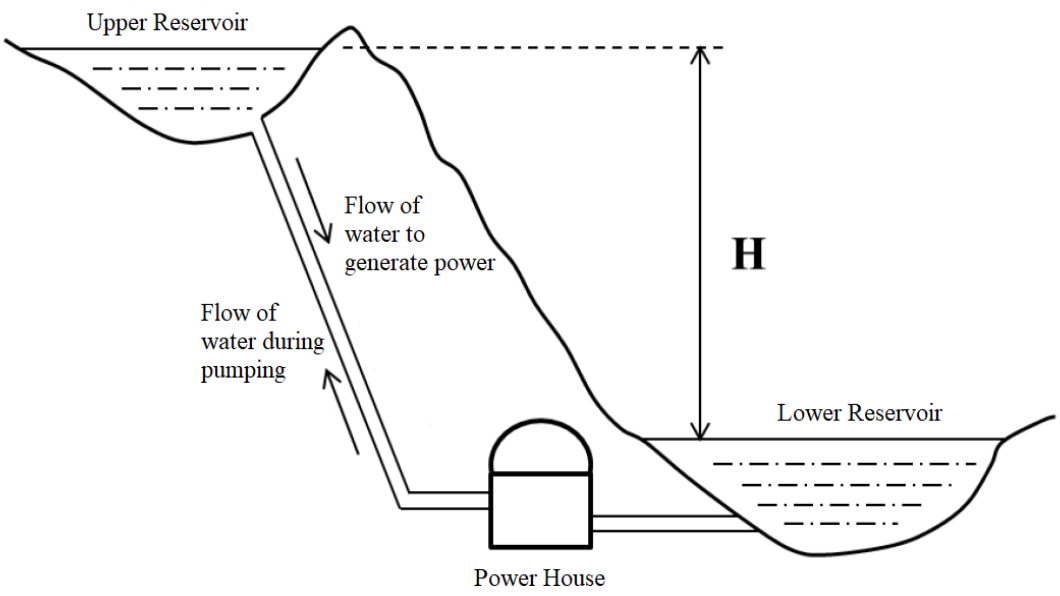

Figure 2.14: generalized structure of a pumped–storage power station [105]

The upper and lower reservoirs, as the facilities for water storage, must be able to meet the needs of pumping at times of off-peak load and to store sufficient water for generating electricity during times of peak load. The upper reservoir must be higher than the lower reservoir, and the height difference must be larg, so as to increase the water's potential energy and allow the creation and storage of electrical energy [106]. The upper reservoir can be built either using an existing reservoir or a natural lake or can be constructed from new. The lower reservoir is used to store the water discharged after power generation so that this water can be recycled, preventing unnecessary loss. It can be built by using an existing reservoir, natural lake or river channel, or purpose-built taking advantage of local geography. The water conveyance system transports water between the upper and lower reservoirs. The plant building, as the power

production centre, is where critical mechanical and electrical equipment, such as the pumped-storage unit, is located.

Pumped−storage power stations can be divided into two types, based on their construction type [107].

1) Pure pumped storage (PPS) station. In this type of HPS, the upper reservoir has either no or very small natural water inflow, so water needs to be pumped from the lower reservoir to the upper reservoir, for storage, and is recycled between the upper and lower reservoirs, so the two reservoirs must have sufficient capacity. The PPS station must be operated in coordination with other power stations in the power grid, and cannot function as an independent power source, but can be used as an operating reserve. Given that the upper and lower reservoirs of PPS stations do not need natural inflows and are characterized by high water head, small flow rate, and small storage capacity, a wide range of sites are suitable for constructing this type of pumped-storage power station.

2) Hybrid pumped combined storage power station. Its upper reservoir has natural inflows, so it has high requirements for the construction site. The lower reservoir needs to be constructed in the downstream river channel, according to the capacity required for pumped-storage, and a small dam is required at the exit of the lower reservoir to maintain its storage capacity. In a hybrid pumped-storage power station, an ordinary

hydroelectric generator unit is installed to generate electricity using river runoff, while the pumped-storage unit is installed to pump and store water from the lower reservoir for power generation and to carry out peak regulation, frequency modulation, and phase modulation.

HPS has two main operating conditions: one for pumping and the other for power generation [108]. During off-peak hours, the power station generally operates in pumping mode and the pumped-storage unit is in the motor state. Excess power from the system is converted into gravitational potential energy and stored in the upper reservoir. During peak hours, the power station operates in generator operation mode and the pumped-storage unit is in the generator state. The gravitational potential energy in the upper reservoir is converted into electrical energy for power supply. The pumped-storage power station is primarily a device for energy storage and conversion. It redistributes electrical energy over time, by storing energy during off-peak hours and discharging electrical energy during peak hours; the energy conversion relationship in an HPS system is shown in Figure 2.15.

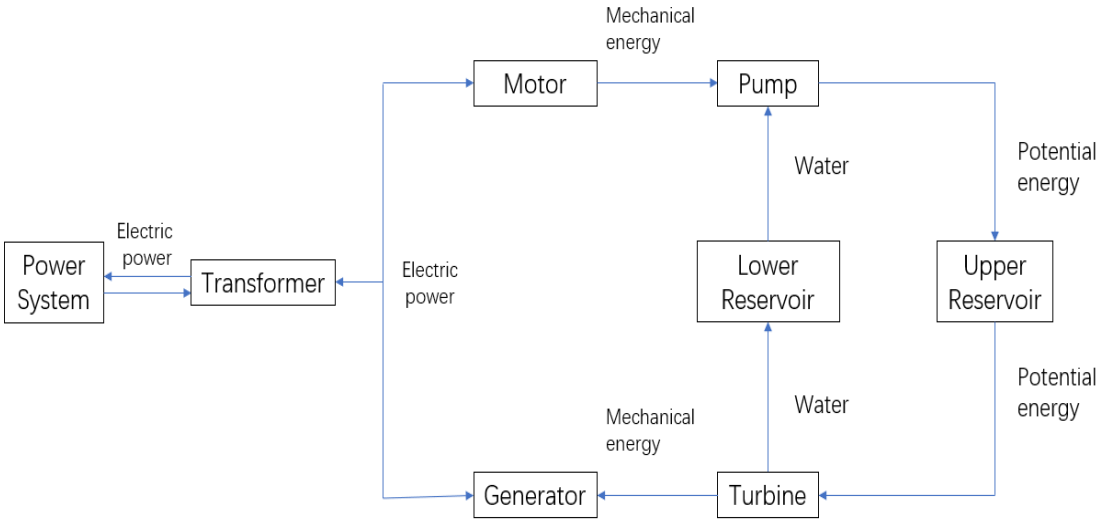

Figure 2.15: HPS system energy conversion relationship

HPS can reduce the start/stop frequency and runtime delays for various types of generator sets in power grids, including those of hydropower, coal power, nuclear power, etc., enabling them to run smoothly in optimal conditions, reducing hazardous emissions and energy consumption, and supporting operational safety.

Generally, HPS functions include the following:

Power generation: When the power supply cannot meet demand, and the HPS system acts as a generator. It has a high ramp rate and short response time, although HPS systems used as generators are subject to storage capacity limitations and by the installed capacity of the upper reservoir [109].

Peak shaving: HPS acts as a motor when the power supply exceeds demand. It stores excess electrical energy in the upper reservoir as potential energy. At this point, HPS

is equivalent to a load that can be used to fill a load trough and to reduce peak-to-trough differences in the system [110].

Frequency modulation and phase modulation: Due to the high ramp rate and short response time of an HPS system, it can be used for operational reserve and load tracking, allowing it to function as a system voltage stabilizer [111].

HPS system functions also include reducing the required system backup capacity and implementing black starts [112].

HPS does have disadvantages, however: 1. Normal HPS system operation requires appropriate terrain, sufficient water resources, and a large water level difference between two reservoirs, making suitable sites hard to find, and HPS system operation highly reliant on topography. 2. Long construction time: it usually takes a number of years to build an HPS system, and it is very difficult to increase its capacity quickly. 3. High costs: despite the low operation and maintenance costs of HPS, due to the large capacity of HPS, its capital investment is higher [113].

With the rapid development of wind power, demand is rising for operating reserve capacity in power systems. HPS is attractive because it can increase the OR capacity of the system which allows the installed capacity of wind power to be increased. Today, wind power and HPS cooperation system is receiving increased attention, and are

considered to be the most effective way to overcome wind power system integration impacts. HPS can store excess wind power into power systems with the high potential energy of water, reduce wind energy wastage, and respond quickly by providing power to the system when wind power input is low, thus improving power system reliability. Mathematical modelling of HPS will be described in detail in Section 5.

2.7 Summary

This chapter firstly described the global installation situation of wind turbines, then wind power development in four representative countries was considered as example cases to enumerate the policies that have been implemented to support the wind power industry. Next, taking China as an example, the situation of limiting wind power was described, despite the proportion of wind power in the generation system was increasing.

In the following sections, wind turbine technology is briefly explained from the wind power generation principle and the types of WTG. In addition, the common wind speed models and wind turbine output models are introduced, through these two models the output of the wind power can be simulated. The two ways to utilize wind power are also described.

The last sections explained the characteristics of wind power and the associated issues when large scale wind power integrated into the power system, and HPS is proposed as an operating reserve to mitigate the influence of wind power integration, the structure and advantages of HPS are introduced. Due to the high cost of HPS, the next section will discuss the impact of wind power integration on the method of determining reasonable capacity from the reliability perspective.

Chapter 3. Overview of power system reliability

3.1 Introduction

The essential task of a power system is to guarantee a sustained supply of standards-compliant electric energy to users [114]. However, along with the expansion in the scale of power systems, the number of components and devices included has grown increasingly large. Meanwhile, incidents of equipment failure, human factors, and external climate factors affecting the normal power supply have continued to surface from time to time. Moreover, in current wind turbine technology, the generated output of the wind turbine depends on the real-time wind speed, which can lead to an increase of the fluctuant load of the system [15]. Hence, it has become increasingly urgent that initiate quantitative assessment and research on improving the reliability of power systems [115][116].

The reliability of a system is closely related to its Operating Reserve (OR) capacity. To guarantee a safe and stable operation of the power system, it is necessary to increase system operating reserve capacity to compensate for the influence of wind power integration. The larger the OR capacity is, the safer is the system operation, and the higher the OR cost is. Therefore, ways to ascertain the OR capacity of the power

system so as to ensure that it not only meets the standard of system reliability but also minimizes cost have received considerable attention.

In section 2.6.3, the advantages of utilizing HPS as system OR have been analyzed in detail. When HPS is used to mitigate the impact of wind power on the system reliability, it is necessary to propose a reasonable control strategy for wind power and HPS to ensure that the reliability of the power system can be maximized.

This chapter focuses on the theoretical background of reliability and methods for evaluating the reserve capacity. The basic concepts of power system reliability are briefly introduced in Section 3.2. Section 3.3 describes two traditional deterministic methods for calculating OR capacity. Reliability-based probabilistic methods are described in Section 3.4, which also introduces the commonly used methods to assess reliability: the analytical method and the simulation method. Section 3.5 briefly introduces the application of cost-benefit analysis in OR capacity calculation. Finally, the impact of wind power on existing OR capacity calculation methods is discussed in Section 3.6.

3.2 Overview of Power system reliability

3.2.1 The basic concept of power system reliability

Power system reliability is generally defined as a power system's ability to maintain sufficient power supply for its users. Power system reliability can be divided into two categories: adequacy and security [117]–[119]. The former mainly involves the static running of the power system and is defined as the power system's ability to maintain the normal operation of equipment and meet the power demands of users. It requires the generator sets to hold sufficient installed capacity and generation power so that the transmission and distribution systems are able to transfer adequate electrical energy to users. The installed capacity of the system, rated capacity of the equipment, equipment failure rate, maintenance frequency, etc. can significantly influence the capacity of the power system. On the other hand, the latter category, security, evaluates the system's ability to meet the load demands with its given capacity under dynamic conditions within a short time of undergoing a sudden disturbance. It is mainly focused on the dynamic characteristics of the system. System security is closely related to the size of the disturbance and the system status before disturbance.

The increasing size of power systems and the growing complexity of the network structure have caused greater difficulties in the integrated analysis of an entire power system; therefore, in most research, the power system has been divided into several

subsystems covering the functions of power generation, transmission, transformation, and distribution, respectively. According to the different scopes of the objects of evaluation, the evaluation of adequacy is generally categorized into three levels, as shown in Figure 3.1.

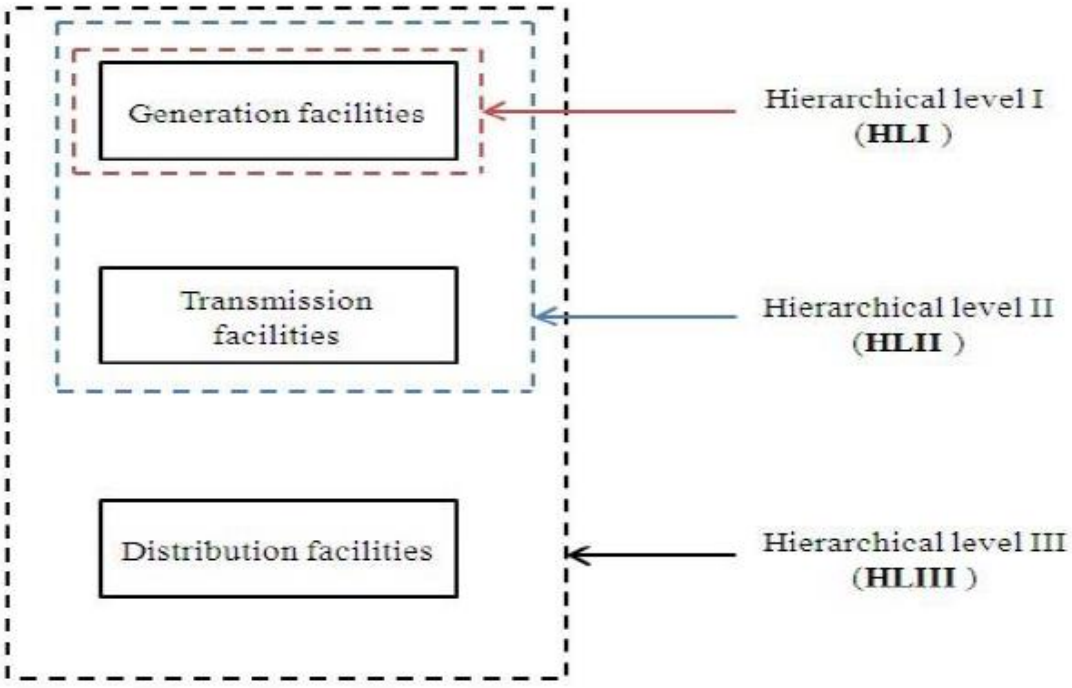

Figure 3.1: Hierarchical levels of reliability evaluation [120]

Hierarchical level 1 (HL1) refers to power generation system, the second level 2 (HL2) contains generation and transmission facilities, the last level (HL3) relates to the whole power system including distribution [121]. This thesis mainly studies adequacy evaluation at generation system.

3.2.2 Adequacy evaluation of the generation system

The generation system is the energy provider for the power system. When carrying out a reliability evaluation of a power generation system, it is usually assumed that the rest of the power system is completely reliable and that the power generated by the units can meet the load without any loss. Therefore, under this assumption, the only way to judge the power system condition (operational or malfunctioning) is by determining whether the power generated meets the load requirements. In the reliability assessment, two mathematical models need to be established: the generating model and the load model. According to such criteria, many risk indicators are obtained by combining the power generation capacity model with the load model of the power system. These risk indicators can reflect, to a certain extent, the improvement or impact on reliability by different combinations of power generation equipment or different capacities, thus providing a unified standard through comparison of different schemes. Figure 3.2 illustrates this concept.

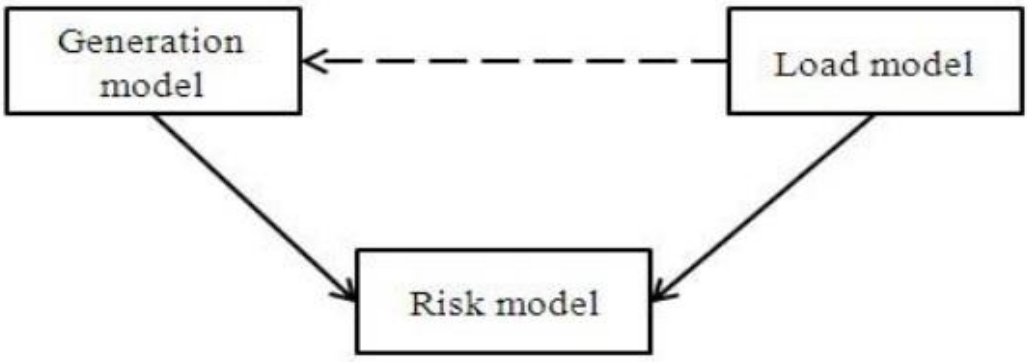

Figure 3.2: Model for generation system reliability evaluation [122]

Therefore, it is very important to evaluate the adequacy of a power generation system irrespective of whether the purpose is for system planning and design or operation and power generation.

3.2.3 Power system unit reliability model

In reliability evaluation, the generation units needs to be modelled. Before modelling, the following factors that affect system reliability modelling are analyzed.

(a) Mean time to failure

When applied in a power system reliability assessment, Mean time to failure (MTTF) represents the average time that a component operates normally before a failure occurs. The higher the reliability of the system, the larger the value of MTTF. The multiplicative inverse of MTTF is the failure rate λ of components during the operating time.

(b) Mean time to repair

Mean time to repair (MTTR) refers to the average repair time of a component, from time of beginning failure to time of repair finishing. The multiplicative inverse of MTTR is the repair rate of component μ.

(c) Mean time before failure

Mean time before failure (MTBF) is the average time between each occurrence during the operating duration, including the failure and repair time, that is, MTBF=MTTF+MTTR. In some publications, MTTF is used instead of MTBF, because MTTR is usually much smaller than MTTF, but these two factors are different. The relationships among these three factors are shown in Figure 3.3.

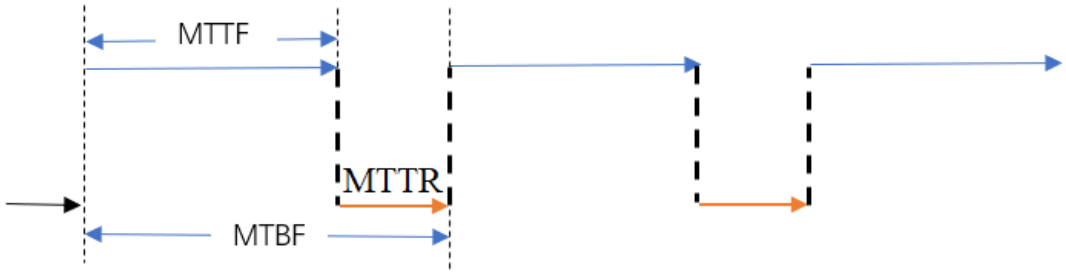

Figure 3.3: Relationships among MTTF, MTTR, and MTBF

(d) Forced outage rate

The forced outage of a component can be described as a process of continuous cycling between the operating state and the outage state. System availability and system unavailability are utilized to describe the state of the component. The system unavailability of the component is usually expressed as a dimensionless factor called the forced outage rate (FOR), and its definition is the percentage of time that a component in the power system is nonfunctional due to forced outages.

System unavailability (FOR):

$$U = \frac{\lambda}{\lambda+\mu} = \frac{MTTR}{MTTR+MTTF} = \frac{\sum[down-time]}{\sum[up-time]+\sum[down-time]} \quad (3.1)$$

System availability:

$$\mathrm{A} = 1 - \mathrm{U} = \frac{\mu}{\lambda+\mu} = \frac{MTTF}{MTTR+MTTF} = \frac{\sum[up-time]}{\sum[up-time]+\sum[down-time]} \quad (3.2)$$

where λ is expected failure rate, μ is expected repair rate.

The following is an example illustrating the calculation, assuming that there are three different generators and that their reliability data are those in Table 3-1.

Table 3-1: Reliability data of example generators

Unit no.	Unit size (MW)	Failure rate λ	Repair rate μ
1	10	0.01	0.49
2	20	0.01	0.49
3	40	0.02	0.48

The FOR of these three generators can be calculated using Equation 3.1:

$$\mathrm{U\ (Unit\ 1)} = \frac{\lambda}{\lambda+\mu} = \frac{0.01}{0.01+0.49} = 0.02$$

$$\mathrm{U\ (Unit\ 2)} = \frac{\lambda}{\lambda+\mu} = \frac{0.01}{0.01+0.49} = 0.02$$

$$\mathrm{U\ (Unit\ 3)} = \frac{\lambda}{\lambda+\mu} = \frac{0.02}{0.02+0.48} = 0.04$$

In the power system reliability analysis, for conventional generators, it is always assumed that the fuel source is adequate. Therefore, in the reliability modeling, only

the equipment running–outage model, including a two-state model or multi-state model, needs to be established.

The forced outage process of the generator can be described as a continuous circulation process between the running state (up state) and the outage state (down state). The availability and unavailability are two important probabilities for the description of the generator state. As shown in Figure 3.4, this is a two-state model.

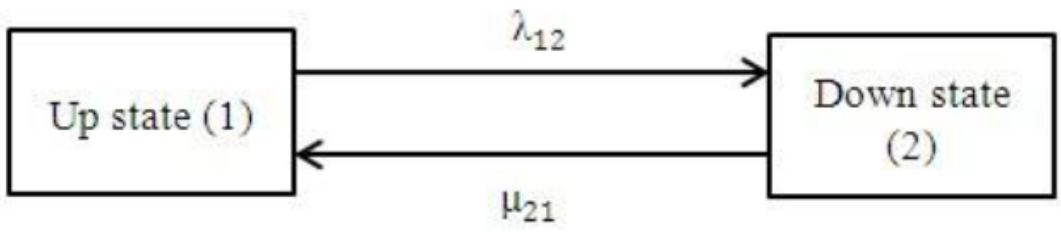

Figure 3.4: Two-state model for reliability analysis

If the derated state of the generator set is also taken into consideration, a multi-state model can be employed for its description, the transitions of the three-state model is shown in Figure 3.5. When considering a partial failure mode, it is necessary to add a derated capacity state in addition to the full-capacity and full-outage states to describe this intermediate process.

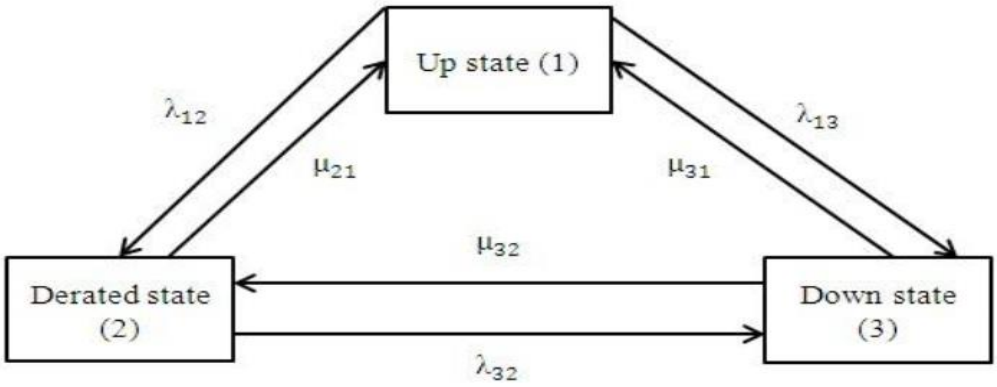

Figure 3.5: Three-state model for reliability analysis

Obviously, considering the derated state will increase the complexity of the system reliability evaluation. The focus of this thesis is to research the impact of wind power integration. Therefore, a two-state model is adopted in the reliability evaluation, ignoring the influence of the derated state and simplifying the computation.

3.2.4 Commonly used indices in generation reliability

In the reliability evaluation of power systems, the reliability indices vary for different subsystems, and the determination of which indices to use is a task of vital significance and an important decision concerning power production and planning. According to the focuses of this thesis, the following reliability indices as being applicable to the power generation system is listed [123].

(a) Loss of load probability

Loss of load probability (LOLP) refers to the total probability of the load demand exceeding the available generation capacity. The LOLP indicator, which indicates the probability of a power shortage accident in the system, has been applied widely, but it cannot evaluate the severity of an accident. The LOLP value within a year can be obtained as per Equation 3.3:

$$\text{LOLP} = \sum_i^m p_i \tag{3.3}$$

where m is the total number of inadequate states in a year and p_i is the inadequate probability of state i.

(b) Loss of load expectation (hours/year)

Loss of load expectation (LOLE) refers to the expected time value when load demand exceeds the available generation capacity within a studied time period. The LOLE within a year is given by Equation 3.4:

$$\text{LOLE} = \sum_{i=1}^m p_i T_i \tag{3.4}$$

where T_i is the duration of state i.

(c) Loss of energy expectation (MWh/year)

Loss of energy expectation (LOEE) refers to the expectation value of energy loss in power shortage within a certain period. This index can indicate system failure-caused user losses and measure the severity of an accident. With an analytical method, the LOEE value within a year can be calculated by Equation 3.5:

$$\text{LOEE} = 8760 \times \sum_i^m \sum_j^{T_i} (P_i - LD_{ij}) \tag{3.5}$$

where LD_{ij} is the load demand of the j^{th} hour in state i and P_i is the generating capacity of state i.

(d) Loss of load frequency and duration (occ./year and hours/occ.)

A frequency indicator is a reliability index as important as a probability index. Frequency refers to the number of shortages occurring in the system within the investigated scope; duration refers to the average length of time of each shortage accident. Equations 3.6 and 3.7 below define Loss of load frequency (LOLF) and Loss of load duration (LOLD), respectively:

$$\text{LOLF} = \sum_i^m f_i \tag{3.6}$$

$$\text{LOLD} = \frac{LOLE}{LOLF} \tag{3.7}$$

where f_i is the frequency of shortage state i.

3.2.5 Role of operating reserve

Theoretically, in the normal operation of a power system, the total active power produced by a power station at any time must be balanced with the load demand [124]. Ideally, the system installed capacity should be equivalent to the maximum load demand. However, in the actual operation of a system, all generator units cannot be guaranteed to be in operation incessantly. Moreover, random fluctuation and estimation error in the system and malfunction of the transmission line may result in system power imbalance. In such a situation, the system installed capacity must be larger than the maximum system load. The difference between them becomes the system reserve. The system reserve indicates the adequacy of the system installed capacity, which is an essential factor for an uninterrupted power supply and the reliability of the system. The system reserve is divided into the Maintenance Reserve (MR) and the Operating Reserve (OR) [125].

The MR is designed for the planned maintenance of the generators, which is related to factors like the shape of system's annual load demand curve, the number of generator units, the generator capacity, and repair cycle. The maintenance plan is generally arranged at a time when the load is low, therefore, the MR capacity does not necessarily need to be designed particularly. The OR is designed to balance the continuously changing load fluctuations aside from the planned system load, which is adjusted hourly, the estimated error of system load, and the accident malfunctioning

and breakdown of power generation and transmission equipment to provide a guarantee for extra capacity of the equipment for local load demand. The OR in a power system is the foundation of system safety. The primary purpose of the OR is to address the power imbalance caused by risk factors including load fluctuation, forced outage of generator, and malfunction of equipment.

3.3 Conventional OR calculation method

In the operation mode of a traditional power system, conventional deterministic methods are usually adopted to ascertain reserve capacity. There are two common approaches: the percentage reserve margin method and the rule of thumb method [32].

3.3.1 Percentage reserve margin

The meaning of "percentage reserve margin" is that the OR capacity of the power system cannot be less than a fixed percentage of the load demand. To explain this approach, assuming a power system with a $200\ \mathrm{MW}$ load demand and a reserve percentage for the system that is set to 20%. Therefore, the capacity of the generating system is $200 \times (1 + 20\%) = 240\ \mathrm{MW}$. Table 3-2 shows three possible generating unit capacity scenarios.

Table 3-2: Generating unit reliability data of three scenarios

Scenario No.	Unit Size (MW)	No. of Units	Forced Outage Rate
1	10	24	0.02
2	20	12	0.02
3	20	12	0.03

By combining the sampling distribution theory described in [126] with the forced outage rate, the system reliability results can be obtained. In addition, there are two important concepts in the calculation that need to be explained. One is the Individual Probability (IP), which means that the probability of each outage is equal to the exact outage level. The other is the Complementary Cumulative Probability (CCP), which refers to the probability that a given outage is equal to or greater than the exact outage level. If n is the total number of units with the same reliability level and generating capacity, k of them have fault, the IP (p_k) and CCP (P_k) can be calculated by Equations 3.8 and 3.9, respectively.

$$p_k = FOR^k(1 - FOR)^{n-k}C_n^k \tag{3.8}$$

$$P_k = P(k) = \sum_{i=k}^{n} p_i \tag{3.9}$$

The calculation process of scenario 1 is shown below.

The value of IP at each outage:

$\mathrm{p}(0) = 0.02^0 \times (1 - 0.02)^{24} \times C_{24}^0 = 0.615780$

$\mathrm{p}(10) = 0.02^1 \times (1 - 0.02)^{23} \times C_{24}^1 = 0.301607$

$$p(20) = 0.02^2 \times (1 - 0.02)^{22} \times C_{24}^2 = 0.070785$$

$$p(30) = 0.02^3 \times (1 - 0.02)^{21} \times C_{24}^3 = 0.010594$$

$$p(40) = 0.02^4 \times (1 - 0.02)^{20} \times C_{24}^4 = 0.001135$$

The value of CCP at each outage:

$$P(0) = 1$$

$$P(10) = P(0) - p(0) = 0.384220$$

$$P(20) = P(10) - p(10) = 0.082613$$

$$P(30) = P(20) - p(20) = 0.018828$$

$$P(40) = P(30) - p(30) = 0.001234$$

$$P(50) = P(40) - p(40) = 0.000099$$

The reliability result of percentage reserve margin for Scenario 1 is shown in Table 3-3.

Table 3-3: Reliability data of Scenario 1 based on percentage reserve margin

In Service (MW)	Out of Service (MW)	IP	CCP
240	0	0.615780	1
230	10	0.301607	0.384220
220	20	0.070785	0.082613
210	30	0.010594	0.018828
200	40	0.001135	0.001234
190	50		0.000099

The value of CCP at a 50 MW outage means the probability of the generating capacity of the system being equal to or smaller than 190 MW. In this situation, loss of load has occurred. Thus, the LOLP of Scenario 1 is 0.000099. Applying the same process to the remaining two scenarios produces the results summarized in the tables below.

Table 3-4: Reliability data of Scenario 2 based on percentage reserve margin

In Service (MW)	Out of Service (MW)	IP	CCP
240	0	0.784717	1
220	20	0.192175	0.215283
200	40	0.021571	0.023108
180	60		0.001537

Table 3-5: Reliability data of Scenario 3 based on percentage reserve margin

In Service (MW)	Out of Service (MW)	IP	CCP
240	0	0.693842	1
220	20	0.257509	0.306158
200	40	0.043803	0.048649
180	60		0.004846

From Tables 3-3 to 3-5, the LOLP values of Scenarios 1, 2, and 3 are 0.000099, 0.001537, and 0.004846, respectively. This example shows that even though OR capacity is fixed to the same marginal percentage, the reliability levels of these three scenarios are quite different. It indicates that the system risk depends on the numbers and FORs of generating units and the load demand in the power system. The capacity of OR based on the percentage reserve margin cannot truly reflect the reliability level of the generating system.

3.3.2 Rule of thumb

The other one of the conventional deterministic approaches is the rule of thumb approach, which means that the OR capacity of the power system is equal to an integral multiple of the capacity of the largest generating unit. If the capacity of the largest generator set is N MW, the capacity of the OR will be fixed to N MW, 2 × N MW, 3 × N MW, etc.

It is assumed that the load demand is 200 MW. At the same time, according to the "rule of thumb," the OR capacity is set to one time the capacity of largest generating unit, and three possible scenarios are established, as shown in Table 3-6.

Table 3-6: Generating unit reliability data of three scenarios

Scenario No.	Unit Size (MW)	No. of Units	Forced Outage Rate
1	10	21	0.02
2	20	11	0.02
3	20	11	0.03

Utilizing the reliability risk assessment method mentioned in Section 3.3.1, the outage probabilities of these scenarios are listed in Table 3-7.

Table 3-7: Outage probabilities of three scenarios

No. of Scenario	LOLP
1	0.065349
2	0.019513
3	0.041349

As for the example of percentage reserve margin, differences between risk indicators of the three scenarios still appear. The capacity of OR based on the "rule of thumb" also cannot reflect the true reliability level of the generating system.

3.4 OR calculation method based on reliability

The probabilistic method based on reliability level consists of analyzing the risk indices that affect the reliability level of the power system, considering the impact of various uncertainties on the reliability of the system, and evaluating the capacity of OR by setting the reliability indices that the system needs to meet [127]–[129]. Before determining the capacity of OR, the reliability of the system should be evaluated.

Given the large scale of modern power systems and the diversity of equipment, the possible number of permutations for system conditions during operation is massive, so it is often quite complicated to make a reliability evaluation. In the actual evaluation, multiple selections of possible system conditions are usually adopted to analyze each of their occurrence probabilities and impacts. Based on this approach, the reliability indicator value of the target system is calculated. Depending on the method of selecting the system conditions, the reliability evaluation of a power system can be carried out by two main methods: the analytical method and the simulation method.

3.4.1 The analytical method for reliability evaluation

When the analytical method is used to obtain the indicators of power generation reliability, the power generation system model that needs to be established is also called the Capacity Outage Probability Table (COPT) [130]. The COPT uses the reliability parameters of the power generating units in the system to obtain the

occurrence probability of the various levels of capacities generated by the combinations of the power generation units to reflect the relationship between the forced outage capacity of the system and the corresponding cumulative probability for the condition. When the type of generating unit is the same, the approach to formulate COPT is the same as the approach described in subsection 3.3.1. If the type of unit is not the same, the recursive approach is utilized to build COPT.

If the power generation system already has a certain number of generators, then a new unit with a rating capacity of C MW is added. The IP and CCP given that the outage capacity is X MW after the new unit is added are calculated by Equations 3.10 and 3.11.

$$\mathrm{p(X)} = \big(1 - \mathrm{p(C)}\big) \times \mathrm{p'(X)} + \mathrm{p(C)} \times \mathrm{p'(X - C)} \tag{3.10}$$

where $\mathrm{p(X)}$ and $\mathrm{p'(X)}$ are the IP of outage capacity X MW after and before the new unit is added, respectively. For the first unit, $\mathrm{p(0)} = 1 - \mathrm{p(C)}\ and\ \mathrm{p(C)} = FOR$.

$$\mathrm{P(X)} = \big(1 - \mathrm{p(C)}\big) \times \mathrm{P'(X)} + \mathrm{p(C)} \times \mathrm{P'(X - C)} \tag{3.11}$$

where $\mathrm{P(X)}$ and $P'(\mathrm{X})$ are the CCP of outage capacity X MW after and before the new unit is added, respectively. For the first unit, $\mathrm{P(0)} = 1\ and\ \mathrm{P(C)} = FOR$.

An example illustrating this approach is provided here, and the reliability data of the generators are shown in Table 3-8.

Table 3-8: Reliability data of three generators

Gen. No.	Capacity (MW)	Forced Outage Rate
1	60	0.01
2	80	0.02
3	100	0.03

Step 1: Adding the first unit to the system, there are $2^1 = 2$ states for one unit.

Table 3-9: COPT for one unit

State *i*	Available Capacity (MW)	Outage Capacity (MW)	IP	CCP
1	60	0	1-0.01=0.99	1
2	0	60	0.01	0.01

Step 2: Adding the second unit to the system, there are $2^2 = 4$ states for the two units.

Table 3-10: COPT for two units

State *i*	Available Capacity (MW)	Outage Capacity (MW)	IP	CCP
1	140	0	$0.99 \times 0.98 + 0.02 \times 0 = 0.9702$	1
2	80	60	$0.01 \times 0.98 + 0.02 \times 0 = 0.0098$	0.0298
3	60	80	$0 \times 0.98 + 0.02 \times 0.99 = 0.0198$	0.02
4	0	140	$0 \times 0.98 + 0.01 \times 0.02 = 0.0002$	0.0002

Step 3: Adding the third unit to the system, there are $2^3 = 8$ states for the three units.

Table 3-11: COPT for three units

State i	Available Capacity (MW)	Outage Capacity (MW)	IP	CCP
1	240	0	$0.97 \times 0.9702 + 0.03 \times 0 = 0.941094$	1
2	180	60	$0.97 \times 0.0098 + 0.03 \times 0 = 0.009506$	0.058906
3	160	80	$0.97 \times 0.0198 + 0.03 \times 0 = 0.019206$	0.049400
4	140	100	$0.97 \times 0 + 0.03 \times 0.9702 = 0.029106$	0.030194
5	100	140	$0.97 \times 0.0002 + 0.03 \times 0 = 0.000194$	0.001088
6	80	160	$0.97 \times 0 + 0.03 \times 0.0098 = 0.000294$	0.000894
7	60	180	$0.97 \times 0 + 0.03 \times 0.0198 = 0.000594$	0.000600
8	0	240	$0.97 \times 0 + 0.03 \times 0.0002 = 0.000006$	0.000006

The reliability indices of the generation power system can be obtained by combining the COPT of the generation system with the load model. Here, LOLP is taken as an example. Figure 3.6 shows a simple weekly load model that assumes that the maximum daily loads last for a whole day (one year has 52 weeks and every weekly load has the same curve). The LOLP can be calculated by Equation 3.3, which was discussed in Section 3.2.5.

The LOLP calculation table can be obtained by combining COPT and the load model and is shown in Table 3-12.

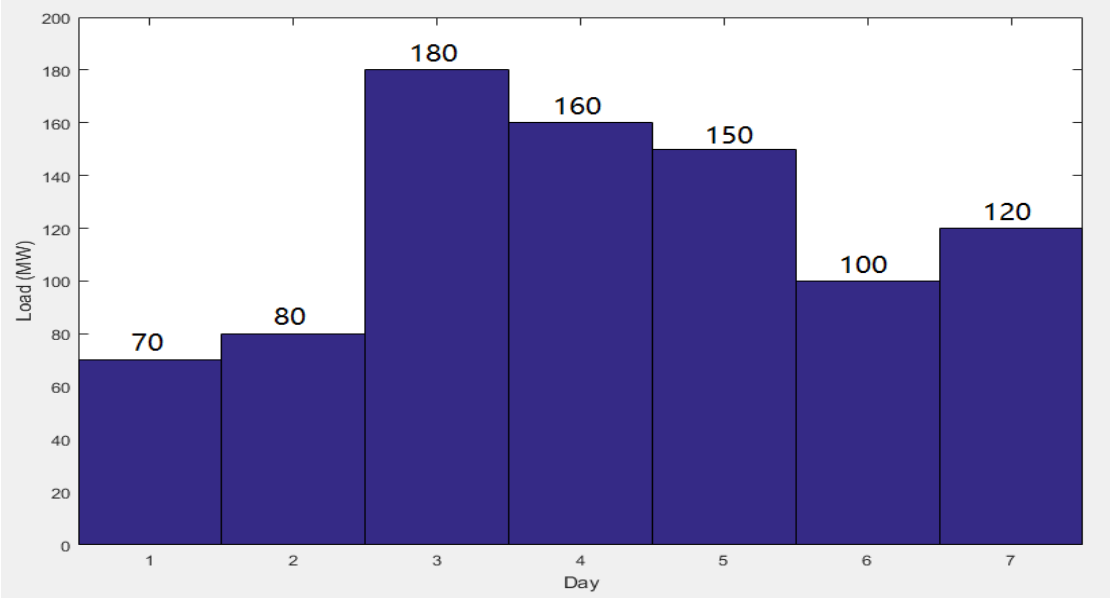

Figure 3.6: Weekly load curve

Table 3-12: LOLP calculation table

Day	Load demand (MW)	Outage Capacity (MW)	LOLP for each day
Monday	70	180	0.000600
Tuesday	80	180	0.000600
Wednesday	180	80	0.049400
Thursday	160	100	0.030194
Friday	150	100	0.030194
Saturday	100	160	0.000894
Sunday	120	140	0.001088

From Table 3-12, the LOLP of this generation system follows:

$$\text{LOLP} = \sum_{i=1}^{7} p_i$$
$$= 0.0006 + 0.0006 + 0.0494 + 0.030194 + 0.030194 + 0.000894 + 0.00108$$
$$= 0.11297$$

3.4.2 The Simulation method for reliability evaluation

The simulation method, also named the Monte Carlo Simulation (MCS) method, takes probability statistics as the theoretical basis and random sampling as the basic method [131]. To obtain a relatively precise result, many experiments need to be conducted, but it is difficult to conduct these manually. In recent decades, with the development of digital computing, MCS has gained rapid popularization and development. Modern MCS utilizes the computer's high-speed capacity, instead of manual labour, to make the experiment easier. MCS is widely used in large-scale electric system evaluation [132].

3.4.2.1 Probability distribution

MCS can utilize different types of probability distribution functions to generate random numbers to simulate the operating state of power system units. The probability distribution describes the values associated with the random event and the corresponding probabilities. These values must cover all possible events, so the cumulated probabilities must equal 1. In general, the reliability characteristics of a system or system unit are described by the probability distribution. The probability distribution functions commonly used in power system reliability assessment are described below.

(1) Normal distribution

The normal distribution is the distribution of the two continuous random variables μ and σ. It can be expressed by Equation 3.12 [5]:

$$f(x) = \frac{1}{\sigma\sqrt{2\pi}} \exp\left[-\frac{(x-\mu)^2}{2\sigma^2}\right] \tag{3.12}$$

The first parameter μ is a mean value of a random variable following the normal distribution; the second parameter σ is the standard deviation of the distribution. The characteristic of the density function of the normal distribution is symmetric about μ, peaking at μ, and reaching 0 at positive/negative infinity. Its image is a bell-shaped curve above the x-axis, as is shown in Figure3.7.

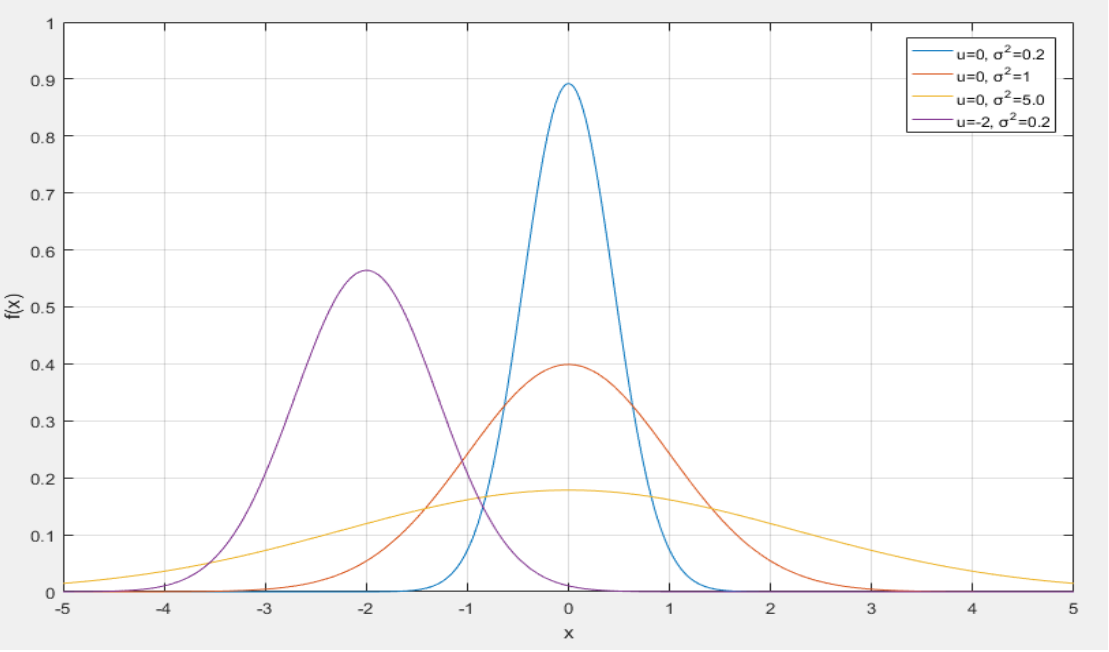

Figure 3.7: Normal density distribution functions of four different parameters

(2) Exponential distribution

The exponential distribution is the most widely used probability distribution function in reliability evaluation because the failure rate in the reliability evaluation of an electric power system is constant [32]. The probability density function of the exponential distribution is expressed by Equation 3.13 and its form is shown in Figure 3.8 [133].

$$f(x) = \begin{cases} \lambda e^{-\lambda x} & x \geq 0 \\ 0 & x < 0 \end{cases} \tag{3.13}$$

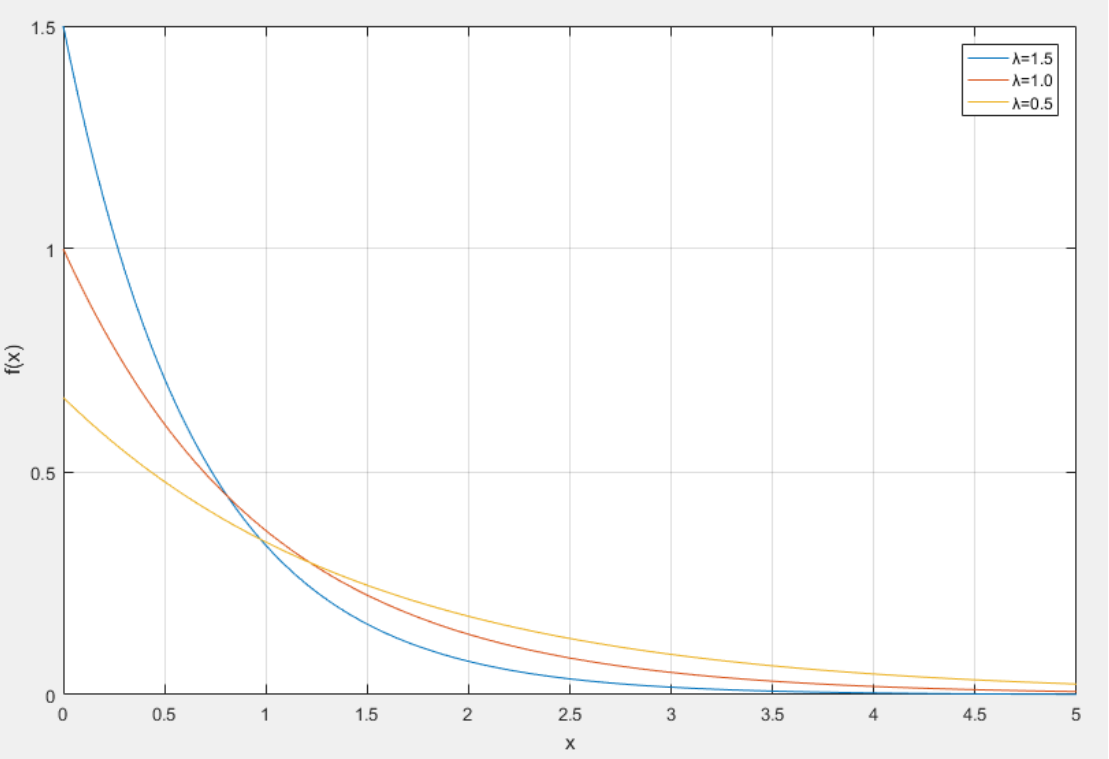

Figure 3.8: Exponential density functions of three different parameters

(3) Weibull distribution

The individual probability distribution function conforming to Weibull distribution is expressed in Equation 3.14:

$$f(v) = \frac{k}{c^k} v^{k-1} \times e^{-(\frac{v}{c})^k} \tag{3.14}$$

In Equation (3.14), v is the probability of a wind velocity, c is the scale parameter, and k is shape parameter. One important feature of the Weibull distribution is that it has no particular shape. By changing the values of c and k (as long as the values are above 0), the shape of Weibull distribution is changed. When the experimental data cannot be described with the normal distribution or exponential distribution, the Weibull distribution can be used to fit the data. The Weibull distribution has become a popular tool of experimental data statistical analysis for this reason [134], more details will be analyzed in Chapter 4.

The basic idea of the MCS method is to change practical problems to a random process or probability model and then take its parameters as the solution of the problem. Statistical characteristics of these parameters can be calculated by observation of this processor model, or by sampling test, and then the solution's approximate value can be obtained. Although the MCS method provides only estimated rather than precise

results and it requires a long time to study, it is an effective method for solving complex problems. MCS includes two methods: sequential MCS and non-sequential MCS [135].

3.4.2.2 Non-sequential and Sequential Monte Carlo simulation

The Non-sequential Monte Carlo Simulation (NMCS) method is also named the state sampling method. It conducts sampling on random states of the system unit directly, without considering the unit's state transition and time series [136]. Therefore, it is a simple model with low memory requirements and a fast rate of convergence, which is suitable for occasions with a high calculation speed requirement. Meanwhile, because states extracted by the NMCS method are not correlated with each other, the method does not consider state transition and time series of components, so some time related indexes cannot be calculated. The state of the entire power system depends on the combination of all component states, but the latter is determined by sampling. If setting s_i as the state of the i_{th} component and FOR_i to be unavailability, a random number R_i evenly distributed between [0,1] is generated. Then, the following exists:

$$s_i = \begin{cases} 0, R_i < FOR_i \\ 1, R_i \geq FOR_i \end{cases} \tag{3.15}$$

The Sequential Monte Carlo Simulation (SMCS) method is a method of conducting emulation in a certain time span per time series. It calculates the reliability index by simulating random system operation. SMCS is based on the probability distribution of

the duration of the sampling component state [137]. It needs to simulate the transfer process of component states per time sequence by sampling and then remerge the result to form the transfer process of system states per time sequence [138]. The unit's state transfer rate is set to be λ, and then the state duration time is described by Equation 3.15:

$$\mathrm{T} = -\frac{1}{\lambda}\ln U \tag{3.16}$$

In the formula above, U is an evenly distributed random number in [0,1]. If it is in the normal state, λ refers to the failure rate and T refers to the duration of normal operation. If it is in the failure state, λ refers to the repair rate and T refers to the duration of trouble.

NMCS does not consider the system's time sequence or the repair of fault components. It develops reliability index statistics per sampling frequency. NMCS is a simple computing method and enables fast computing speed. However, as it does not consider the time sequence of an electric system, it fails to calculate the index of failure frequency and time of duration in the reliability computation. This is a major defect. SMCS considers the system's time sequence and the change of load over time to simulate the system's actual running accurately. It can be used to calculate reliability indices such as failure frequency and time of duration and economic indicators such as shortage cost. SMCS is suitable for time-varying power supply and load, such as in

hydroelectric generation, wind power generation, solar power supplies, and loads with a great node peak to valley difference. However, the calculation amount in SMCS is so large that it is somewhat difficult to apply it to large electric systems.

Each method has advantages and disadvantages. Considering wind energy's randomness and time sequence and the correlation of the running state of the electric power system, this thesis adopts the SMCS method to evaluate the influence of the wind power plant on electric power reliability. The steps of this method are listed below.

(1) Each initial state of a unit is designated as up or down.

(2) Sampling is conducted for each unit's current state time by Equation 3.15 within a certain period of time, the state transfer process of the unit will be obtained.

(3) Merging each unit's state transfer process to obtain the system's available generating capacity.

(4) With the provided load profile, the system reliability indices could be calculated.

3.4.2.3 Simulation termination criteria

Because MCS is a continuously changing convergence process, a large number of iterations are required to make the simulated result close to the true value. Figure 3.9 shows the process of MCS calculations fluctuating but also converging with number of iterations.

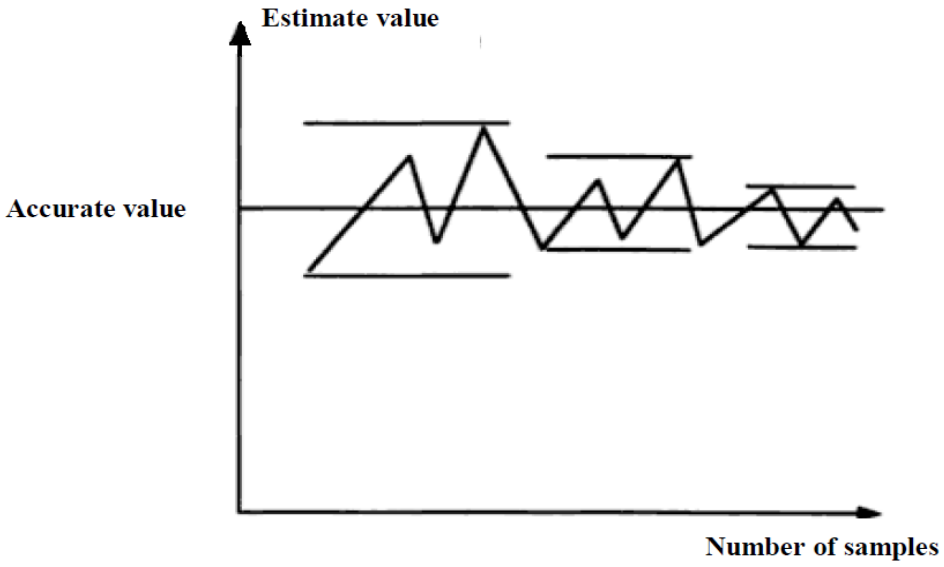

Figure 3.9: Convergence process in Monte Carlo simulation [115]

It can be seen from Figure 3.9 that adding a few more samples does not necessarily make the error smaller [115]. However, as the number of samples increases, the error bounding decreases. It is necessary to achieve a certain degree of accuracy in the simulation results, but it is not appropriate to obtain extremely high accuracy through a large number of sample simulations. There are normally two terminating criteria for stopping simulation.

(1) Setting the size of samples to a fixed value before simulation: For example, if the sample size is set to 2000, it means that the simulation will terminate when the sample size reaches 2000. This criterion is easy to program on the computer, but the number of samples is very important. If the number of samples is too small, the simulation results cannot meet the accuracy requirements. If the quantity is too large, computation time and cost are wasted.

(2) Taking a small value for the sample size: In this case, the simulation will pause after the sample number reaches this value and check whether the required level has been attained. If not, the simulation will continue to run the set number of samples and then check again until the simulation results meet the requirement.

The first criterion will be utilized for simulation termination in this work, and more details will be provided in Chapter 4. After running the MCS N times, the basic system reliability indices in Section 3.2.5 can be evaluated by following equations [10]:

a) Loss of load expectation, LOLE (hours/year)

$$\text{LOLE} = \frac{1}{N}\sum_{i=1}^{S} LLD_i \tag{3.17}$$

where N is the sampling numbers, S is total number of inadequate states in the one sampling period and LLD_i is sampled loss of load duration for shortage state i.

b) Loss of energy expectation, LOEE (MWh/year)

$$\text{LOEE} = \frac{1}{N}\sum_{i=1}^{S} ENS_i \tag{3.18}$$

where ENS_i is the sampled energy not supplied in MWh for state i.

c) Loss of load frequency and duration, LOLF (occ./year) and LOLD (hours/occ.)

$$\text{LOLF} = \frac{1}{N}\sum_{i=1}^{S} LLO_i \tag{3.19}$$

where LLO_i is the sampled loss of load occurrence for state i.

$$\text{LOLD} = \frac{LOLE}{LOLF} \tag{3.20}$$

3.4.3 Comparison between analytical and simulation methods

The advantage of the analytical method is that it utilizes rigorous mathematical method and effective mathematical algorithm to analyze the reliability in detail and systematically. The obtained reliability indices are highly accurate. However, for large and complex systems, the analytical method is not easy to calculate. As was discussed above, assuming that the system has n units, then the system has 2^n states, which makes the mathematical model difficult to build and computationally intensive.

The MCS method mainly reflects the probability distribution of components and system by using the computer to generate a series of random numbers. It simulates the system's actual operation by large amounts of sampling, and then obtains accumulative results to obtain the system's reliability index. When analyzing system reliability with the MCS method, each component's state should be sampled in the electric system. Sampling of the probability distribution function of components can be conducted to confirm the state of system components. Then, the entire system's state can be confirmed by combination of all component states.

MCS has obvious advantages in judging system reliability. Firstly, random sampling is conducted to obtain the computation. This basic idea is very easy to interpret and apply for staff and researchers. Secondly, on the premise of meeting the required precision, the sampling frequency is not associated with system sizing, so the MCS method is usually applied in the assessment of large electric power system reliability, etc. Thirdly, through reliability assessment with the MCS method, we can obtain the probability index, frequency index, and duration index to make the reliability information more practical and comprehensive. Fourthly, the mathematical model of this method is relatively simpler than that of other methods. It is easy to simulate random factors such as wind speed and load change and various control strategies of the system. The obtained result is more consistent with engineering practice.

3.4.4 Method based on reliability level

The method based on reliability level consists of analyzing the risk indices that affect the reliability level of the power system, considering the impact of various uncertainties on the reliability of the system, and evaluating the capacity of OR by setting the reliability indices that the system needs to meet [127]–[129]. The method proposed by Pennsylvania—New Jersey—Maryland is commonly used to determine the OR capacity that the operated power capacity over a certain period in the future can barely meet or fail to meet the expected load demands. This probability is called the Unit Commitment Risk (UCR), and this certain period is the leading time during which no newly added units are allowed to be put into operation [139]. Therefore, UCR can represent the level of risk of whether the operated power capacity over the leading time can meet the load demands.

In the PJM method, the traditional power generating units are expressed by a two-state model. Suppose that both the mean time between failures and the mean repair time show an exponential distribution. Then, if the units are in normal operating condition at $t = 0$, the probability of outage within T is the following:

$$P_D = \frac{\lambda}{\lambda+\mu} - \frac{\lambda}{\lambda+\mu} e^{-(\lambda+\mu)T} \tag{3.21}$$

As the leading time is usually short, the maintenance process can be neglected. Therefore, the above formula can be changed as follows:

$$P_D = 1 - e^{-\lambda T} \tag{3.22}$$

Likewise, given the low unit failure rate and the short leading time, Equation 3.21 can be simplified further:

$$P_D \approx \lambda T \tag{3.23}$$

The result of the Equation 3.22 is called the Outage Replacement Rate (ORR), which represents the probability of unit failure within the leading time. The power generation model adopted in the PJM method can follow the method of establishing COPT in the previous chapter, with the difference that ORR is used instead of FOR to represent unit regular stable performance. Moreover, considering the short study time of the operating reserve risk evaluation, it is assumed that the load remains constant during study. Therefore, the power generation model does not need to be combined with a load model, and the UCR indicators can be obtained by the accumulated probability in the COPT table.

3.5 OR calculation method based on cost–benefit analysis

Cost–benefit analysis is an economic method covering the whole process of estimating and evaluating the investment cost of an engineering effort and the benefit arising the effort in order to realize a clear public goal [140]. According to the analysis of the system OR cost and the economic value of the reserve, the minimum total marginal power supply cost is used as the objective function to build a mathematical model for determining the reserve capacity, thus seeking the optimal point of the objective function to determine the optimal reserve capacity of the system.

Reliability cost refers to the cost increase by the power supply department for improved power supply reliability, which primarily includes the investment cost, and the operating cost. Reliability benefit refers to the economic and social benefit obtained due to the achieved predetermined power supply reliability level of the power network [41]. It is difficult to estimate the social and economic benefit produced under a certain power supply reliability level, so the reliability benefit can be analyzed indirectly according to the economic impact of the power supply reliability on the society, which refers to the Customer Interruption Cost (CIC) caused by unreliable power supply and reflects the power supply reliability directly from the economic point of view [141]. Thus, it can be seen that CIC is an important parameter for study of the reliability and economy of the power system, and it is indispensable for reliability

optimization during power system expansion. Also, in the actual implementation of the project, CIC can be used as an additional indicator for reliability evaluation.

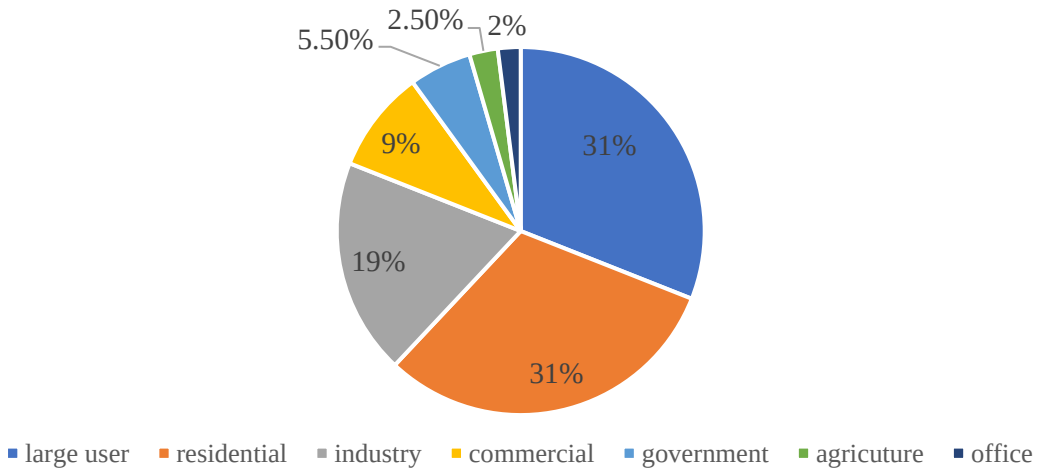

Figure 3.10: Seven categories used in the customer damage function [115]

The approach to evaluating CIC is called the Customer Damage Function (CDF). Different types of customers have different power shortage characteristics, so the customers are divided into the following seven types according to Standard Industrial Classification (SIC): large user, residential, industry, commercial, government, agriculture, and office [115]. Their respective proportions are shown in Figure 3.10. After market research and analysis of historical data, the economic losses of each customer in the event of power interruption can be obtained, as shown in Table 3-13. The expected CIC can be evaluated by Equation 3.23:

$$f_{CIC} = \sum_{i=1}^{N} C_i \times F_i \times W(D_i), \tag{3.23}$$

where N is the total number of load loss events in the sampling time, C_i is the load curtailment of load loss of event i (WM), F_i is the frequency of occurrence of event i, and $W(D_i)$ is the customer damage function (£/MW).

Table 3-13: Customer damage function for the seven categories

Customer Damage Function ($/kWh)							
Duration	Large user	Res.	Indus.	Com.	Govern.	Agri.	Office
1 min	1.005	0.001	1.625	0.381	0.044	0.06	4.778
20 min	1.508	0.093	3.868	2.969	0.369	0.343	9.878
1 h	2.225	0.482	9.0825	8.552	1.492	0.649	21.038
4 h	3.968	4.914	25.163	31.317	6.558	2.064	68.83
8 h	8.24	15.69	55.808	83.008	26.04	4.12	119.16

Typically, the concepts of marginal cost and benefit in economics can be used to explain the relationship between reliability cost and benefit. The marginal cost of reliability refers to the investment cost increase for improved system reliability level. The marginal benefit of reliability refers to the benefit obtained, or the power interruption cost reduced by improving the system reliability level, which is also called the marginal shortage cost. Figure 3.11 shows the changing trends of the marginal cost of reliability, the marginal benefit of reliability, and the total marginal cost with the change of reliability.

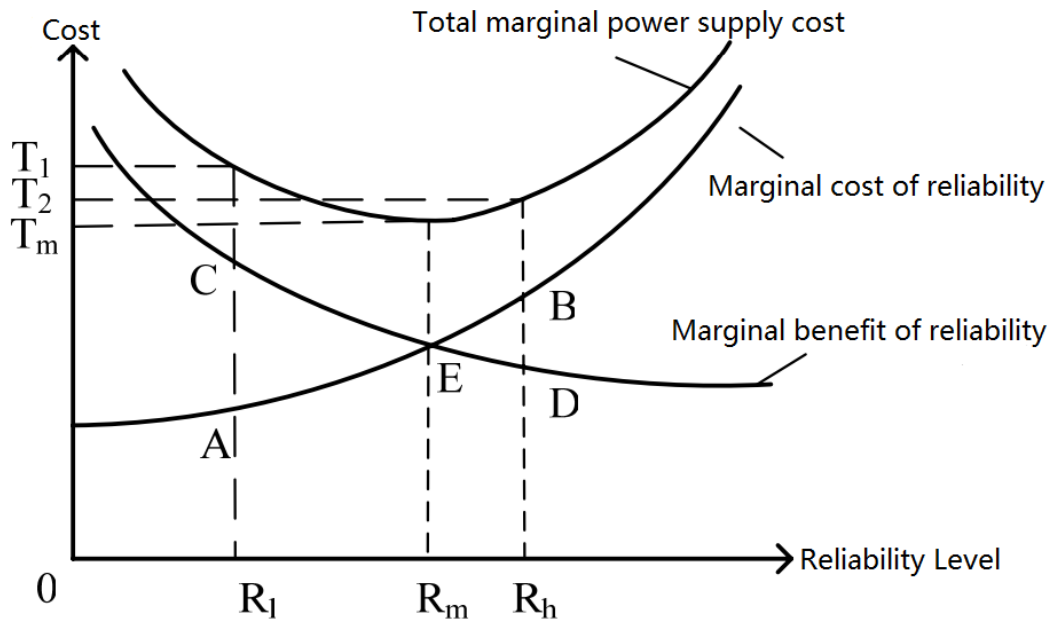

Figure 3.11: relationship between reliability cost and reliability benefit [142]

According to the relation curves in Figure 3.11, when the curve of the marginal cost of reliability intersects the curve of the marginal benefit of reliability, as shown by point E in the figure, the total marginal power supply cost is at its minimum, which corresponds to the optimal reliability of the network.

3.6 Effect of wind power generation on OR calculation method

The conventional determination method is simple and easy to use, but it still has some disadvantages. It does not take the actual situation that different structure of power supply results in different level of reliability into consideration, it does not take the relationship between OR cost and the loss caused by shortage into account, and it does

not consider the features, structure, and demand of system load. As for the wind power system, as mentioned above, because equivalent load (the result of original power load minus wind power) is more fluctuant than original power load, if OR capacity is still ascertained by traditional deterministic methods without considering the influence of the uncertainty of wind power on the system, the operating reserve capacity may be inadequate or excessive, which is harmful to the safe and economical operation of the system. Moreover, it is increasingly difficult for deterministic methods to meet the demand of fine system operation [37].

Although the influence on the reserve demand caused by uncertainties in the system is taken into account in the reliability-based probabilistic method, namely, by the influence on the system reliability, the cost minimization is used as the objective function in the method and the economy of the whole power system is not considered. With the introduction of large-scale wind power to the system, there is an increasing requirement for the OR capacity. Meanwhile, due to the volatility of wind power, it is not possible to simply use a two-state model to simulate the output of wind. Therefore, the traditional method of assessing reliability cannot assess the reliability level of a power system with wind power integration.

There is no need to set in advance the system reliability level that must be met in RCBA method; however, through seeking the equilibrium point between the reserve cost and benefit, the reserve capacity and the system reliability level under such reserve

capacity are determined, and the reliability required by the system is essentially turned into the economic index. The reliability level is not taken into consideration in this method. However, an important target of the electrical power system is to ensure that the total available gross generation can meet the load demand, so the impact of wind power integration on power system reliability cannot be ignored. Many countries have their own reliability standards, as shown in Table 3-14 below [143], but the electrical power system under the optimal economy may not meet the reliability demand.

Table 3-14: Reliability standards for various countries [143]

Country	LOLE (days/year)	LOLE (hours/year)
Australia		5~7
Belgium		16
Brazil	2.5	
Canada	0.1	
France		3
Japan	0.3	
Republic of Ireland		8
Spain	0.1	
China	1~2	
UK		3

Reliability and economy are two essential requirements that need to be met in the operation of an electrical power system, and two influences should be taken into consideration to determine the system OR capacity. After the introduction of wind

power to the system, an appropriate solution meeting the reliability demand is determined using the probability-based reliability assessment method, then the solution with the highest social benefit is selected as the optimal reserve capacity through the economic study; in this way, the reliability and economy of the operation of the system can be met at the same time.

3.7 Summary

A literature review of power system reliability and three main OR calculation methods: conventional determination, probability method based on reliability, and cost–benefit analysis, was presented in this chapter.

This chapter first explained the basic concepts of power system reliability assessment. Several indicators commonly used in adequacy analysis were then explained under the interpretation of their formulae and definitions. Subsequently, the important elements for building the reliability model of the generation system were discussed.

There are two conventional OR determination methods: the percentage reserve margin method and the rule of thumb method. The shortcomings of these two methods were analyzed in detail.

The OR capacity also can be evaluated by the reliability-based probability method, which evaluates the optimal OR capacity according to the reliability index corresponding to different reserve capacities. Therefore, the methods of reliability assessment, analytical method and simulation method, were also introduced in this section. The analytical method evaluates the reliability indices of the power system by establishing a COPT. A detailed example of constructing the COPT was explained in this section. Another way to assess the reliability level of a power system is the Monte Carlo simulation method. The state duration sampling approach for the NMCS method and the SMCS method were explained and compared.

The latter section explained how to use the cost benefit method to calculate OR capacity. Then, the approach for assessment of the benefit of OR to the power system, which is most difficult part of this method, was also explained.

Finally, the impact of wind power integration on three OR capacity calculation methods was briefly described. Unlike the case of the conventional generator, the output of wind power is fluctuating and uncontrollable, so the methods useful for the former case are not applicable to a power system with wind power, and OR capacity needs to be calculated from both reliability and economy, and the next section will describe how to evaluate the reliability of power systems with wind power.

Chapter 4. Reliability Evaluation of a Power System with Wind Power

4.1 Introduction

Chapter 3 introduced the power system reliability and the effect of OR capacity on system reliability, also analyzed the impact of wind integration on the method of determining OR capacity. This chapter describes the method of simulating wind power output and explains why it is necessary to increase OR capacity by analyzing the impact of wind power on power system reliability. Due to the intermittent and random nature of wind power generation, and since it is still difficult to achieve the desired accuracy at the current level of prediction of this natural resource, it is basically difficult to schedule wind power generation. The increased integration of wind power capacity into a power system will have a major impact on the reliable operation of that power system. In order to evaluate its impact on power system reliability, it is necessary to study the characteristics of wind energy and to establish a reliability model for wind power generation using wind speed energy conversion formula based on specific research and applicable technical methods.

Wind speed models and wind speed power conversion formulas were briefly introduced in Chapter 2. Chapter 3 introduced the reliability model for system

components, power system reliability assessment methods and analyzed the advantages of the SMCS simulation method, by comparing to NMCS.

When a wind power output model is established, firstly, it is important for wind speed randomness, volatility, and intermittency to be included in the model. Secondly, the relationship between wind speed and wind turbine power output should be determined—that is, a wind turbine power output function should be determined, with wind speed as the horizontal coordinate. Thirdly, for precise calculation, the forced outage rate of the wind turbine should also be considered, so that a wind turbine outage model can be established. These three aspects are described in detail in this chapter.

In this chapter, application of the SMCS method to the reliability assessment of power systems with wind power is presented. Details of artificially generating wind speeds, using the Weibull distribution, are discussed in Section 4.2, while a wind turbine output model is described in Section 4.3. In Section 4.4, a wind turbine reliability model is discussed, and in Section 4.5, the results and discussion of the reliability assessment of integrating wind power into an IEEE-30 BUS system are presented.

4.2 Wind speed model

The power available from a wind turbine changes in real-time, along with wind speed. Therefore, when the reliability level of the power system with wind power is analyzed

by the SMCS method (presented in Section 3.4.2.2), the basic issue is to simulate the hourly wind speed—using actual conditions as much as possible. Given the great randomness of wind, the statistical characteristics of wind in various regions should be relied on to determine local wind regimes. In order to reflect the statistical characteristics of wind, the frequency distribution of the wind speed at the chosen site is an important and indispensable parameter in a technical study associated with farm planning, design, and grid connection.

4.2.1 Weibull Distribution

As mentioned in Section 2.5.2, there are numerous statistical models of wind speed. As shown in a large number of research studies and field assessments, wind speed change during a year is unimodal, in most regions, and a Weibull distribution can correctly fit the curve of the actual probability density distribution [144]–[146]. The individual probability distribution function conforming to Weibull distribution is expressed in Equation 4.1:

$$f(v) = \frac{k}{c^k} v^{k-1} \times e^{-(\frac{v}{c})^k} \tag{4.1}$$

In Equation (4.1), v is the probability of a wind velocity, c is the scale parameter, and k is shape parameter.

The cumulative probability of wind velocity smaller than v can be obtained from the cumulative Weibull distribution function, according to Equation 4.2.

$$\mathrm{F(v)} = 1 - e^{-(\frac{v}{c})^k} \tag{4.2}$$

When wind speed is simulated by the Weibull distribution, c reflects the value of windspeed where the cumulative probability function has a value of 0.632 and k mainly represents the distribution of the wind speed..

4.2.2 The parameters of Weibull distribution

The two-parameter Weibull distribution curve is a probability model with a simple form and exhibits a fine and sufficient match with actual wind speed distributions. Provided that the Weibull distribution parameters k and c are given, the wind speed distribution form is thereby given. On that basis, effective information, such as the average wind speed, may be simply obtained without having to summarize all the wind speed observational data—this aspect is of important and practical convenience [147]. Based on this advantage, the Weibull distribution probability model enjoys an extensive application in wind energy analyses and wind farm design. The two-parameter Weibull distribution will be used in this thesis, to represent wind speed probability distribution.

The probability densities of wind speeds, when the scale parameter, c, is valued at 6, 8, and 10 respectively, while the shape parameter, k, is valued at 2.3, are compared in Figure 4.1. It can be seen in the figure that the wind speed distribution probability at relatively high speeds (such as > 10 m/s), when c = 10, is far higher than for the other two scenarios, whereas the wind speed distribution probability at relatively low speeds (such as < 5 m/s) is lower than the value, when c = 6. This comparison suggests that larger scale parameter, c, brings about a greater probability for the wind farm to gain relatively fast wind speed.

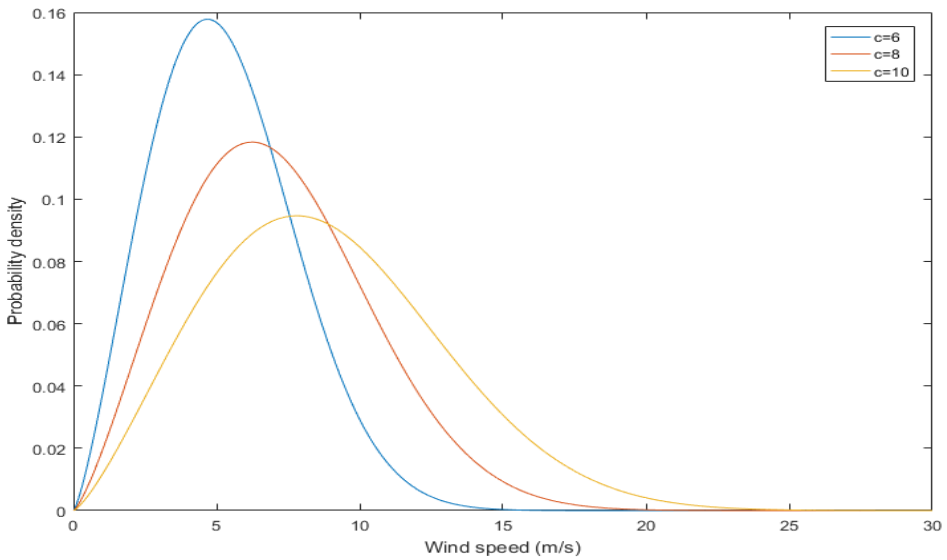

Figure 4.1: Wind speed probability under different values of c, and with k constant at 2.3

In Figure 4.2, cumulative wind speed distributions when the scale parameter, c, is valued at 6, 8, and 10, respectively, and the shape parameter, k, is valued at 2.30, have been compared. It can be seen from the figure that, as c grows, the cumulative

distribution function curve rise tends to be moderate, indicating that a comparatively large c brings about relatively sparse wind speed distribution.

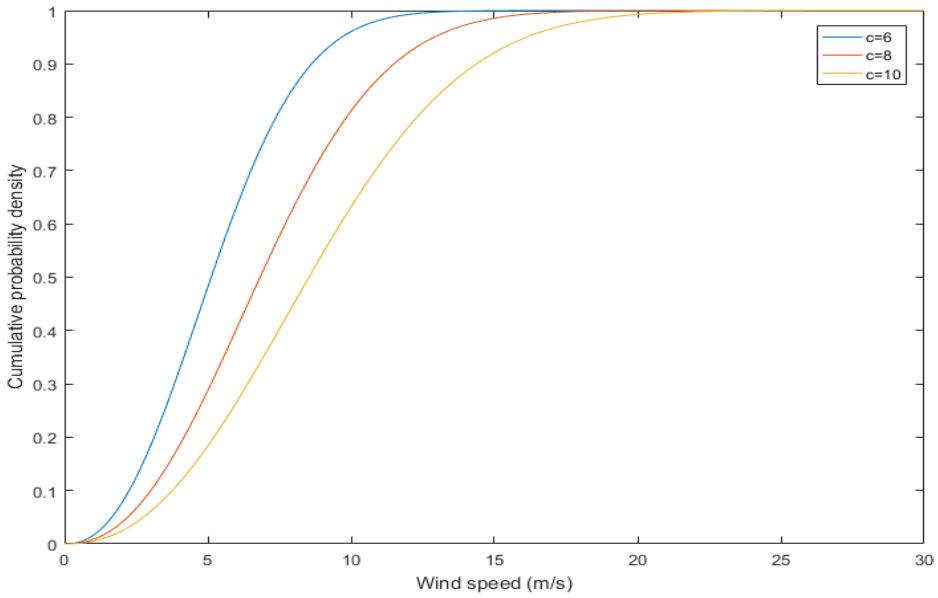

Figure 4.2: Cumulative wind speed probability under different values of c, and with k constant at 2.3

In Figure 4.3, wind speeds probability densities when the shape parameter, k, is valued at 1.8, 2.3, and 2.8, respectively, while the scale parameter, c, is valued at 6, are compared. It can be seen in the figure that, when k is valued at 2.8, the wind speeds are more concentrated than they are in the other two scenarios, indicating that greater k leads to the more concentrated distribution of wind speed, whereas smaller k leads to the sparse distribution of wind speed.

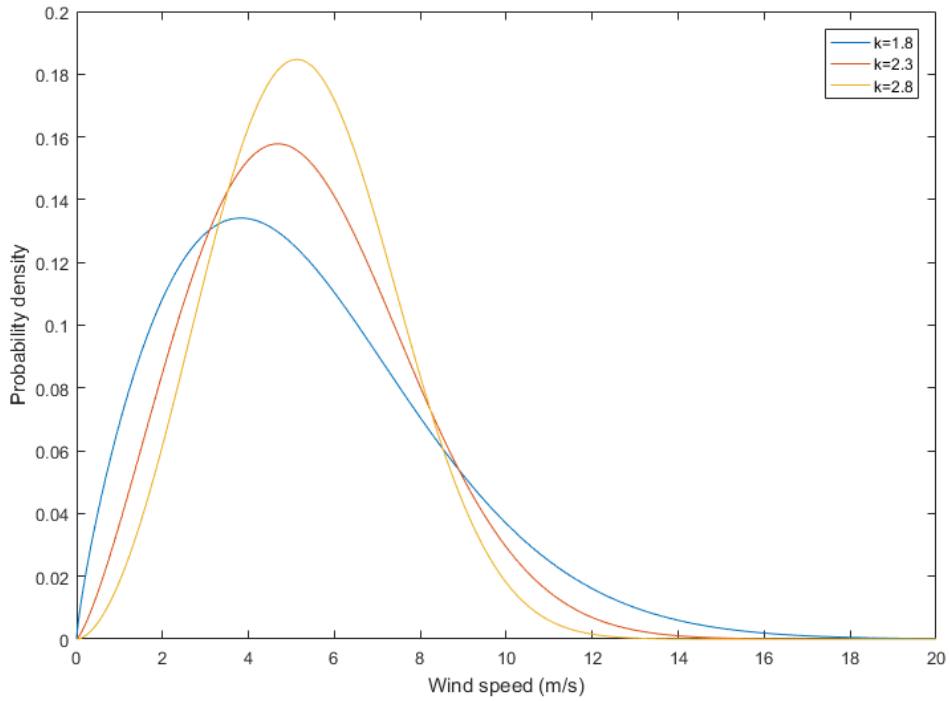

Figure 4.3: Wind speed probability under different values of k, with c constant at 6

Simulated calculation via random sampling is available for the hourly wind speed of a wind farm, provided that the Weibull distribution parameters c and k for that wind farm are obtained by means of statistical calculation, using historical observation data. Inverse transformation is used [148], and so Equation 4.3 is firstly solved with an inverse function, as follows:

$$v = c[-\ln(1 - F(v))]^{1/k} = c[-\ln(1 - \gamma)]^{1/k} \qquad (4.3)$$

where γ is a uniformly distributed random number, in the range of zero to one.

4.2.3 Example: Wind speed in West Inner Mongolia

The wind speed data is arranged in time series, where each data represents the instantaneous wind speed at that time point or the average wind speed at a fixed time interval [149]. The data used in this example is measured by the Chahar Right Middle Banner wind speed station in the central part of Inner Mongolia Autonomous Region at a height of 10 meters, with hourly wind speed data measured between 2015 and 2018 being recorded 35040 times [150]. The wind speed data can be sorted into a frequency distribution so that the frequencies at which the wind speeds appear in various ranges can be obtained. Table 4-1 summarizes the frequency of wind speeds in the various wind speed ranges in the Chaqihal right-wing Zhongqi area. The table divides the wind speed into 21 intervals based on the maximum and minimum wind speeds. The frequency (number) indicates the number of times the wind speed appears in this interval, and the frequency (%) indicates the ratio of the wind speed in this interval to the total number of records. It can be clearly seen from the table that strong winds are rare and wind speeds are mainly distributed between 2 m/s and 10 m/s.

Table 4-1 : Wind speed data at Chahar Right Middle Banner from 2015 to 2018 [150]

State No.	Wind speed (m/s)	Frequency (number)	Frequency (%)
1	From 0 to 1	163	0.47
2	From 2 to 3	2541	7.25
3	From 3 to 4	4855	13.89
4	From 4 to 5	4549	12.98
5	From 5 to 6	4764	13.59
6	From 6 to 7	3952	11.28
7	From 7 to 8	3623	10.34
8	From 8 to 9	2397	6.84
9	From 9 to 10	2386	6.80
10	From 10 to 11	1614	4.61
11	From 11 to 12	1392	3.97
12	From 12 to 13	960	2.74
13	From 13 to 14	660	1.88
14	From 14 to 15	489	1.40
15	From 15 to 16	247	0.70
16	From 16 to 17	208	0.59
17	From 17 to 18	96	0.27
18	From 18 to 19	69	0.19
19	From 19 to 20	31	0.09
20	From 20 to 21	16	0.05
21	From 21 to 22	8	0.02
22	From 22 to 23	8	0.02

The wind speed distribution curve can be obtained by taking the wind speed interval as the horizontal axis and the corresponding probability as the vertical axis. The parameters of Weibull fitting wind speed in this region are c=6.2648 and k=1.7050 [150]. The wind speed distribution of real data and artificial data is shown in Figure 4.4. It can be seen from this figure that although there are some deviations between the simulated data and the real data in a few individual wind speed intervals, the Weibull distribution can simulate the probability distribution of wind speed well.

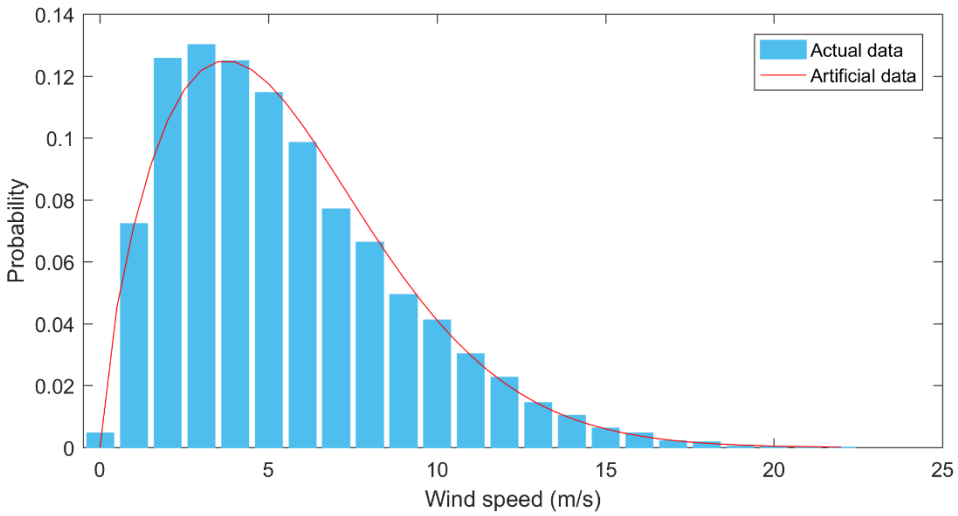

Figure 4.4: Wind speed distribution of Chahar Right Middle Banner from 2015 to 2018 [150]

4.3 Wind turbine output model

Three wind turbine output models have been described in detail in Section 2.5.2. Due to the lack of specific wind farm data, the quadratic function was introduced, to simulate wind turbine output. The available wind turbine output, at time t, can be expressed by Equation 4.4:

$$AP_{wi}[t] = \begin{cases} 0, v_{wind}[t] \le v_{ci} \text{ or } v_{wind}[t] > v_{co} \\ \left(A - B \times v_{wind}[t] + C \times v_{wind}^2[t]\right) \times P_{w\_rate}, v_{ci} < v_{wind}[t] \le v_r \\ P_{rate},\ v_r < v_{wind}[t] \le v_{co} \end{cases} \quad (4.4)$$

where v_{ci}, v_r, and v_{co} are the designed wind turbine cut-in speed, rate speed, and cut-out speed (m/s), respectively; $v_{wind}[t]$ is the wind speed at time t (m/s); P_{w_rate} is the rated power output of the wind turbine (MW), and $AP_{wi}[t]$ is the available output of the i^{th} wind turbine generator (WTG) at time t. A, B, and C can be calculated using v_{ci}, v_r, and v_{co}.

$$\begin{cases} A = \frac{1}{(v_{ci}-v_r)^2}\left[v_{ci}(v_{ci}+v_r) - 4v_{ci}v_{cr}\left(\frac{v_{ci}+v_r}{2v_r}\right)^3\right] \\ B = \frac{1}{(v_{ci}-v_r)^2}\left[-(3v_{ci}+v_r) + 4(v_{ci}+v_r)\left(\frac{v_{ci}+v_r}{2v_r}\right)^3\right] \\ C = \frac{1}{(v_{ci}-v_r)^2}\left[2 - 4\left(\frac{v_{ci}+v_r}{2v_r}\right)^3\right] \end{cases} \quad (4.5)$$

4.4 Wind turbine reliability model

In the reliability evaluation of wind power, the states of WTGs are the same as those of CGUs, and are determined by sampling, which, as described in Section 3.2.3. The SMCS method is utilized in this thesis, and state duration sampling is used to simulate the wind turbine outage model. The WTG is also simulated using a two-state outage model.

The available generation output of the WTG during the up state is determined by wind speed—and is 0 MW in the down state. The Mean Time to Failure (MTTF) and Mean Time to Repair (MTTR) of WTG are exponentially distributed, and the failure rate, λ,

and repair rate, μ, are constant. Sampling of WTG continuous operation, t_1, and repair times, t_2, were described using the following:

$$t_1 = -\frac{\ln \gamma_1}{\lambda} = -MTTF \ln \gamma_1 \tag{4.5}$$

$$t_2 = -\frac{\ln \gamma_2}{\mu} = -MTTR \ln \gamma_2 \tag{4.6}$$

where γ_1 and γ_2 are uniformly distributed random numbers, either [0,1].

In general, WTGs in a particular wind farm are the same type, and their locations in the same wind farm are very close—so the wind conditions for each wind turbine in the same wind farm will be similar, meaning that their output power can also be expected to be approximately the same. The available output power, AP_w, of a wind farm composed of *m* wind turbines, can be calculated as shown in Equation 4.7, where a_i is the running status of the i^{th} WTG at time t.

$$AP_w[t] = \sum_{i=1}^{m} a_i AP_{wi}[t] \tag{4.7}$$

$$a_i = \begin{cases} 0 & WTG\ in\ down\ state \\ 1 & WTG\ in\ up\ state \end{cases}$$

SMCS has been adopted in this thesis to build the wind farm power generation model. The biggest difference between wind turbines and conventional power generators lies in the fact that the former's available output power is not necessarily rated and could

even be zero, even in an up state. The available output power of wind turbines in the up state depends largely on wind speed, so simulations of available wind farm output power should consider the situation in three stages. Firstly, obtain simulated wind speeds for different periods; secondly, convert these simulated wind speeds into the wind turbine outputs, using the wind speed power conversion formula; finally, sample the continued state durations of the wind farm and system components, during different time periods. Using this information as the basis, the available output power of the wind farm and the system can eventually be determined.

The specific steps would be as follows:

1) Input the system units' parameters, including the installed capacity and the reliability factors for of all conventional generators and wind turbines in the system, as well as the wind speed distribution parameters for the wind farm in the system (or historical data on wind speed). In the meantime, the duration time (NY) in years for the simulation should be determined.

2) Begin the wind speed simulation from Year 1, and obtain wind speed values for each time period, for one year.

3) Begin the SMCS simulation for both the conventional units and the wind turbines, to obtain the status and continuous time series' for the units.

4) Combine the status of each conventional unit and the continuous time series with their corresponding rated capacities, to obtain a comprehensive time series for available output power from the conventional units.

5) Based on the wind speed obtained in step 2, determine the time series of the available output power from each wind turbine, then combine with the state time series of the wind turbine, to obtain the time series of the available output power from the wind farm.

6) Combine the available output power time series for the wind farm with that for the conventional units to obtain the available output power time series for the generating system.

7) Integrate the power load series to determine the system status, take down the reliability indexes of the system in this simulation run.

8) If year > NY, record the reliability indexes and end the simulation; otherwise, proceed to year + 1, and go back to step 2 for the next round of calculations.

4.5 Illustrated example

4.5.1 Description of an IEEE-30 bus system

The IEEE 30-bus system represented a portion of the American Electric Power System, as of December 1961 [151]; as shown in Figure 4.5, which is a one-line diagram of the IEEE-30 bus system, it has six generator buses and 21 load buses. The total installed generating capacity was 360 MW and the peak load demand was 270 MW. IEEE 30 bus system has fewer nodes and simple lines, and is easy to analyze the impact of wind penetration levels on system reliability. The generating unit capacities and reliability data of IEEE 30 Bus Test System have been listed in Table 4.2.

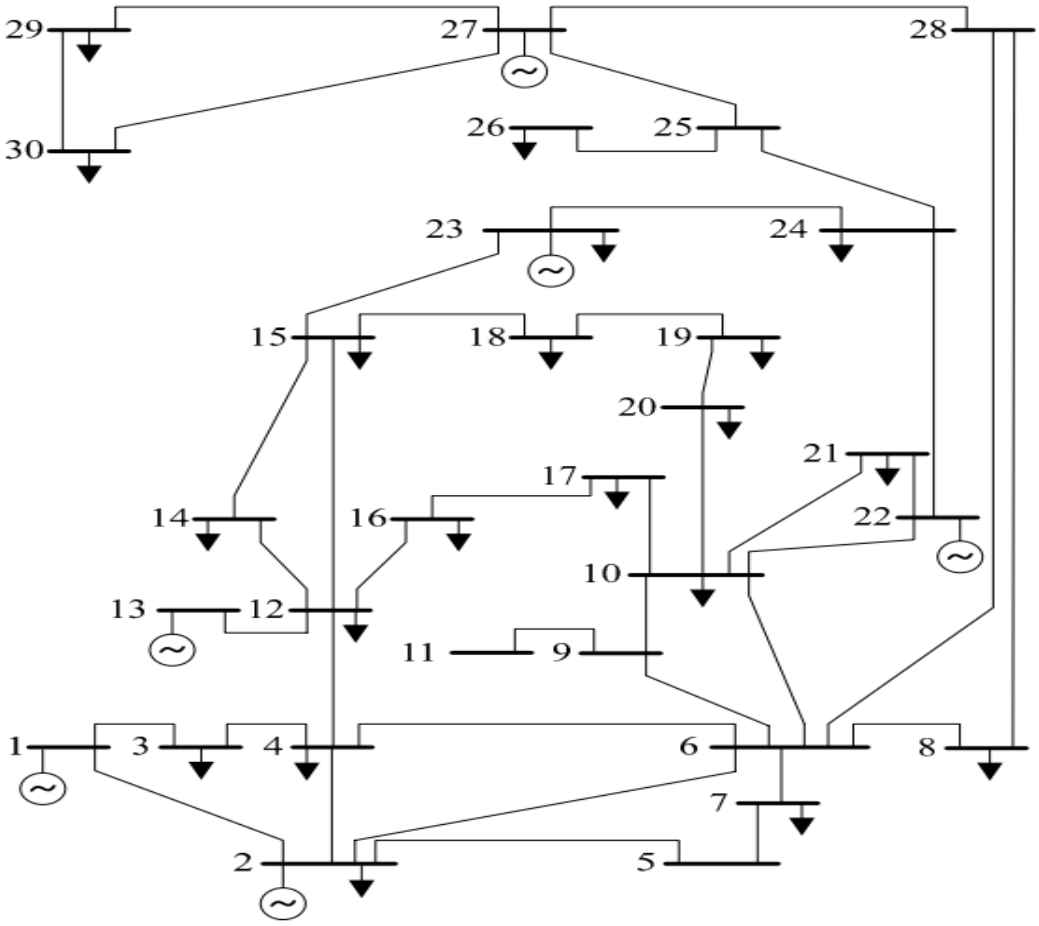

Figure 4.5: One-line diagram of the IEEE 30-bus system

Table 4-2: Generating unit reliability data

Gen no.	Unit size (MW)	FOR	MTTF (hours)	MTTR (hours)	Annual failure rate
1	100	0.03	1460	45	6
2	80	0.02	2920	60	3
3	50	0.025	1752	45	5
4	60	0.015	3650	55	2.4
5	30	0.02	2190	45	4
6	40	0.01	4380	45	2
Wind turbine	3	0.05	2850	65	3

4.5.2 Modelling wind power output

After wind power integration, its stochastic fluctuations will affect power supply reliability. Therefore, in actual operations, the relationship between wind power penetration level and system reliability needs to be evaluated. In this thesis, wind power penetration level δ_{wind} is described as the ratio of the installed capacity of wind power C_{wind} to the total installed capacity of generation system C_{total}, and is usually used to study the maximum installed capacity of wind power stations in large power grids, as shown in Equation 4.8. In this case, when wind power with a certain capacity is integrated into the grid, the same conventional generation unit capacity in the system will be simultaneously reduced.

$$\delta_{wind} = \frac{C_{wind}}{C_{total}} \tag{4.8}$$

To analyze the impacts of wind power integration on system reliability, the wind power penetration level in this simulation will be gradually increased, from 0% to 20%. System parameter details are listed in Table 4.3.

Table 4-3: System data for different wind penetration levels

Scenario	1	2	3	4	5
Wind penetration	0%	5%	10%	15%	20%
Number of wind turbines	0	6	12	18	24
Wind generation capacity (MW)	0	18	36	54	72
Total generation Capacity (MW)	360	360	360	360	360
Peak load (MW)	270	270	270	270	270

In this simulation, the time interval was set to one hour, duration of one sample was one year (8760 hours) and the number of sample was set to 5000. It was assumed that in the wind farm, the probability distribution of the wind speeds approximated a Weibull distribution, wherein parameter c = 7 and parameter k = 2, in which case the wind farm wind speeds could be artificially generated using Equation 4.3.

A sample simulated wind speed curve, extending over 300 hours, is shown in Figure 4.6. Here it can be seen that the wind speeds constantly varied, while remaining within the range of 4–10 m/s, with minor probabilities of either weak or strong winds. Hence, the Weibull distribution's exceptional performance in simulating wind speed lies in its capacity to approximate the actual wind speed probability status for real wind farms, by modifying scale and shape parameters.

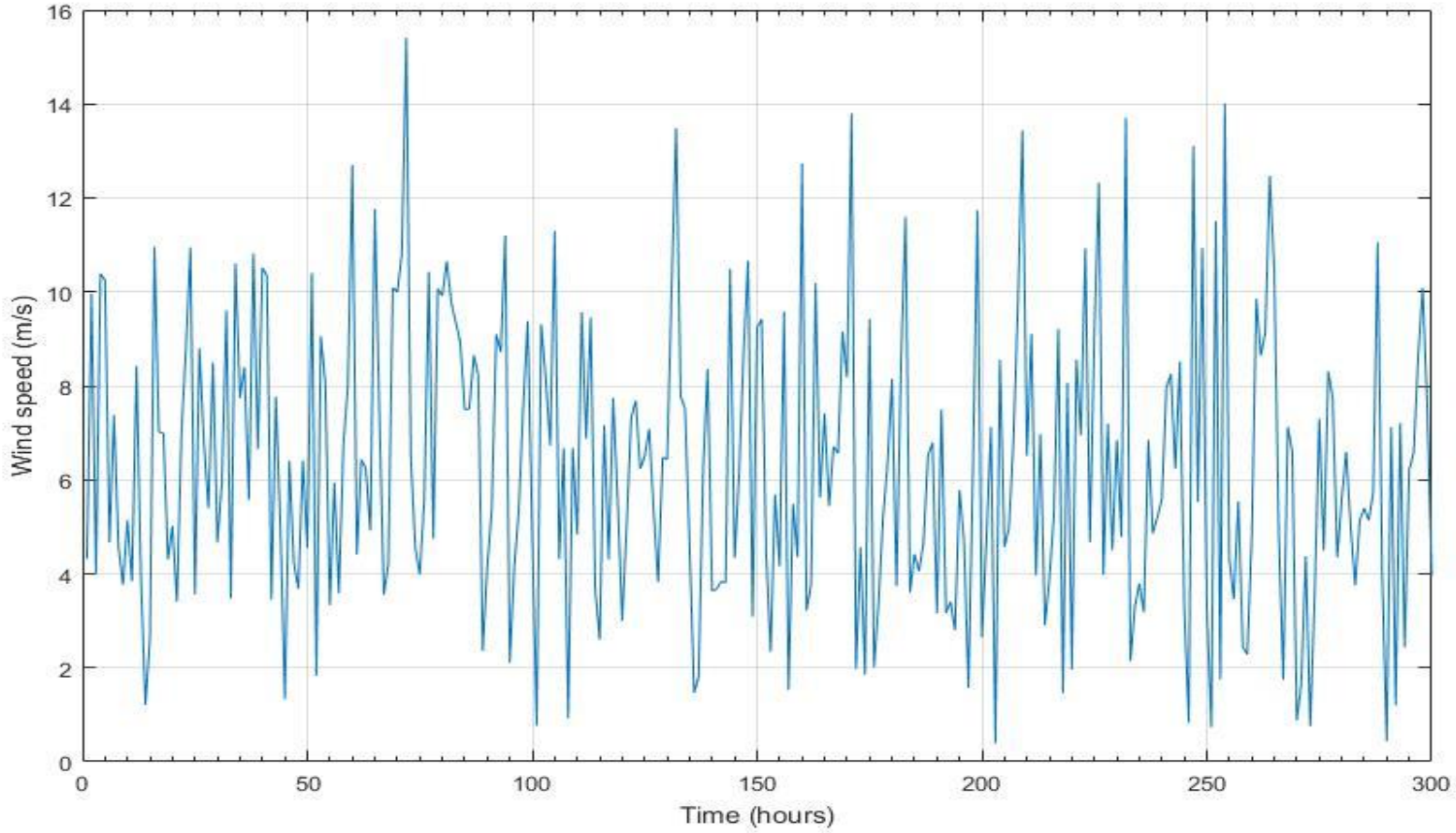

Figure 4.6: 300 hours snap shot of artificially generated wind speeds

The wind turbine data are shown in Table 4-4, and the available wind power output can be obtained by using the wind speed power conversion equation (4.4). Figure 4.7 shows the available output from a single wind turbine, based on the wind speeds shown in Figure 4.6, and as can be seen, although there were no windless periods during the 300 hours simulation, the available wind turbine output was occasionally 0 MW, due to the wind speed is below the turbine cut-in speed and above the turbine cut-out speed. In addition, it can be seen that the available wind turbine output was not constant, changing frequently between 0–3 MW.

Table 4-4: Wind turbine parameters[100]

Rated power output	3 MW
Cut-in speed	4 m/s
Rated speed	10 m/s
Cut-out speed	25 m/s

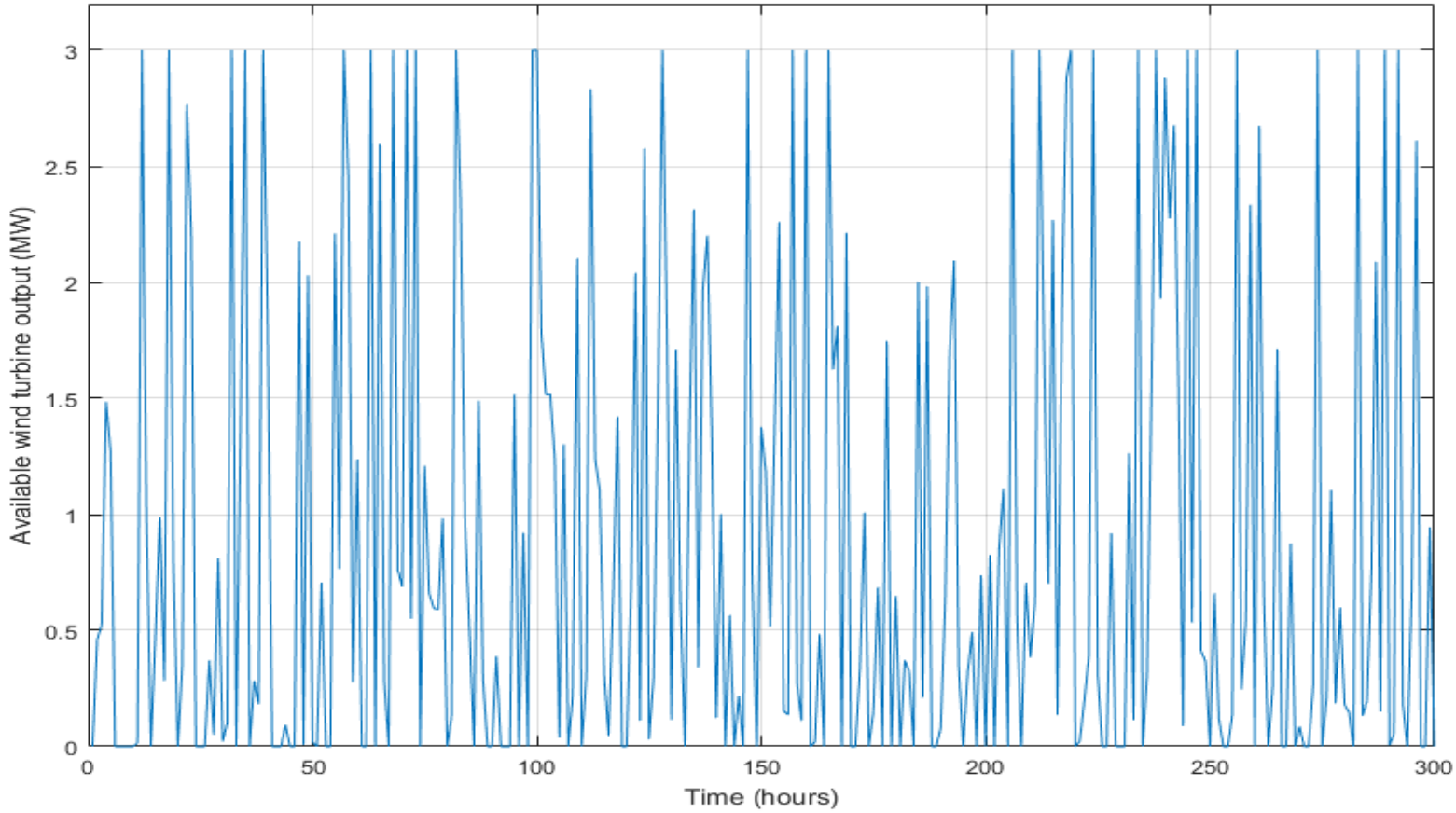

Figure 4.7: Wind turbine output over the 300 hours simulation

According to the wind turbine reliability data in Table 4-2, an average of three failures occurred annually, each lasting for an average of 65 hours. Figure 4.8 shows a sample of a simulated time series reliability state, for one wind turbine, for one year. Apparently, there were three outages in this one-year state simulation, and their durations can be found in the Matlab simulation results, as expressed in Table 4-5.

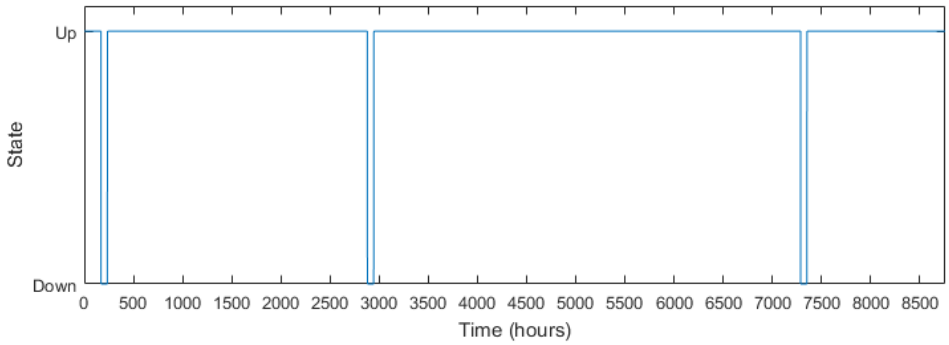

Figure 4.8: One-year sample of wind turbine reliability state

Table 4-5: Wind turbine outage times

From (hours)	To (hours)	Lasted (hours)
171	235	65
2881	2945	65
7289	7353	65

In the 5% wind penetration level scenario, there are six wind turbines in the power system. The wind power system reliability state model for this scenario, as shown in Figure 4.9, can be obtained through simulation. The Y-axis indicates how many wind turbines were in the “up” state at a specific time.

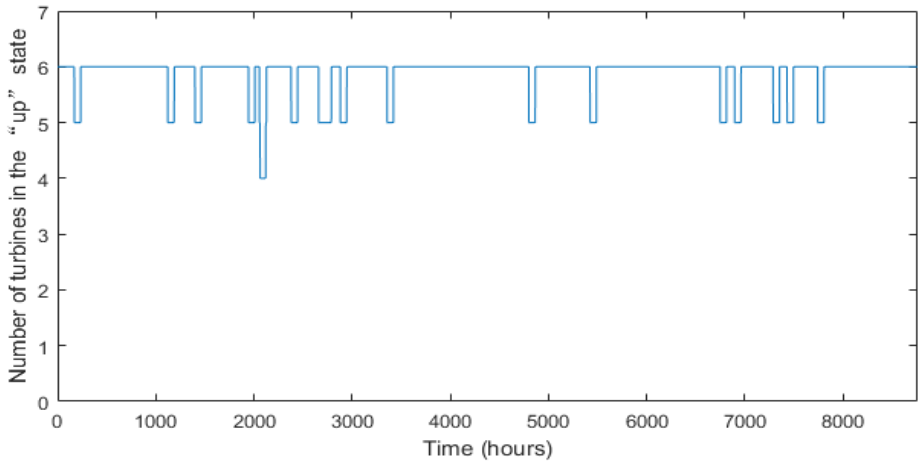

Figure 4.9: Sample of a six-turbine wind power system reliability state over one year

By combining the wind power system reliability model with the available output model, the wind power system's available output curve, for the 300 hours simulation, can be obtained—and has been plotted as Figure 4.10. Since one of the wind turbines was in the outage state from 171 hours to 235 hours, the maximum available wind power system generating output could not reach its installed 18 MW capacity at any time in the 300 hours simulation.

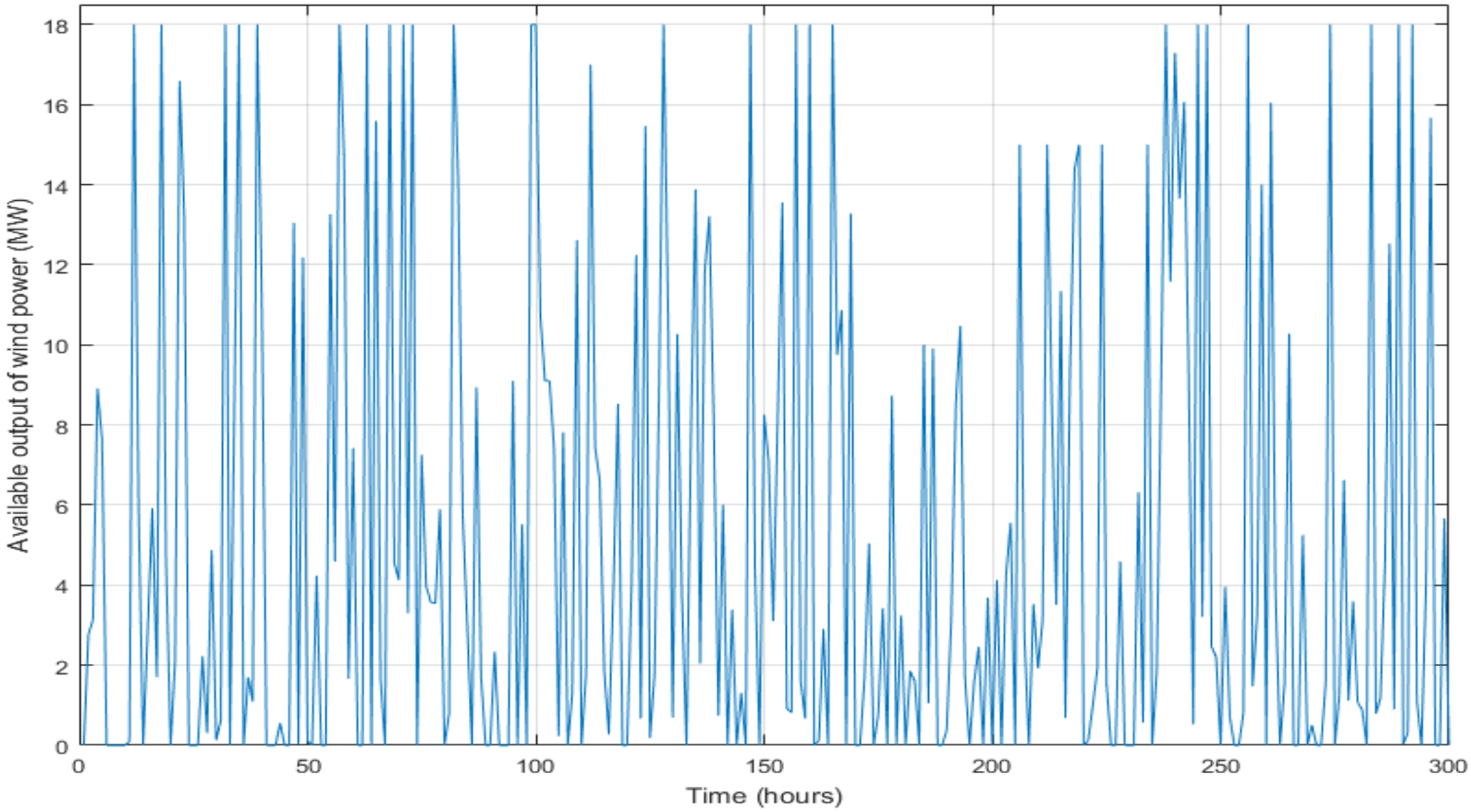

Figure 4.10: Available wind power output across the 300 hours simulation

4.5.3 Results

- Number of samples

Figure 4.11 represents a one-year sample simulation of the IEEE 30 bus test system without integrating wind power, where system available generation output and load demand are compared in a simulation; peak load demand was 270 MW, and the curve has been modified using UK load demand for 2018. When the load exceeded the available generation capacity, insufficient power supply occurred and the system reliability index could be obtained in this simulation. Inspection of Figure 4.11 indicates that in this simulation, the system's available generation output was always higher than the load, which meant there were no instances of insufficient power supply for the year. To make simulated results close to actual results, the system must be tested and repeated enough times.

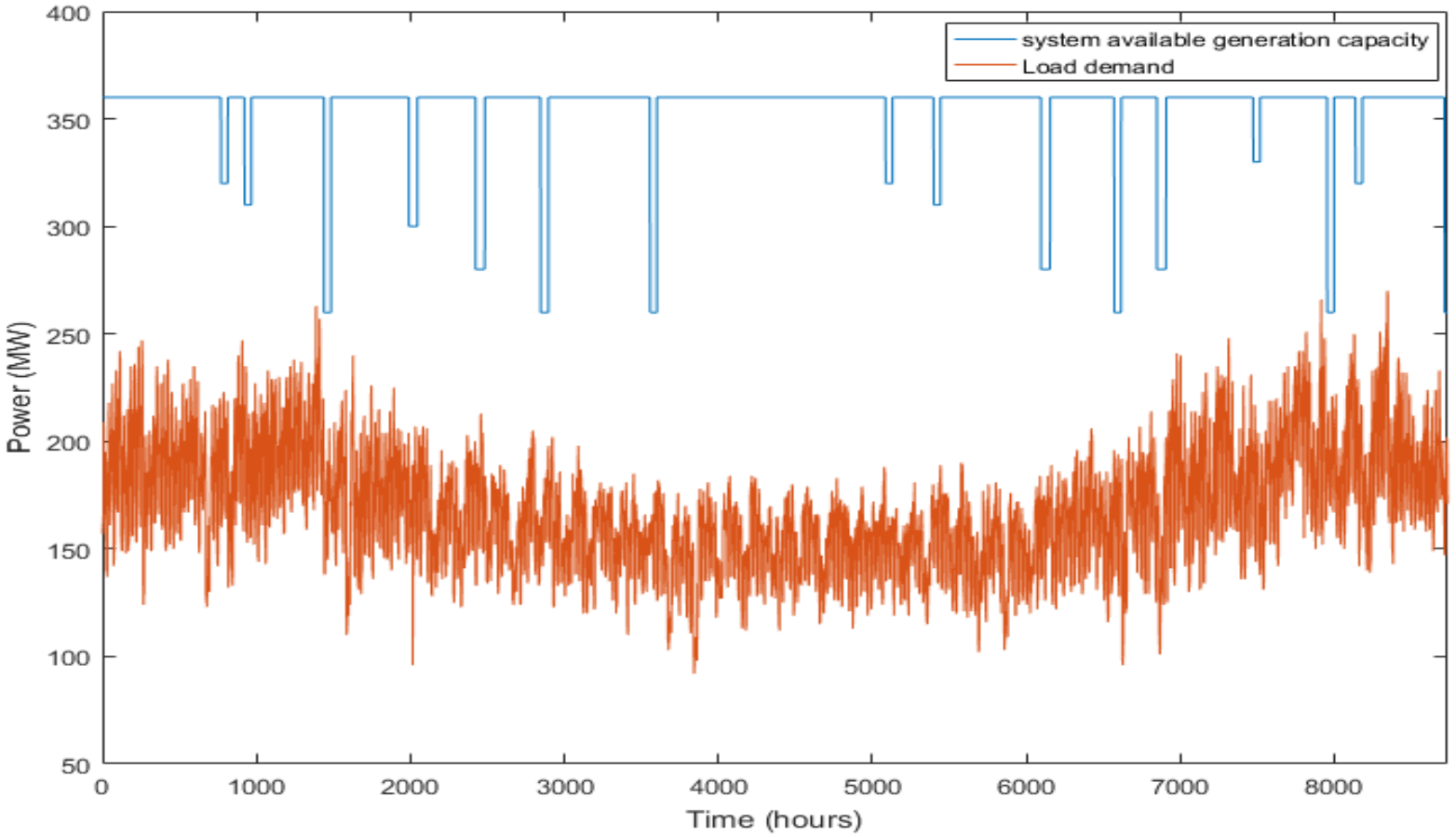

Figure 4.11: Superimposition of available system generation capacity and load demand

Since these are artificially generated, pseudo-random numbers, sufficient simulation repeats must be conducted to make the results close to actual values. In this section, the Loss of Load Expectation (LOLE) reliability index will be used to determine the sample numbers needed for a sufficiently representative simulation.

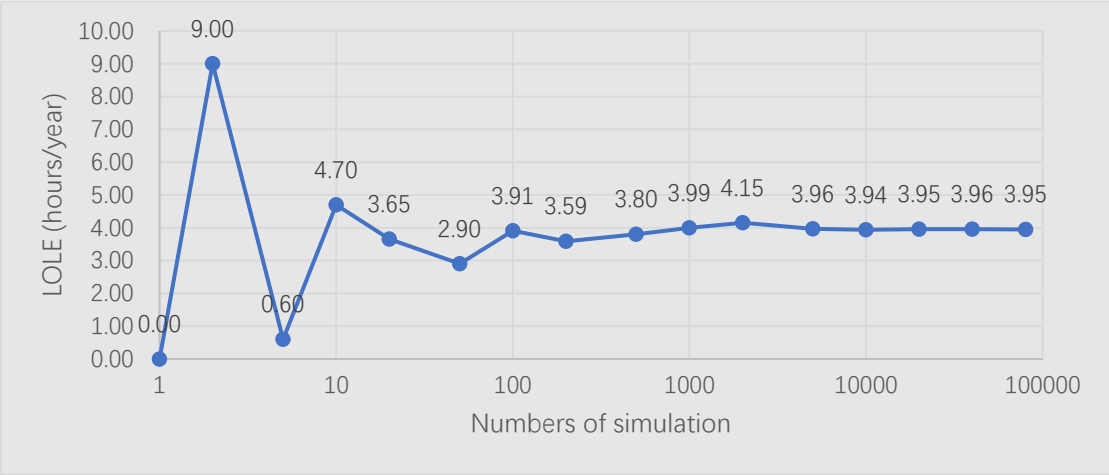

Figure 4.12: LOLE results from different numbers of simulation runs

Table 4-6: LOLE results for different numbers of simulation runs

Sample numbers	LOLE (hours/year)		Sample numbers	LOLE (hours/year)
1	0.00		500	3.80
2	9.00		1000	3.99
5	0.60		2000	4.15
10	4.70		5000	3.96
20	3.65		10000	3.94
50	2.90		20000	3.95
100	3.91		40000	3.96
200	3.59		80000	3.95

The SMCS concluding convergence characteristics for reliability can be seen in Figure 4.12. Very large sample numbers can improve accuracy while increasing simulation time, and it can be seen from Figure 4.12, and from Table 4-6, that the LOLE value became relatively stable after 5000 samples—and so the sample number has been set at 5000 for this thesis.

- No wind power

After the sample number was set to 5000, through SMCS simulation and without integrating wind power, the reliability index for the system is shown in Table 4-7.

Table 4-7: Reliability indices for the system without wind power

Reliability Indices	Value
LOLE (hours/year)	3.96
LOEE (MWh/year)	79.23
LOLF (occ./year)	0.71

From this table, in summary, the average insufficient power supply time, where load exceeded available generation output, was 3.96 hours/year, while the amount of energy which could not be supplied, due to insufficient availability, was 79.23 MWh/year. The number of times where load exceeded the available generation output averaged 0.71 times annually.

- With wind power

The changes in system reliability indicator LOLE when wind penetration level increased are shown in Figure 4.13, where it can be seen that, with increasing wind turbine capacity integrated into the system, the reliability index LOLE of the system gradually increased, meaning system reliability was lower. This was because the available wind power generation output changed with wind speed, and though the CGUs have been reduced in number and replaced with wind power with the same capacity, wind power cannot operate at its rated power most of the time, leading to decreased total available output for the system. Therefore, the insufficient power supply issue became more severe with increased installed wind power capacity.

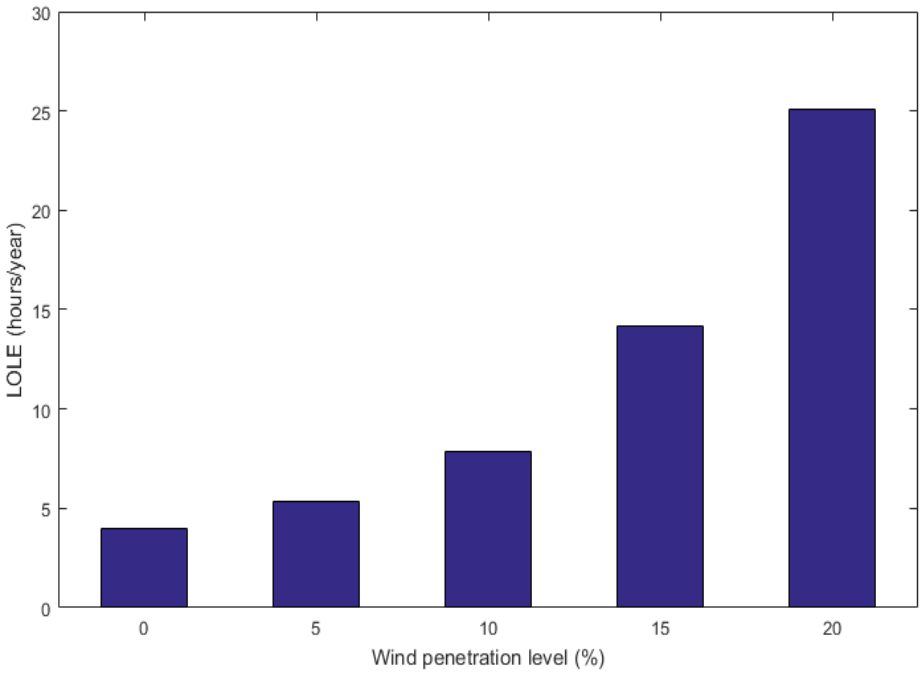

Figure 4.13: Wind penetration level against LOLE

- Impact of the number of wind farms

For this case study, it was assumed that all wind turbines were in one wind farm. In reality, this is difficult to achieve, so it is necessary to study the impact of a number of wind farms on system reliability. Three situations have been considered in this section, scenarios with one wind farm, with two wind farms, and with three wind farms. The wind farms were at different locations, but with the same Weibull distribution parameters,there were different windspeed simulations for the three windfarms calculated on common values of shape and scale.. The wind turbines are evenly distributed in these wind farms. The wind power output curves for a wind penetration level of 10% are shown for the three scenarios in Figures 4.14 and 4.15 respectively.

It can be seen from these two figures that as the number of wind farms increased, the available wind power generation capacity curve became smoother, effectively reducing wind power fluctuation. At the same time, as the number of wind farms increased, it became harder for the available wind power generation output to reach its rated capacity.

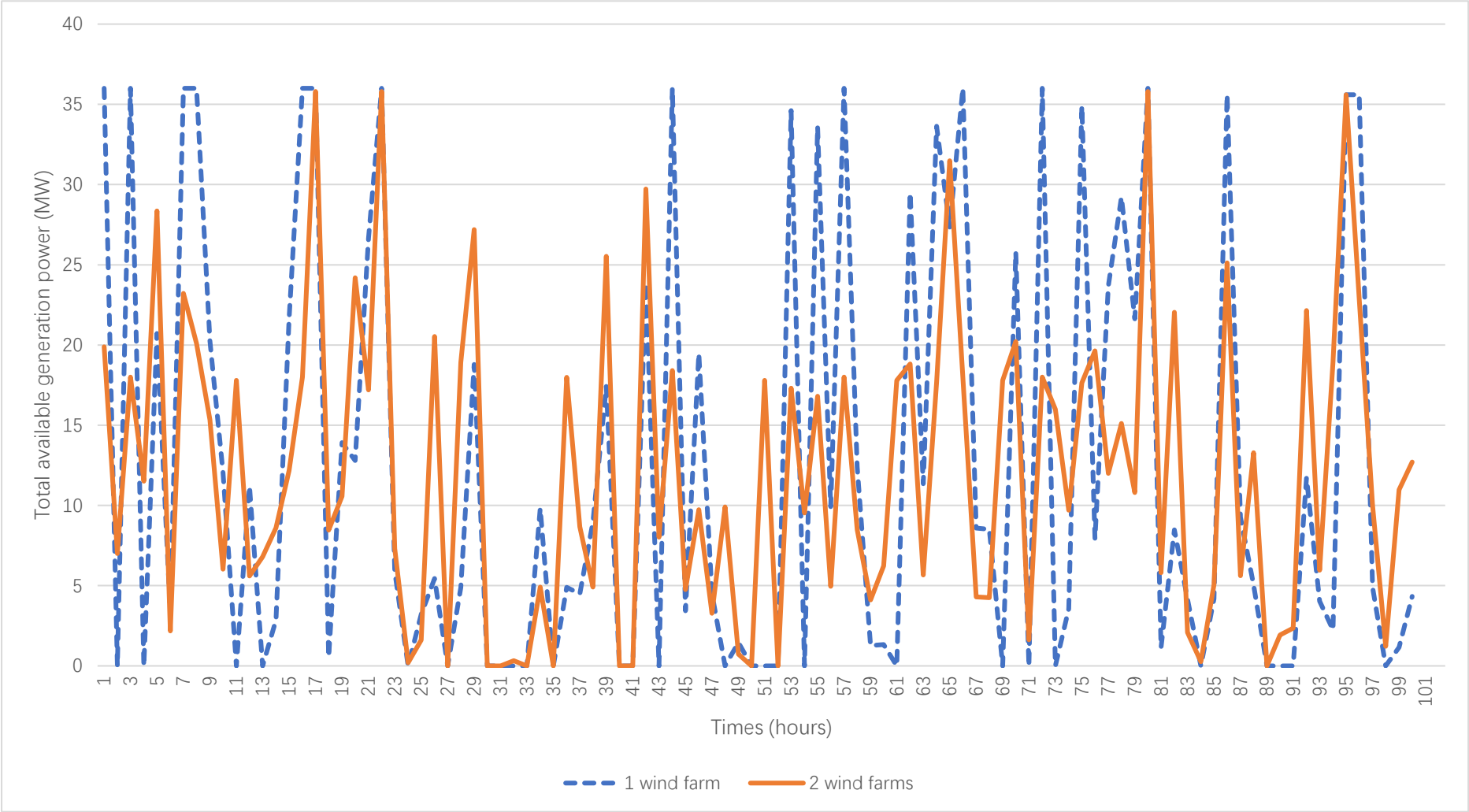

Figure 4.14: Total available power generation by 1 wind farm and 2 wind farms when wind penetration level is 5% (100 hours)

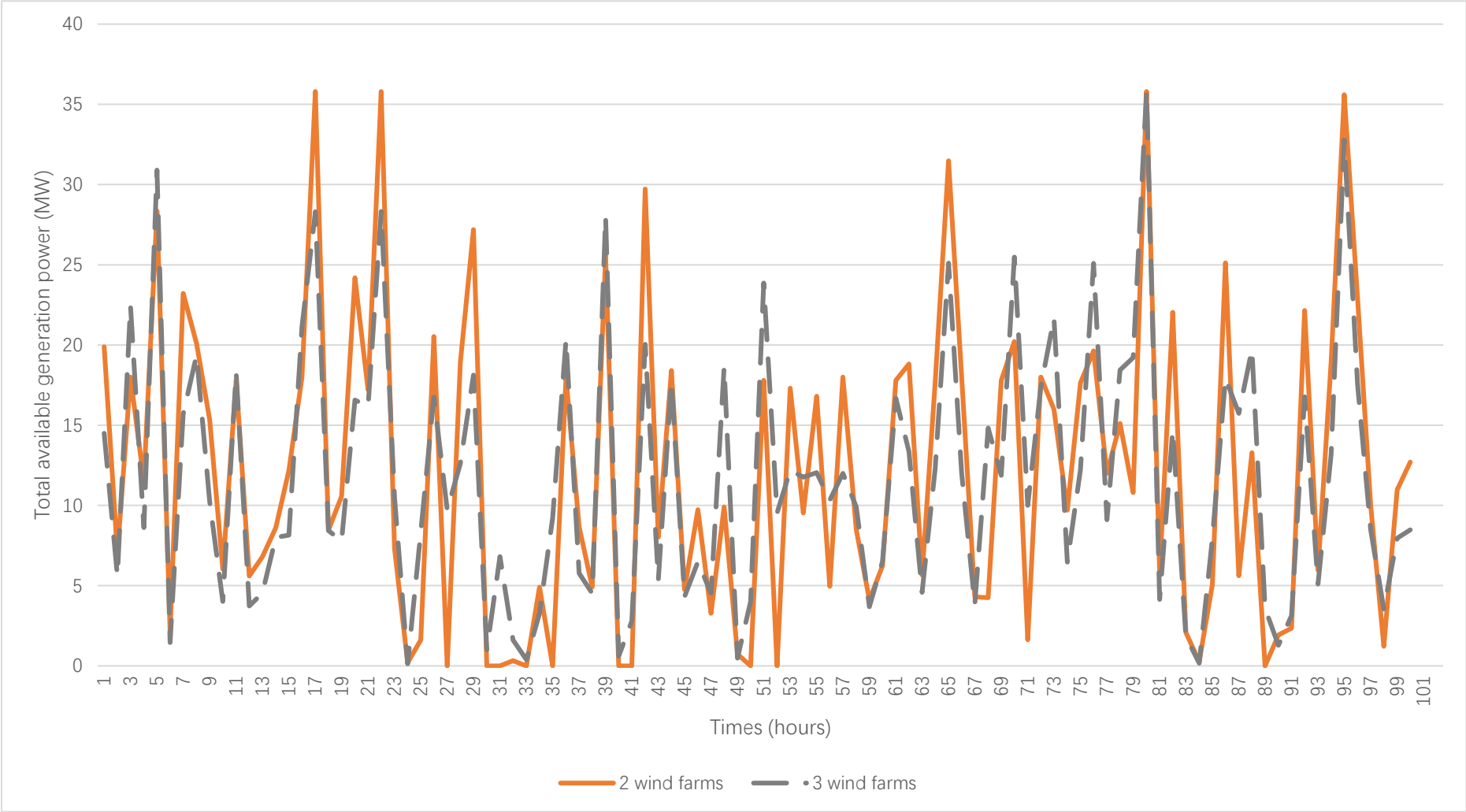

Figure 4.15: Total available power generation by 2 wind farms and 3 wind farms when wind penetration level is 5% (100 hours)

The reliability assessments for the multiple farm scenarios, with various levels of wind power penetration, are summarized in Table 4-8. It can be seen from the table that the increase in the number of wind farms was able to mitigate the impact of wind power fluctuations on the power system, and improve its reliability. However, with the integration of wind power, overall system reliability declined, mandating the addition of extra reserve generation capacity, to reduce the negative impact of wind power.

Table 4-8: Reliability indices for the system with different numbers of wind farms

Reliability index	No. of wind farms	Wind penetration level				
		0%	5%	10%	15%	20%
LOLE (hours/year)	1	3.96	5.38	7.89	14.20	25.06
	2	3.96	5.33	7.38	12.28	20.28
	3	3.96	4.74	5.85	8.62	13.17
LOEE (MWh/year)	1	79.23	105.52	150.79	248.33	448.16
	2	79.23	103.79	140.88	213.39	355.87
	3	79.23	90.79	109.60	148.89	227.49

4.6 Conclusions

This chapter has focused on methods for simulating available wind power output, including the Weibull distribution for artificially generated wind speeds, a wind turbine reliability model, and the wind speed power conversion equation. By combining the

wind farm available output model, the traditional generator model, and the load model, the reliability of the power system with wind power integration can be evaluated.

The evaluation, based on the SMCS method, was established through a sequence of tasks. Firstly, the reason for setting the simulation sample size to 5000 was discussed. Then, based on reliability parameters for conventional generators, the reliability of the power system without wind power was evaluated. Following this, based on wind power penetration rate, the reliability of the power system with wind power was simulated, and the negative impact of wind power connection into the overall system was analyzed. Finally, the influence of the number of wind farms on the system was also reviewed. It can be seen from the evaluation results that the wind power integration has a negative impact on system reliability. Therefore, it is necessary to add more OR capacity to alleviate the volatility of wind power output. The next chapter will present a new cooperation method to wind power and HPS to solve this problem.

Chapter 5
Proposed WP-HPS cooperation method and reliability assessment in IEEE 30 bus test system

5.1 Introduction

In Chapter 4, it was shown that the negative influence of wind power on power system reliability became greater as the amount of integrated wind power capacity increased. Therefore, it is necessary to increase the OR capacity of the system to improve the reliability of the system. Hydro-Pumped Storage (HPS) technology was briefly introduced in Chapter 2. With the increase in wind power capacity, interest in HPS has recently recovered. In power system, most CGUs do not have the flexibility to adjust their output to meet the requirement of the volatility of wind power. HPS is currently the only commercially proven, large-scale energy storage technology. It provides flexible, fast start-up generation, which can be used to smooth intermittent power output, and also has the ability to store excess energy until needed.

Meanwhile, the output of wind power is random and intermittent. If the output of CGUs changes in real time with wind power, the fluctuation of CGUs output will be greatly increased. In order to ensure power system reliability and safety, as well as to

underwrite the power supply quality in the power system, it is necessary to establish a dispatch limitation of wind power if wind power is to be integrated into the power supply system at significant scales.

In Chapter 3, common evaluation and simulation methods for power system OR were discussed, followed by an elaboration on the principles of the methods, as applied. Based on these considerations and advantages, in this chapter, the advantages of HPS as an OR to reduce the influence of wind power fluctuations on power system reliability, and to improve the efficient use of wind power, have been adopted. Although HPS has been widely accepted as an excellent OR supply, it still carries an overly high investment cost. The question of how to improve HPS planning and construction in order to better satisfy power demand supply issues, while simultaneously reducing construction costs, remains to be resolved. This chapter combines SMCS reliability evaluation method with reliability cost-benefit analysis to determine optimal capacity of HPS.

This chapter is organized as follows: Section 5.2 introduces the proposed WP-HPS cooperation method and two possible cooperative strategies of wind power and HPS. The mathematical model of the proposed power system will be described in detail in Section 5.3. Section 5.4 describes the mathematical model of the proposed WP-HPS cooperation method and the calculation procedures in detail. Finally, the two possible

cooperative strategies are applied in the IEEE 30 Bus Test System, and the evaluation results are analyzed and compared in Section 5.5.

5.2 Proposed method: WP–HPS cooperation method

In order to ensure the reliability of the system after wind power integrating, a new WP-HPS cooperation method is proposed to reduce the impact of wind power fluctuations on the power system in this section. The proposed WP-HPS cooperation method should smooth the output of the CGUs by limiting the wind power directly absorbed by the system. The HPS stores excess wind power and discharges when the system is insufficient to improve system reliability. It should also be emphasized that the purpose of adding HPS has been to improve wind power utilization and system reliability; therefore, in this WP-HPS cooperation method, all the stored energy for HPS came from wind power.

The amount of wind power that can be absorbed by a power system depends, however, on the performance of its CGUs and dispatch limitation [152]. The dispatch limitation is to limit the wind power that can be directly absorbed by the system to a certain value, if the available wind power output is larger than this value, a portion of the wind power output needs to be abandoned, in order to achieve adequate and dynamic control in the system [153]. The advantage of limiting the wind power output is stability of power

supply, while the disadvantage is the waste of wind power resources and reduced wind power utilization.

In an actual operating grid, the system operator typically limits the amount of wind energy dispatched to a fixed percentage of the load demand. This percentage can be expressed as shown in Equation 5.1 and 5.2.

$$\mathrm{X}\% = {}^{P_{w\_limit}[t]}\Big/_{LD[t]} \tag{5.1}$$

$$100\% - \mathrm{X}\% = {}^{P_{cgu\_limit}[t]}\Big/_{LD[t]} \tag{5.2}$$

where $P_{w\_limit}[t]$ is the dispatch limit of wind power in time t, $\mathrm{X}\%$ is the wind power dispatch ratio, and $P_{cgu\_limit}[t]$ is the dispatch limit of CGUs in time t.

With continuous development in the intelligence and automation of wind power system management, this WP-HPS cooperation method becomes easier to implement, as it can be implemented through coordination of the wind turbine yaw mechanism, blade pitch system, and power system, although it also requires accurate prediction of load and wind power.

In proposed dispatch limitation, The part of wind power that exceeds its dispatch limitation will be abandoned. Above this level of potential supply, HPS can be used to

store wind power above the limit of available power generation, thus storing electricity which can be used to alleviate power shortages when the power received into the system does not meet load demand.

There are two common HPS operating modes: 1. Fixed cycle—for example, storing water at night when the load is small, and discharging during the day [154]. 2. Free cycle—for example, storing water when the electricity price is low, and discharging otherwise [155]. However, due to features of wind power such as volatility, reverse peak modulation, and uncertainty, these two schemes may reduce system reliability, and are therefore not suitable for HPS operations in power systems with higher wind penetration levels [156]. In order to make a more reasonable plan for power generation, thus improving both wind power uptake and system reliability, it is necessary to minimize the output volatility for the power generation equipment affected by wind power; this not only improves equipment efficiency, but also reducing damage and the effects of ageing, and increasing service life.

To address these issues in practical terms, the HPS system operating mode in this thesis takes system reliability into account. HPS is only for storing excess wind power, so when the available wind power output larger than the wind power dispatch limitation, HPS runs in the pumping mode. Otherwise, when the available wind power output smaller than the wind power dispatch limitation, HPS runs in generating mode. Since

in this WP-HPS cooperation method, HPS is for storing excessive wind power and balancing the supply and demand of the system.

The available generation output of CGUs meets the requirements dispatch limitation in most time. However, due to the FOR (forced outage rate) of CGUs, there are some time periods that the available generating output of CGUs cannot meet the requirements of dispatch limitation.

During the period when the available CGUs output is less than its dispatch limitation, the available output of wind power may be greater than the dispatch limitation of wind power. Therefore, when the available power generation output of CGUs is insufficient, there are two possible control strategies—Strategy 1 and Strategy 2, as given below.

Strategy 1: HPS system supports CGUs with wind power supplying basic load. When the available CGUs output is less than its dispatch limitation, which implies that the CGUs supply is insufficient, HPS can only run during the hydro period to support the system load, and the wind power output is still limited to wind power dispatch limitation.

Strategy 2: both HPS and wind power support CGUs. When CGUs supply is insufficient and wind power larger than the dispatch limitation of wind power, both HPS and wind power can support the CGUs and there is no limit to the wind power directly absorbed by the system..

In these operation strategies, data in [157] shows that HPS takes up to 240 seconds for a pumping unit to change from full power generation to full pumping. In this chapter, the time interval to theoretically and technically implement the strategies above has been set to 1 hours.

The proposed WP-HPS cooperation method has the following features:

1. In the proposed WP-HPS cooperation method, although HPS only absorbs excess wind power to improve wind power utilization, HPS supplies power when either wind power or CGUs inputs are insufficient, based on the power supply and demand relationship of the power system, thus increasing the reliability of the system to a greater extent.

2. In the proposed WP-HPS cooperation method, setting the dispatch ratio of CGUs can reduce the fluctuation of the output of CGUs, thus preventing the aging and damage of the generation units caused by the frequent fluctuation of output of CGUs the and prolonging theirs service life.

3. In the proposed WP-HPS cooperation method, a form based on reliability indicators can be created; for each level, the reasonable installed generation capacity, reservoir capacity, and HPS dispatch ratio can be listed. Then, the wind power and HPS capacity

for the specified area can be planned, using the RCBA method and taking account of power system reliability requirements.

5.3 Mathematical model of the proposed power system

HPS is used to mitigate the impact of wind power fluctuations on system reliability, and the generation system will become a proposed power system containing WTGs, CGUs and HPS. Chapter 4 has introduced mathematical modeling approach for WTGs and CGUs output. Before modeling the proposed power system, the mathematical model of HPS needs to be considered. Four operational constraints will be encountered when modelling an HPS unit:

1) Reservoir capacity constraint:

The energy stored by the HPS at time t, $E_{hps}[t]$, will always be limited by the capacity of the HPS reservoir.

$$0 \leq E_{hps}[t] \leq E_{rate} \tag{5.3}$$

where E_{rate} is the maximum amount of energy that the HPS can store (MWh).

2) HPS pumping and generation capacity constraint:

Reversible pumped turbines were utilized in this study; their pumping capacities were assumed to be equal to their generation capacities—and a constant value was assumed for them in this chapter.

$$0 \leq P_h[t] \leq P_{h\_rate} \tag{5.4}$$

$$0 \leq P_p[t] \leq P_{p\_rate} \tag{5.5}$$

$$P_{h\_rate} = P_{p\_rate} = P_{hps\_rate} \tag{5.6}$$

In (5.4) to (5.6), P_{p_rate} and P_{h_rate} are the power ratings of the HPS during the pumping and generation periods, respectively (as MW); $P_p[t]$ is the pumping input of the HPS at time t (as MW), and $P_h[t]$ is the generation output of the HPS at time t (as MW).

3) State uniqueness constraint:

It is not possible for the HPS system to be simultaneously pumping and generating energy. Therefore, it will be necessary to avoid simultaneous HPS system pumping and generation.

$$P_h[t] \times P_p[t] = 0 \tag{5.7}$$

4) Power balance constraint:

This constraint defines the relationship between the energy stored in the water reservoir and the pumping/generation power of the HPS system.

$$E_{hps}[t] = E_{hps}[t-1] + T \times \eta_p \times P_h[t] - T \times P_h[t]/\eta_h \quad (5.8)$$

In (5.8), η_p and η_h are HPS system efficiency during pumping and generation periods, respectively.

The security, reliability, and economy of the system require that the total power supply must equal the total load, when the proposed power system transmits power to the grid, as shown in the Equation (5.9), where $\mathrm{LD}_{total}[\mathrm{t}]$, and $P_{total}[t]$ are the total load and total power of the local grid, respectively.

$$\mathrm{LD}_{total}[\mathrm{t}] = P_{total}[t] \quad (5.9)$$

The total power supply consists of outputs from CGUs, wind power, and the generation model of HPS:

$$P_{total}[t] = P_{cgu}[t] + P_w[t] + P_h[t] \quad (5.10)$$

Where $P_{cgu}[t]$, and $P_w[t]$ are the power supplied by CGUs and the wind power directly absorbed by power system, respectively.

Total load consists of the demand load and the load from HPS pumping period:

$$\mathrm{LD}_{total}[\mathrm{t}] = \mathrm{LD}[\mathrm{t}] + P_p[t] \tag{5.11}$$

Where LD[t] is the power required by the load.

The HPS system operating mode in WP-HPS cooperation method proposed in Section 5.2 takes system reliability into account. HPS is only for storing excess wind power, so when $AP_w[t] > P_{w\_limit}[t]$, HPS runs in the pumping mode. Otherwise, when $AP_w[t] < P_{w\_limit}[t]$, HPS runs in generating mode. Since in this system, HPS is for storing excessive wind power and balancing the supply and demand of the system, Equation 5.12 holds:

$$AP_w[t] = P_w[t] + P_p[t] + P_{w\_c}[t] \tag{5.12}$$

where $P_{w\_c}[t]$ is the amount of wind power which needs to be curtailed.

Therefore, the curtailment ratio of wind power can be expressed as follows.

$$\mathrm{CR} = \frac{\sum_{t=1}^{8760} P_{w\_c}[t]}{\sum_{t=1}^{8760} AP_{wind}[t]} \tag{5.13}$$

where CR is the curtailment ratio of wind power. It represents the ratio of wind power that cannot be absorbed by the system or stored in HPS to the total amount of wind power generated in one year (8760 hours).

5.4 Mathematical model of the WP–HPS cooperation method

In Chapter 4, it was assumed that all wind power output could be absorbed by the system, which is normal for lower wind penetration levels, so, in this case, the wind power characteristics had little effect on system reliability. However, as described in Section 5.2, when the wind penetration level is large, the amount of wind power that can be absorbed by a power system depends on the performance of its CGUs and dispatch limitation [152]. For this reason, Section 5.2 proposed the WP-HPS cooperation method. This section will mathematically model the proposed method, then, the main purposes in chapter are to evaluate and compare the impacts of two HPS and wind power operating strategies.

The reliability of proposed power system with HPS and wind power will be evaluated by the probability-based reliability assessment method (presented in Section 3.4.3). Reliability Cost-Benefit Analysis (RCBA) (presented in Section 3.5) is utilized to determine the optimal HPS capacity due to the extremely high construction cost of HPS.

5.3.1 Simulation reliability evaluation method

Reliability indexes for the power system are obtained using SMCS method, ensuring a sufficient number of simulations was conducted, such that the results were close to those of the actual operating system.

The reliability index calculation steps and related mathematical models applied in this chapter to reduce wind power impact on the power system are as follows:

1. Reliability models for each power generation units (including CGUs and WTGs) in the generation system were simulated by using the SMCS method to obtain the available power generation output. Meanwhile, system reliability indicators were obtained by taking into account the time series for the dispatching scheme and for load demand.

The reliability model of the power generation unit refers to the outage models, and is directly related to the available power generation output of the power generation system. In this chapter, reliability models for each unit have been simulated in chronological order, with SMCS lasting one year (8760 hours), and an interval of 1 hour per simulation. Reliability parameters were revised based on IEEE-RTS.

As described in Chapter 4, the available power output of the system is obtained by combining the available power output generated by CGUs and wind power, with the methods summarized as follows:

The available power output of the CGUs was based on the two-state model, and the time series was simulated by the method of state duration sampling in SMCS, according to forced outage rate (FOR) and mean time to repair (MTTR), for each generating unit.

For the available power output of wind power, the wind speed time series was firstly simulated using Weibull distribution. Then, the wind speed series was converted into available single wind turbine output series, using the wind speed power conversion formula.

Next, the reliability model was established for each WTG, using the same method as the CGUs reliability model, but based on wind turbine reliability parameters. The available wind power output series can then be obtained, by combining the reliability model with the output sequence of the WTG.

According to the dispatch ratio for power generation and the load time sequence, the reliability indicators of the power system can be evaluated using the available wind

power and CGUs output time sequences. Taking LOLE as an example, when $AP_w[t] < X\% \times LD$, or $AP_{cgu}[t] < (1 - X\%) \times LD$, a power shortage occurs, and the length of this shortage is set at one time duration (one hour).

$$\mathrm{LOLE}_i = \begin{cases} 1 & AP_w[t] < P_{w\_limit}[t] \; or \; AP_{cgu}[t] < P_{cgu\_limit}[t] \\ 0 & AP_w[t] \geq P_{w\_limit}[t] \; and \; AP_{cgu}[t] \geq P_{cgu\_limit}[t] \end{cases} \quad (5.15)$$

Then Equation 5.16 can be used to calculate the power system reliability index of the Monte Carlo method, after N simulations.

$$\mathrm{LOLE} = \frac{1}{N}\sum_{i=1}^{8760\times N} \mathrm{LOLE}_i \quad (5.16)$$

2. The proposed WP-HPS cooperation method is utilized to deal with wind power impact on system reliability and to reduce reliability indicator readings to a reasonable level.

The remaining wind power, which has been stored via HPS, will be used to balance the power supply shortage. The wind power and CGUs outputs absorbed by the system time series were derived by modifying the load demand time series, the available output from the wind power time series, and the CGUs time series, using equations 5.17 and 5.168 respectively.

$$P_w[t] = \min\left(AP_w[t], \mathrm{X}\% \times LD[t]\right) \quad (5.17)$$

$$P_{cgu}[t] = \min\left(AP_{cgu}[t], (1 - \mathrm{X}\%) \times LD[t]\right) \quad (5.18)$$

Based on the two strategies introduced in Subsection 5.2, the HPS output in the pumping and generation period time series was calculated using equations 5.19–5.22, which take reservoir capacity constraints, HPS efficiencies during pumping and generation periods, and the installed HPS generation capacity into account.

Strategy 1: Only HPS system could supports CGUs.

If $P_w[t] + P_{cgu}[t] \geq LD[t]$

$$P_p[t] = \min\{P_{rate}, (AP_w[t] - P_w[t]), (E_{rate} - E_{hps}[t-1])/T\} \quad (5.19)$$

Otherwise, $P_w[t] + P_{cgu}[t] < LD[t]$

$$P_h[t] = \min\{P_{\mathrm{rate}}, (\mathrm{LD}[t] - P_w[t] - P_{cgu}[t]), E_h[t-1]/T\} \quad (5.20)$$

In (5.19) and (5.20), P_{p_rate} and P_{h_rate} are the HPS power ratings during pumping and generation periods, respectively (MW), E_{rate} is the maximum amount of energy that the HPS could store (MWh), and $E_{\mathrm{hps}}[t-1]$ is the amount of energy that the HPS stored at time t - 1 (MWh).

Strategy 2: HPS and wind power could support CGUs.

If $AP_w[t] + P_{cgu}[t] \geq LD[t]$

$$P_p[t] = \min\{P_{rate}, (AP_w[t] - P_w[t]), (E_{rate} - E_{hps}[t-1])/T\} \quad (5.21)$$

Otherwise $AP_w[t] + P_{cgu}[\mathrm{t}] < LD[\mathrm{t}]$

$$P_h[t] = \min\{P_{\mathrm{rate}}, (LD[t] - AP_w[t] - P_{cgu}[t]), E_{hps}[t-1]/T\} \quad (5.22)$$

By comparing the load demand time sequence with generation unit outputs, the reliability indicators for the power system, with HPS, can be determined, take LOLE as an example:

Strategy 1:

$$\mathrm{LOLE}_i = \begin{cases} 1 & P_w[t] + P_{cgu}[t] + P_h[t] < \mathrm{LD}[t] \\ 0 & P_w[t] + P_{cgu}[t] + P_h[t] \geq \mathrm{LD}[t] \end{cases} \quad (5.23)$$

Strategy 2:

$$\mathrm{LOLE}_i = \begin{cases} 1 & AP_w[t] + P_{cgu}[t] + P_h[t] < \mathrm{LD}[t] \\ 0 & AP_w[t] + P_{cgu}[t] + P_h[t] \geq \mathrm{LD}[t] \end{cases} \quad (5.24)$$

The reliability index LOLE, after N times SMCS simulattions, can be obtained using Equation 5.25.

$$\mathrm{LOLE} = \frac{1}{N}\sum_{i=1}^{8760\times N} \mathrm{LOLE}_i \quad (5.25)$$

In this chapter, LOLE is taken as the standard by which to evaluate how HPS enhances the reliability of the power system, with wind power. For a system with fixed wind power and CGUs installed capacity, each HPS scenario (HPS installed capacity, HPS reservoir capacity and dispatch ratio) will alter the system reliability. Therefore, the values for these three factors can be adjusted to enable a specific system to achieve the required level of reliability.

5.3.2 Reliability cost-benefit analysis

It is known that the larger the OR capacity of the system, the more reliable the system becomes, so there are many HPS capacity scenarios that can satisfy system reliability requirements. The optimal HPS scenario will be determined based on reliability cost-benefit method, and this method identifies the optimal capacity by calculating the costs and benefits of the reliability improvement achieved by adding HPS, while still satisfying system reliability criteria.

Consider the benefit and cost for one year. The main WP-HPS cooperation system annualized reliability costs considered herein are the HPS capital, installation, operation, and maintenance costs. The annualized reliability benefit of this cooperation method is divided into two aspects: one is that by adding HPS to a conventional power generation system, more wind energy can be supplied to the grid, which will reduce coal costs. The other is that HPS cooperates with wind power to improve the reliability

of the system and reduce the Costumer Interruption Cost (CIC). The optimum capacity of the HPS system is determined by identifying those power rating and reservoir rating values that not only satisfy system reliability requirements, but also provide the maximum difference between the annualized reliability benefit and cost.

The annualized reliability benefit from reducing the coal cost by adding an HPS system can be calculated according to the differences in expected energy not used (EENU), before and after adding an HPS system, for different year-based scenarios. These values are a function of HPS size—that is, the capacity of HPS generation and reservoir—as these factors will influence reliability.

$$\mathrm{EENU} = \sum_{t=1}^{N} AP_w(t) - \sum_{t=1}^{N} P_w(t) - \sum_{t=1}^{N} P_h(t) \tag{5.26}$$

$$B_{EENU}(P_{rate}, E_{rate}) = (EENU_b - EENU_a) \times r_{fuel} \tag{5.27}$$

In Equations (5.26) and (5.27), r_{fuel} is the fuel price (£/MWh), and $EENU_b$ and $EENU_a$ are the values of EENU before and after adding an HPS, respectively.

It is difficult to evaluate the reliability benefit from adding an HPS directly, and assessing the customer interruption cost (CIC) caused by insufficient power supply is a practical alternative. This can be evaluated using a Customer Damage Function (CDF), which represents the relationship between the outage cost for a given type of

customer, and the duration of the outage [34]. A fixed LOEE cost rate was used to evaluate the CIC, and sector CDFs were used to develop more accurate results.

$$B_{CIC}(P_{rate}, E_{rate}) = (LOEE_b - LOEE_a) \times r_{cic} \tag{5.28}$$

In Equation (5.28), r_{cic} is the LOLE cost rate (£/MWh); $LOEE_b$ and $LOEE_a$ are the values of LOEE before and after adding HPS, respectively.

Therefore, the annualized reliability benefit obtained by adding HPS can be expressed as following equation:

$$RB(P_{rate}, E_{rate}) = B_{EENU}(P_{rate}, E_{rate}) + B_{CIC}(P_{rate}, E_{rate}) \tag{5.29}$$

The annualized reliability cost of an HPS system is composed of its capital cost, C_{cap}, and installation, operation, and maintenance costs, C_{IOM}, which depend on its rated power and reservoir capacity. C_{IOM} can be evaluated using functions for fixed and variable costs [158], so that the annualized reliability cost of an HPS system is as shown in Equation (5.30), where: C_P (£/MW) and C_E (£/MWh) are the cost rates associated with installing power and reservoir capacity, respectively, α is the yearly discount rate, and r_F (£/MW) and r_V (£/MWh) are the cost rates for the fixed and variable costs, respectively.

$$\mathrm{RC}(P_{rate}, E_{rate}) = C_{cap}(P_{rate}, E_{rate}) + C_{IOM}(P_{rate}, E_{rate})$$

$$= \alpha \times (C_P \times P_{rate} + C_E \times E_{rate}) + (r_F \times P_{\mathrm{rate}} + r_V \times E_{rate}) \quad (5.30)$$

Based on the above reliability cost and benefit concept, the total benefit of adding an HPS system can be expressed as shown in Equation (5.31).

$$\begin{cases} LOLE(P_{rate}, E_{rate}) \le LOLE_{required} \\ Max\big(TB(P_{rate}, E_{rate})\big) = \mathrm{RB}(P_{rate}, E_{rate}) - \mathrm{RC}(P_{rate}, E_{rate}) \end{cases} \quad (5.31)$$

Given that HPS acts as the OR of the system, the larger the HPS capacity, the more reliable the system, but the greater the cost. There are therefore many schemes able to satisfy system reliability requirements, and the reliability of their benefits and costs differ. Using the RCBA method, the scheme with the most appropriate HPS capacity is that which is identified as representing the maximum comprehensive benefit.

5.3.3 The calculation procedures flow chart

The calculation procedures flow chart of the proposed WP-HPS cooperation method is shown in Figure 5.1.

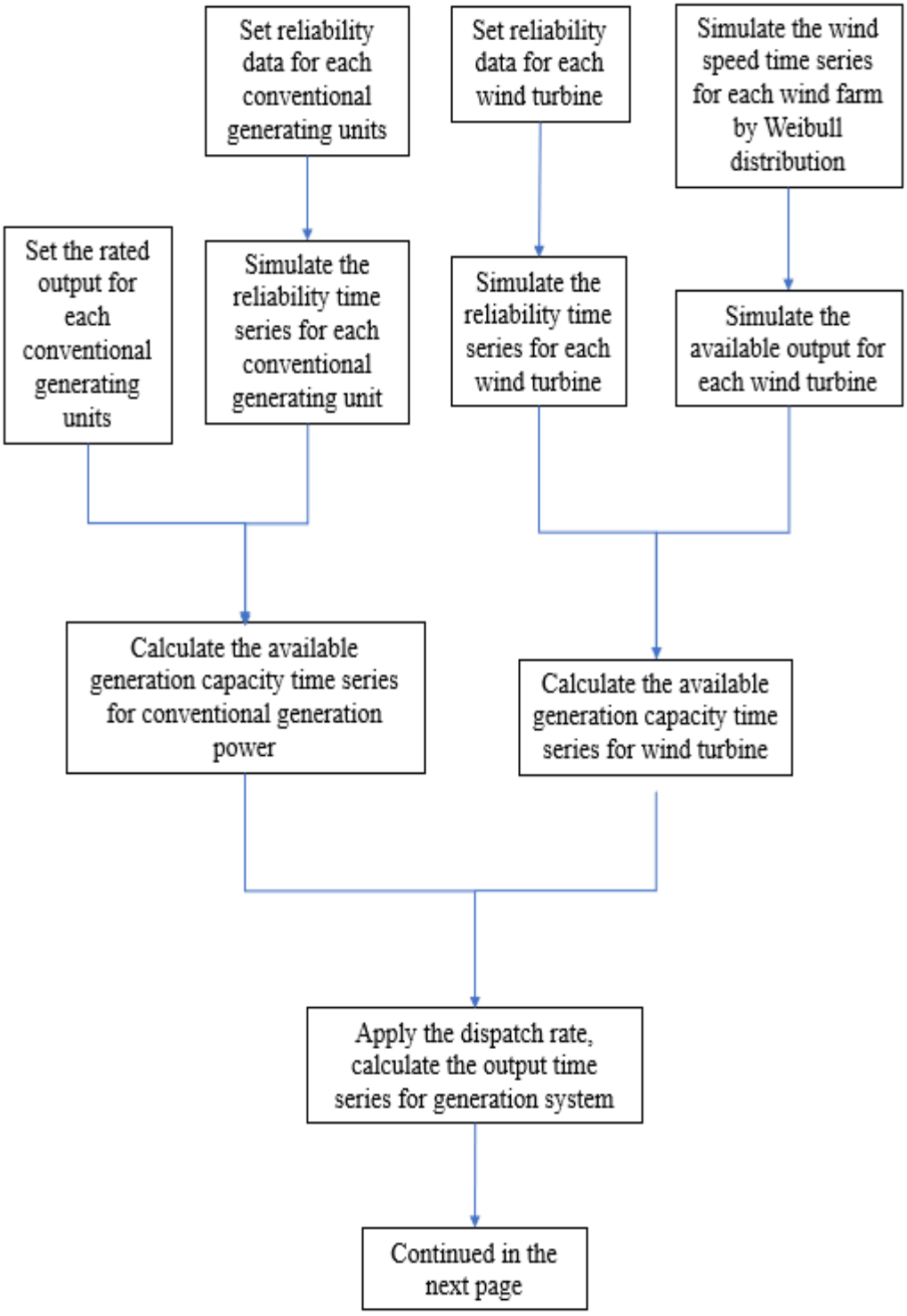
Set reliability data for each conventional generating units
Set reliability data for each wind turbine
Simulate the wind speed time series for each wind farm by Weibull distribution
Set the rated output for each conventional generating units
Simulate the reliability time series for each conventional generating unit
Simulate the reliability time series for each wind turbine
Simulate the available output for each wind turbine
Calculate the available generation capacity time series for conventional generation power
Calculate the available generation capacity time series for wind turbine
Apply the dispatch rate, calculate the output time series for generation system
Continued in the next page

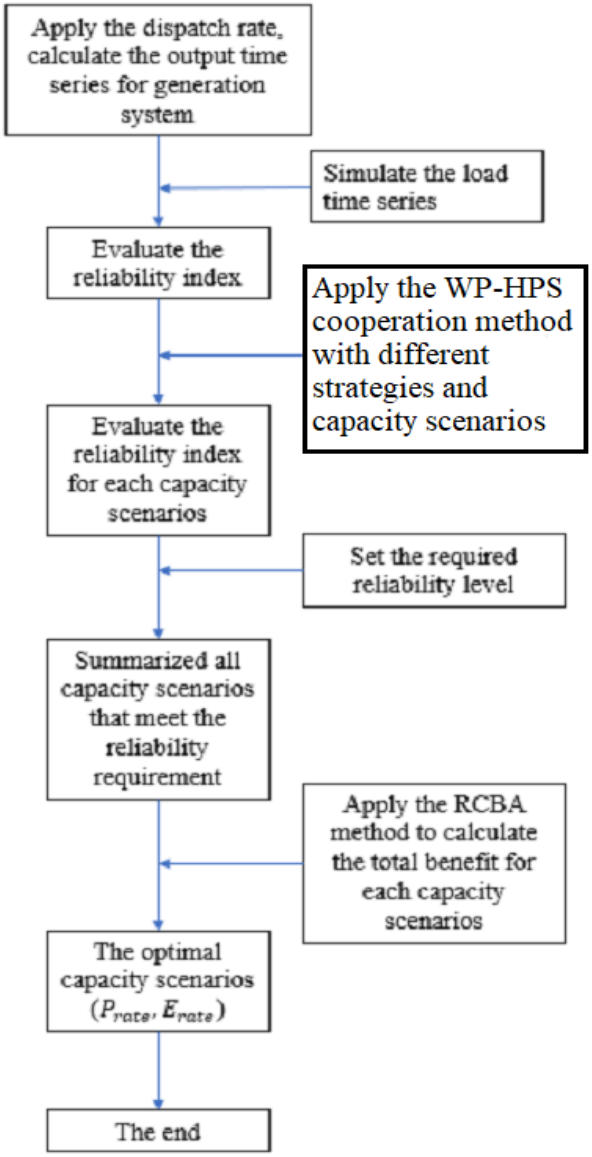

Figure 5.1: The proposed WP-HPS cooperation method calculation flow chart

5.5 Illustrative Example

The system presented in this case was modified IEEE 30 Bus system, with the purpose of showing how the methods put forward in this chapter could reduce the impact of reliability reduction on the system, brought about by the addition of wind power. As previously described, HPS can enhance system reserve capacity, and the case analysis below is focused on illustrating the cooperation achieved between the wind power and HPS generation and to explain, the positive contributions of this method to the reliability of the power system with wind power. In this part, the role of WP-HPS cooperation method in enhancing reliability is considered, and the two operational strategies are compared. To achieve this, wind penetration level in this instance was fixed at 10%, with a more comprehensive case analysis to be presented in Chapters 6 and 7, respectively.

5.5.1 Description of the test system

In this section, a comparison between the two operating scenarios, in terms of generation capacity and HPS reservoir capacity effects on the reliability benefit from the addition of an HPS system, and in terms of the amount of wind power that can be stored, is presented. The test system used here is the same as was used in Chapter 4,

and basic information, together with RCBA system parameters, have been listed in Tables 5-1 and 5-2, respectively.

Table 5-1: test system basic data

Generators	6
Buses	30
Load points	21
Total generation capacity (MW)	360
Peak load (MW)	270

Table 5-2 reliability cost and benefit parameters [159]

Parameter	r_{fuel} (k£/MWh)	r_{cic} (k£/MWh)	C_P (k£/MW)	C_E (k£/MWh)	α	r_F (k£/MW)	r_V (k£/MWh)
Value	0.4	10	200	25	0.06	10	1.25

When the wind power penetration level is 10%—that is, when the installed wind power capacity is 36 MW—CGUs with equivalent capacity will be replaced. The scale and shape parameters values for these wind farms' Weibull distributions were all set to 7 and 2, respectively, and the wind turbine parameters were as mentioned in Chapter 4.

Wind power available power output can be obtained using the methods for generating artificial wind speed and the formula for wind speed power conversion introduced in Chapter 4, while the method for sampling the available CGUs power generation

capacity durations was introduced in Subsection 3.3.2. The system power generation capacity can be calculated with this method, while taking wind power output into account at the same time.

The same load demand model as that previously used, in Chapter 4, has been applied, modified for this simulation, to reflect the UK 2018 (8760 hours) load demand. In the meantime, the transmission network was determined to have cleared the reliability test, so there were no system adequacy issues due to transmission congestion to be addressed [99]. The test system reliability assessment results from Chapter 4 will also be used in this section.

5.5.2 Results and discussions

To test the ability of the proposed WP-HPS cooperation method to improve power system reliability, a research program covering four areas was applied:

- Use SMCS method to evaluate the reliability of the power system and study the impacts of wind power integration and dispatch ratio on the test system reliability

- Add HPS to the test power system, through operational Strategy 1, to cooperate with wind power, and to facilitate studying the impact of power generation capacity and reservoir capacity of HPS on system reliability improvement.

- Add HPS to the test power system, through operational Strategy 2, to cooperate with wind power, and to facilitate studying the impact of power generation capacity and reservoir capacity of HPS on system reliability improvement.

- Compare the ability of the WP-HPS cooperation method of two operational strategies to improve system reliability in the presence of different cooperating strategies, with wind penetration level and dispatch limitations the same.

5.5.2.1 The impacts of wind power integration and dispatch ratio on the test system reliability, at 10% wind penetration level

The simulated test system reliability indices, before and after 10% wind penetration level wind power was integrated, have been listed in Table 5-3. The aim of this study was to determine a method for improving reliability of the power system, after wind power integration into the system, by adding an HPS system of optimum capacity. Thus, the reliability index value of the original system, before wind power was integrated, $LOLE_{required}$, was set to 3.96 hours/year, as derived in Section 4.5.

Table 5-3: Reliability indices for the test system at 0% and 10% wind penetration

Wind penetration level	Reliability indices		
	LOLE (hours/year)	LOEE (MWh/year)	LOLF (occ./year)
0% (without wind power)	3.96	79.23	0.71
10%	7.89	152.41	2.84

As can be seen in Table 5-3, wind power integration has a significant negative impact on power system reliability. The time for power shortages in one year has nearly doubled (from 3.96 hours/year to 7.89 hours/year) when 10% of the CGUs installed generation capacity was replaced with wind power. In addition, with increased wind power integration, the LOEE and LOLF values have also increased rapidly.

Wind power characteristics are the main cause of power system reliability reduction, as wind power is relatively uncontrollable compared to CGUs. At lower wind speeds, the available wind power generation capacity will be reduced to the point that the number of times when the total available power generation capacity of the system cannot meet the load demand will increase—and so the reliability of the system will be deemed to have decreased.

In addition to reduced system reliability, the integration of wind power into the power system will also affect the CGUs. System reliability is affected since power generated by wind power is fully absorbed by the system, and the CGUs output needs to be

adjusted continually to compensate for wind power fluctuation. Figure 5.2 presents a snapshot of CGUs output, over 200 hours based on this activity, and it is clear that the CGUs output curve fluctuates frequently—which will reduce CGUs efficiency, increase carbon dioxide emissions and generating cost, accelerate equipment ageing, and reduce its service life.

To address this problem, dispatch limitation is proposed, and the CGUs output curve with 10% wind power dispatch limitation is also shown in Figure 5.2. Here, it can be seen that, when dispatch limitation is applied to the power system, the CGUs output curve has become smoother, with less fluctuation, compared to the curve for no wind power limitation.

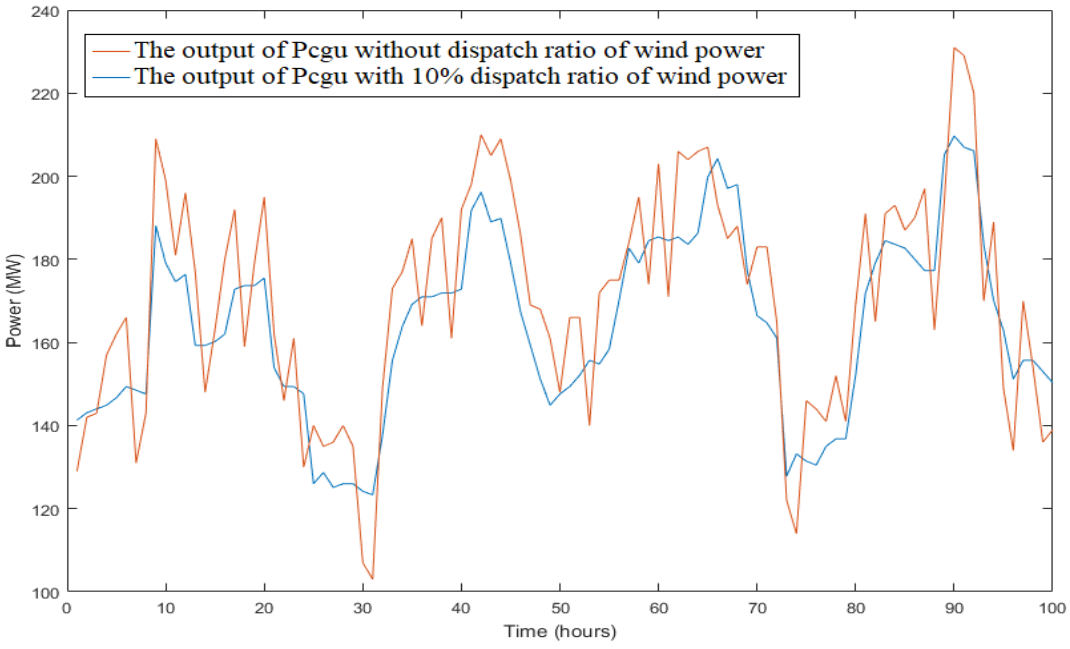

Figure 5.2: 200 hours CGUs output curves before and after dispatch limitation applied

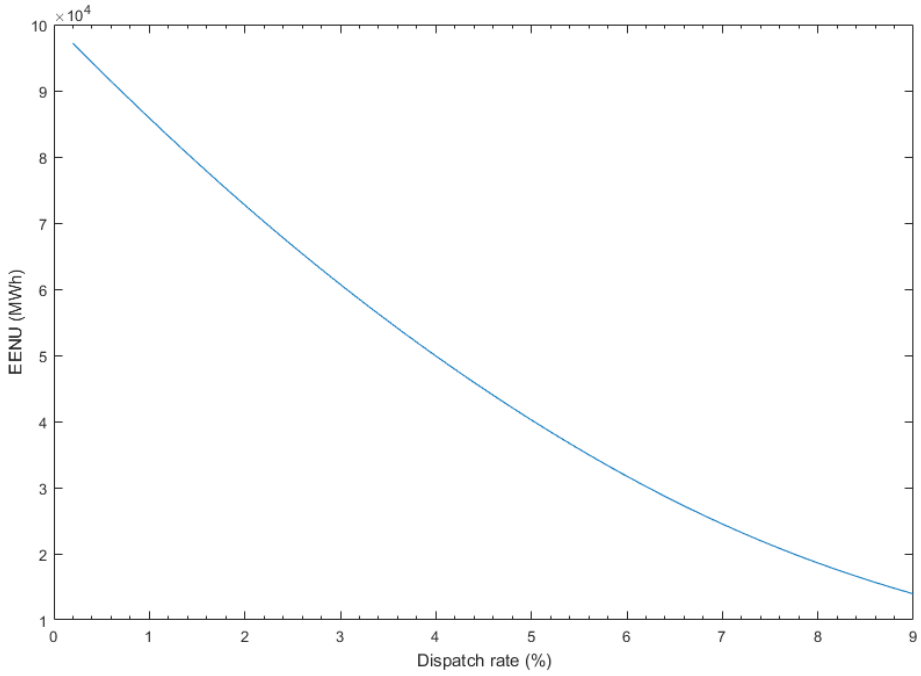

Figure 5.3: EENU against dispatch ratio at 10% wind penetration level

Dispatch limitation not only can minimize CGUs output curve fluctuations, but can also reduce wind power waste. Figure 5.3 shows the relationship between EENU and the dispatch ratio. It can be seen from this figure that, as the dispatch ratio value increased, there was less and less unused wind power. When the dispatch ratio was 0.01, the wasted wind power larger than 9×10^4MWh, and this value decreased to 1.5×10^4MWh when the dispatch ratio rose to 9%. Dispatch ratio enhancement can allow more wind power to be absorbed by the power system, thereby improving wind power utilization.

Figure 5.4 shows the effect of dispatch ratio on system reliability LOLE. Dispatch limitation will make the system unreliable, with LOLE increasing with the increasing dispatch ratio; this happens because wind power is required to supply part of the load demand, but wind power fluctuations make power shortages inevitable. Then, the increased dispatch ratio will increase the amount of power that wind power needs to supply, so the reliability will become worse, indicating that the system must have additional OR capacity, in order to improve system reliability. Although the increase in dispatch limitation can reduce the curtailment of wind power, it has a negative impact on system reliability.

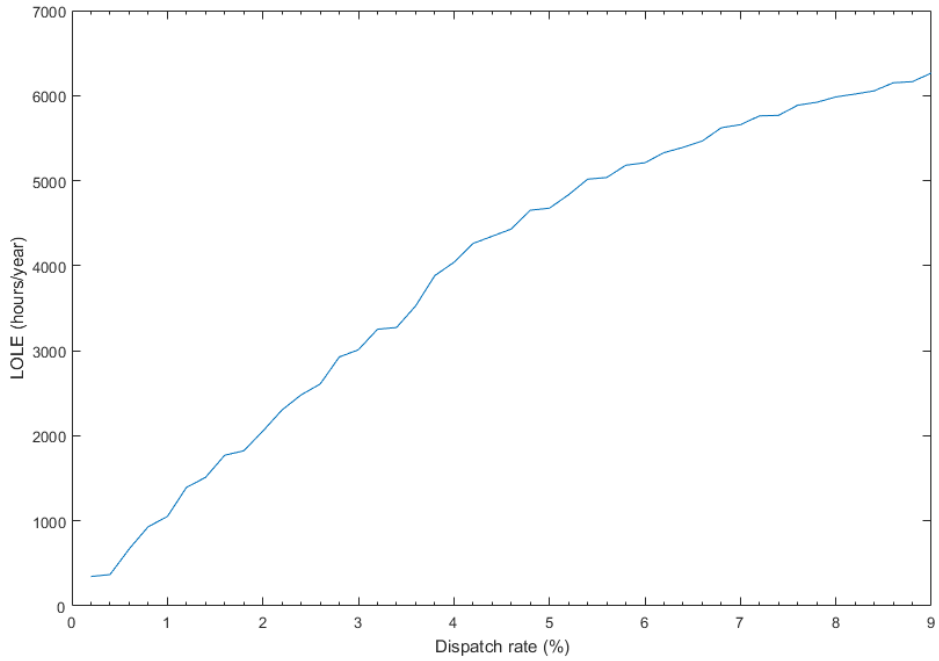

Figure 5.4: LOLE against dispatch ratio when wind penetration level is 10%

5.5.2.2 The proposed WP-HPS cooperation method through Strategy 1 at 10% wind penetration

The larger the HPS capacity, the more reliable the system will be. Nevertheless, HPS capacity cannot be limitless, so the wind power installed capacity has been taken as representing the HPS generation capacity upper limit, to evaluate the impact of WP-HPS cooperation (strategy 1) method on system reliability. HPS reservoir capacity is generally eight to twenty times that of the installed capacity [160], and the purpose of this chapter is to analyze whether the proposed method can effectively alleviate the impact of wind power on power system reliability. Therefore, the minimum value of 8 is taken as the maximum limit of the reservoir capacity. In addition, in order to shorten simulation time, the dispatch ratio will start from 1%, and increase by 1% increments until the HPS can no longer meet system reliability requirements, even at maximum capacity.

In this chapter, 10% of the installed wind power capacity was taken as the base HPS generation capacity, to allow 10% increments each time, until the upper limit was reached, so that a total of ten HPS power generation capacity scenarios were generated. The same method was applied when the reservoir capacity was chosen, leading to ten scenarios in terms of reservoir capacity. In reality, however, HPS installed capacity and reservoir capacity can be adjusted according to the capacity of the actual installed

hydro turbine type and the applicable hydraulic conditions—and this will be discussed in more detail in Chapter 7.

In order to analyze the effects of HPS capacity on system reliability for Strategy 1, a dispatch ratio of 3% was assumed. In this situation, the system reliability index, LOLE, was 1662 hours/year, when there was no HPS.

HPS generation and reservoir capacities are two important parameters when considering HPS effects on reliability: The maximum water-pumping power and power generation depend on the HPS generation capacity, P_{rate}, and HPS reservoir capacity, E_{rate}, determines the HPS energy storage capacity upper limit.

Capacity Scenario (CS) is the term used to describe the evaluation results, when different HPS capacities are incorporated into the power system, and can be expressed as (P_{rate},E_{rate}).

HPS balances system power generation and demand by storing redundant wind power, which not only improves system reliability but also reduces wind power wastage. Evaluation results for the reliability index, LOLE, for the WP-HPS cooperation (strategy 1) method, under various Capacity Scenarios, have been summarized in Figure 5.5.

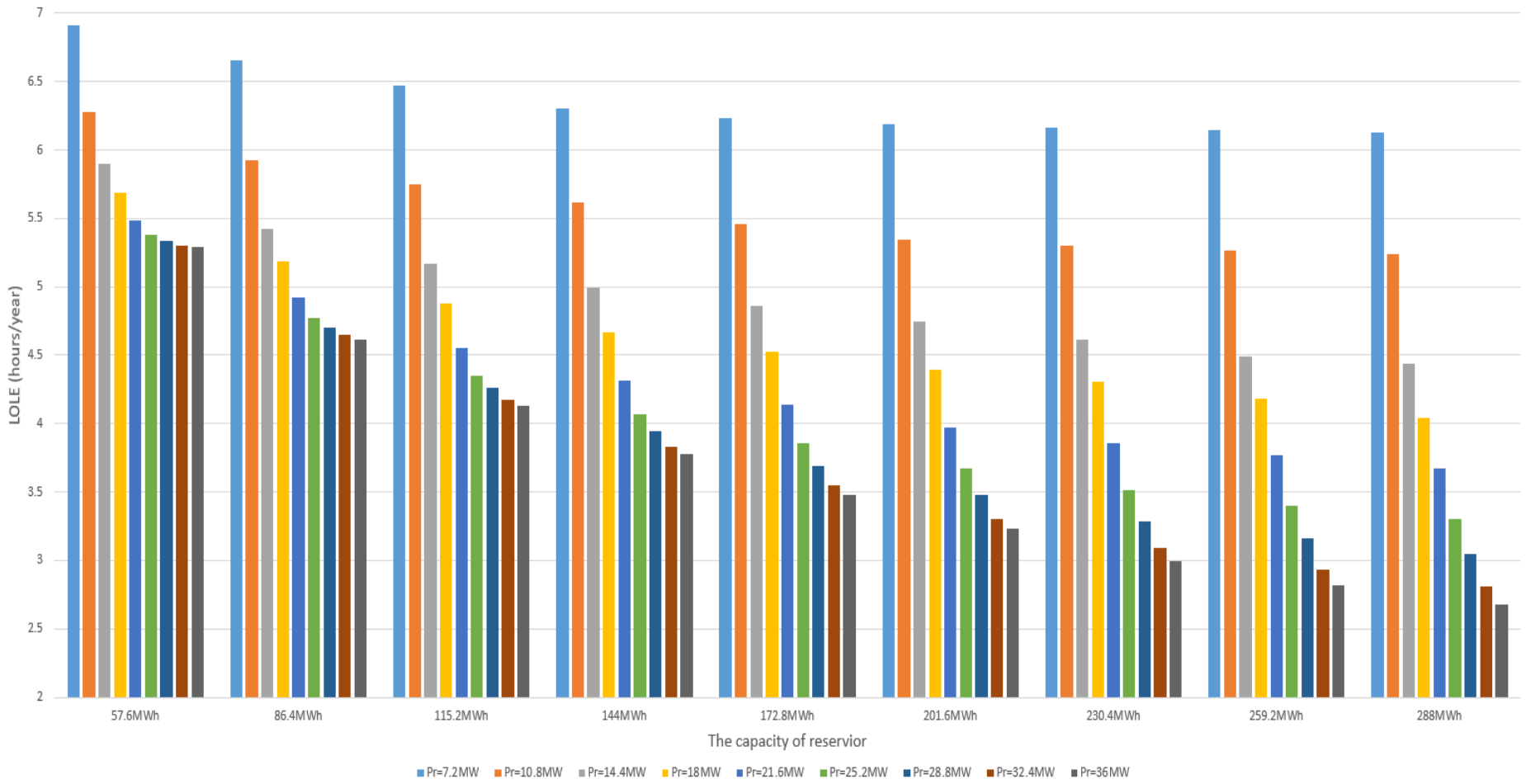

Figure 5.5: Effect of Capacity Scenarios on LOLE for strategy 1, at a 3% dispatch ratio

The reliability index LOLE values for different HPS generation and reservoir capacities for strategy 1 are shown in Figure 5.5, where system reliability improvement by HPS through Strategy 1 can be clearly seen. Even the smallest CS (7.2 MW, 57.6 MWh) can reduce LOLE from the excessive 1662 hour/year to an acceptable 6.9 hour/year. The figure also shows that increased capacity can improve system reliability: for example, when $E_{rate} = 57.6\ MWh$, LOLE continues to decline as the same generation capacity continues adding to the system. Moreover, the value of LOLE drops rapidly to begin with, after which the rate of decline slows significantly, meaning that increasingly more generation capacity was required to reduce LOLE by the same value.

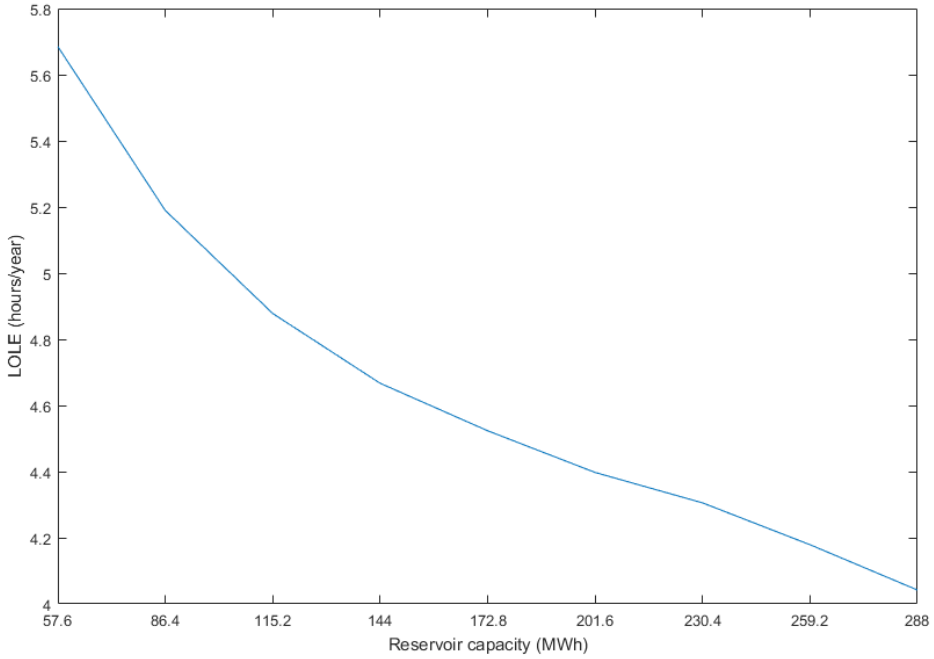

Figure 5.6: HPS reservoir capacity against LOLE, for strategy 1, at 18 MW HPS generation capacity

As the effect of HPS reservoir capacity on LOLE for strategy 1 could not be clearly shown on Figure 5.5, the simulation LOLE results for different reservoir capacities have been displayed in Figure 5.6, under an 18 MW generation capacity of HPS scenario. Larger HPS reservoir capacity contributes to improved system reliability, however, since improving the reliability of the system cannot be based on unlimited increases to either HPS reservoir or generation capacity, a reasonable balance must be found between these two kinds of HPS capacity.

As mentioned above, the power system reliability requirement is for achievement of an LOLE < 3.96 hour/year, and by review of the results in Figure 5.5, it can be seen that there were many HPS capacity scenarios that fulfilled this reliability requirement, so it has been necessary to use RCBA to identify the optimal result.

Variations in the RCBA indices when a fixed reservoir capacity and different HPS generation capacities were added to the power system are shown in Figure 5.7. RC increased linearly as generation capacity increased, while RB increased rapidly at first and then slowly rose to a fixed value. This was because the HPS RB comes mainly from the reduction of system LOEE and the provision of more wind power to the power system, both of which are limited. Therefore, for different generation capacities, the RCBA first increased rapidly, and was then approximately stable, before starting a slow

decline. The impact of HPS reservoir capacity on the RCBA outcomes was similar to that of generation capacity (refer to Table 5-4 for specific data).

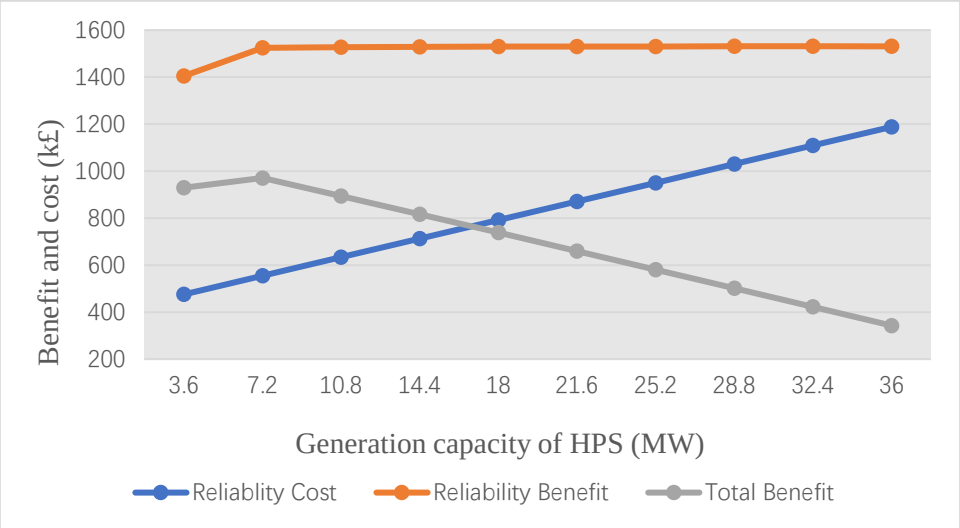

Figure 5.7: Effect of HPS generation capacity on the RCBA for strategy 1, at 144 MWh reservoir capacity

Table 5-4: Effect of HPS reservoir capacity for strategy 1 on the RCBA indices, at 18 MW generation capacity

HPS Reservoir Capacity (MWh)	RCBA Indices (k£)		
	RB	RC	TB
28.8	1513.55	475.2	1038.35
57.6	1520.01	554.4	965.61
86.4	1523.80	633.6	890.20
115.2	1527.13	712.8	814.33
144	1530.03	792	738.03

The dispatch ratio not only affects the wind power that is absorbed by the system, but also affects system reliability. To facilitate review of the dispatch ratio upper limit for strategy 1, assuming that the system was incorporated into the HPS with the largest capacity scenario (36 MW, 288 MWh), the reliability evaluation results have been summarized in Figure 5.8.

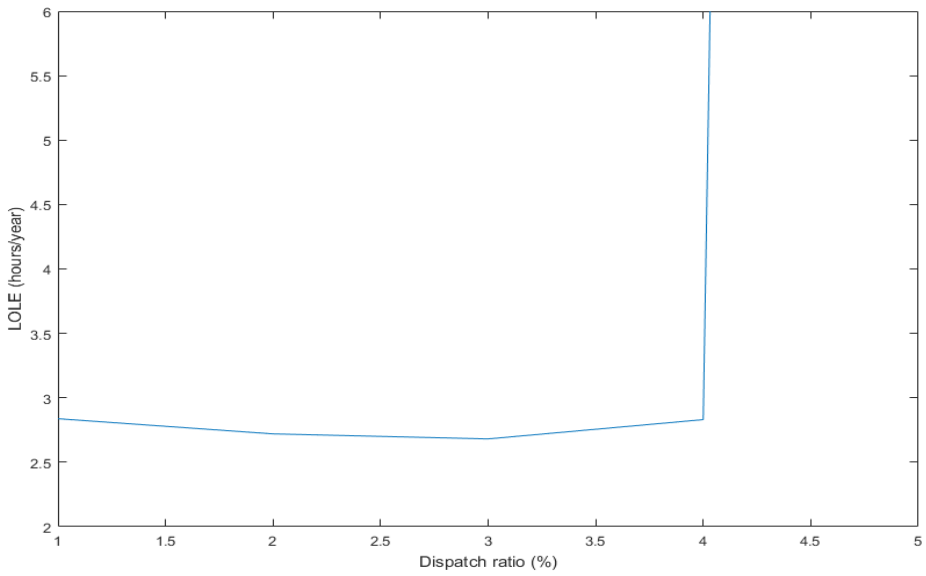

Figure 5.8: Effect of dispatch ratio on LOLE for Strategy 1 (10% wind penetration)

In strategy 1, because wind power output was limited, in case of insufficient power supply, more wind power was absorbed by the system during the dispatch ratio increase, gradually relieving the CGUs of responsibility for a larger amount of load. Therefore, the reliability of the system initially improved, due to the increase in the wind dispatch ratio. However, when the wind dispatch ratio exceeded a certain value (in this case, the

value was 3%), the intermittent influence of wind power became obvious, the reliability of system decreased rapidly, and the maximum dispatch ratio value able to satisfy the reliability requirement was 4%.

RCBA indicator evaluation results for the gradual increase in the dispatch ratio from 1% to 4% are summarized in Table 5-5—where it can be seen that RC remained unchanged, while RB and TB gradually increased. This occurred because the HPS capacity was fixed, so the RC remained unchanged. Under the premise of meeting the reliability requirements, the higher the power dispatch ratio, and the worse the system reliability without HPS became, the greater the WP-HPS cooperation (strategy 1) method improved the power system, and the more wind power was absorbed by the system—and so RCBA indicators RB and TB became larger. It should be noted that the negative TB value meant that the cost exceeded the benefit, and that this capacity scenario was therefore not worthy of being adopted, from the perspective of reliability improvement.

Table 5-5: The effect of dispatch ratio on the RCBA for strategy 1 (10% wind penetration)

Dispatch ratio (%)	RCBA indices (k£)		
	RB	RC	TB
1	243.1828	1584	-1340.82
2	732.02	1584	-851.98
3	1543.426	1584	-40.5738
4	2690.463	1584	1106.463

Applying the RCBA method to all capacity scenarios that satisfied the reliability requirements at each dispatch ratio, the TB for each scenario could be obtained—with the optimal capacity scenario being that with the highest TB. The optimal capacity scenarios and corresponding reliability and RCBA index TB assessment results (which meet the reliability requirements under each dispatch ratio), have been summarized in Table 5-6.

Table 5-6: The optimal capacity scenarios for each dispatch ratio on the RCBA, for strategy 1 (10% wind penetration)

Dispatch Ratio (%)	LOLE (hours/year)	P_{rate} (MW)	E_{rate} (MWh)	TB (k£)
1	3.92	28.80	172.80	-876.37
2	3.93	25.20	172.80	-307.83
3	3.85	25.20	172.80	504.00
4	3.95	21.60	230.40	1576.41

Based on this comparison, the optimal capacity scenario from the ISO point of view, was (21.60 MW, 230.40 MWh), at 4% dispatch ratio.

At 10% wind penetration level, the reliability of the system required LOLE to be < 3.96 hours/year. This mandates that, to decrease wind power fluctuation impact on the power system and restore reliability to its original level, with maximum TB, the optimum HPS capacities, under Strategy 1, should be 21.60 MW and 230.40 MWh, with a 4% dispatch ratio.

5.5.2.3 WP-HPS cooperation method through strategy 2 at 10% wind penetration

In order to analyze the effect of HPS capacity on system reliability under strategy 2, it was assumed that the dispatch ratio was 3%. The simulation steps and the capacity scenario selection methods were the same as were used previously for strategy 1.

The reliability index LOLE values for different HPS generation and reservoir capacities are illustrated in Figure 5.9, where the system reliability improvement achieved by employing various HPS sizes under strategy 2 can be seen. Even the smallest CS (7.2, 57.6) could reduce LOLE from the exaggerated 1662 hours/year down to an acceptable 5.08 hours/year. The figure also shows that the impact of HPS capacity on system

reliability, through strategy 2, was similar to that achieved by strategy 1. The added HPS system generation capacity improved power system reliability, although, as the generation capacity increased, system reliability improvement decreased—and HPS system reservoir capacity had a similar effect on power system reliability.

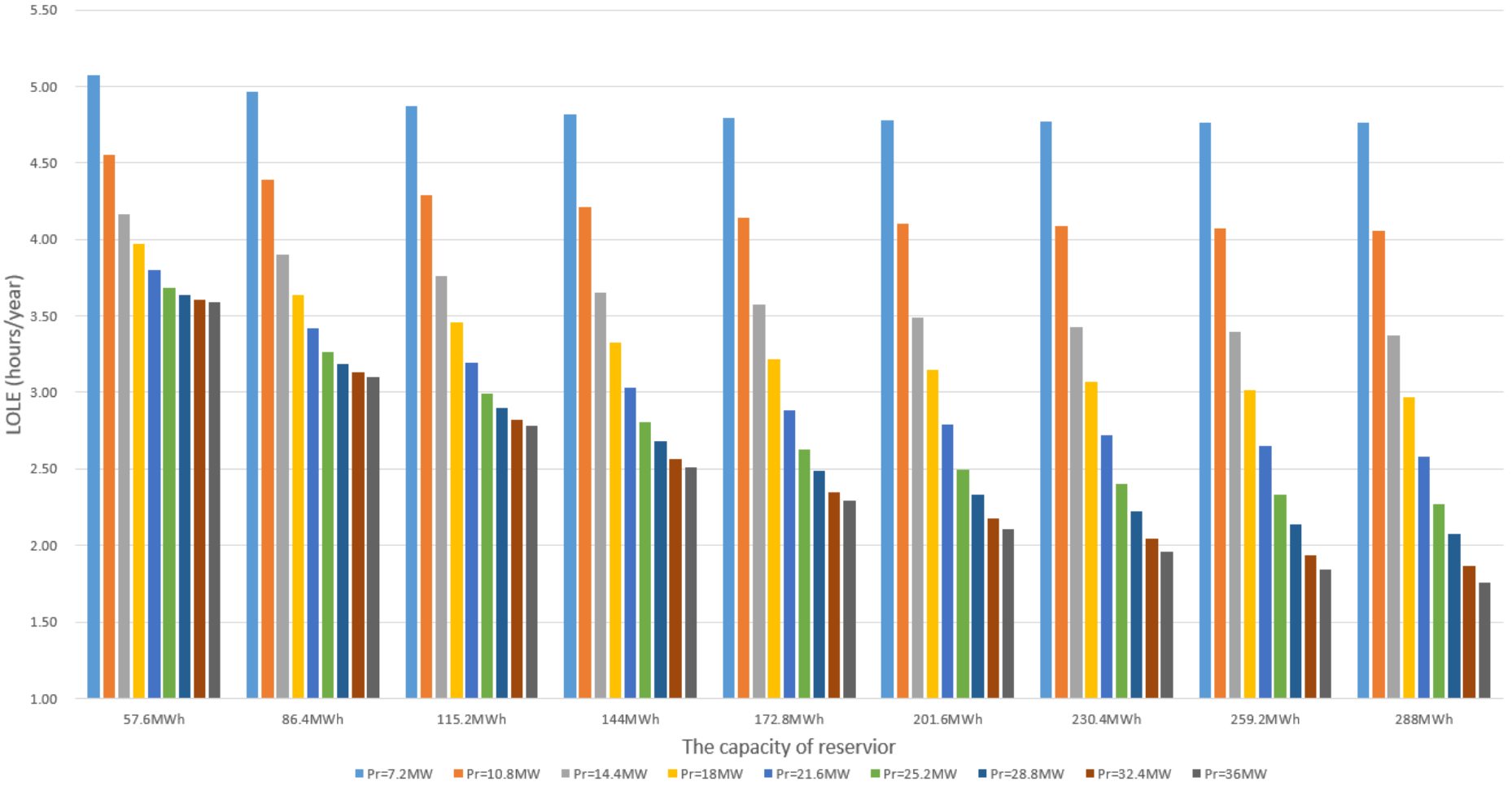

Figure 5.9: Effect of Capacity Scenarios on LOLE for Strategy 2 (3% dispatch rate)

By reviewing the power system reliability requirement with the capacity scenarios reliability results in Figure 5.9, it can be seen that many capacity scenarios for strategy 2 fulfilled the reliability requirement. It was necessary, therefore, to use RCBA to determine the optimal capacity HPS scenario.

Figure 5.10 and Table 5-7 show the RCBA indices variations when an HPS system was added to the power system through strategy 2. It can be seen from Figure 5.11 that TC increased linearly as generation capacity increased, while TB increased rapidly at first and then slowly rose to a fixed value. Therefore, for different generation capacities, the RCBA initially increased rapidly, then plateaued, before commencing a slow decline that was approximately linear. Reservoir capacity impact on the RCBA was similar to that of generation capacity.

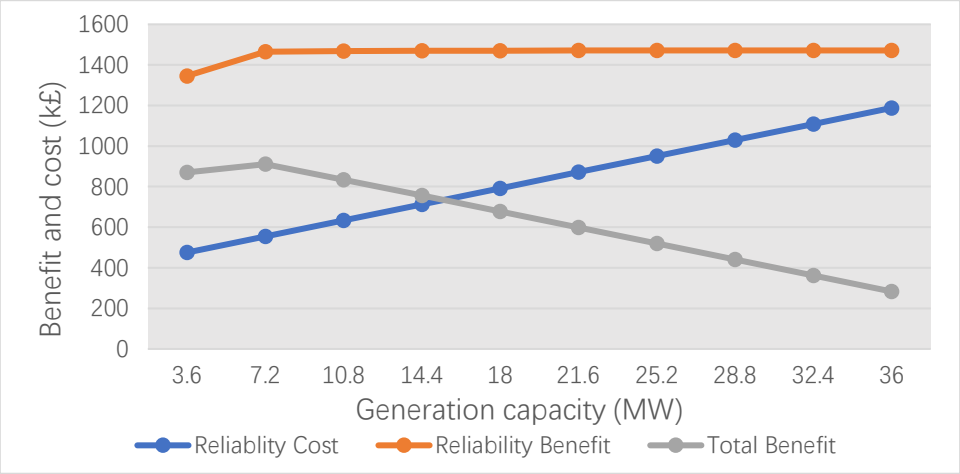

Figure 5.10: HPS generation capacity effect on the RCBA for strategy 2, at 144 MWh reservoir capacity

Table 5-7: HPS reservoir capacity effect for strategy 2 on the RCBA indices, at 18 MW generation capacity

HPS Reservoir Capacity (MWh)	RCBA Indices (k£)		
	RB	RC	TB
28.8	1457.14	475.2	981.94
57.6	1461.91	554.4	907.51
86.4	1465.10	633.6	831.50
115.2	1467.79	712.8	754.99
144	1470.11	792	678.11

In order to review the dispatch ratio upper limit for strategy 2, assuming that the system was incorporated into the HPS with the largest capacity scenario (36 MW, 288 MWh), the reliability evaluation results have been illustrated in Figure 5.11.

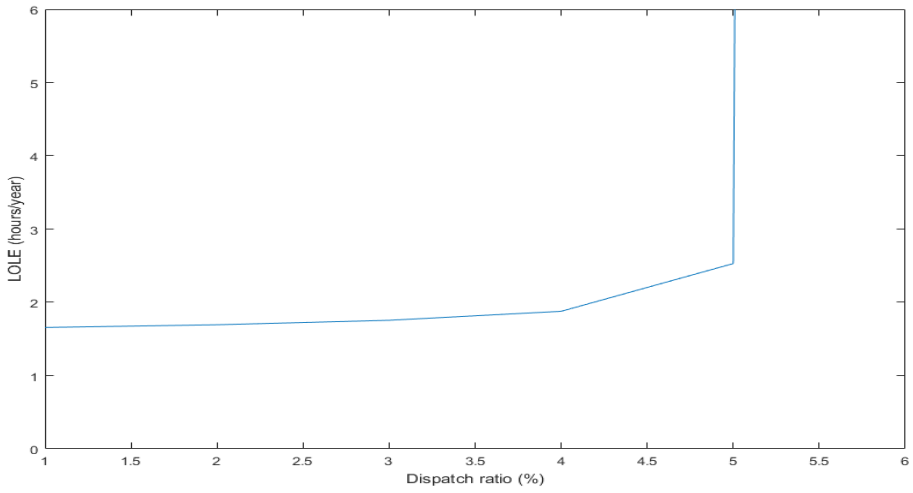

Figure 5.11: Dispatch ratio effect on LOLE for Strategy 2 (10% wind penetration)

In strategy 2, because there was no limitation on wind power output when power supply was insufficient, the increased dispatch ratio did not contribute to system reliability. As shown in Figure 5.11, when the dispatch ratio increased, the value of LOLE rose, slowly at first and then sharply. Further, the dispatch ratio had an upper limit. When its value exceeded this limit (here, 5%), neither scenario could maintain reliability at the original level, even by adding HPS.

The evaluation results achieved for the RCBA indicators, while gradually increasing the dispatch ratio from 1% to 5%, have been summarized in Table 5-8. Here, it can be seen that, under strategy 2, the dispatch ratio had the same effect on the RCBA index as it did under strategy 1, as the increased dispatch ratio led to a corresponding rise in the benefit achieved from using HPS.

Table 5-8: Dispatch ratio effect on RCBA for Strategy 2 (10% wind penetration)

Dispatch Ratio (%)	RCBA indices (k£)		
	RB	RC	TB
1	208.3014	1584	-1375.7
2	682.3824	1584	-901.618
3	1481.464	1584	-102.536
4	2611.648	1584	1027.648
5	4061.287	1584	2477.287

By applying the RCBA method to all capacity scenarios that satisfied the reliability requirements at each dispatch ratio, the TB for each scenario was obtained, with the optimal capacity scenario being that with the highest TB. The optimal capacity scenarios, and corresponding reliability and RCBA indices assessment results that meet the reliability requirements under each dispatch ratio, have been summarized in Table 5-9.

Table 5-9: The optimal capacity scenarios for each dispatch ratio on the RCBA, under Strategy 2 (10% wind penetration)

Dispatch ratio (%)	LOLE (hours/year)	P_{rate} (MW)	E_{rate} (MWh)	TB (k£)
1	3.77	14.40	86.40	-362.80
2	3.82	14.40	86.40	111.2683
3	3.90	14.40	86.40	910.28
4	3.94	14.40	115.20	1963.68
5	3.83	14.40	288.00	2948.60

Based on this comparison, the optimal capacity scenario from the ISO point of view, was (14.40 MW, 288.00 MWh), at the 5% dispatch ratio.

At the 10% wind penetration level, the reliability of the system requires that LOLE should be < 3.96 hours/year, so the optimum HPS capacities should be 14.40 MW and 288.00 MWh, under Strategy 2, with 5% dispatch ratio, to decrease wind power

fluctuation impact on the power system, and restore reliability to the original level, with maximum TB.

5.5.2.4 Comparison between strategy 1 and 2

Using the data in Figure 5.5 and Figure 5.9, the capacity scenario reliability indices under reservoir capacities of 144 MWh, 172.8 MWh and 201.6 MWh were selected, to compare the proposed WP-HPS cooperation method performance in reducing wind power integration influence, as shown in Figure 5.12. First, it can be seen from the figure that both WP-HPS cooperation strategies contributed positively to system reliability, and can effectively mitigate the negative impact of wind power volatility on reliability. In addition, the LOLE curve for strategy 2 was lower than that for Strategy 1, which meant that strategy 2 had higher system reliability—and a smaller LOLE value—using the same HPS capacity. This was because there were no limits on the maximum wind power output when power supply was insufficient, in strategy 2. Hence, strategy 2 can improve the reliability of the system from its original state, using a smaller HPS capacity scenario, and at the same dispatch ratio.

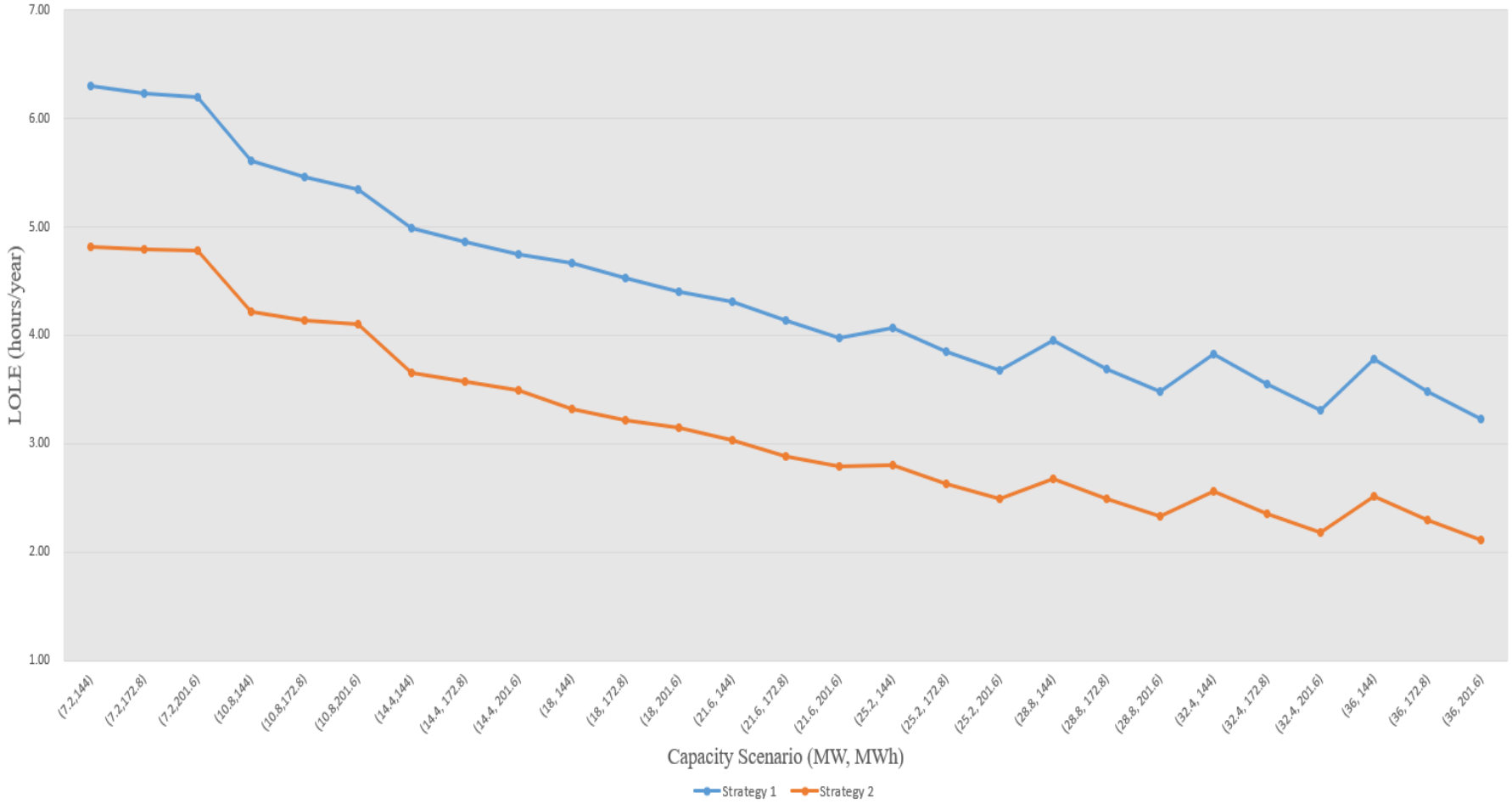

Figure 5.12: Effect of Capacity Scenarios on LOLE for strategy 1 and 2 at 3% dispatch ratio and 10% wind penetration level

It should be noted that, if wind power is used as a reserve power source when CGUs power generation is insufficient, wind power forecasting must be highly accurate, to prevent sudden decreases in wind power available generation capacity caused by wind speed changes. As described in Chapter 2, forecast errors are always present for a variety of reasons, and are typically in the order of 10–30%, so therefore, in strategy 1, wind power is only used as a power generation source, and there is no need to use a OR power supply, which sacrifices some reliability, but the prediction error has less impact on the system. In strategy 2, the system reliability is higher, but the wind power forecast error will have a certain impact on the system.

The optimal HPS capacity scenario for each strategy and relative RCBA result have been summarized in Table 5-10: here, it can be seen that strategy 2 can support a higher dispatch ratio while still meeting reliability requirements, which helps to increase wind power use, thereby achieving higher total benefits. This is achieved as HPS stores the surplus wind power to help achieve the balance between energy supply and demand of power system, so more wind power is utilized, as HPS.

Table 5-10: Optimal HPS capacity for each Strategy, at 10% wind penetration level

Strategy	Dispatch ratio (%)	P_{rate} (MW)	E_{rate} (MWh)	LOLE (hours/year)	TB (k£)
1	4	21.60	230.40	3.95	504
2	5	14.40	288.00	3.83	2948.60

5.5.2.5 Voltage amplitude of nodes in IEEE 30 Bus Test System with the WP-HPS cooperation method

The previous analysis in this section focus on the effect of the WP-HPS cooperation method under different strategies on the reliability of power systems with wind power. It can be concluded from the evaluation results that the proposed method has the ability to mitigate the negative impact of wind power volatility on the reliability of the power system, and the improvement of strategy 2 is better.

Whether the proposed method can be reliably operated in the system under strategy 2 remains to be proven. Therefore, this section will use the power flow calculations to analyze whether the voltage amplitude of each node in the test system meets the requirements for the node voltage. MATPOWER software is a package based on MATLAB package to solve the problem of power flow and optimize power flow. The 30 Bus Test System packages of Matpower software include detailed busbars data, branches data and generators data to facilitate power flow calculation. Through Matpower software, the voltage magnitude of each bus can be obtained.

Same as the evaluation result in Section 5.4.2, the wind penetration level was set to 10%. The optimal capacity scenario (14.4 MW, 288 MWh) of HPS is added to IEEE 30 Bus Test system, and corresponding dispatch ratio is 5%. This section will comprehensively analyze whether the proposed method can operate in the system from

the three scenarios of minimum load demand, average load demand and maximum load demand. In these three scenarios, wind power output is also divided into three situations: minimum wind power output, average wind power output and maximum wind power output, a total of nine cases. Due to the requirements of the dispatch ratio, the wind power actually absorbed by the system is adjusted according to the load demand. The specific data is summarized in Table 5-11.

Table 5-11: Various load scenarios and corresponding wind power conditions of IEEE 30 Bus Test System

Maximum Load demand (270 MW)	Maximum wind power output	13.5 MW
	Average wind power output	6.75 MW
	Minimum wind power output	0 MW
Average load demand (169 MW)	Maximum wind power output	8.45 MW
	Average wind power output	4.23 MW
	Minimum wind power output	0 MW
Minimum load demand (96 MW)	Maximum wind power output	4.8 MW
	Average wind power output	2.4 MW
	Minimum wind power output	0 MW

The output of HPS and CGUs will be adjusted according to the difference between the load and the wind power and the respective installed capacity. This section does not adopt the optimum power flow calculation. Due to the influence of the dispatch ratio, the wind power output accepted by the system is limited to X% of the load. The purpose

of this section is to verify that the proposed WP-HPS cooperation (strategy 2) method can operate in the power system, so the harsh situation is adopted, that is, the output of wind farms is injected into the grid from the same node, bus 17 is an example from a set of results where a selection of different nodes were used for injection of wind and HPS power.

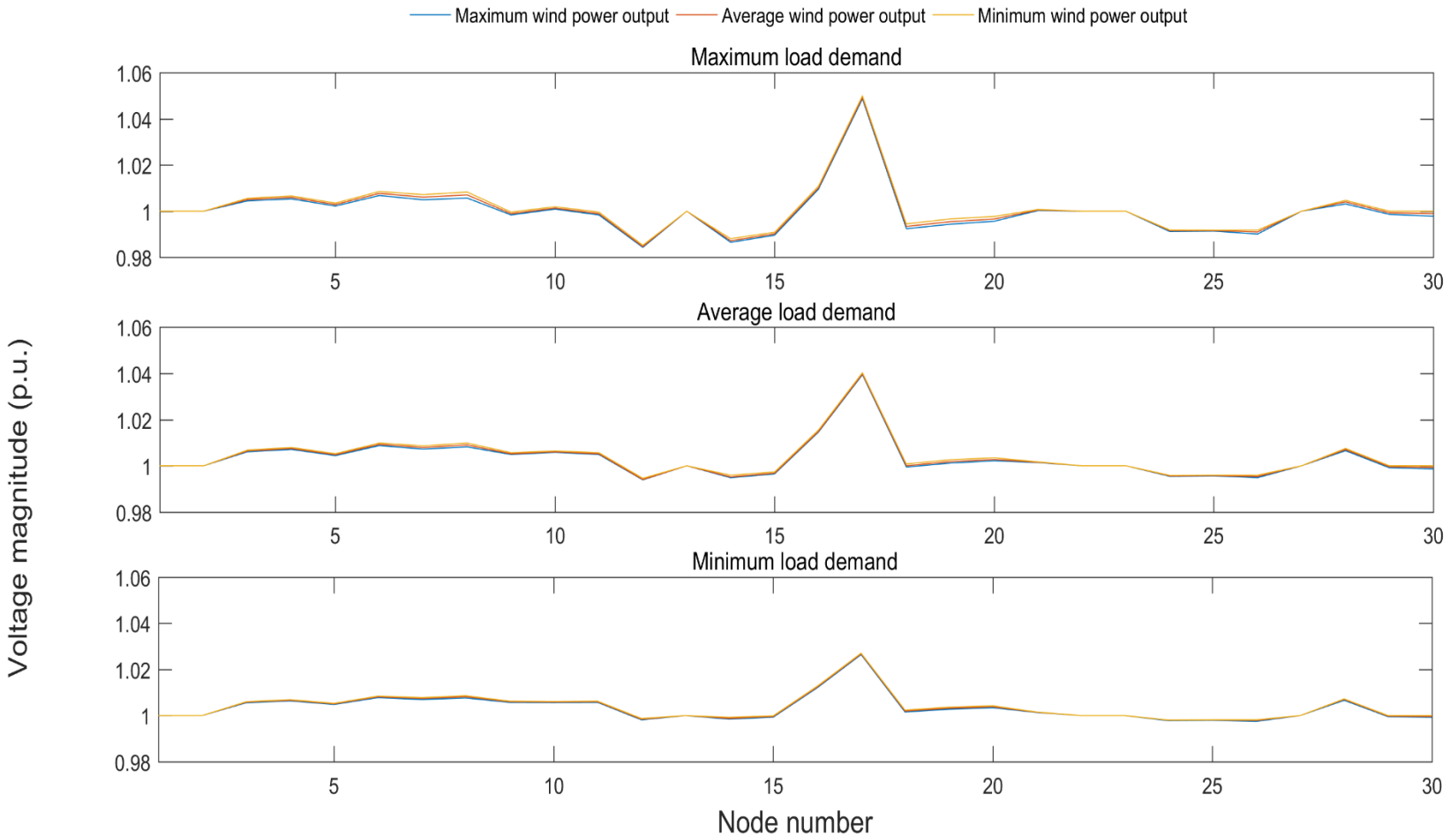

Figure 5.13: Voltage magnitude of each node of IEEE 30 Bus Test System for three wind power output situations under different load scenarios

Figure 5.13 illustrates the effects of different wind power outputs on the voltage amplitude of each node in the three load scenarios. It can be seen from the figure that in the three load scenarios, the change of wind power output has little effect on the voltage amplitude of each node of the system, but since the wind power is integrated into the grid through the node 17, the voltage amplitude of the node 17 is increased. Moreover, an increase in the load demand will increase the fluctuation of the voltage amplitude of the node. In general, the voltage amplitude of all nodes is between 0.98 and 1.05, which meets the voltage requirements of the system operation. Therefore, the WP-HPS cooperation method can operate reliably in the system.

5.6 Summary

In this chapter, the WP-HPS cooperation method has been fully analyzed. HPS modelling mathematical constraints, and a WP-HPS cooperation reliability evaluation process have been described in detail. RCBA has also been introduced in this chapter, to determine the optimal HPS capacity.

The analyses conducted in this chapter gave rise to the following conclusions:

(1) For a power system incorporating wind power, the SMCS method can effectively simulate system output and evaluate various reliability indicators. The results showed that wind power volatility will reduce the ability of the system to continue reliable power supply, and will increase the number of changes required to CGUs output, thereby reducing its efficiency.

(2) The WP-HPS cooperation method allows surplus wind power to be stored, through HPS, and provides power when the power supply is insufficient. Both of the control strategies analyzed can effectively alleviate negative wind power impact on the power system, and improve system reliability. Both HPS power generation capacity and reservoir capacity are positively related to system reliability, and an ISO can apply RCBA to determine the optimal capacity scenario, based on the reliability requirements of the system.

(3) From the perspective of reliability, Strategy 2 produced greater improvement in system reliability, and allowed use of a smaller capacity HPS scenario to fulfil system reliability requirements. This result came about as Strategy 1 imposed a strict limit on the amount of wind power that can be absorbed by the system, which reduced the impact of wind power prediction error, and also reduced system reliability, requiring larger capacity HPS to still satisfy reliability requirements.

Compared to strategy 1, the proposed WP-HPS cooperation (strategy 2) method can more effectively reduce the impact of wind power fluctuations, while maintaining the test system reliability at its original level. Later on, the WP-HPS cooperation (strategy 2) method will be trailed in a larger power system, to verify its feasibility and effectiveness at higher wind penetration levels.

Chapter 6

Reliability assessment of the WP-HPS cooperation method in IEEE 118 Bus Test System

6.1 Introduction

Chapter 5 analyzed the proposed WP-HPS cooperation method to alleviate wind power fluctuations with surplus wind power. This method not only improves system reliability and increases the utilization of wind power, but it also reduces the output fluctuation of CGUs. Two feasible cooperative strategies were compared using the IEEE 30 Bus Test System with a wind penetration level of 10%. The comparison results show that strategy 2 is better than strategy 1 in terms of reliability improvement; thus, strategy 2 is adopted in the analysis to improve system reliability.

In this chapter, the proposed WP-HPS cooperation (strategy 2) method is examined in the larger power system IEEE 118-Bus Test System. This test system is a simplified model of the power system in the Midwest United States in December 1962 and is widely used in the power system industry. Therefore, the test system has sufficient system data to verify the effectiveness of this method.

Unlike the test in the Chapter 5 which aims to examine the ability of the WP-HPS cooperation (strategy 2) method to improve the reliability of power system with wind power, the test in this chapter is divided into long-term planning and short-term operation, with the durations of one year and 24 hours respectively.

The long-term planning investigation is to test whether the WP-HPS cooperation (strategy 2) method can still effectively mitigate the impact of wind power fluctuation on system reliability when the wind penetration level is increasing. Six different wind penetration levels are used to evaluate the system reliability improvement of the proposed method, and the optimal capacity scenario and power generation ratio are determined based on RCBA.

In the short-term operation test, power flow analysis of daily load curve is carried out to power system using the proposed WP-HPS cooperation (strategy 2) method. From small to large, four different wind penetration levels are used to examine the impact of this method on network losses in the short-term system operation.

The structure of this chapter is as follows. The details of the data for each power component in the IEEE 118-Bus Test System and the six different wind penetration level cases are briefly described in Section 6.2. In Section 6.3, the improvement of the reliability of six different wind penetration levels by the WP-HPS cooperation (strategy 2) method is analyzed based on the simulation results. Section 6.4 analyzes the impact of the WP-HPS cooperation (strategy 2) method on network losses.

6.2 Description of IEEE 118 Bus System

In this section, the use of the IEEE 118-Bus Test System to evaluate system reliability is discussed, and the use of the proposed WP-HPS cooperation (strategy 2) method to mitigate the negative impact of wind power is analyzed. Also analyzed is the impact of power dispatch ratio, wind penetration level, and scheme maintenance on reliability. The one-line diagram of the IEEE 118-Bus Test System is shown in Figure 6.1 [161]. The basic system data are summarized in Table 6-1.

Table 6-1: IEEE 118-Bus Test System basic data

Buses	118
Generators	54
Load	99
Peak load	7780 MW
Minimum load	2460 MW
Total generation capacity	9000 MW

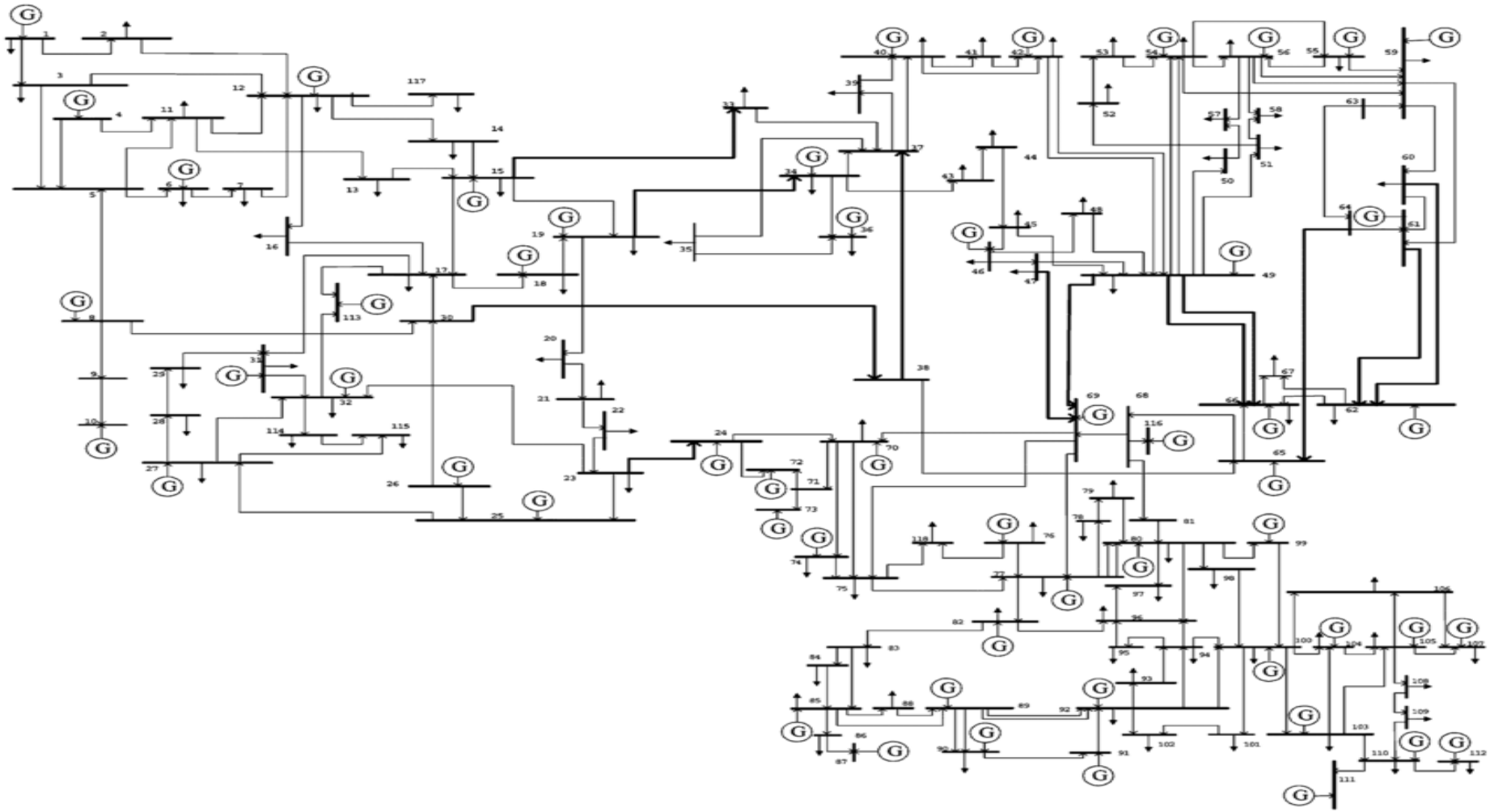

Figure 6.1: One-line diagram of IEEE 118-Bus Test System [161]

(1) Conventional generating system

The reliability parameters of the CGUs are modified based on IEEE Reliability Test System (RTS) [32] for SMCS (Sequential Monte Carlo Simulation). It is assumed that the reliability parameters of the generators with the same rated power are the same. Table 6-2 summarizes the reliability parameters of CGUs .

Table 6-2: Reliability data of CGUs in IEEE 118-Bus Test System

Rated Output (MW)	No. of Generators	MTTF (hours)	Failure rate per year	MTTR (hours)
400	6	950	7.9	150
350	8	1050	7.6	100
200	8	900	9.2	50
100	12	1150	7.3	50
50	20	1960	4.4	20

(2) Wind power system

Assuming that the wind conditions of the wind farms in the IEEE 118-Bus Test System are the same as those in Chapter 5, the average wind speed is 7 m/s, and the Weibull shape parameter is 2, the wind speeds of the WTGs in the same wind farm are the same, and the wind conditions of each wind farm are independent of each other. The output

of the WTG can then be obtained by the Weibull distribution and SMCS. All WTGs performance and reliability parameters are the same and are summarized in Table 6-3.

Table 6-3: Reliability data of WTGs in IEEE 118-Bus Test System

Rated Output	Cut-in Speed (m/s)	Rated Speed (m/s)	Cut-out Speed (m/s)	MTTF (hours)	Failure Rate per Year	MTTR (hours)
5 MW	4 m/s	12 m/s	25	2620	3	300

It is assumed that the IEEE 118-Bus Test System has six wind farms and the wind turbines are evenly distributed across these wind farms. The system reliability of this thesis is the adequacy of the power generation system (Chapter 3). When the available output of the power generation system is less than the load demand, the system is considered to have insufficient power supply. The location of the injection node of the wind farm does not change the available output of the wind farm, so in the reliability analysis, the injection nodes of the wind farm will not affect the adequacy of the power generation system. In this thesis, the impact of the different injected nodes is the node voltage and network loss. In Chapter 5, only a low wind penetration level was studied for the test system. In this chapter, six different wind penetration level cases are utilized to analyze the effective of WP-HPS cooperation (strategy 2) method to mitigate wind power fluctuations and to increase system reliability to an acceptable level. As described in Chapter 5, in this thesis, the wind penetration level is defined as the ratio of the installed capacity of wind power to the total installed generation capacity of the

system. With the fixed total installed generation capacity, the integrated wind capacity replaces the equivalent of CGUs capacity. The number of CGUs remains unchanged, and the rated capacity of each conventional generators will decrease according to the level of wind penetration level.Table 6-4 summarizes the installed capacity of the power generation system under each wind penetration level.

Table 6-4: Basic generation capacity data for cases 1 to 6

Case No.	1	2	3	4	5	6
Wind penetration	10%	15%	20%	30%	40%	50%
Wind turbine numbers	180	270	360	540	720	900
Wind generation capacity (MW)	900	1350	1800	2700	3600	4500

(3) Load demand

The load demand variation curve is the same as utilized in Chapter 4, is shown in Figure 4.11. It is based on the UK load demand in 2018 which has been modified so that the peak load and the minimum load correspond to those used on the IEEE 118 bus system.

(4) Reliability cost-benefit analysis parameters

A reliability cost-benefit analysis (RCBA) will be used to determine the optimal capacity scenario for the system reliability requirements, and the parameters of RCBA are the same as in Chapter 5 (see Table 5.2 in detail).

6.3 Capacity planning of WP-HPS cooperation (strategy 2) method

From the perspective of long-term planning, the reliability evaluation results of the IEEE 118-Bus Test System can be divided into the following three categories:

1. Use the SMCS method described in Section 3.4.2.2 to evaluate the impact of the six wind penetration levels mentioned above on the reliability of the power system.

2. Use the WP-HPS cooperation (strategy 2) method (presented in Section 5.3.1) to mitigate the negative effects on wind power at each wind penetration level and to assess the impact of dispatch ratio and HPS capacity on reliability.

3. Calculate total benefit (TB) by the RCBA method (presented in Section 5.3.2) and determine the optimal capacity scenario for the WP-HPS cooperation (strategy 2) method under each wind penetration level.

6.3.1 Impact of wind penetration level on system reliability

Combined with the reliability model time series and the rated capacity of CGUs, the time series of the available generation capacity of CGUs can be simulated by SMCS which has been explained in detail in section 3.4.2. The available generation time series of wind power is obtained by the combination of the wind speed time series simulated by the Weibull distribution, the wind speed power conversion equation, and SMCS. When the total available generation capacity is less than the load demand, the system has an insufficient power supply. Table 6-5 summarizes the results of the reliability index loss of load expectation (LOLE), loss of energy expectation (LOEE), and loss of load frequency (LOLF).

Table 6-5: Reliability indices evaluation results of IEEE 118-Bus Test System

Wind penetration level	0%	10%	15%	20%	30%	40%	50%
LOLE (hours/year)	3.80	24.41	59.51	134.61	514.51	1425.46	2950.98
LOEE (MWh/year)	820.33	6238.38	16926	43312	218401	782912	2122358
LOLF (occ./year)	1.43	9.89	25.53	59.68	223.51	597.85	1088.85

Table 6-5 shows that the replacement of CGUs by WTGs has a negative impact on system reliability, and, as the wind penetration level increases, the reliability of the system continues to decrease. This is because the available power generation capacity of wind power is unstable, which causes fluctuations in the total power generation

capacity of the power system. As the wind penetration level increases, the OR capacity of the system continues to decrease, this fluctuation becomes more and more obvious, and the reliability of the system decreases.

Table 6-6 summarized a comparison of the reliability indices LOLE for each wind penetration level with the original system. This table shows that the wind penetration level significantly reduces system reliability. When the wind penetration level increases by five times (from 10% to 50%), the value of the system reliability index LOLE increases by 120 times (from 24.41 to 2950.98 h/year), and one-third of the year there is insufficient power supply. Therefore, as the wind penetration level increases, the system's demand for OR becomes increasingly urgent.

Table 6-6: Comparison of LOLE for each wind penetration level with the original system

Wind penetration level (%)	LOLE (hours/year)	Increase degree
10	3.80→24.41	6.43 times
15	3.80→59.51	15.66 times
20	3.80→134.61	35.43 times
30	3.80→514.51	135.42 times
40	3.80→1425.46	375.17 times
50	3.80→2950.98	776.67 times

6.3.2 Promotion of system reliability by the WP-HPS cooperation (strategy 2) method

The purpose of the WP-HPS cooperation (strategy 2) method as stated in Chapter 5 is threefold. First, reduce the impact of wind power volatility on the power system through the pumping and generating actions of HPS. Second, reduce the waste of wind power through the cooperation of HPS and wind power. Finally, smooth the output fluctuation of CGUs through the dispatch ratio, improving the coal combustion efficiency and service life of CGUs.

The WP-HPS cooperation (strategy 2) method for the IEEE 118-Bus Test System was evaluated under each wind penetration level, and the evaluation results are described by the capacity scenario (CS), which can be expressed as (P_{rate},E_{rate}). Also, the installed wind power capacity is taken as the upper limit of HPS generation capacity to evaluate the impact of the WP-HPS cooperation (strategy 2) on the system reliability. HPS reservoir capacity is generally eight to twenty times that of the installed capacity [160], this chapter is to analyze the maximum wind penetration level of power system that the proposed WP-HPS cooperation (strategy 2) method could maintain to original reliability level, twenty times the WP installed capacity is taken as the upper limit of the HPS reservoir capacity. According to the evaluation results in Section 6.3.1, the reliability index LOLE of the original system is 3.8 hours/year. This value is set to the

target that the power system with wind power needs to satisfy after the WP-HPS cooperation (strategy 2) method is applied to the system.

To shorten the simulation time, the dispatch ratio starts from 0. 5%, increasing by 0.5% each time, and the process continues until even the maximum capacities of HPS cannot meet the system reliability requirements. In addition, the research results in Chapter 5 show that the capacity of HPS plays an important role in the reliability of the system. If its capacity is too small, although it can improve the reliability of the system, it is difficult to achieve the reliability level required by the power system. Hence, 0.6 times the wind power installed capacity was taken as the basis generation capacity of HPS to allow an increment of 0.1 times each time until the upper limit is reached so that a total of five kinds of possibility in terms of HPS power generation capacity can be generated. The same method is applied when the reservoir capacity is chosen, leading to five kinds of possibilities in terms of reservoir capacity.

Case 1: 10% wind penetration level

The dispatch ratio not only affects the amount of wind power directly absorbed by the system but also affects the reliability of the system. It is assumed that the system is incorporated into the HPS with the largest capacity scenario (900 MW, 18,000 MWh) to analyze the upper limit of the dispatch ratio, the reliability evaluation results of different dispatch ratios are shown in Figure 6.2.

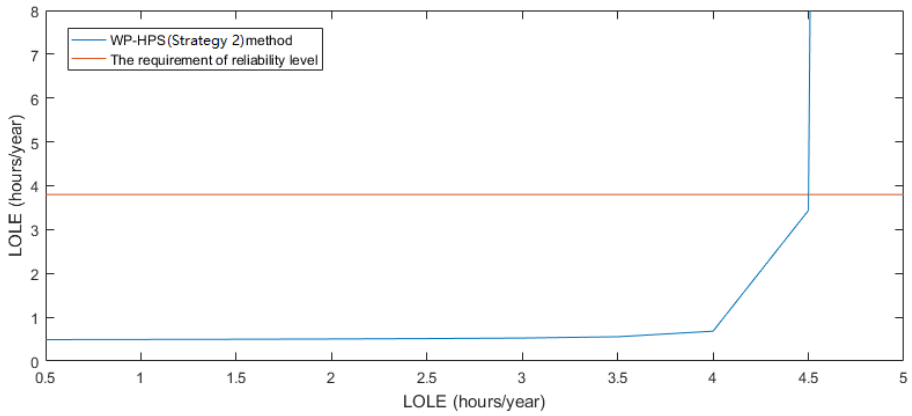

Figure 6.2: Effect of dispatch ratio on reliability (10%)

Because there was no limitation on the wind power output when the power supply was insufficient, the increase in the dispatch ratio did not contribute to the system reliability. As shown in Figure 6.2, when the dispatch ratio increased, the value of LOLE rose slowly at first and then sharply. Furthermore, the dispatch ratio had an upper limit. When its value exceeded this limit (in this case, the value was 4.5%), even the largest capacity scenario could not maintain reliability at the required level.

As discussed in Chapter 5, the larger the value of dispatch ratio, the more wind power is absorbed by the system, and the higher efficiency of wind power, so the upper limit of the dispatch ratio (4.5%) is applied to the system. Figure 6.3 summarizes all capacity scenarios for and corresponding reliability assessment results for the test system with 10% wind penetration level.

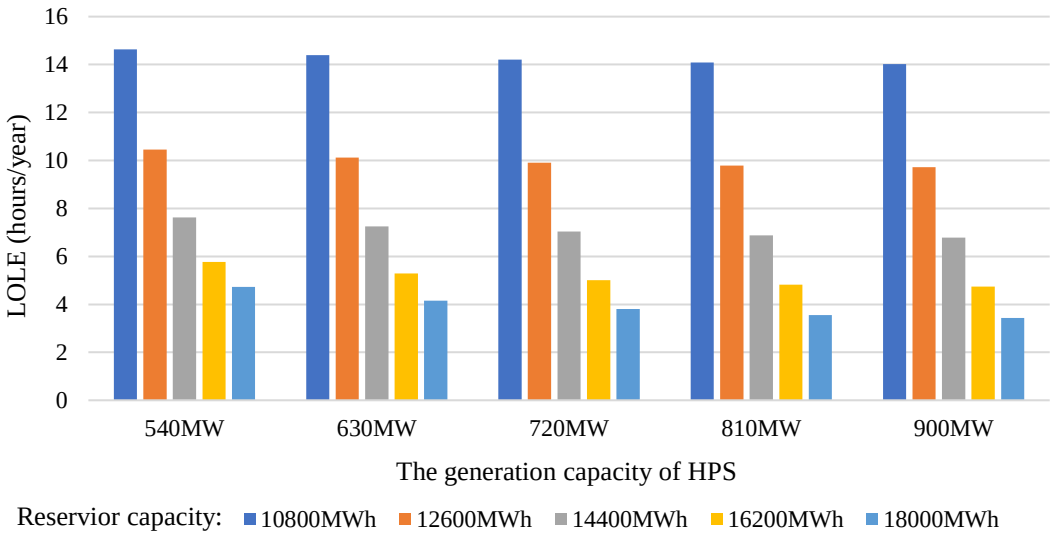

Figure 6.3: Effect of capacity scenarios of HPS on reliability (10%)

Figure 6.3 clearly shows the improvement of the system reliability by the WP-HPS cooperation (strategy 2) method. The added generation and reservoir capacity of the HPS improved the reliability of the power system; however, as the generation capacity increased, the improvement in system reliability decreased. Therefore, improving the reliability of the system cannot done by increasing the reservoir or generation capacity of HPS blindly — it needs a reasonable combination of HPS generation capacity and reservoir capacity.

The reliability requirement of the power system is LOLE less than 3.80 hours/year, there are three capacity scenarios that meet this reliability requirement. These suitable capacity scenarios and associated TB are summarized in Figure 6.4 to determine the optimal capacity scenario.

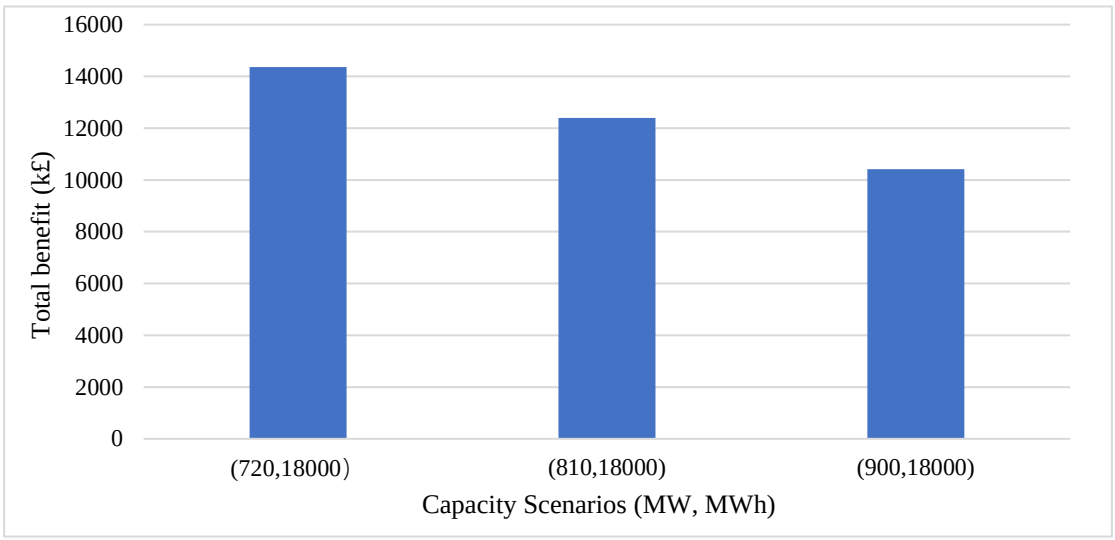

Figure 6.4: Total benefit of suitable capacity scenarios of HPS (10%)

As Figure 6.4 shows, the capacity scenario (720 MW, 18000 MWh) can obtain better TB. It can be summarized from the perspective of an independent system operator (ISO): at 10% wind penetration level, the reliability of the system requires that LOLE should be smaller than 3.80 hours/year, and the optimal HPS capacities should be 720 MW and 18000 MWh. The dispatch ratio of the WP-HPS cooperation (strategy 2) method is 4.5% dispatch ratio and can decrease the impact of wind power fluctuation on the power system and can return the reliability to the original level with better TB, and the corresponding CR is 1.85%.

Case 2: 15% wind penetration level

It is assumed that the system is incorporated into the HPS with the largest capacity scenario (1350 MW, 27,000 MWh) to analyze the upper limit of the dispatch ratio for

the WP-HPS cooperation (strategy 2) method. The reliability evaluation results of different dispatch ratios are shown in Figure 6.5.

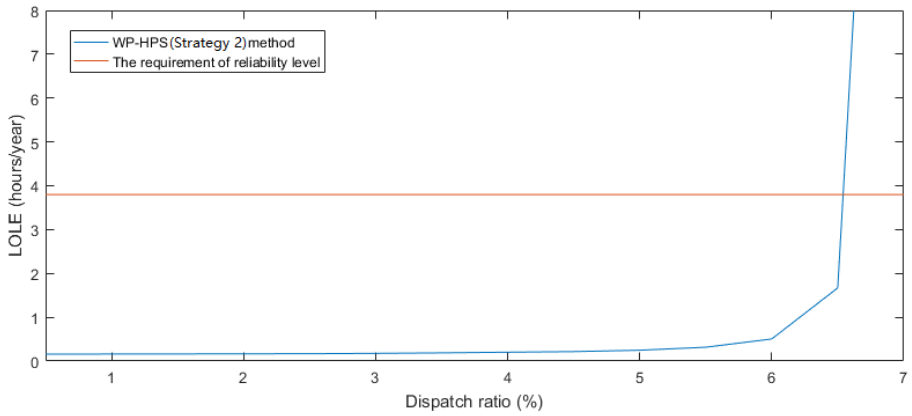

Figure 6.5: Effect of dispatch ratio on reliability (15%)

Figure 6.5 shows that when the dispatch ratio is increased, the value of LOLE rose, slowly at first and then sharply. Furthermore, the dispatch ratio had an upper limit. When the dispatch ratio exceeded 6.5% and even with the largest capacity scenario still could not maintain to required reliability level.

The upper limit of the dispatch ratio (6.5%) for the WP-HPS cooperation (strategy 2) method was applied to the system. Figure 6.6 summarizes all capacity scenarios of HPS and corresponding reliability assessment results for the power system with 15% wind penetration level.

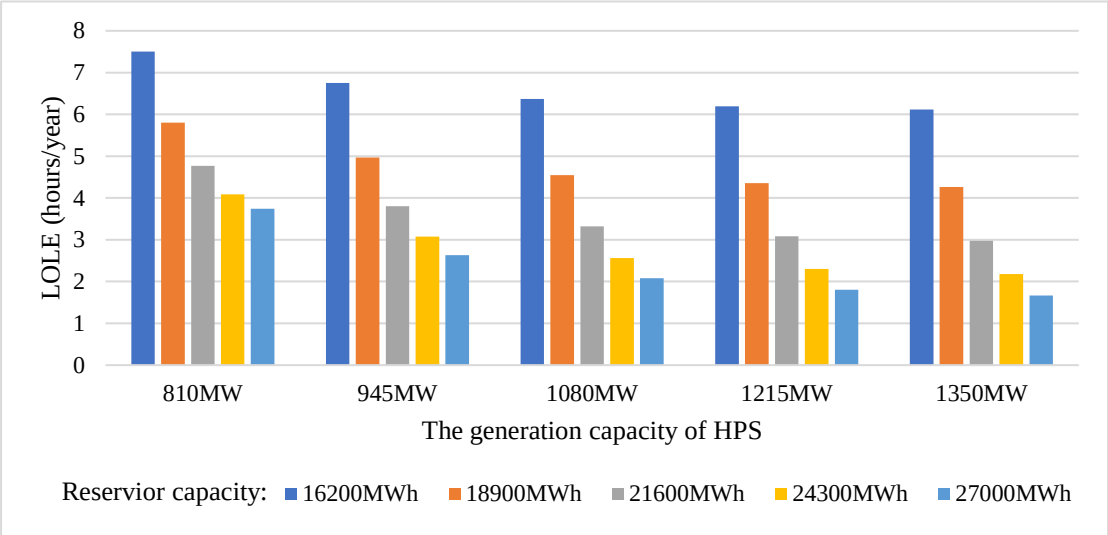

Figure 6.6: Effect of capacity scenarios of HPS on reliability (15%)

Figure 6.6 clearly shows that the added generation and reservoir capacity of the HPS improved the reliability of the power system. As mentioned above, the reliability requirement of the power system is LOLE less than 3.80 hours/year, and there are 12 capacity scenarios that meet this reliability requirement. The results of RCBA to determine the optimal capacity scenario are shown in Figure 6.7.

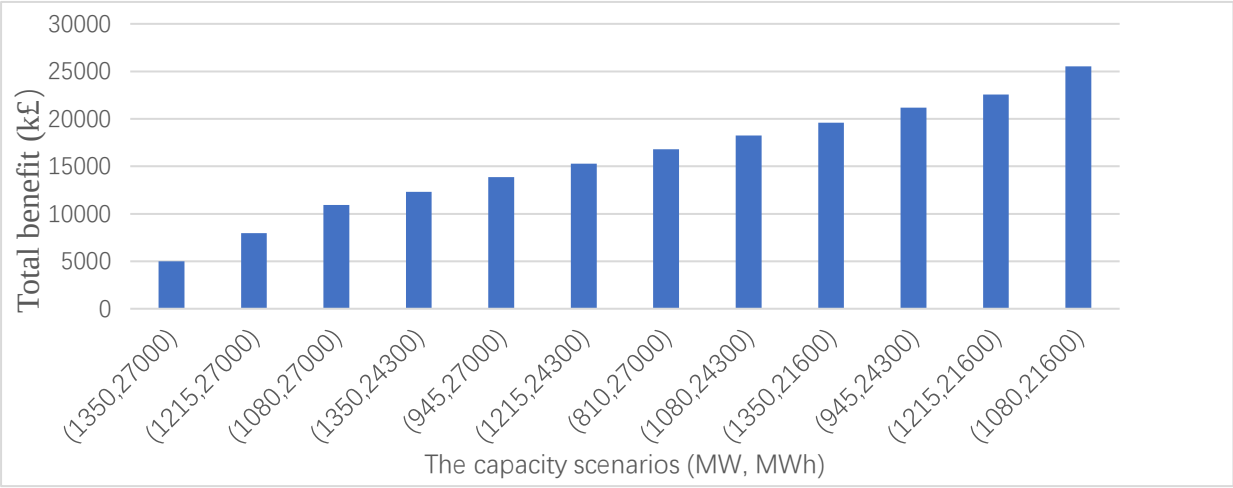

Figure 6.7: Total benefit of suitable capacity scenarios of HPS (15%)

As Figure 6.7 shows, the capacity scenario (1080 MW, 21,600 MWh) can obtain the maximum TB. It can be summarized from the perspective of an ISO: at 15% wind penetration level, the reliability of the system requires that LOLE should be smaller than 3.80 hours/year, and the optimal HPS capacities should be 1080 MW and 21600 MWh respectively with a 6.5% dispatch ratio. This scenario could decrease the impact of WP fluctuation on the power system and return the reliability to the original level with maximum TB, and the corresponding CR is 13.40%.

Case 3: 20% wind penetration level

It is assumed that the system is incorporated into the HPS with the largest capacity scenario (1800 MW, 36,000 MWh) to analyze the upper limit of the dispatch ratio for WP-HPS cooperation (strategy 2) method, and the reliability evaluation results are summarized in Figure 6.8.

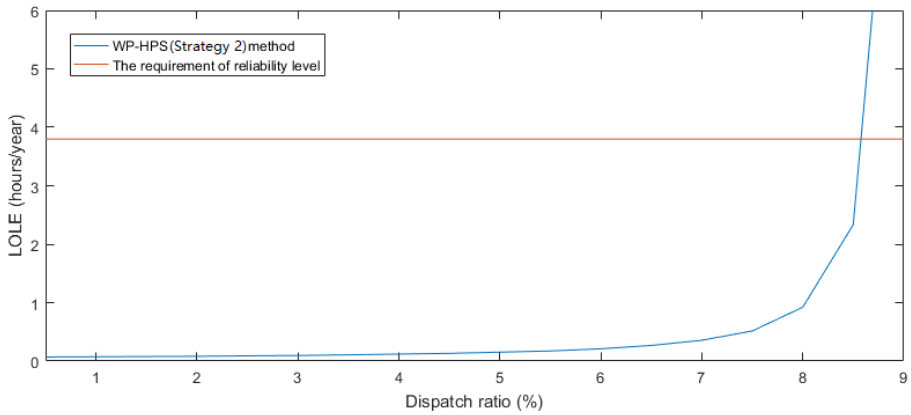

Figure 6.8: Effect of dispatch ratio on reliability (20%)

As shown in Fig 6.8, when the dispatch ratio increased, the value of LOLE rose, slowly at first and then sharply. Furthermore, the dispatch ratio had an upper limit. When its value exceeded 8.5% at a 20% wind penetration level, even the largest-capacity scenario could not maintain reliability at the required level.

The upper limit of the dispatch ratio (8.5%) was applied to the WP-HPS cooperation (strategy 2) method. Figure 6.9 summarizes all capacity scenarios and corresponding reliability assessment results for the test system with 20% wind penetration level.

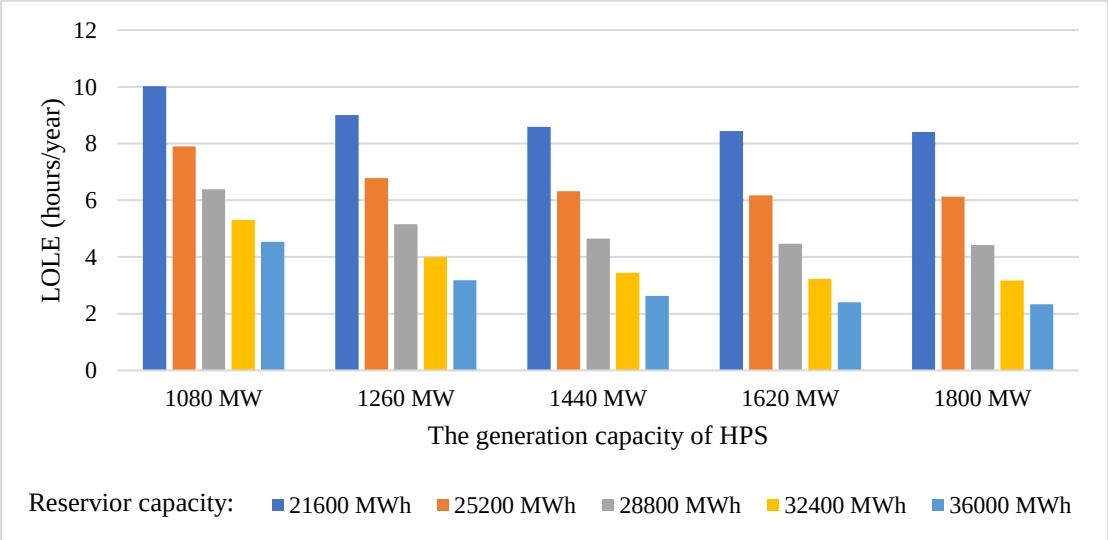

Figure 6.9: Effect of capacity scenarios of HPS on reliability (20%)

Figure 6.9 clearly shows that the impact of HPS capacity on system reliability as the capacity of HPS increases, the value of LOLE continues to decline. The reliability requirement of the power system is LOLE less than 3.80 hours/year, and there are seven capacity scenarios that meet this reliability requirement. These suitable capacity

scenarios and associated TB are summarized in Figure 6.10 to determine the optimal capacity scenario.

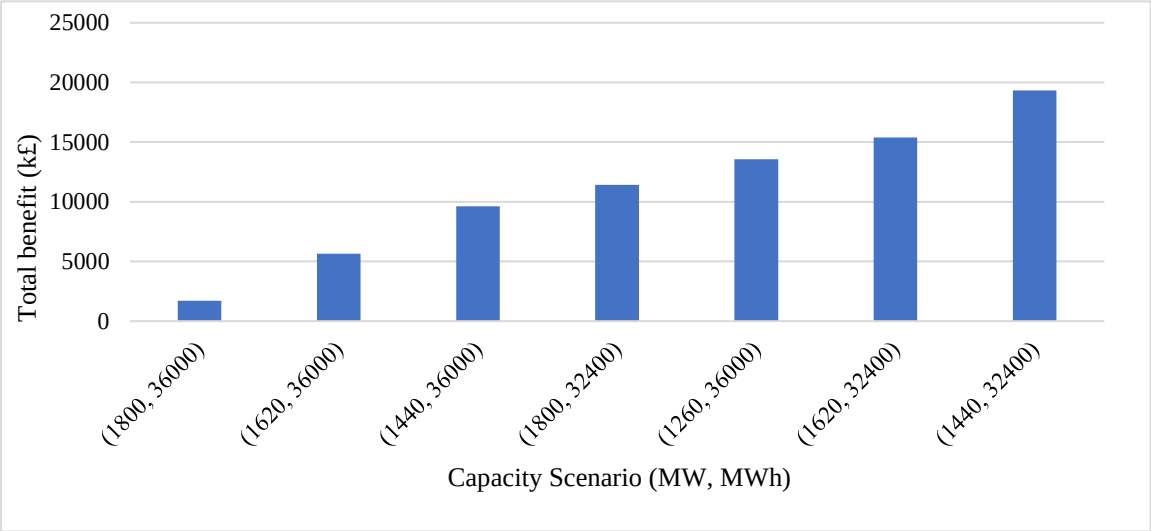

Figure 6.10: Total benefit of suitable capacity scenarios of HPS (20%)

Figure 6.10 shows that the capacity scenario (1440 MW, 32,400 MWh) can obtain the maximum TB. It can be summarized from the perspective of an ISO: at a 20% wind penetration level, the reliability of the system requires that LOLE should be smaller than 3.80 hours/year. The optimal HPS capacities should be 1440 MW and 32,400 MWh for the WP-HPS cooperation (strategy 2) method. An 8.5% dispatch ratio can decrease the impact of wind power fluctuation on the power system and retrieve the reliability to the original level with maximum TB, and the corresponding CR is 20.59%.

Case 4: 30% wind penetration level

It was assumed that the system is incorporated into the HPS with the largest capacity scenario (2700 MW, 54,000 MWh) to analyze the upper limit of the dispatch ratio, and the reliability evaluation results of different dispatch ratios are shown in Figure 6.11.

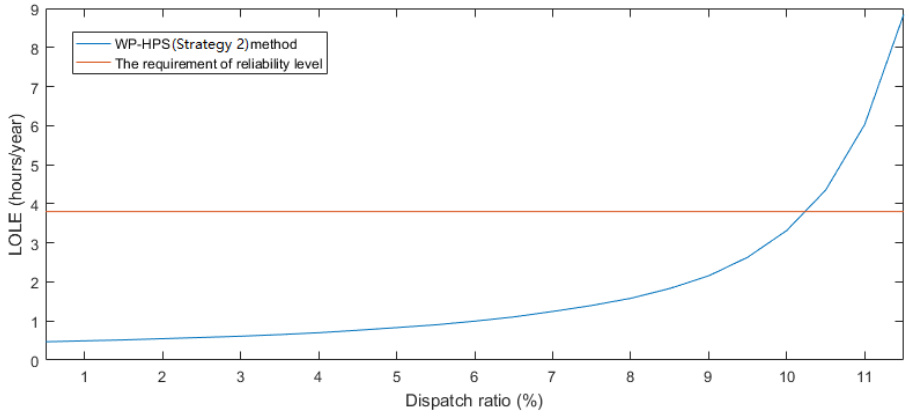

Figure 6.11: Effect of dispatch ratio on reliability (30%)

This figure shows that, if an HPS with the same installed capacity as WP is added to the system, the LOLE still can be smaller than 3.80 hours/year with the WP-HPS cooperation (strategy 2) method. This means the proposed method can improve the reliability of power systems with 30% wind penetration level to the required level. The maximum value of the dispatch ratio is 10%.

The upper limit of the dispatch ratio (10%) was applied to the system. Figure 6.12summarizes all capacity scenarios and corresponding reliability assessment results for the test system with 30% wind penetration level.

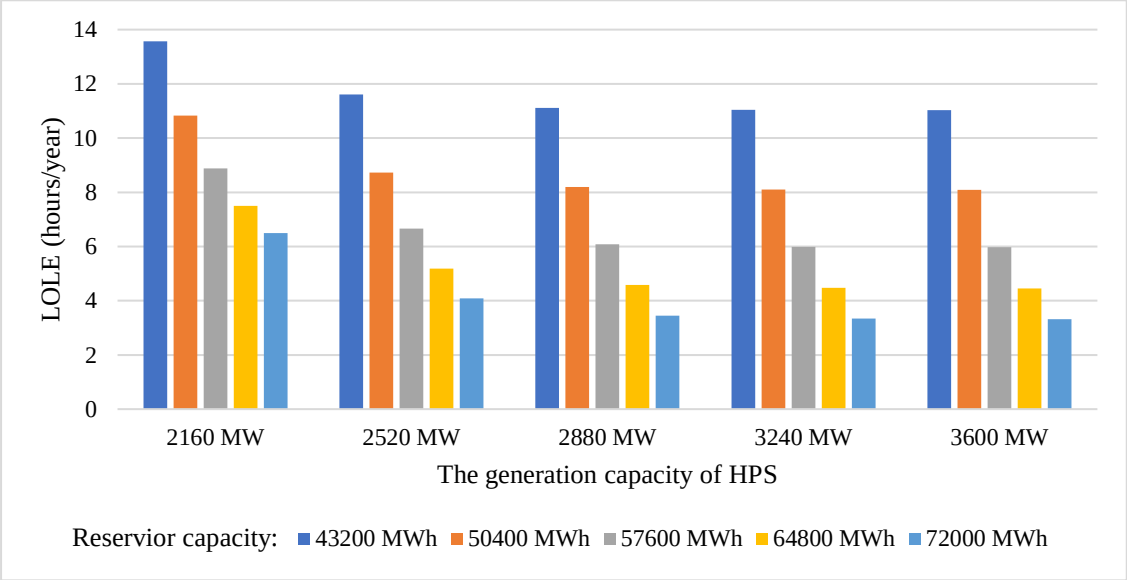

Figure 6.12: Effect of capacity scenarios of HPS on reliability (30%)

Figure 6.12 shows that, as the capacity of HPS increases, the value of LOLE continues to decline. The reliability requirement of the power system is LOLE which should be less than 3.80 hours/year, and there are three capacity scenarios that meet this reliability requirement. These suitable capacity scenarios and the associated TB are summarized in Figure 6.13 to determine the optimal capacity scenario.

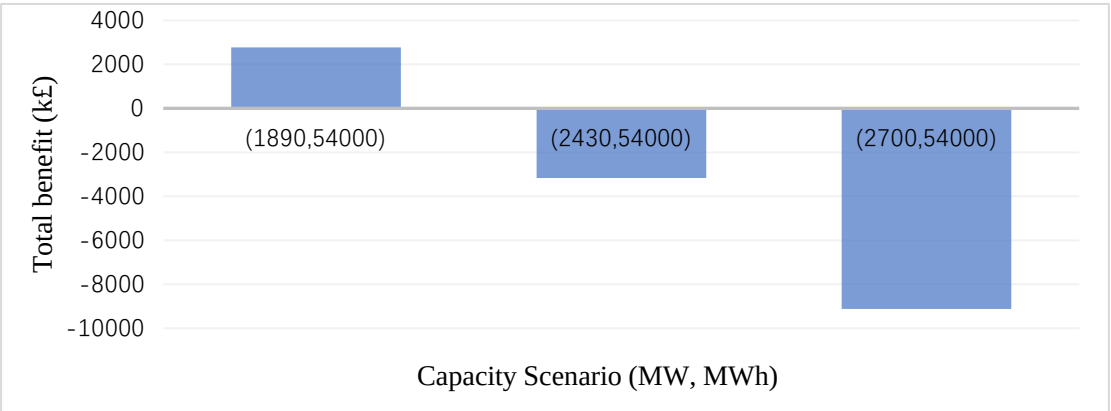

Figure 6.13: Total benefit of suitable capacity scenarios of HPS (30%)

As Figure 6.13 shows, the capacity scenario (1890 MW, 54,000 MWh) can obtain the maximum TB. Besides that, unlike in the previous cases, TB of two capacity scenarios are less than 0 here, which means that the benefits of improving reliability are less than the cost. Although it can be improved to the reliability level of the original system, it is not worthwhile financially. The results can be summarized below.

At 30% wind penetration level, the reliability of the system requires that LOLE should be smaller than 3.80 hours/year, and the optimal HPS capacities should be 1890 MW and 54,000 MWh. This will allow the WP-HPS cooperation (strategy 2) method with 10% dispatch ratio to decrease the impact of WP fluctuation on the power system and return the reliability to the original level with maximum TB. The corresponding CR is 33.51%.

Case 5: 40% wind penetration level

It was assumed that the system is incorporated into the HPS with the largest capacity scenario (3600 MW, 72,000 MWh) to analyze the upper limit of the dispatch ratio, and the reliability evaluation results of different dispatch ratios are shown in Figure 6.14.

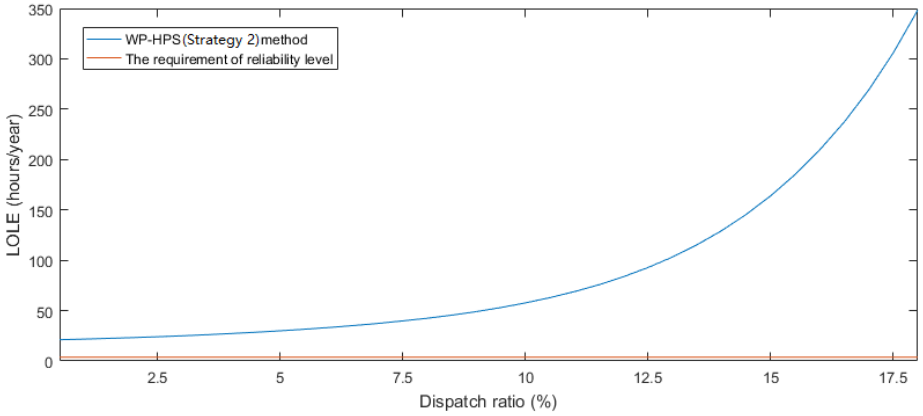

Figure 6.14: Effect of dispatch ratio on reliability (40%)

This figure shows that, even if an HPS with the same installed capacity as WP is added to the system, the minimum LOLE is 21.12 hours/year, which is much larger than the required system reliability level, and the reliability cannot be improved to the required level. There are two solutions without increasing the total installed capacity.

a) Increase the capacities of HPS regardless of cost

Based on the scenario capacity (3600 MW, 72,000 MWh), one can continue to increase HPS capacity until system reliability meets the requirements. The reliability evaluation results are shown in Figure 6.15.

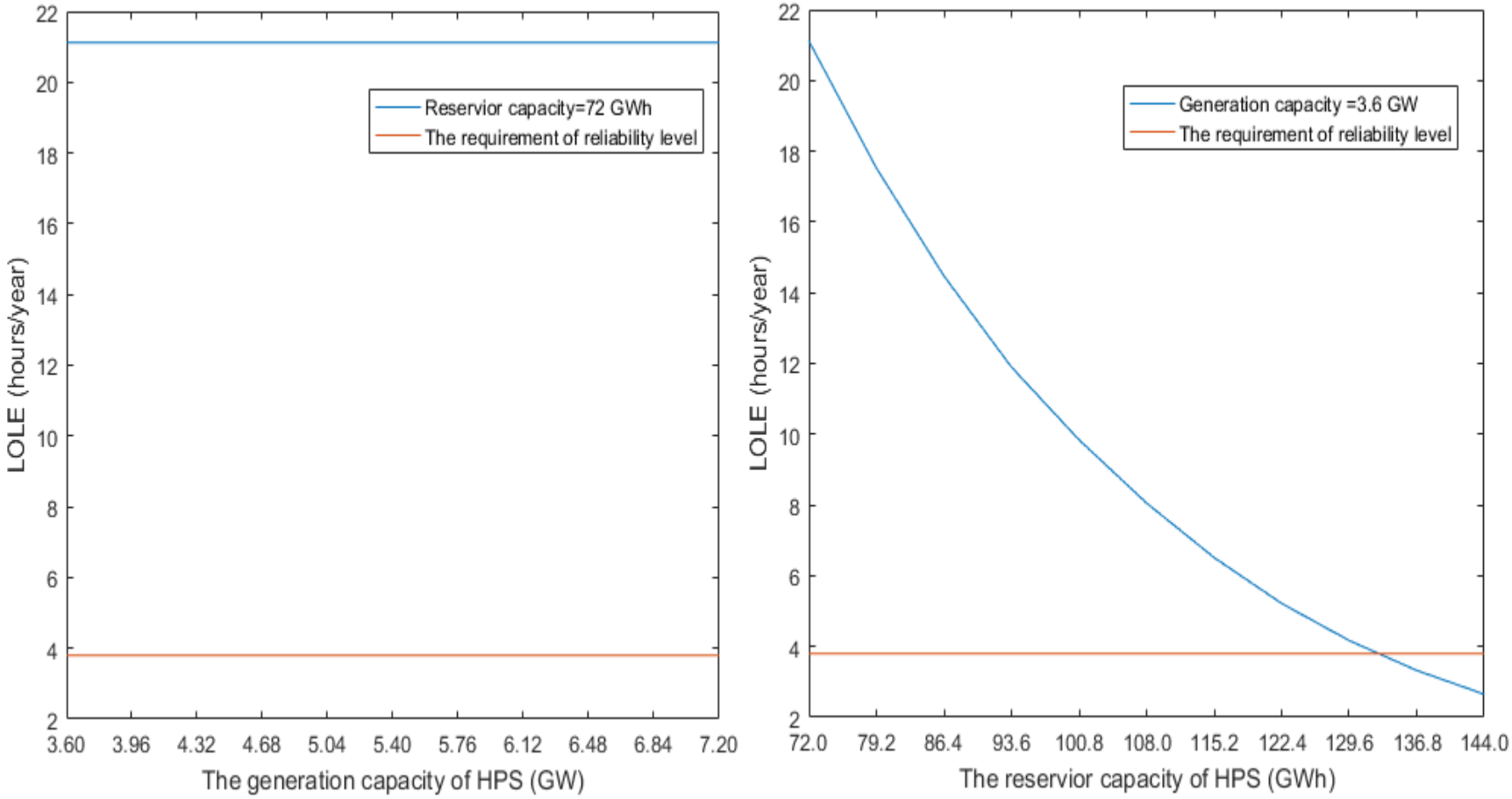

Figure 6.15: Effect of generation capacity and reservoir capacity of HPS on reliability (40%)

Figure 6.15 shows the relation between the reservoir capacity of HPS and generation capacity of HPS which effect on LOLE when one of the capacities is fixed and the other capacity is varied. Figure 6.15 shows that the reservoir capacity of HPS is kept constant (72,000 MWh), the power generation capacity is adjusted, and the reliability is hardly changed. Keeping the power generation capacity constant (at 3600 MW) and increasing the reservoir capacity can improve system reliability and reduce the value of LOLE. When the capacity scenario (3600 MW, 72,000 MWh) of HPS is connected to the system, the generation capacity can meet the system requirements, , and the failure to reach the required reliability level is due to insufficient reservoir capacity. When the reservoir capacity exceeds 129,600 MW, the system reliability can be raised to the original system level. However, the results of the RCBA at this time show that the TB is -232.3 M£.

b) Increase the acceptable level of LOLE

To permit higher wind penetration levels, the reliability requirements of the system may need to be appropriately reduced. Here, it is proposed to reduce reliability level to incorporate a certain capacity scenario (for example, 3600 MW, 72,000 MWh) of HPS to obtain positive TB. Figure 6.16 summarizes the relationship between dispatch ratio and TB.

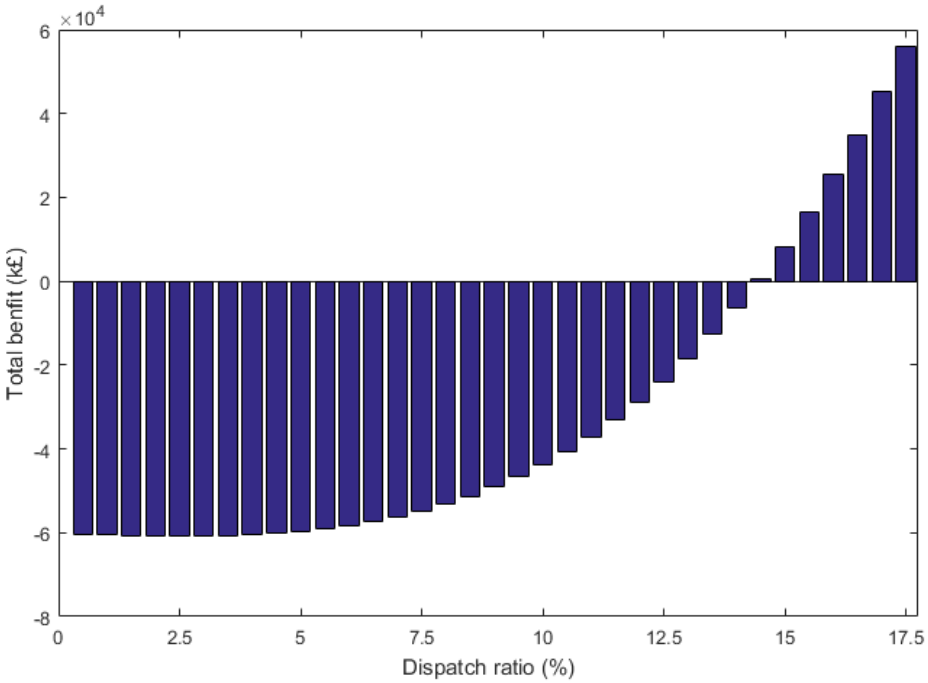

Figure 6.16: Effect of dispatch ratio on TB when the capacity scenario of HPS is 3600 MW, 72,000 MWh (40%)

As Figure 6.16 shows, when the capacity scenario (3600 MW, 72,000 MWh) of HPS is connected to the power system, increasing the power generation ratio can increase the TB of the WP-HPS cooperation (strategy 2) method. When the dispatch ratio is greater than 14.5%, the TB is positive for the first time (697.14 k£). It is suitable to utilize HPS to alleviate the negative impact of WP integration on the system, and the corresponding LOLE value is 145.45 hours/year.

Case 6: 50% wind penetration level

It was assumed that HPS with the largest capacity scenario (4500 MW, 90,000 MWh) is incorporated to analyze the upper limit of the dispatch ratio, and the reliability evaluation results of different dispatch ratios are summarized in the following Figure 6.17.

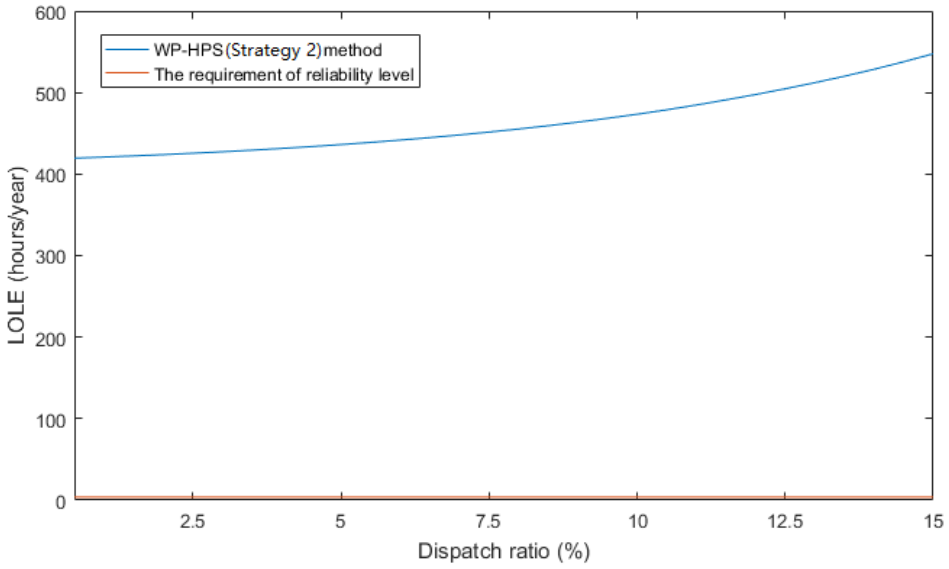

Figure 6.17: Effect of dispatch ratio on reliability (50%)

This figure shows that, even if an HPS with the same installed capacity as WP is added to the system, the minimum LOLE is 419.56 hours/year which is much larger than the required system reliability level and cannot be accepted by an ISO. Increasing the reliability of the system by increasing the capacity of the HPS regardless of cost, it is difficult to reduce the LOLE from such a high value to the required level of the system by merely increasing the power generation capacity or the reservoir capacity. Figure

6.18 shows the relationship between the multiple of HPS capacity scenario (4500 MW, 90,000 MWh) and reliability.

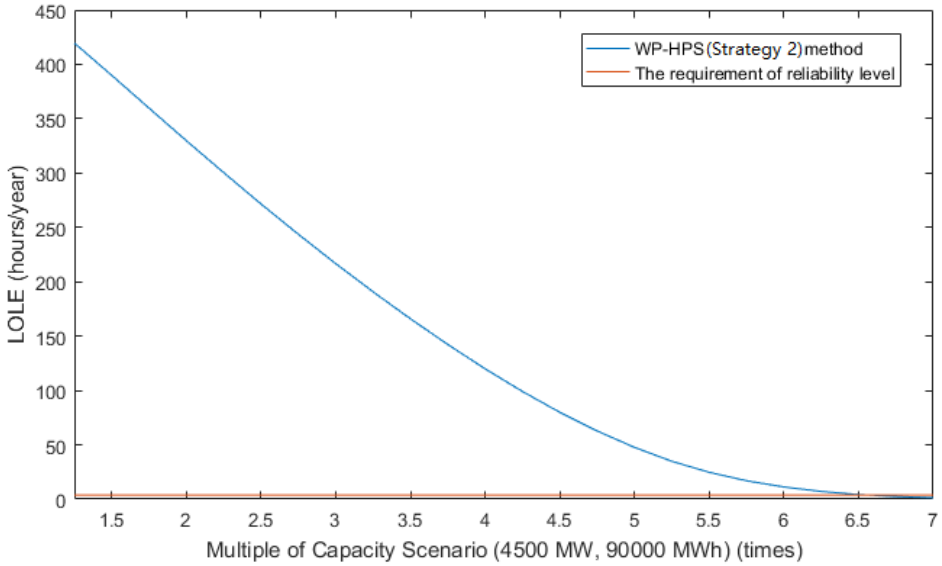

Figure 6.18: Effect of multiplied capacity scenario of HPS on LOLE

Figure 6.18 shows that, to improve the reliability of the system to the level of the original system when the wind penetration level is 50%, it is necessary to increase the capacity scenario of the HPS by at least 6.5 times, which is (29,250 MW, 1,800,000 MWh). The corresponding TB is -3,135,019 k£, so, although the WP-HPS cooperation (strategy 2) method with this HPS capacity scenario can meet the requirements of system reliability, it is not worthwhile from the perspective of RCBA.

6.3.3 Voltage amplitude of nodes in IEEE 118 Bus Test System with the WP-HPS cooperation (strategy 2) method

The previous analysis in this section focus on the effect of the WP-HPS cooperation (strategy 2) method on the reliability of power systems with different wind penetration level. Under the requirement of satisfying both reliability and economy, the proposed method can improve the reliability of the power system of the four cases with wind power penetration level from 10% to 30% to the required level. Table 6-7 summarizes the optimal capacity scenarios and dispatch ratios for the four different wind penetration levels.

Table 6-7: Optimal capacity scenarios and dispatch ratio in different wind penetrations

Wind penetration level	Optimal Capacity Scenario (MW, MWh)	Dispatch ratio (%)	CGUs capacity (MW)
10%	(720,18000)	4.5	8100
15%	(1080,21600)	6.5	7650
20%	(1440,32400)	8.5	7200
30%	(1890,54000)	10	6300

Whether the proposed method can operate reliably in the power systems of these four cases remains to be determined. Therefore, this subsection will utilize the MATPOWER software for power flow analysis to determine whether the magnitude of

each node voltage of the system meets the requirements. Same as Chapter 5, this subsection will detect each case from three scenarios: minimum load demand, average load demand, and maximum load demand. In these three scenarios, wind power output is also divided into three situations: minimum wind power output, average wind power output and maximum wind power output, a total of nine situation. Due to the dispatch ratio, the wind power actually accepted by the system will be adjusted according to the load demand. The specific data is summarized in Appendix 1.

The output of HPS and CGUs will be adjusted according to the difference between the load and the wind power and the respective installed capacity. This subsection does not adopt the optimum power flow calculation. Due to the influence of the dispatch ratio, the wind power output accepted by the system is limited to X% of the load. The purpose of this section is to verify that the proposed WP-HPS cooperation (strategy 2) method can operate in the power system, so the harsh situation is adopted, that is, the output of wind farms is injected into the grid from the same node, and bus 107 is an example from a set of results where a selection of different nodes were used for injection of wind power.. Due to the regional restrictions on the construction of large HPS, HPS is difficult to integrate with wind power through the same node and it is assumed that the injection point of HPS is 61 bus. Figures 6.19 to 6.22 summarize the effects of different wind power outputs on the voltage magnitude of each node in the three load scenarios of the four cases.

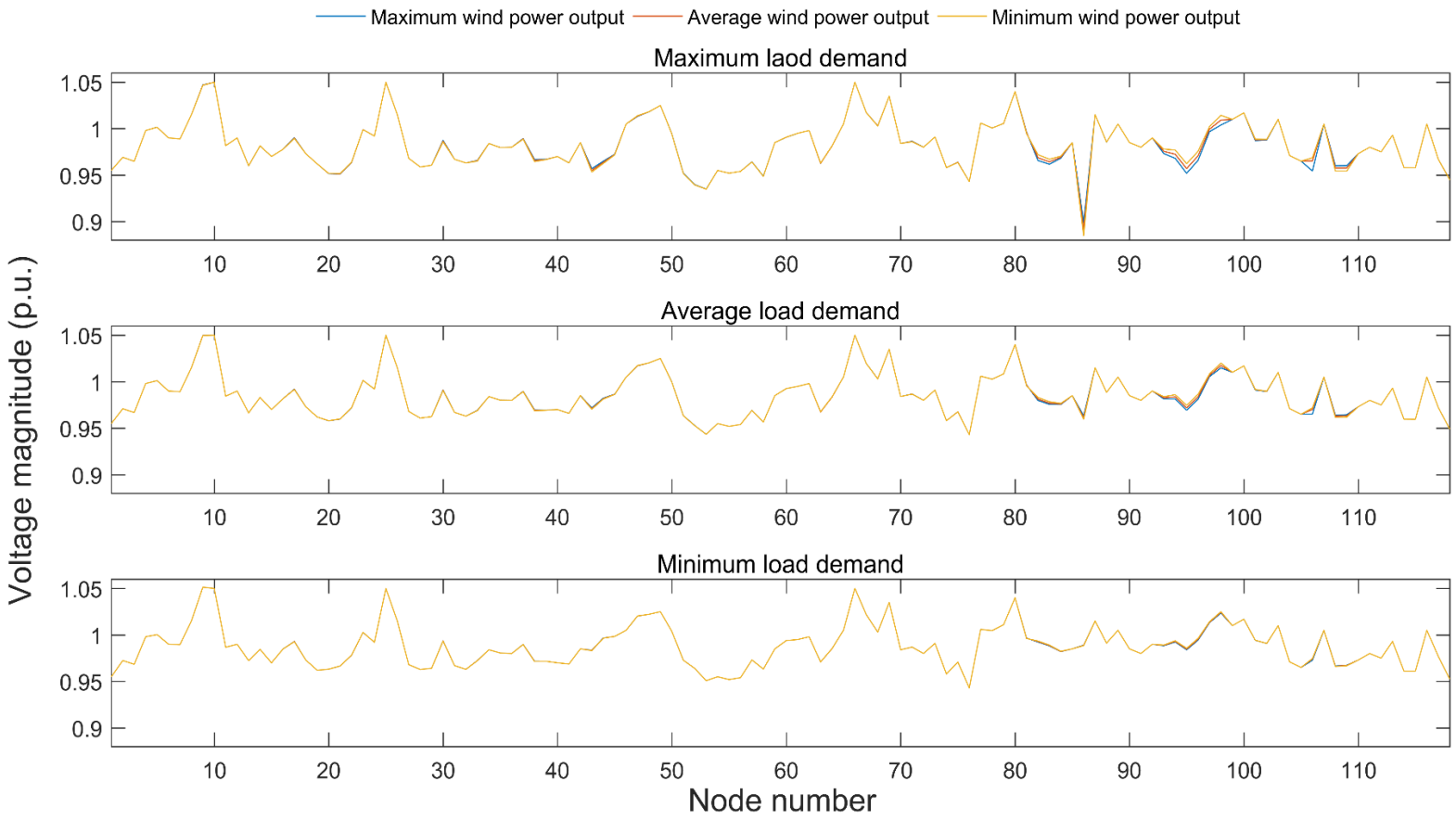

Figure 6.19: Voltage magnitude of each node of IEEE 118 Bus Test System for three wind power output situations under different load scenarios when wind penetration is 10%

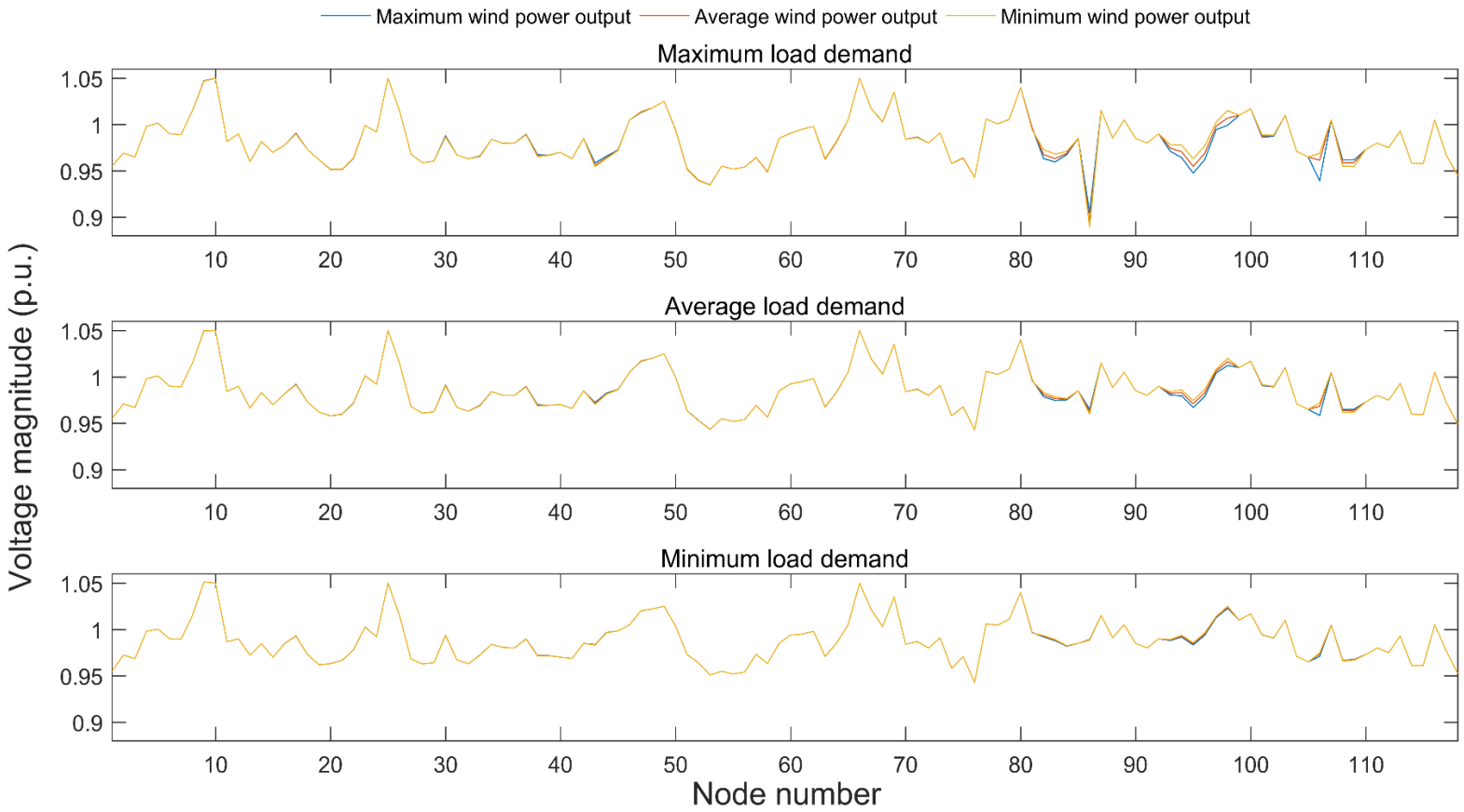

Figure 6.20: Voltage magnitude of each node of IEEE 118 Bus Test System for three wind power output situations under different load scenarios when wind penetration is 15%

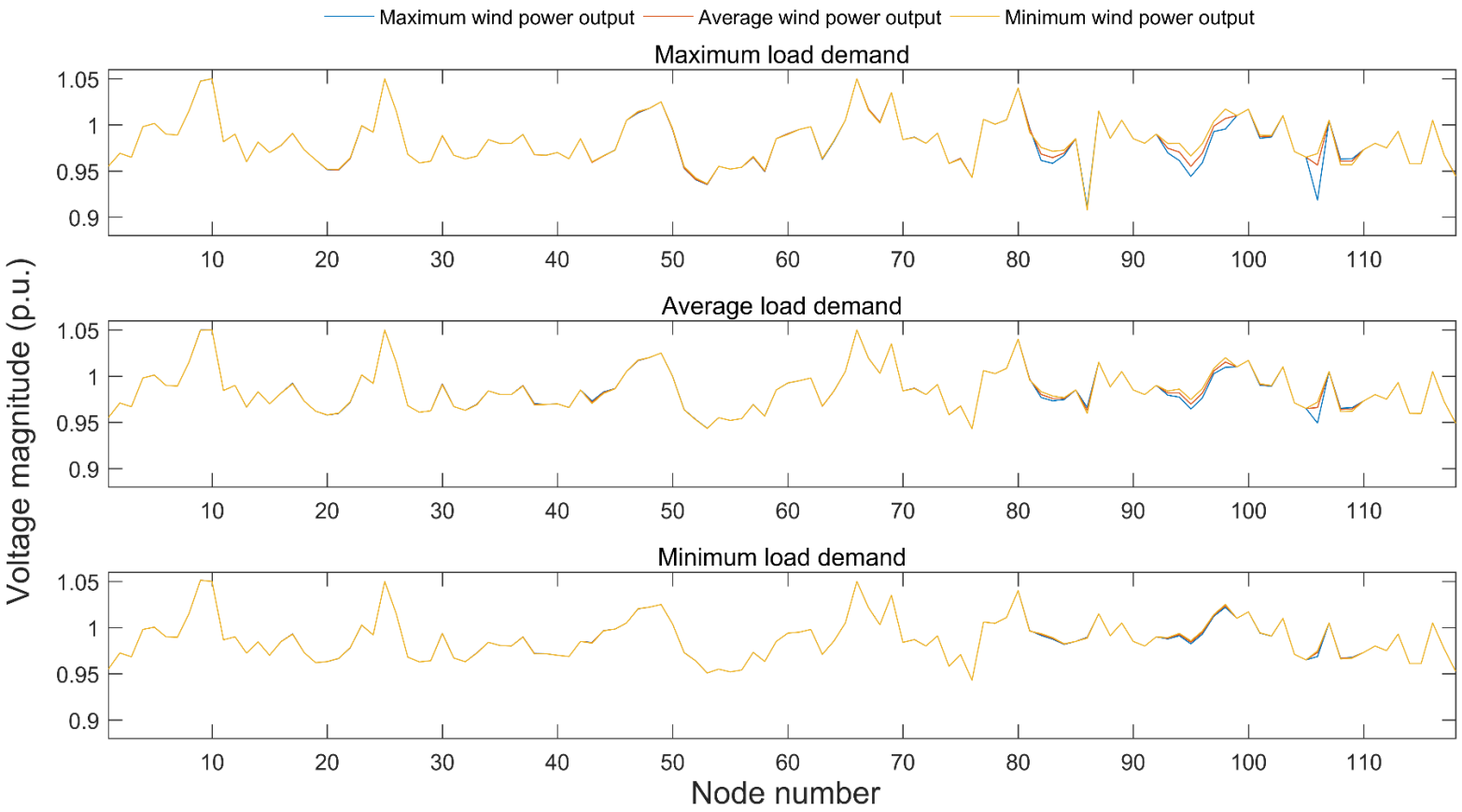

Figure 6.21: Voltage magnitude of each node of IEEE 118 Bus Test System for three wind power output situations under different load scenarios when wind penetration is 20%

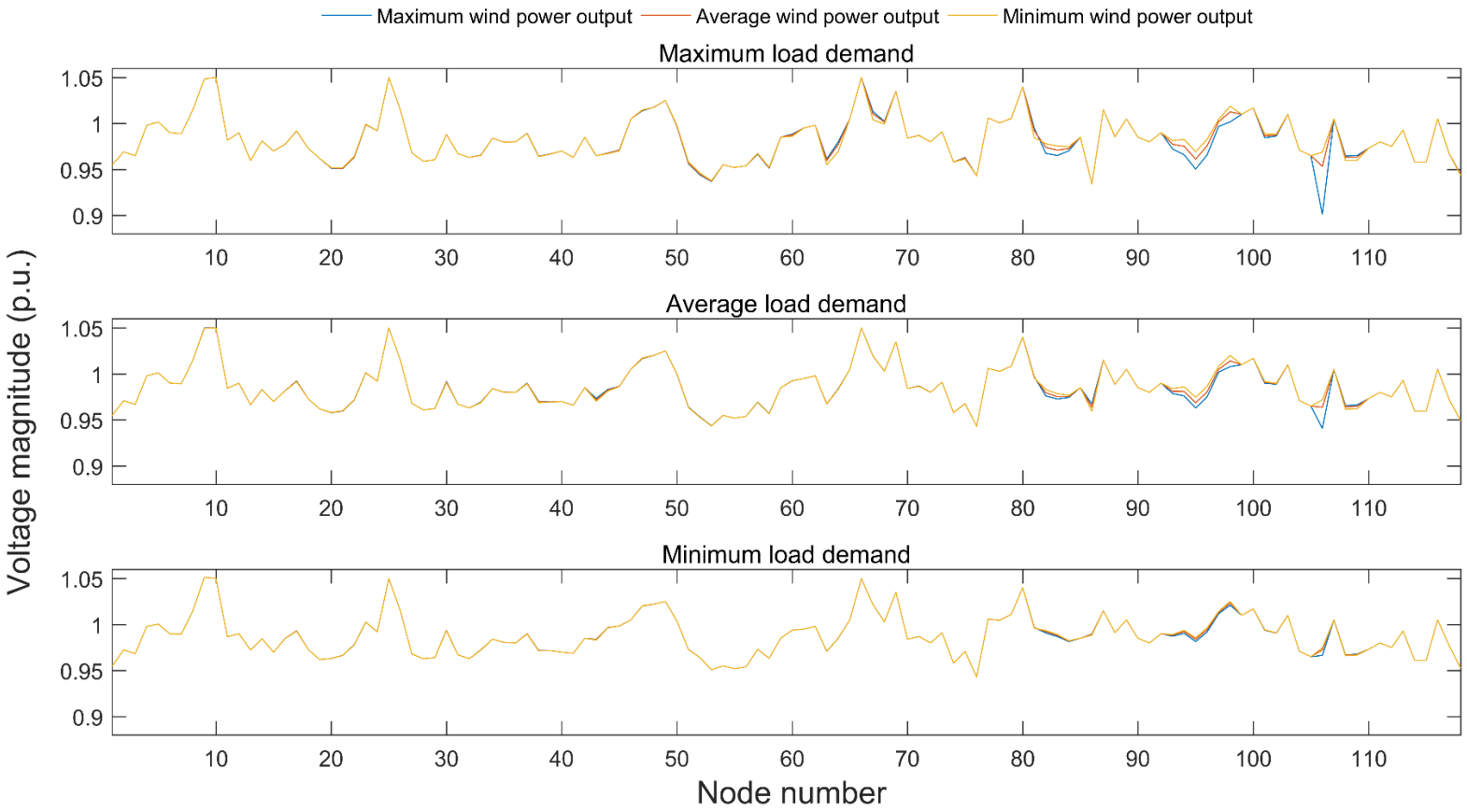

Figure 6.22: Voltage magnitude of each node of IEEE 118 Bus Test System for three wind power output situations under different load scenarios when wind penetration is 30%

It can be seen from Figure 6.19 to 6.22 that the increase of the wind power output will reduce the voltage magnitude of the nodes that wind power injection and adjacent nodes, and the degree of influence increases as the wind power penetration level increases. Moreover, the increase in load demand will increase the influence of wind power fluctuation on the node voltage magnitude. For example, when the wind power penetration level is 30% and at minimum load demand, the wind power output increase has little effect on the node voltage. During the maximum load demand, the influence of wind power output change on the node voltage can be clearly seen. This is due to the dispatch ratio, and the wind power output directly absorbed by the system is limited to reduce the influence of wind power changes on the system voltage magnitude. In general, the voltage amplitudes of all nodes in the four cases are between 0.9 p.u. and 1.05 p.u., which meets the voltage requirements of the system operation. Therefore, the proposed method can operate reliably in the system.

6.4 Daily Operation of WP-HPS cooperation (strategy 2) method

The previous analysis in this chapter focuses on the impact of proposed method on IEEE 118 Bus system reliability integrating wind power in one year. The test result shows that the method can effectively mitigate the negative impact of wind power fluctuation on system reliability.

Network losses are an important base to determine the power system planning and operation method. Therefore, conducting power flow analysis for WP-HPS cooperation

(strategy 2) method in the short-term planning is necessary in order to evaluate the impact of the method on network losses of power system with wind power.

This section evaluates the impact of WP-HPS cooperation (strategy 2) method on power network losses by simulating wind-powered system for 24 hours. The daily load curve is modified based on the British load curve on January 1, 2018, at half hour intervals, as shown in Figure 6.23, from which it can be seen that the load peak is from 14:00 to 20:00.

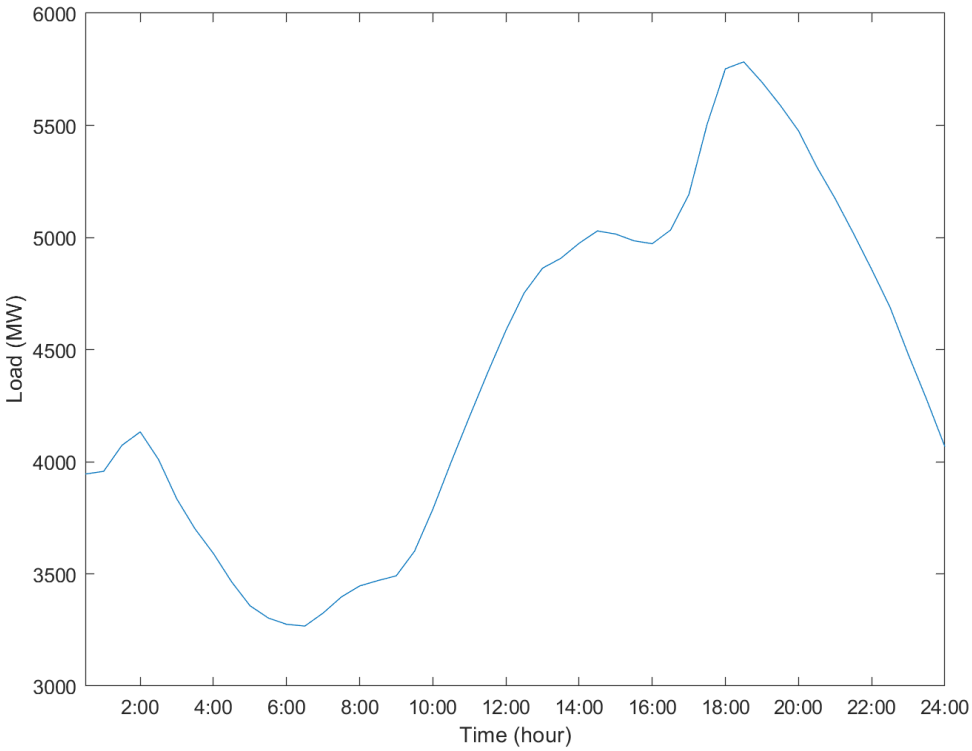

Figure 6.23： Daily load demand with 30 min interval

Through MATPOWER software, the corresponding network losses can be obtained by simulating the power flow of 118 Bus Test System at different wind penetration levels. This chapter does not adopt the optimum power flow calculation. Due to if there is no HPS, all wind power injected into the system through the same node will cause the node

voltage limit to be exceeded and the system will not operate reliably. Therefore, in order to comprehensively analyze the impact of the proposed method on the network loss of the system, this section assumes that wind power is injected through three randomly nodes, and in all simulations in this section, wind power is injected from these same three nodes. The injection point of HPS is set to 61 first, and the impact of other injection points on the system will be analyzed in detail in 6.4.3. The simulation results are analyzed from the following three aspects:

1. The impact of load change and wind power fluctuations on the network losses are analyzed, by taking cases at four wind penetration levels (10%, 15%, 20%, 30%).

2. HPS is connected to the system by cooperation with wind power proposed in the thesis, to evaluate the impact of the proposed method on network losses. The optimal capacity scenarios and dispatch ratios for the four different wind penetration levels are summarized in Table 6-7.

3. The impact of the injection of the HPS into the grid on the grid loss is analyzed, by changing location into the grid.

6.4.1 The effect of wind power integration on power losses

In a previous analysis the wind speed data in this chapter was generated by taking Weibull distribution and Monte Carlo simulation and is suitable for reliability evaluation. The wind output data at intervals of 30 minutes are modified based on the simulation results obtained using the Weibull distribution function and the SMCS method in Section 6.3. The available wind power output is summarized in Table 6-8 as

the percentage of rated output. Combined with the installed wind power capacity of each wind penetration level, the available output of wind power can be obtained.

Table 6-8: Wind power Output in one day with 30 Minutes time interval

Load No.	Time interval	Output (%)		Load No.	Time interval	Output (%)
1	0:00~0:30	0.00		25	12:00~12:30	86.33
2	0:30~1:00	10.78		26	12:30~13:00	57.44
3	1:00~1:30	58.89		27	13:00~13:30	80.22
4	1:30~2:00	20.22		28	13:30~14:00	95.56
5	2:00~2:30	31.11		29	14:00~14:30	37.00
6	2:30~3:00	0.00		30	14:30~15:00	88.00
7	3:00~3:30	10.78		31	15:00~15:30	0.00
8	3:30~4:00	20.00		32	15:30~16:00	46.78
9	4:00~4:30	67.00		33	16:00~16:30	26.22
10	4:30~5:00	0.00		34	16:30~17:00	77.44
11	5:00~5:30	95.56		35	17:00~17:30	0.00
12	5:30~6:00	0.00		36	17:30~18:00	94.44
13	6:00~6:30	32.33		37	18:00~18:30	0.00
14	6:30~7:00	37.00		38	18:30~19:00	45.11
15	7:00~7:30	95.56		39	19:00~19:30	94.44
16	7:30~8:00	27.33		40	19:30~20:00	0.00
17	8:00~8:30	47.00		41	20:00~20:30	37.56
18	8:30~9:00	95.56		42	20:30~21:00	83.78
19	9:00~9:30	0.00		43	21:00~21:30	0.00
20	9:30~~10:00	28.33		44	21:30~22:00	27.22
21	10:00~10:30	0.00		45	22:00~22:30	2.67
22	10:30~11:00	95.56		46	22:30~23:00	89.44
23	11:00~11:30	0.00		47	23:00~23:30	32.22
24	11:30~12:00	13.78		48	23:30~0:00	30.44

Figure 6.24 shows the the behavior of the daily load and corresponding network power losses when no wind power is connected to the power grid. According to these curves, the load increases during peak hours, resulting in increase of network power losses, and vice versa. Therefore, the change of network power losses is consistent to the load and such change happens in a smooth manner.

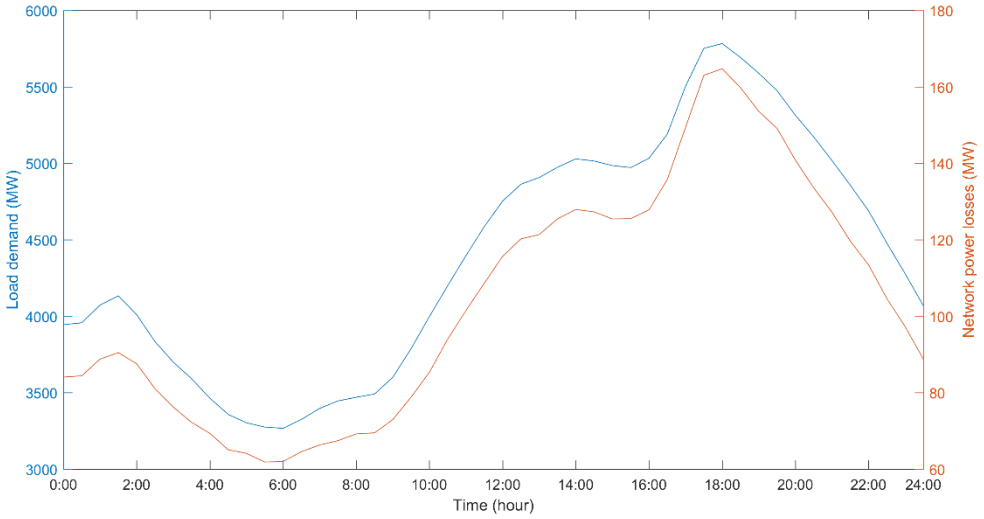

Figure 6.24: Impacts of load variations on network power losses

Figure 6.25 compares the curve of network power losses changes of the original system and that of the system with 10% wind penetration level. The figure clearly shows that the curve of network power losses fluctuates violently compared with the previous curve when wind power is connected to the power grid. Moreover, the network power losses exceed that of the original system after wind power is connected to the power grid. The maximum increase is at 11:30 where the network power losses increases by more than thrice the original 73.4 MW to 270 MW.

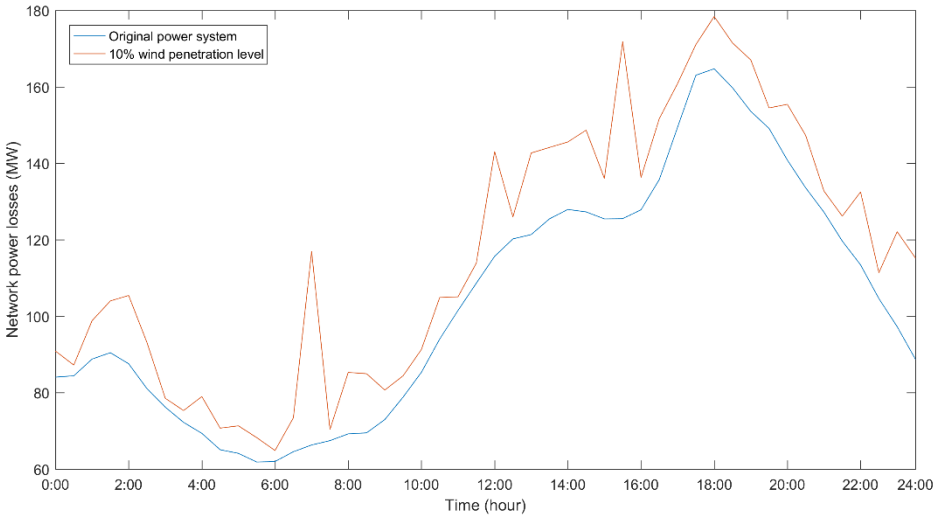

Figure 6.25: Network power losses of power system with and without wind power and 10% wind penetration level

Figure 6.26 summarizes the wind power output curve and corresponding network power losses when the wind penetration level is 10%. It clearly shows that the fluctuation of network power losses is almost consistent with the wind power fluctuation. Therefore, after the wind power is integrated to the power grid, the fluctuation of network power losses is caused by the wind power fluctuation.

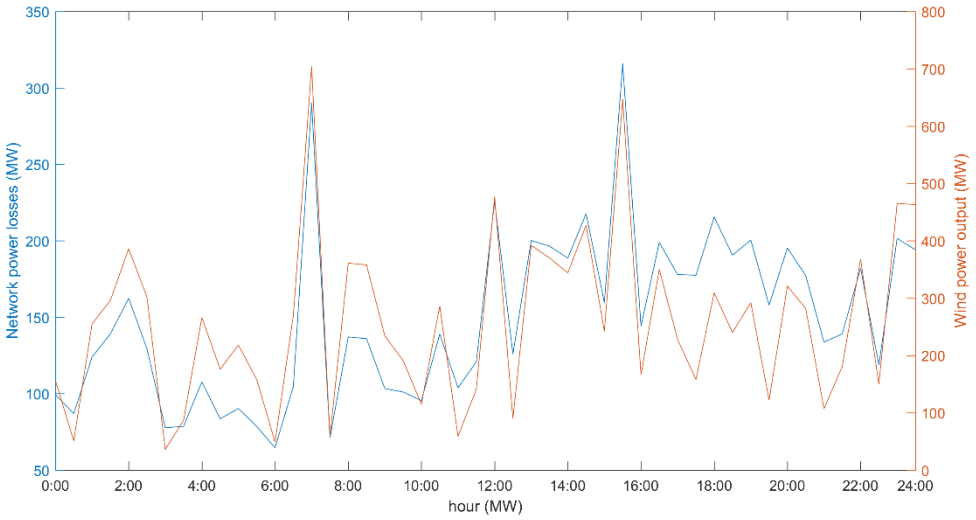

Figure 6.26: Impacts of wind power fluctuations on network power losses (10% wind penetration level)

Figure 6.27 shows the network power losses curve of the power system at four different wind penetration levels (10%, 15%, 20%, 30%) respectively. Detailed data is summarized in Appendix 2. As the wind penetration level increases, the network power losses can fluctuate to a larger extent, and the value of network power losses mostly become larger. Table 6-9 summarizes the daily network energy losses at different wind penetration levels and compares with the data of the original system. The table shows clearly that the integration of wind power to the grid has a negative impact on network energy losses, which constantly increases with the increase of wind penetration levels. When the wind penetration level is increased to 30%, the energy losses increase to 169.08% of the original system.

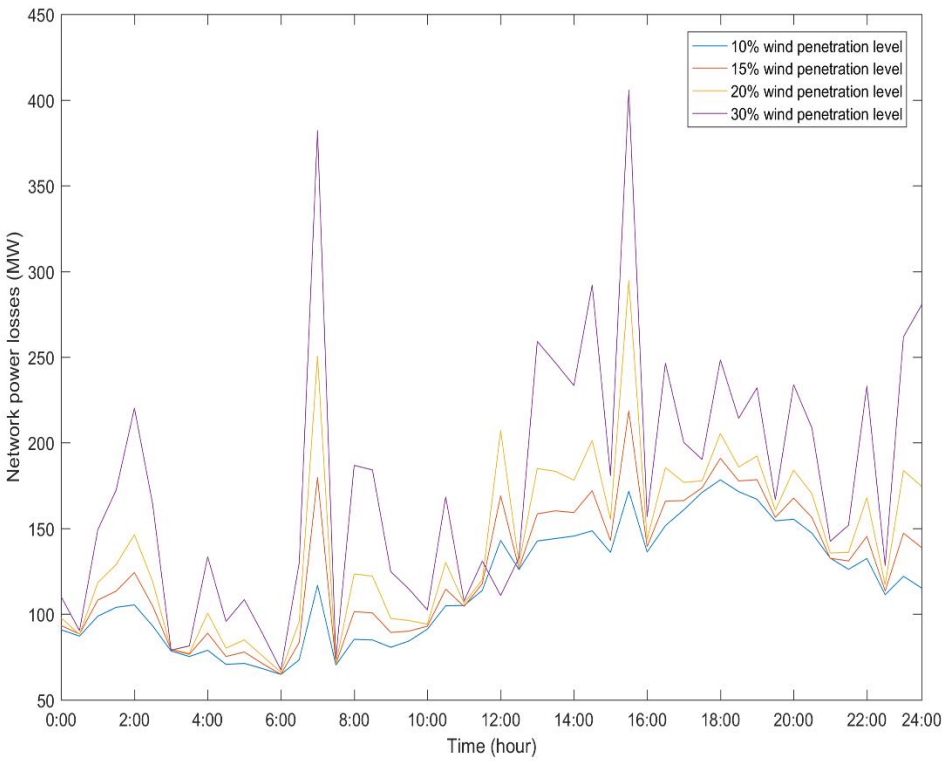

Figure 6.27: Impact of wind penetration level of network power losses

Table 6-9: Daily network energy losses at four different wind penetration levels

Wind penetration level	Daily network energy losses (MWh)	Growth ratio (%)
10%	4983.09→5590.99	12.20%
15%	4983.09→6102.54	22.46%
20%	4983.09→6803.50	36.53%
30%	4983.09→8425.50	69.08%

6.4.2 The impact of WP-HPS cooperation (strategy 2) method on network losses

For WP-HPS cooperation (strategy 2) method, the available output of wind power is not completely absorbed by the power grid due to dispatch limitation. The wind power absorbed by the system in WP-HPS cooperation (strategy 2) method is analyzed, by taking 10% wind penetration level as an example. Figure 6.28 shows the available output of wind power and corresponding wind power dispatch limitation, where the wind power stays within the specified scope of dispatch limitation can directly be absorbed by the system and the residual part stored in HPS. Therefore, the actually used wind power is the sum of the wind power directly absorbed by the system and the power stored in HPS, and the rest to be curtailed.

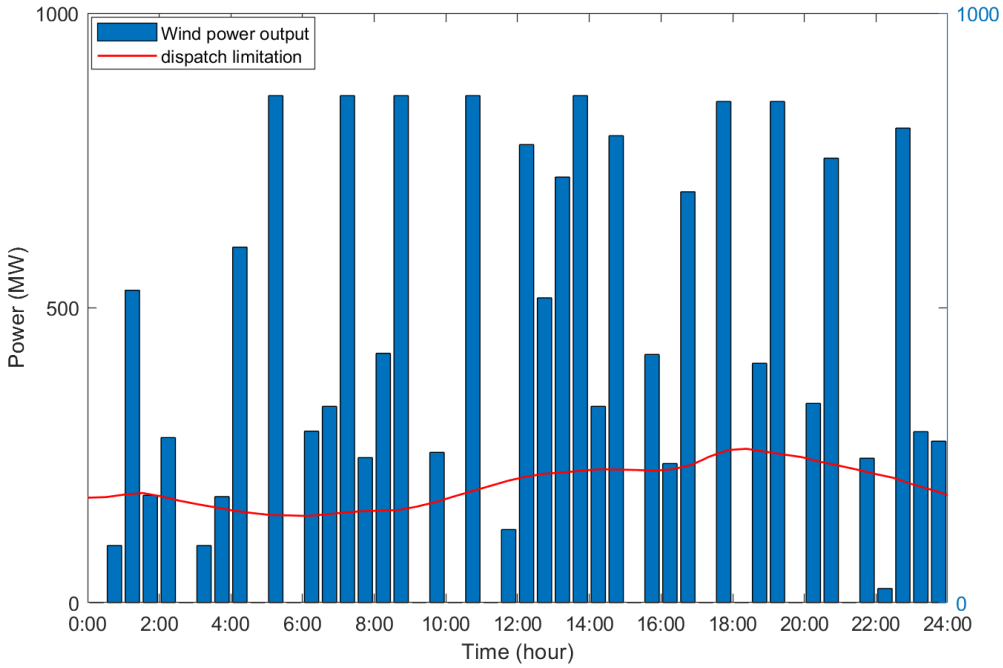

Figure 6.28： Daily available wind power output and dispatch limitation

Figure 6.29 compares the relationship between the available wind power output and the wind power actually absorbed by the system. As can be observed from this figure, the wind power is completely absorbed by the system or mostly stored in HPS. However, the wind power cannot be fully used during a short time period and has to be curtailed due to limited reservoir volume of HPS and limitation of dispatch ratio, for example, from 16:30 to 17:00.

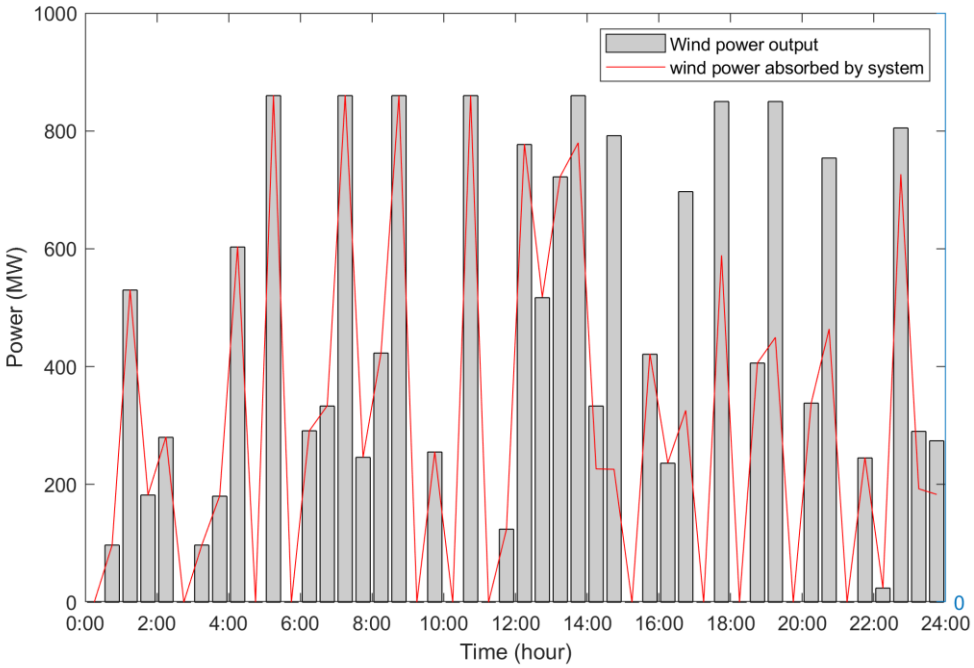

Figure 6.29: Relationship between wind power output and wind power absorbed by the system

The pumping power and generating power for 24 hours of HPS and the actually used wind power are added to the power flow simulation of IEEE 118 bus system. The power system network power losses at different time can be analyzed by MATPOWER flow simulation. For detailed data, please refer to Appendix 3.

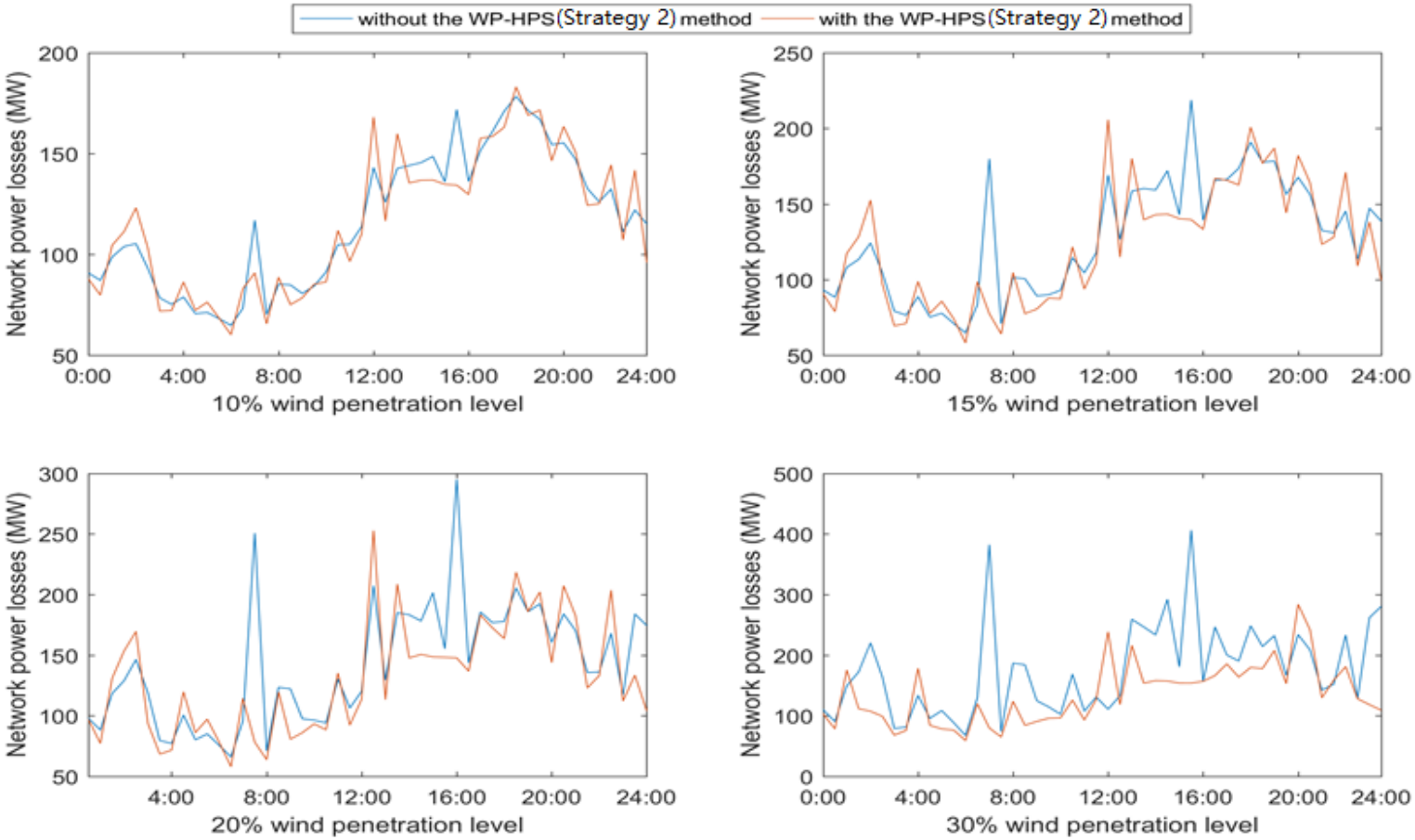

Figure 6.30: Impact of HPS on network power losses at four wind penetration levels

Figure 6.30 compares the network power losses curve of the power system at four wind penetration levels with and without WP-HPS cooperation (strategy 2) method. According to this figure, WP-HPS cooperation (strategy 2) method can effectively reduce the fluctuation of network power losses caused by wind power under the four wind penetration levels. In most of the cases, the system network power losses greatly reduce after HPS was integrated to the power system.

Table 6-10 summarizes the daily network energy losses under different wind penetration levels when HPS is connected to the system and compares them with the data of the original system. The table shows that the daily network energy losses in the system increase with increase in wind penetration level, which is similar to the situation of system without HPS (strategy 2) method. However, due to WP-HPS cooperation (strategy 2), although the daily network energy losses do not decrease to the same level as the original system, the energy losses do not increase greatly. Particularly, at 30% wind penetration level, the daily network energy losses for WP-HPS cooperation (strategy 2) method only increases by 30.18% compared with the original system, while the daily network energy losses of the system without WP-HPS cooperation (strategy 2) method are 69.08% of the original system.

Table 6-10：Daily network energy losses after applying WP-HPS cooperation (strategy 2) method at different wind penetration

Wind penetration level	Daily network energy losses (MWh)	Growth ratio (%)
10%	4983.09→5547.30	11.32%
15%	4983.09→5867.82	17.75%
20%	4983.09→6289.69	26.22%
30%	4983.09→6487.11	30.18%

6.4.3 The impact of HPS injection point on network losses

The analysis in the previous section assumes that the injection point of the HPS is node 61. Since the construction of HPS requires specific geographical conditions, there are fewer alternative construction sites. It is therefore necessary to study the impact of HPS injection node on network energy loss and provide recommendations for selecting HPS construction sites and planning HPS injection points. Figure 6.31 shows the effect of each node that HPS injected into the grid on daily energy losses through four different wind power penetration levels. Detailed data is documented in Appendix 4.

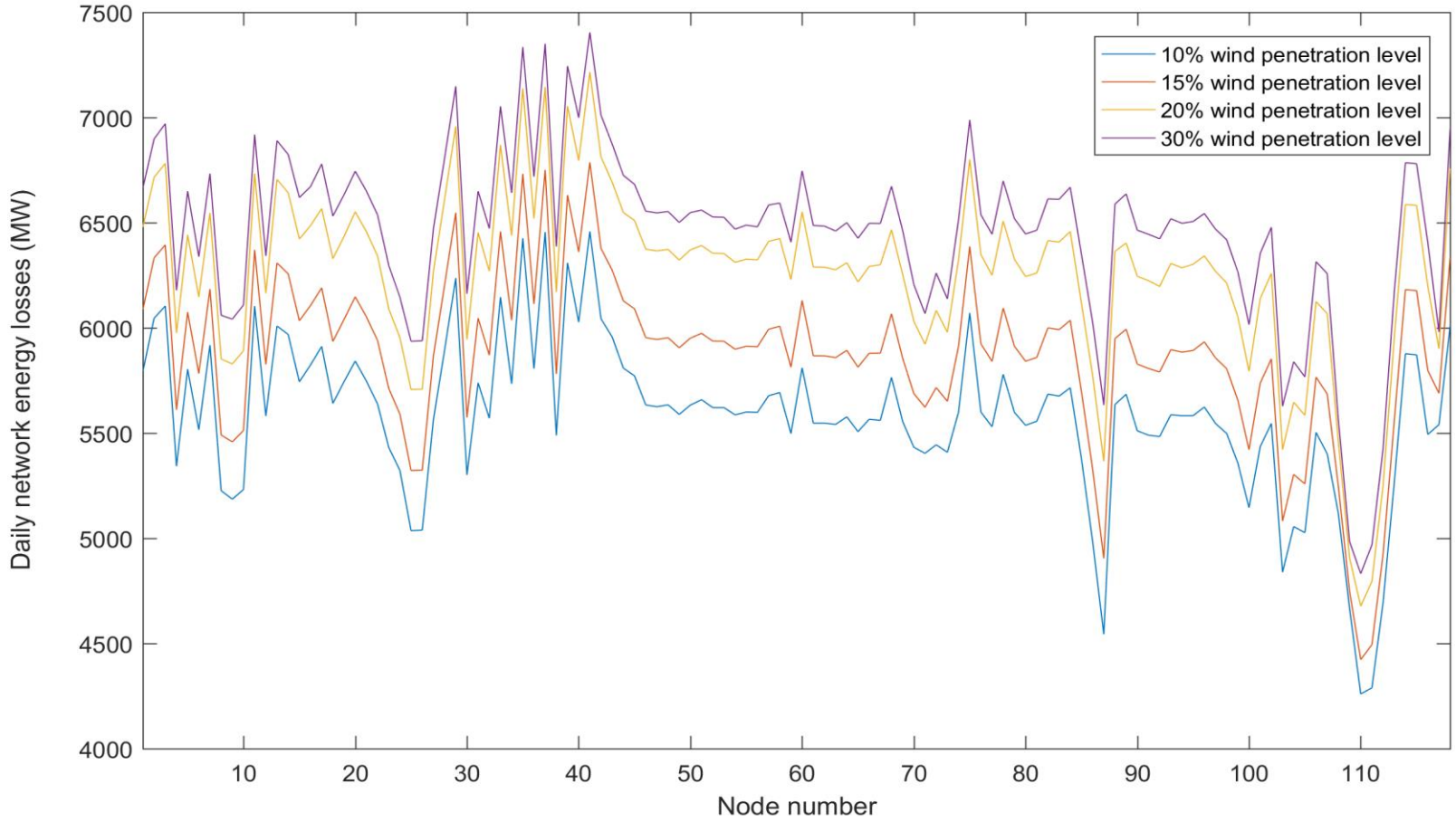

Figure 6.31: The impact of HPS injection point on daily network energy losses at 4 wind penetration level

It can be seen from Figure 6.31 that the injection node of HPS has a great influence on the daily energy loss, and different injection nodes have different daily energy losses. Although the increase in the level of wind penetration level will increase the daily energy loss at the same injection point, the trend of the curve at each wind penetration level is the similar. Besides that, the best HPS injection points at the four wind power penetration levels are all at node 109. Therefore, when planning the construction site of HPS, priority should be given to whether there is a geographical condition suitable for the construction of HPS near node 109.

6.5 Summary

In this chapter, the WP-HPS cooperation (strategy 2) method was applied to the IEEE 118-Bus Test System to verify the effectiveness of the proposed method. Six different wind penetration levels from low to high were applied to verify the improved system reliability of the method. Through several simulation results, it can be concluded that the WP-HPS cooperation (strategy 2) method can be used for:

1. Comparing reliability indicators to assess the impact of different wind penetration levels on system reliability

2. Collaborating of HPS with wind power to reduce the impact of wind power volatility on system reliability and CGU output

3. Quantifying the improvement of HPS on system reliability, evaluating reliability costs and benefits, and determining the optimal capacity scenario for HPS

The case study in this chapter is a long-term plan for systems with different levels of wind penetration. With the increase of integrated wind power capacity, the impact of wind power volatility is deepened, the available generation capacity of the system becomes more fluctuating and difficult to control, and the reliability of the system is significantly reduced.

The proposed WP-HPS cooperation (strategy 2) method can reduce the impact of wind power fluctuation on CGUs output, balance the supply and demand of electric energy by storing excess wind power, improve the system reliability to the level of the original system, and then determine the optimal capacity scenarios through RCBA. This method also has limitations. As in the case study, if the wind penetration level reaches 40%, although the method can improve the reliability to the original level, from the RCBA point of view, the reliability cost is greater than the reliability benefit. When the wind penetration level reaches 50%, this method cannot meet the system reliability requirements.

Finally, the impact of WP-HPS cooperation (strategy 2) method on power system network losses in short-term operation is also analyzed. It can be concluded from the power flow simulation results that the WP-HPS cooperation (strategy 2) method can

effectively smooth the network power loss and reduce the network energy loss for the power system with wind power. Therefore, the WP-HPS cooperation (strategy 2) method is feasible in short-term operation.

The feasibility of the WP-HPS cooperation (strategy 2) method was evaluated and analyzed in detail in the modified IEEE 118 Bus Test System. However, the test system is only an ideal model for educational purposes, so it is necessary to apply the proposed method to a real power system to solve the actual problem. The next chapter will analyze in detail the application of this method in practical cases.

Chapter 7
Reliability assessment of the WP-HPS cooperation (strategy 2) method in Western Inner Mongolia Power Grid

7.1 Introduction

In Chapter 6, the feasibility of the WP-HPS cooperation (strategy 2) method in the IEEE 118-Bus Test System was analyzed. The results of these cases demonstrate that the WP-HPS cooperation (strategy 2) method can mitigate the impact of wind power output volatility on system reliability. Therefore, in this chapter, the WP-HPS cooperation (strategy 2) method is applied to a real case and analyzed, and planning suggestions are provided for the Western Inner Mongolia Power Grid (WIMPG).

Inner Mongolia is the province with the most abundant wind resources in China. The power grid of the autonomous region is divided into two parts: WIMPG and the East Inner Mongolia Power Grid (EIMPG). With the support of Chinese government policies, the wind power project in WIMPG has developed rapidly. West Inner Mongolia is rich in coal resources and has few rivers, local power generation is mainly based on thermal-power generation. Wind power relies on the peaking regulation of thermal-power units, while the output regulation of thermal-power units is slow. Therefore, with the continuous expansion of the wind power scale, the problem of

wind power consumption has become increasingly prominent, resulting in a relatively serious problem of wind abandonment.

To optimize the generation power structure of the WIMPG, reduce the wind power curtailment, and improve the system reliability, the first HPS power station in the West Inner Mongolia area — the Hohhot Hydro Pumped Storage Power Station — was completed at the end of 2014. With the rapid growth of wind power installed capacity, the Hohhot Pumped Storage Power Station has been unable to meet the requirements of power system reliability, and WIMPG has stipulated the proportion of abandoned wind in 2020. To smooth the output of the CGUs, the WP-HPS cooperation (strategy 2) method limits the amount of wind power directly received by the system, stores the excess wind power, and supplies the electric energy when power is insufficient, which is suitable for the WIMPG.

This chapter evaluates the reliability of the power system of the WIMPG at three time points, December 2010, December 2015 and December 2020. In 2010, WIMPG had a low level of wind penetration and without hydro pumped storage power station. In 2015, the first hydro pumped storage power station was put into operation. In 2020, it plans to build more pumped storage power stations to accommodate larger capacity wind power integration. Using the WP-HPS cooperation (strategy 2) method to improve the reliability of the system while reducing the curtailment rate of wind power.

7.2 Description of Western Inner Mongolia Power Grid

The Inner Mongolia Autonomous Region is a vast area in the northernmost part of China. It accounts for one-eighth of China's area, has a long span from east to west, and is rich in wind energy resources. The wind energy resources that can be used are mainly distributed in grasslands and desert areas. According to national resource statistics, the total wind energy reserves in the region are 1.052 TW, and the developable capacity is approximately 300 GW, accounting for 40% of the national wind energy resource reserves, ranking first in the country [162].

The Inner Mongolia Power Grid is divided into the WIMPG and EIMPG [163], as shown in Figure 7.1. The power supply area of WIMPG is approximately 710,000 km^2, accounting for 59.1% of the total autonomous land area. The power supply range mainly includes Alashan League, Bayannaoer City, Erdos City, and the provincial capital Hohhot, and it is located within the range of 97° to 114° east longitude [164]. The cities of Alxa League and Bayannaoer are on the national border, and the north is bordered by Outer Mongolia. This place has sufficient wind energy all year round. It is one of the regions suitable for developing wind farms in China. Therefore, the development of wind power in the Western Inner Mongolia area is very suitable because of the natural conditions. In addition, these places are geographically remote, economic development is relatively backward, and power supply is not sufficient. For these reasons, it is necessary to build wind power generation to promote development.

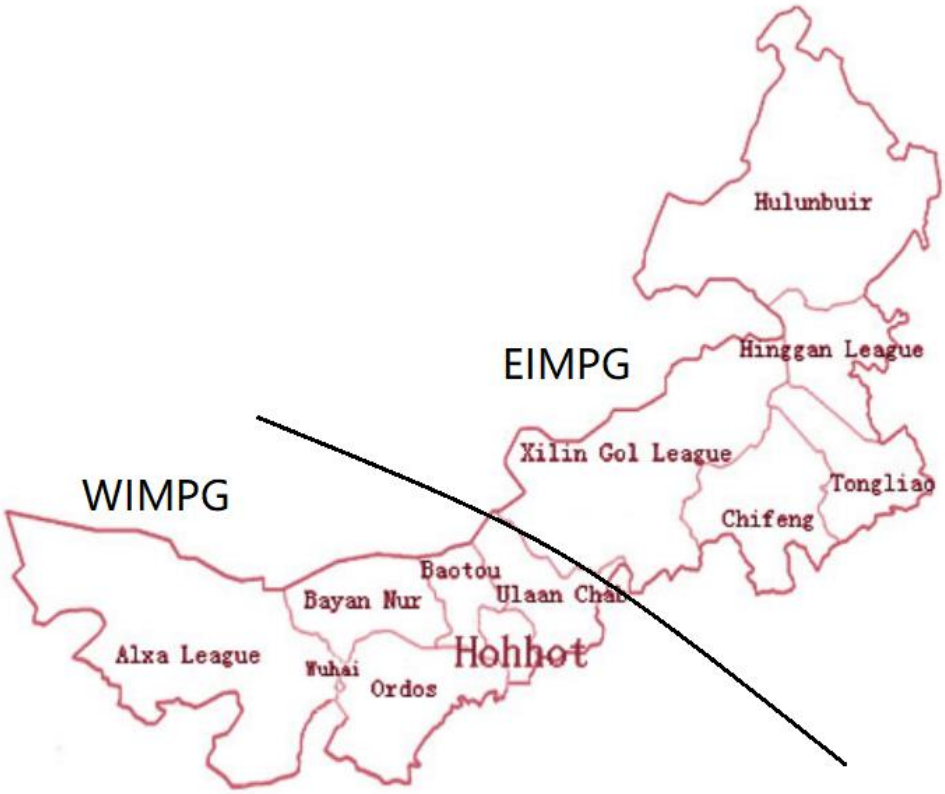

Figure 0.1: WIMPG city distribution schematic [165]

WIMPG plays an important role in the development of wind power in China. Especially in 2009, the installed capacity of wind power in WIMPG was 4,314 MW, accounting for 25% of total wind power installed capacity in China. After 2016, the capacity of newly installed wind power gradually stabilized. The proportion of installed capacity of wind power in Western Inner Mongolia has dropped to 14% compared with national installed wind power capacity, as shown in Figure 7.2 [166]. As of the end of 2018, the installed capacity of wind power in WIMPG accounted for 29.6% of the total installed generation capacity of the region, and the capacity of

integrated wind power ranked first in China. According to China's wind power outlook [167], there will be 14-GW-class large-scale wind farm bases in the Western Inner Mongolia area in 2020, which will be distributed in seven cities — Wulanchabu City, Xilin Gol League, Baotou City, Bayannaoer City, Hohhot City, Erdos City, Alxa League City, and Erenhot City — and the total installed capacity is expected to reach 30,120 MW [7].

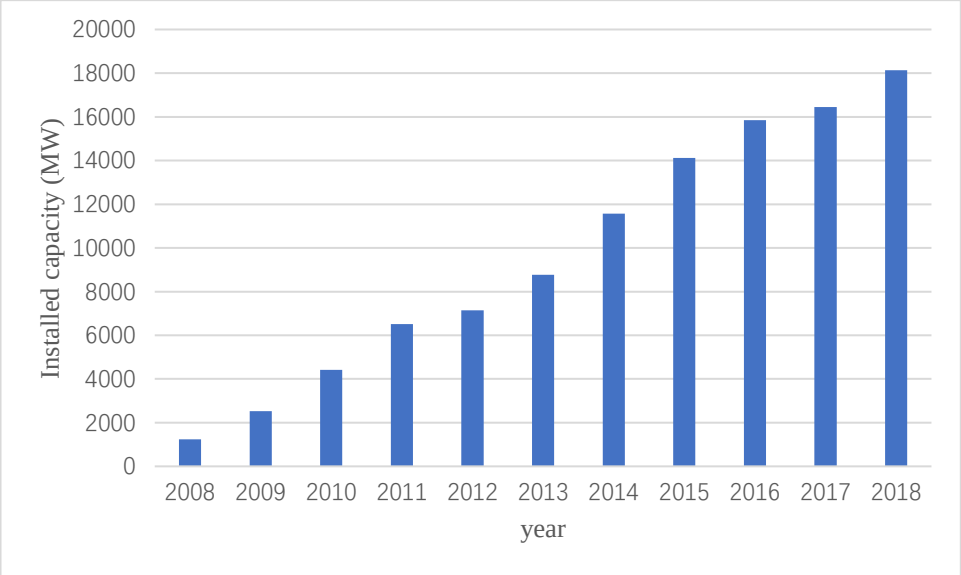

Figure 0.2: Wind power installed capacity of WIMPG over the years[166]

In recent years, with the rapid development of wind power, WIMPG has a large surplus of wind power, and a part of wind power relies on the expansion of power transmission channel. Inner Mongolia is adjacent to eight provinces of North China, Northeast China, and Northwest China. The geographical position is superior, and it is close to the load centre in North China and Northeast China. Therefore, the wind power of the WIMPG has the natural conditions of centralized delivery. For example, the already

established ultrahigh-voltage external transmission channels, such as Western Inner Mongolia-Shandong, Western Inner Mongolia-Jiangsu, and Western Inner Mongolia-Southern Tianjin, are improving WP utilization [168].

The remaining part of wind power is locally absorbed by the WIMPG. There is much coal and less water in the western part of Inner Mongolia, so the power supply structure is mainly composed of CGUs, and there are few hydropower and gas generation units [169]. Wind power mainly relies on CGUs for peak regulation. The output of CGUs has a small ramp rate which cannot meet the peaking requirements of the power grid under the condition of large fluctuations in wind power. In addition, WIMPG belongs to the alpine region, and the winter heating period lasts for six months, from October to April r. The CGUs are the main supply of electrical energy to households and businesses to provide heating. To ensure heating, it is impossible to participate in system peak shaving, which leads to further reduction of the OR capacity of the power grid.

To reduce the impact of wind power volatility on the power system, WIMPG built the first HPS power station in 2014, which is located in Hohhot with a total installed capacity of 1200 MW. According to China's 13th Five-Year Plan (2015-2020), WP that needs to be locally consumed in Western Inner Mongolia will increase from 5,200 MW in 2015 to 10,300 MW in 2020 [170]. One HPS is no longer sufficient to meet the system reliability requirements, so there are three HPSs in the plan, namely,

Xilinhot HPS (installed capacity of 800 MW), Wuhai HPS (installed capacity of 1200 MW), and Baotou HPS (installed capacity of 1600 MW).

7.3 Reliability evaluation of WIMPG

The purpose of this chapter is to utilize the proposed WP-HPS cooperation (strategy 2) method to build an optimal-capacity HPS under the condition of increased wind power capacity integrated into the power system, alleviate the fluctuation of wind power output, smooth the output of CGUs, and improve the reliability of the system to the required level. According to the Inner Mongolia 12th Five-Year Plan (2010-2015) and the Inner Mongolia 13th Five-Year Plan (2015-2020), the basic conditions of power systems and the WP needed in the Western Inner Mongolia area in 2010, 2015, and 2020 are as summarized in Table 7-1 respectively [170] [171]. In these 10 years, the wind penetration level increased from 11.6% in 2010 to 22.6% in 2020. The reliability details of this decade are analyzed later.

Table 0-1: Basic data of the WIMPG in 2010, 2015, and 2020 [170] [171]

Year	2010	2015	2020
Peak load demand (MW)	17,490	28,430	38,220
Valley load demand (MW)	12,010	18,480	23,696
Conventional Gen (MW)	19,500	28,100	35,200
Wind power (MW)	2550	5200	10,300
Wind penetration level (%)	11.6	15.7	22.6

The maximum and minimum load demand values in each year are listed in Table 7.1. It is based on the China load demand in 2018 which has been modified so that the peak load and the minimum load correspond to those used in Table 7.1.

Compared with other power grids, the WIMPG is relatively simple, and most of the generation units are thermal-power generators. To simplify the calculation process and simulation time, it is assumed that the power generation system of the Inner Mongolia Power Grid has only two types of generators: thermal-power generators and wind turbines. Because the reliability data of each power plant are not available to the public, the reliability data of all generation components are modified by the IEEE Reliability Test System [11]. The reliability evaluation of thermal-power generators utilizes the two-state model, described in Section 3.2.3, and its available output model combines failure rate (λ), mean time to repair (MTTR), and rated power through SMCS. The available output of one CGU can be evaluated by combining the failure rate per year

and MTTR into SMCS (presented in Section 3.4.2.2). Combining the output of all CGU, the total available output of CGUs can be calculated.

It is assumed that WTGs in West Inner Mongolia are rated at 3 MW, because there is no detailed industry information, and the wind conditions of each wind farms in WIMPG are the same as those in Chapter 5 and 6, the Weibull scale parameter is 7, and the Weibull shape parameter is 2, the wind speeds of the WTGs in the same wind farm are the same, and the wind conditions of each wind farm are independent of each other. Next, the wind power output can be simulated by combining the Weibull distribution (presented in Section 4.2) and the reliability of the wind turbine by SMCS (presented in Section 4.4). When the total available generating capacity is less than the load demand, the system has an insufficient power supply.

Same as in the previous chapters, the SMCS method (presented in Section 3.4.2.2) is utilized in this chapter to evaluate the reliability level of the system. The results of the simulation are described using three reliability indicators: LOLE (loss of load expectation, hours/year), LOEE (loss of energy expectation, MWh/year) and LOLF (loss of load frequency, occ./year). The processes of the reliability evaluation are explained in detail in Section 5.3.

7.3.1 Reliability evaluation of Western Inner Mongolia Power Grid in 2010

According to the power system data in Table 7.1 and the IEEE Reliability Test System data, the assumed modified power rating and reliability indicators of the CGUs of the WIMPG in 2010 are summarized in Table 7-2.

Table 0-2: Reliability data of conventional generating units in December 2010

Unit size (MW)	No. of units	MTTF (hours)	MTTR (hours)	Failure rate per year
400	13	1100	150	7.9
350	16	1150	100	7.6
200	18	950	50	9.2
100	28	1200	50	7.3
50	46	1980	20	4.4

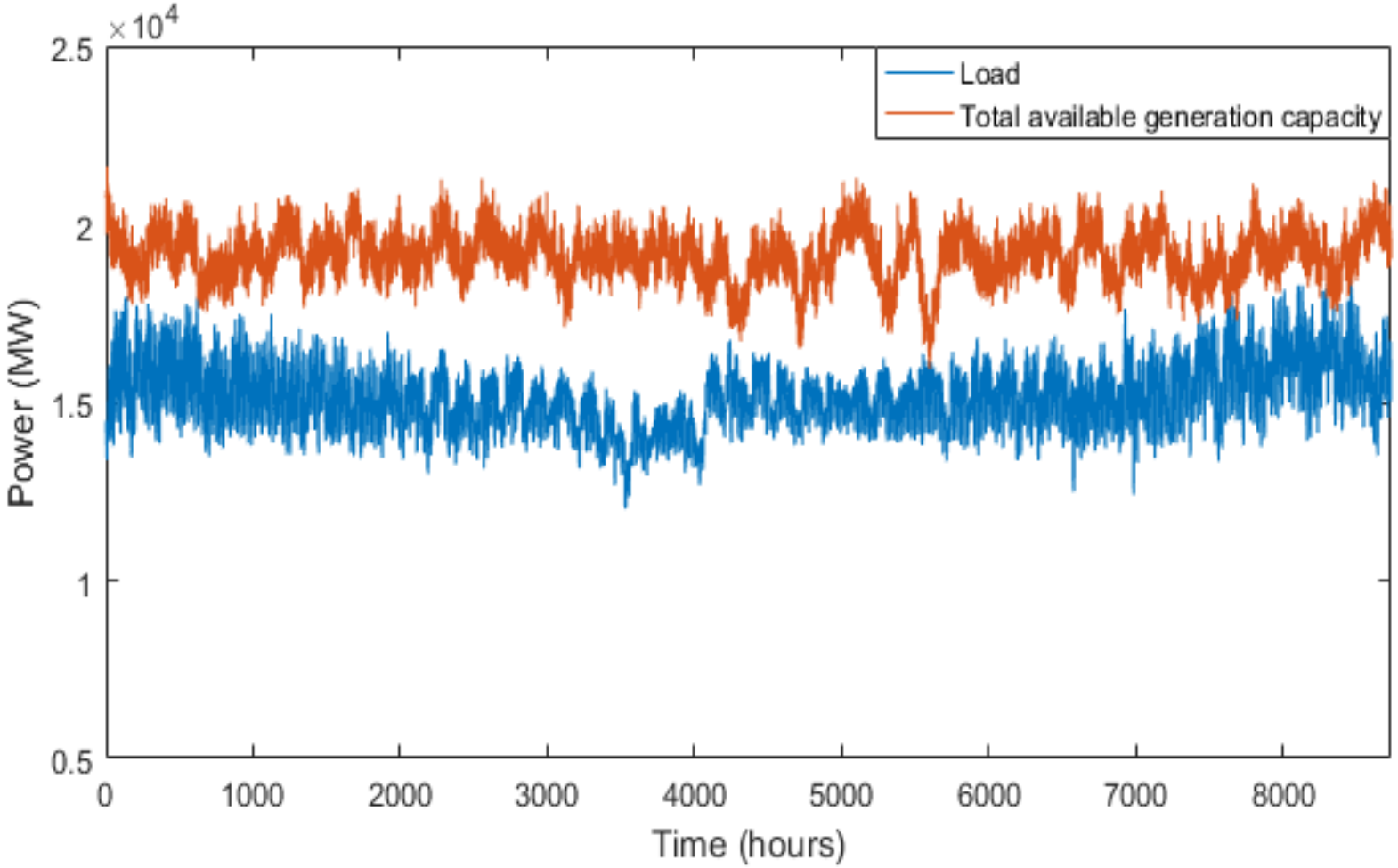

Figure 0.3: Total available generation capacity and load in West Inner Mongolia (December 2010)

One simulation sample of the total available generation capacity and load demand curve for the system are shown in Figure 7.3. Because the reliability model of CGUs is a two-state model and has only two states of up and down, the available output curve of the conventional generator should be smooth without fluctuation. However, after the wind power is integrated into the power system, the power generation the system becomes more fluctuant. The reliability index results of the SMCS evaluation are summarized in Table 7-3.

Table 0-3: Reliability indices of WIMPG in December 2010

Reliability indices	Value
LOLE (hours/year)	19.72
LOEE (MWh/year)	7207.21
LOLF (occ./year)	11.30

As Table 7-3 shows, the time for insufficient power supply for one year is 19.72 hours, the annually unsupplied electric energy is 7207.21 MWh, and there are 11.30 times of insufficient power supply in one year. The 2010 China Power Yearbook reports that the LOLE value of the West Inner Mongolia area in 2010 was 20.51 hours/year, and the evaluation results were close to the true value. The reliability standard of China's power system is one to two days (24 to 48 hours), so the existing reliability level of WIMPG is acceptable.

7.3.2 Reliability evaluation of Western Inner Mongolia Power Grid in 2015

Due to industrial data is kept secret from the public, according to the system data in Table 7-1 and IEEE Reliability Test System Data, the modified power rating and reliable indicators of the conventional generation components of the WIMPG in 2015 are summarized in Table 7-4. In 2015, the wind power capacity that needs to be consumed by WIMPG had increased from 2,550 MW in 2010 to 5,200 MW, wind penetration increased from 11.6% to 15.7%.

Table 0-4: Reliability data of conventional generating units in December 2015

Unit size (MW)	No. of units	MTTF (hours)	MTTR (hours)	Failure rate per year
400	19	1100	150	7.9
350	24	1150	100	7.6
200	25	950	50	9.2
100	38	1200	50	7.3
50	66	1980	20	4.4

One simulation sample of the total available generation capacity and the load curve for the system are shown in Figure 7.4. This figure shows that, as the wind penetration level increases, the fluctuation of the available power generation capacity of the system increases.

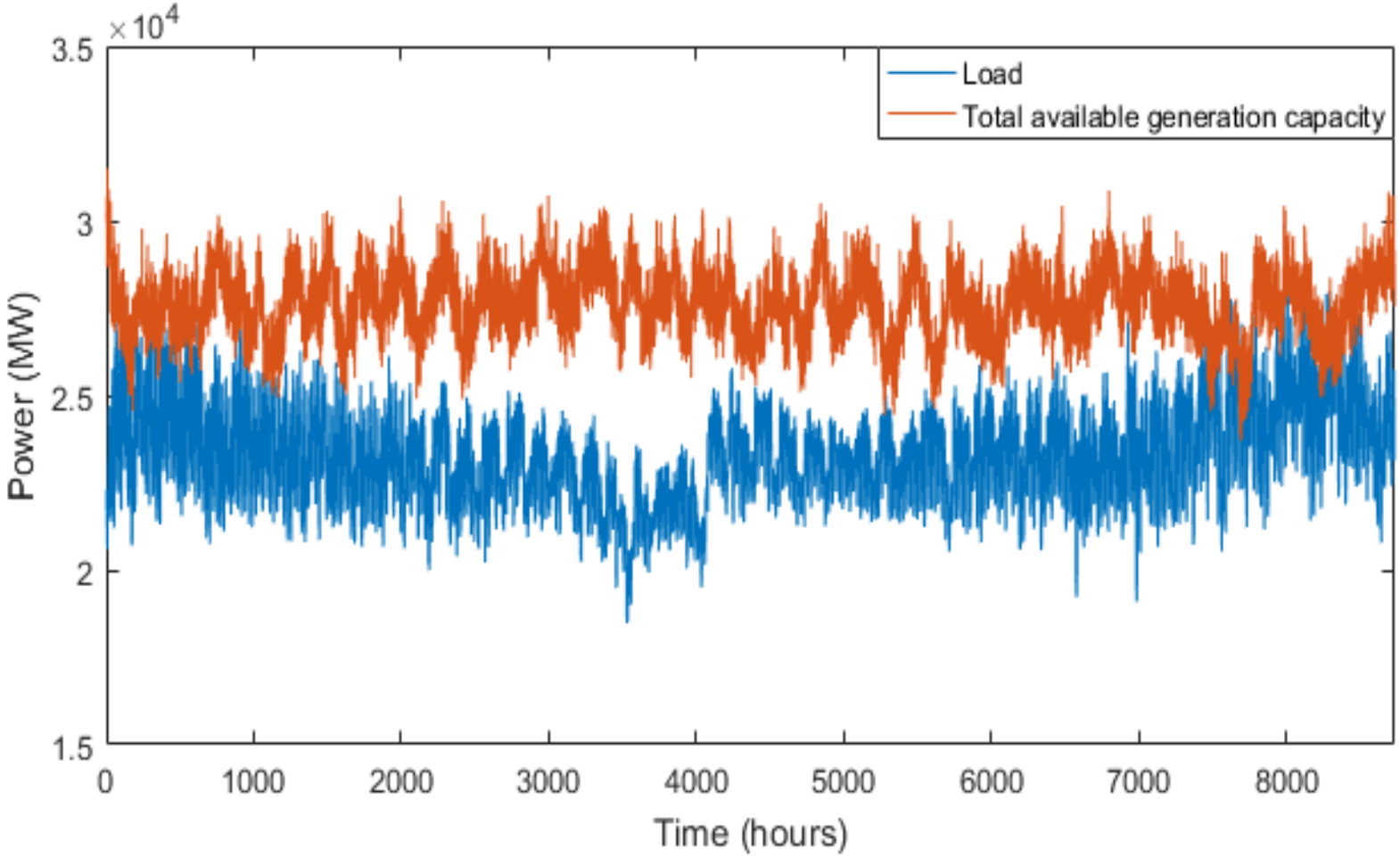

Figure 0.4: Total available generation capacity and load in West Inner Mongolia (December 2015)

The impact of wind power on system reliability can be illustrated by system reliability indicators. The reliability indicators of the WIMPG in 2015 evaluated by SMCS are summarized in Table 7.5.

Table 0-5: Reliability indices of WIMPG in December 2015 without WP-HPS cooperation (strategy 2) method

Reliability indices	Value
LOLE (hours/year)	127.47
LOEE (MWh/year)	81051.50
LOLF (occ./year)	64.82

As this table shows, when the wind penetration level increased from 11.6% to 15.7%, the value of LOLE increased by nearly 6.5 times (from 19.72 to 127.47 hours/year). Therefore, it is necessary to add HPS to mitigate the impact of wind power volatility on system reliability. The 1200-MW Hohhot HPS was built and used at the end of 2014 to increase the operating reserve capacity of the system. Because there is no specific engineering information for the Hohhot HPS, it is assumed that the reservoir capacity of the Hohhot HPS is eight times its generating capacity, and the pumping efficiency and power generation efficiency are consistent with those in Section 5. The HPS stores electric energy at low load and releases electric energy at high load to balance supply and demand. The WP-HPS cooperation (strategy 2) method (presented in Section 5.2)

was used to evaluate the system reliability index for different dispatch ratios after the Hohhot HPS is integrated into the grid, and the results are summarized in Table 7.6.

Table 0-6: Comparison of reliability indices of WIMPG in December 2015 for different dispatch ratios when Hohhot HPS integrated

Dispatch ratio	LOLE (hours/year)	LOEE (MWh/year)	LOLF (occ./year)	Curtailment Rate
0.5%	10151.07	19.59	12.03	91.84%
1.0%	10192.68	19.61	12.03	84.45%
1.5%	10250.37	19.64	12.04	77.04%
2.0%	10328.20	19.68	12.04	69.62%
2.5%	10430.08	19.73	12.05	62.16%
3.0%	10571.66	19.81	12.05	54.66%
3.5%	10770.85	19.93	12.06	47.09%
4.0%	11050.34	20.11	12.06	39.42%
4.5%	11461.84	20.44	12.08	31.64%
5.0%	12222.47	22.41	13.52	23.73%

According to the 2015 China Electric Power Yearbook, the actual system reliability index LOLE of WIMPG in 2015 was 21.06 hours/year, and to prevent the fluctuation of wind power from changing the output of CGU too much, most of the wind power is discarded, and the curtailment ratio of wind power is as high as 32% [172]. By comparison with Table 7-6, it can be concluded that when the dispatch ratio is 4.5%, it is the closest to the actual situation. Therefore, assuming that the system limits the

output of wind power according to a dispatch ratio of 4.5%, Table 7-7 compares the system reliability indicators before and after the integration of Hohhot HPS into the system.

Table 0-7: Comparison of reliability indices of WIMPG in December 2015 without and with WP-HPS cooperation (strategy 2) method

Reliability indices	Without Hohhot HPS→ with Hohhot HPS	Decrement degree
LOLE (hours/year)	127.47→20.44	83.96%
LOEE (MWh/year)	81051.50→11461.84	85.86%
LOLF (occ./year)	64.82→12.08	81.36%

As Table 7-7 shows, the addition of HPS had a positive impact on system reliability. The annual period of power shortage decreased to 20.44 hours, the unserved electric energy drops to 11461.84 MWh, and the number of power shortages declined to 12.08 times. The level of power system reliability was significantly improved.

7.3.3 Reliability evaluation of Western Inner Mongolia Power Grid in 2020

Without access to the industry data of WIMPG, the modified power rating and reliable indicators of the conventional generation components of the WIMPG in 2020 are summarized in Table 7-8. In 2020, the wind power capacity that needs to be consumed

by WIMPG has increased from 5200 MW in 2010 to 10,300 MW, and the wind penetration level will increase from 15.7% to 22.6%.

Table 0-8: Reliability data of conventional generating units in December 2020

Unit size (MW)	No. of units	MTTF (hours)	MTTR (hours)	Failure rate per year
400	24	1100	150	7.9
350	30	1150	100	7.6
200	32	950	50	9.2
100	46	1200	50	7.3
50	82	1980	20	4.4

One simulation sample of the total available generation capacity and the load curve for the system are shown in Figure 7.5. This figure shows that the fluctuation range of the available power generation capacity of the system becomes larger as the installed capacity of the wind power increases.

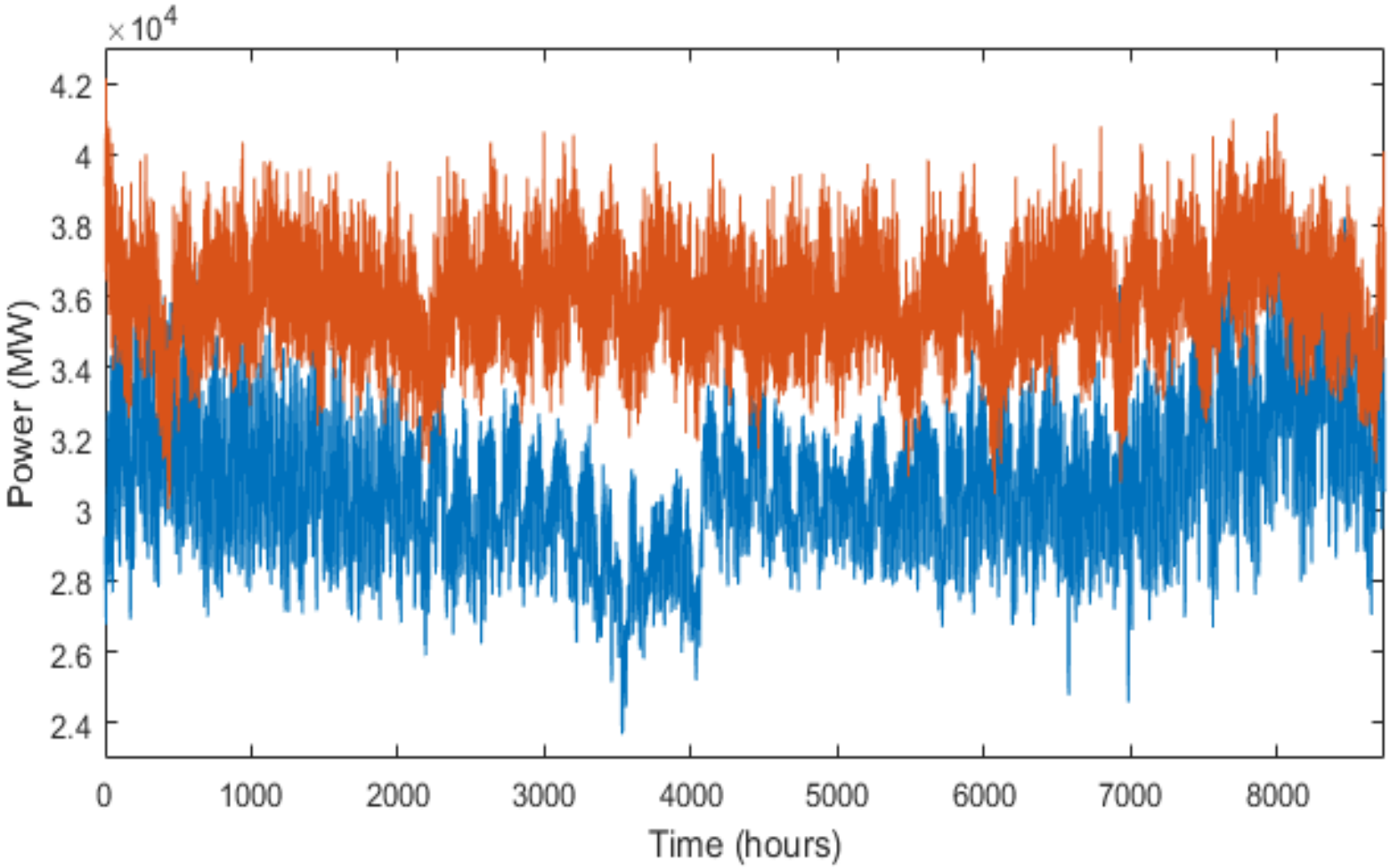

Figure 0.5: Total available generation capacity and load in West Inner Mongolia (December 2020)

Table 7-9 summarizes the system reliability indicators for wind power without restrictions if only the Hohhot HPS is used. Table 7-9 shows that, if the new pumped storage power station is not added, the reliability of the system becomes worse as the level of wind penetration increases.

Table 0-9: Reliability indices of WIMPG in December 2020 only with Hohhot HPS

Reliability indices	Value
LOLE (hours/year)	147.84
LOEE (MWh/year)	147827.90
LOLF (occ./year)	86.80

In the meantime, because of the greater variation of wind power, the output of CGUs also needs to change frequently to accept wind power. Figure 7.6 shows the output of a 300 hours conventional generation output with a wind power unrestricted and a power generation ratio limited to 10%. As the figure shows, wind power limitation based on load demand can smooth the output of CGUs, reduce power generation cost, and help reduce equipment wear and improve unit operating life. Therefore, it is necessary to limit the wind power that can be absorbed by the system and reduce the fluctuation of the CGUs output.

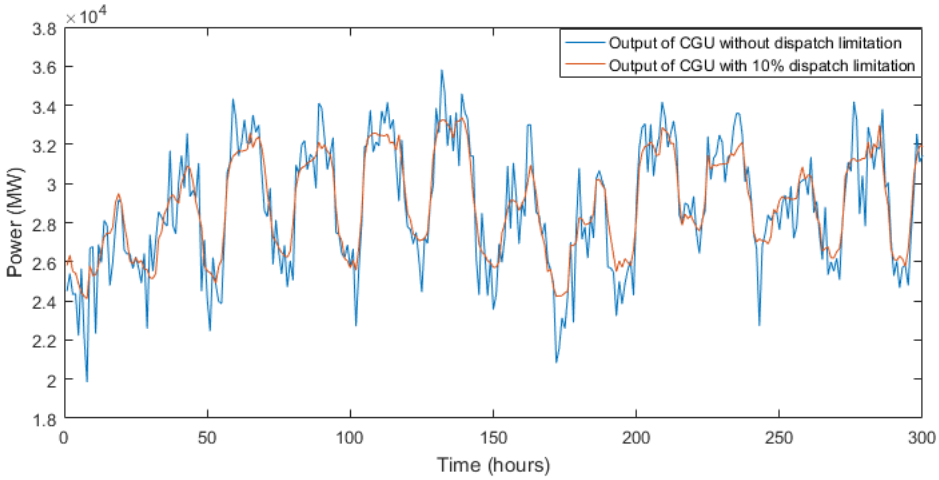

Figure 0.6: Output curve of CGUs with and without dispatch limitation

Inner Mongolia's 13th Five-Year Wind Power Development and Access Grid Rules pointed out that, to accommodate more wind power, WIMPG plans to build three new HPSs, and the Wuhai HPS with an installed capacity of 1200 MW has been confirmed. The Xilinhot HPS with an installed capacity of 800 MW and the Baotou HPS with an installed capacity of 1600 MW whose construction completion time can be adjusted according to suit system requirements [170]. Because there are no specific industrial data, to simplify the calculation and simulation time, the generators of each HPS is regarded as a whole, and the reservoir capacity of these several HPSs is eight times its power generation capacity. Therefore, by 2020, together with the now-operating Hohhot HPS, there are four capacity schemes for the HPSs of WIMPG, and summarized in Table 7-10:

Table 0-10: Four capacity schemes for the HPSs of WIMPG in 2020

Schemes No.	The included HPSs	Capacity scenario
1	Hohhot and Wuhai	(2400 MW, 19,200 MWh)
2	Hohhot, Wuhai and Xilinhot	(3200 MW, 25,600 MWh)
3	Hohhot, Wuhai and Baotou	(4000 MW, 32,000 MWh)
4	Hohhot, Wuhai, Xilinhot and Baotou	(4800 MW, 38,400 MWh)

At the same time, according to the state uniqueness constraint proposed in Chapter 5, all HPS in the power system can only pump water or generate electricity at the same time,; otherwise, energy will be wasted. Applying the proposed WP-HPS cooperation (strategy 2) method to the system, to simplify calculation and simulation time, the dispatch ratio is gradually increased from 0.25% in increments of 0.25% until the reliability requirements of the system are not satisfied. Figure 7.7 shows the reliability index LOLE when the dispatch ratio is at the minimum value (0.25%) for the four capacity schemes.

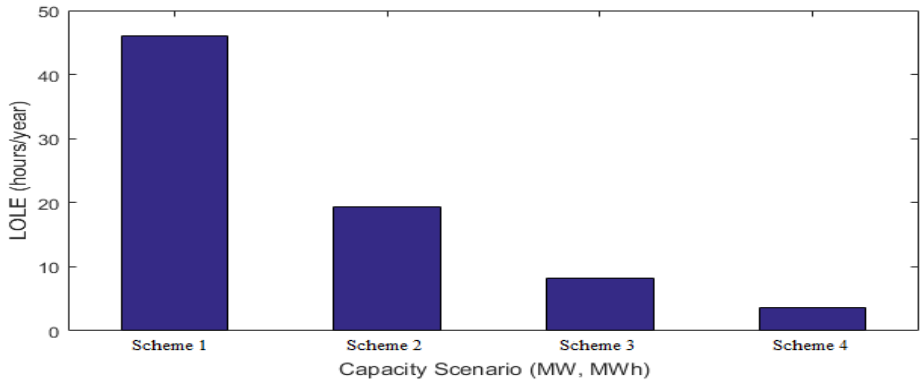

Figure 0.7: LOLE evaluation results for four capacity scenarios when dispatch ratio is 0.25%

The analysis of Chapters 5 and 6 proved that the smaller the dispatch ratio, the higher the system reliability. If the minimum dispatch ratio cannot meet the system reliability requirements, the HPS capacity scheme is not suitable for the power system with the current wind penetration level. As Figure 7.7 shows, the scheme 1 cannot meet the system reliability requirements when the dispatch ratio is at a minimum. In other words, if the WIMPG needs to accept 10,300 MW wind power in 2020, only the construction of the Wuhai HPS will not meet the requirements of system reliability, and at least one more HPS is needed. Figure 7.8 shows the LOLE variation of the remaining three schemes as the dispatch ratio is increased.

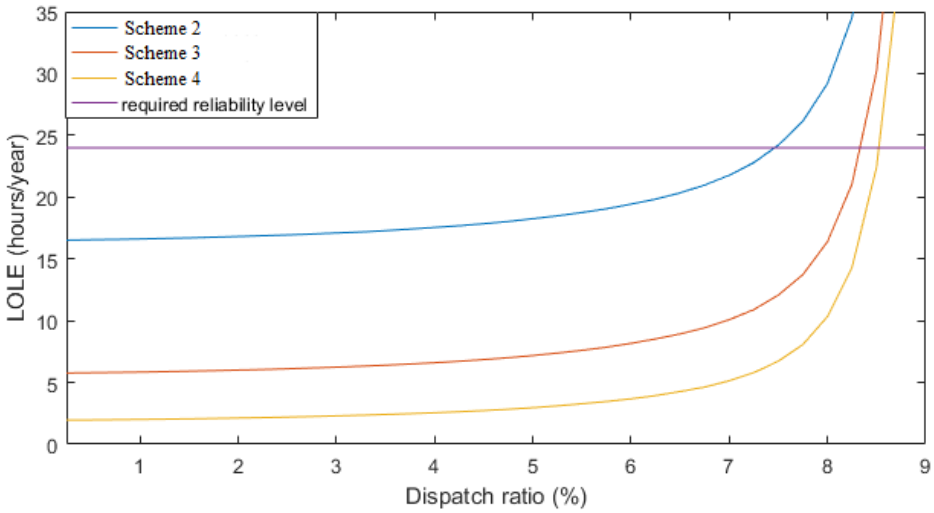

Figure 0.8: LOLE against dispatch ratio of three capacity scenarios

Figure 7.8 shows that all three capacity scenarios can meet the system reliability requirements (less than 24 hours/year), but the maximum acceptable dispatch ratio is different. Specifically, if scheme 2 is adopted in 2020, the dispatch ratio can be as high

as 7.25% when the system reliability requirements are met. If the scheme 3 is put into operation, the dispatch ratio can reach 8.25%. If scheme 4 is adopted, the dispatch ratio can reach 8.5%. The best dispatch ratio and corresponding TB evaluation results for the three schemes are summarized in Table 7-11 after evaluation by the RCBA. The table shows that, although the scheme 4 can accommodate more wind power, the increased reliability cost exceeds the reliability benefit, so the TB is fallen compared to the scheme 3. Therefore, the optimal capacity scheme of HPSs is scheme 3 from the perspective of RCBA.

Table 0-11: Optimal dispatch ratio and TB for each scheme

Scheme No.	2	3	4
Dispatch Ratio (%)	7.25	8.25	8.5
Reliability Benefit (m£)	458.86	667.55	730.13
Reliability Cost (m£)	176.00	220.00	294.00
Total Benefit (km£)	282.86	447.55	436.13

According to the Clean Energy Dissipation Action Plan (2018-2020) proposed by the China Energy Administration in 2018, the wind curtailment rate of the WIMPG needs to be less than 15% in 2020 [173].

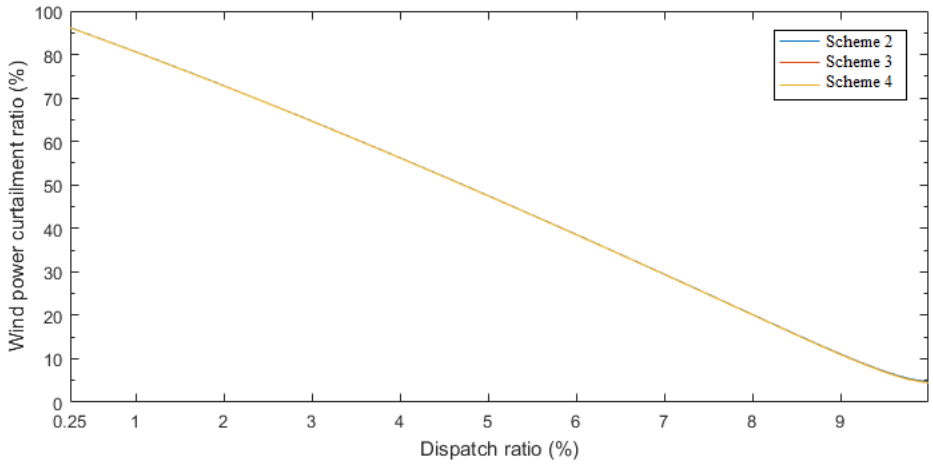

Figure 0.9: Curtailment ratio of wind power against dispatch ratio for three capacity scenarios

Figure 7.9 shows the variation of the CR of the three schemes as the dispatch ratio increases. The figure shows that the three curves are almost coincident, and, as the dispatch ratio increases, the value of CR continuously decreases. If the value of CR needs to be controlled below 15%, the dispatch ratio needs to be increased to 8.5% or more. Only the scheme 4 could satisfy this condition, which means that both the Wuhai HPS, Xilinhot HPS and Baotou HPS need to be put into operation in 2020. It can be summarized from the perspective of the ISO: in 2020, the installed capacity of wind power that needs to be consumed by WIMPG is 10,300 MW, and the wind penetration level is increased to 22.6%. If the last HPS is not built, the system reliability index LOLE will increase from 21.86 to 147.84 hours/year. To alleviate the impact of increased wind power installed capacity on system reliability, from the perspective of RCBA, the Wuhai HPS and Baotou HPS need to be put into operation to obtain the maximum TB, and the corresponding dispatch ratio is 8.25%. The system reliability

evaluation result is that the power shortage time is 21.06 hours per year, the unserved electric energy is 3164.55 MWh, there will be an insufficient power supply of 8.02 times per year, and the corresponding CR is 17.81%.

If it is necessary to achieve a value of CR less than 15%, all three HPSs in the scheme 4 (Xilinhot HPS, Wuhai HPS, and Baotou HPS) should be put into operation, and the corresponding dispatch ratio is 8.5%. The system reliability evaluation result is that the power shortage time is 22.42 hours per year, the unserved electric energy is 3469.70 MWh, there will be 7.45 times power shortages per year, and the corresponding CR is 14.56%.

Whether the proposed method can operate reliably in WIMPG of this optimal scheme (Xilinhot HPS, Wuhai HPS, and Baotou HPS) remains to be inspected. Therefore, matpower software will be utilized for power flow analyze whether the amplitude of each node voltage of WIMPG meets the requirements. The 500 KV line diagram of WIMPG is shown in figure 7.10.

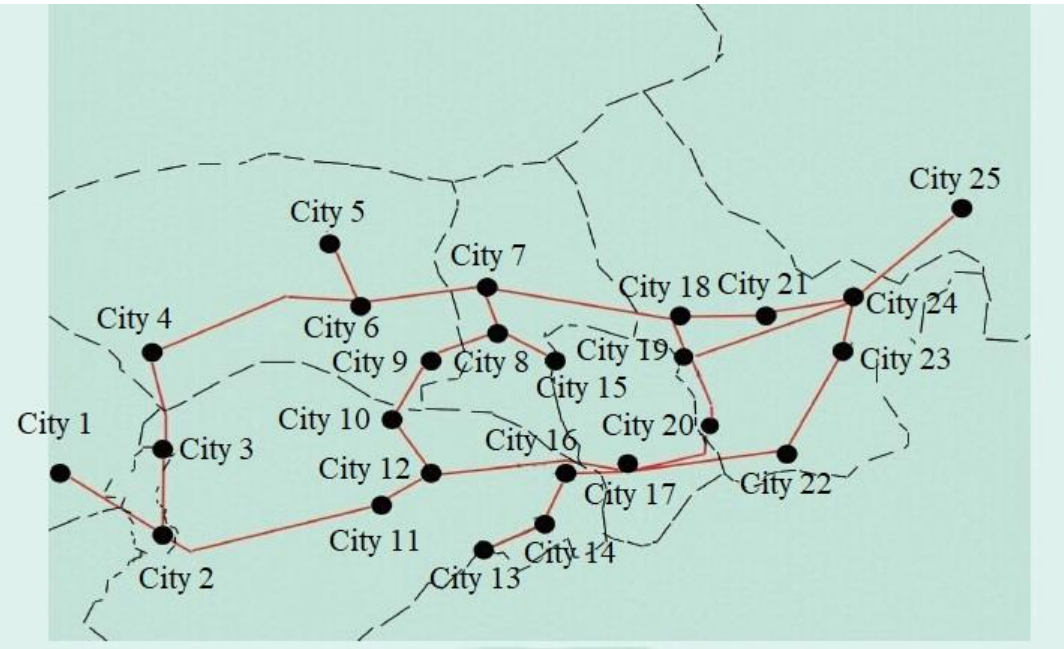

Figure 0.10: The 500 KV line diagram of WIMPG

Same as Chapter 5 and 6, this subsection will consider three cases: at minimum load demand, average load demand, and maximum load demand respectively. In these three cases, wind power output is also divided into three situations: minimum wind power output, average wind power output and maximum wind power output respectively, a total of nine situations. Due to the dispatch ratio, the wind power actually accepted by the system will be adjusted according to the load demand. The specific data is summarized in Table 7-12.

Table 0-12: Various load cases and corresponding wind power conditions of WIMPG in 2020

Maximum Load demand (38220 MW)	Maximum wind power output	3249 MW
	Average wind power output	1624 MW
	Minimum wind power output	0 MW
Average load demand (30868 MW)	Maximum wind power output	2624 MW
	Average wind power output	1312 MW
	Minimum wind power output	0 MW
Minimum load demand (23696 MW)	Maximum wind power output	2014 MW
	Average wind power output	1007 MW
	Minimum wind power output	0 MW

The output of HPSs and CGUs will be adjusted according to the difference between the load and the wind power and the respective installed capacity. This subsection does not adopt the optimum power flow calculation. The injection points of CGUs are city 3, 2, 13, 18, 22 and 25, the injection points of wind power are City 12, 20, 17 and 7, and the injection points of HPSs are City 4, 5, 18 and 25. Figure 7.11 summarizes the effects of different wind power outputs on the voltage amplitude of each node in WIMPG under the three load cases.

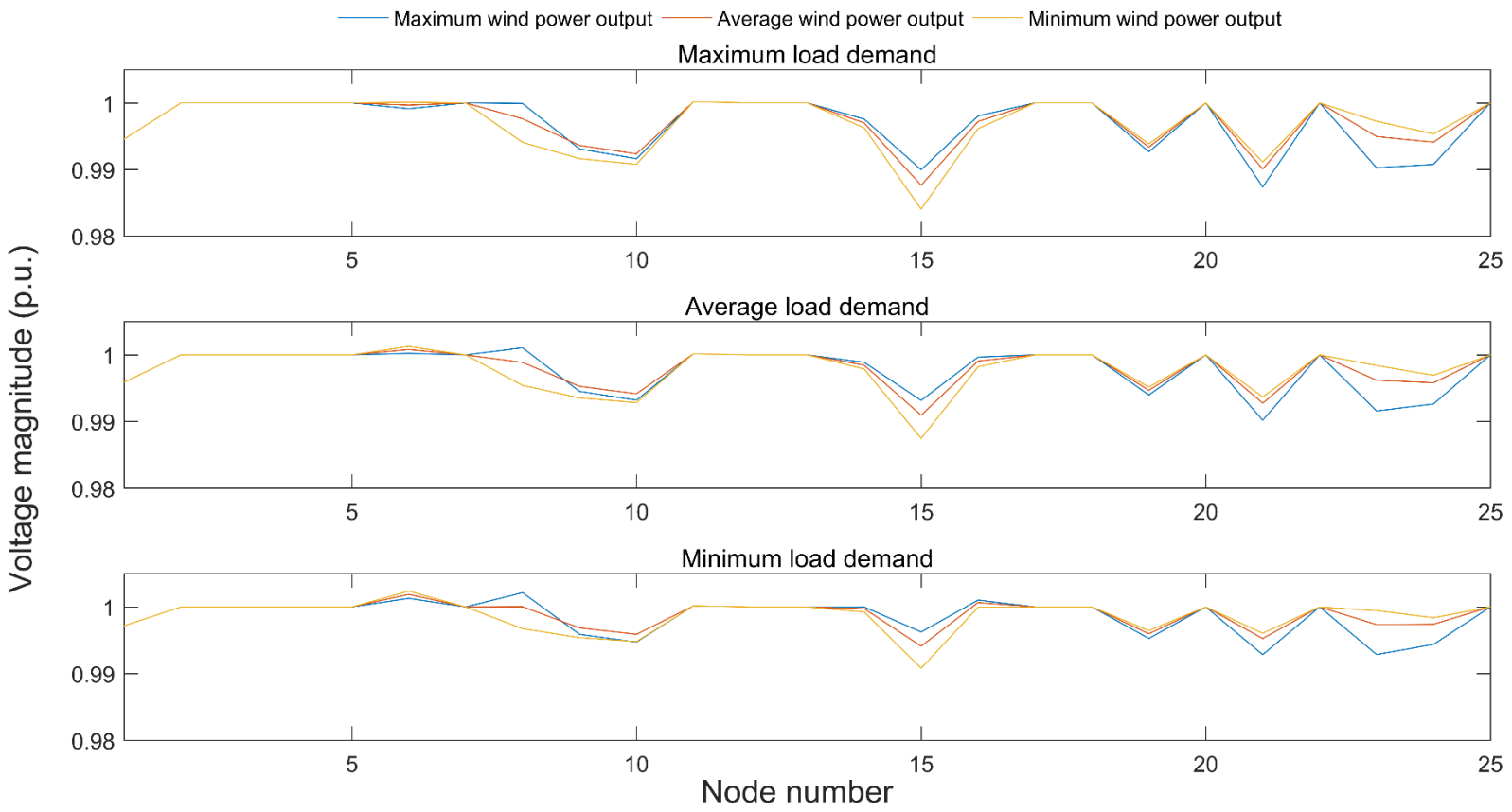

Figure 0.11: The voltage magnitude of each node in WIMPG with three wind power outputs in different load scenarios in 2020

It can be seen from the figure that the fluctuation of the wind power output will cause the voltage magnitude of the node adjacent to the wind power injection node to fluctuate, which is more obvious when the load demand is high. In general, the voltage amplitudes of all nodes in the nine situations are between 0.98 and 1.01, which meets the voltage requirements of the system operation. Therefore, the proposed capacity scenario of HPS can be operated reliably in the system.

7.4 Summary

In this chapter, the WP-HPS cooperation (strategy 2) method was applied to the WIMPG to study its application in practical cases. The Inner Mongolia Autonomous Region is the province with the most wind resources, and it is also the province with the fastest development of wind power in China and the largest installed capacity of wind power. However, the local coal resources are abundant and water resources are scarce. The power generation system of WIMPG is mostly based on thermal-power generation. Therefore, when the wind penetration level increases, the fluctuation of the available power generation capacity of the system becomes larger, and the peak regulation ability of the system is obviously insufficient, which reduces the reliability of the system. It is a reasonable solution for the WIMPG to improve the operating reserve capacity of the system by adding HPS to alleviate the volatility of wind power.

In this chapter, the system reliability of the WIMPG was evaluated at three time points from low to high wind penetration levels. The simulation results in 2010 show that, when the wind penetration level is low, the impact on system reliability is small. The simulation results of 2015 illustrate that the increase in wind penetration level will make

the system reliability worse. Increasing system operation by adding HPS can significantly improve system reliability. In 2015, as much as a 32% abandonment rate also gave HPS another goal besides improving system reliability: cooperation with WTGs to reduce the waste wind power.

The proposed WP-HPS cooperation (strategy 2) cooperation method introduces the dispatch ratio, smooths the fluctuation of the CGUs output, and balances the supply and demand of the power system by absorbing surplus wind power. The 2020 simulation results prove that the WP-HPS cooperation (strategy 2) method can increase the utilization of wind power while improving system reliability to system requirement level.

Chapter 8

Conclusions and future works

8.1 Conclusions

The purpose of this thesis is to reduce the negative impact of wind power characteristics on the power system and to maintain the reliability of the system. Detailed analyses of the output models of the various units (CGUs, WTGs, HPS) of the power generation system were carried out. A new control strategy, based on reliability, for HPS and wind power is proposed, and the method is analyzed and introduced in detail. The well-proven software tools MATLAB and MATPOWER support the study. The following sections describe the main findings of this thesis based on the detailed research contributions outlined in Chapter 1.

Contribution 1: develop the reliability assessment method utilizing SMCS method to analyze power system reliability at different wind penetration levels

The probability-based simulation reliability assessment method proposed in this thesis utilized the SMCS method to simulate the reliable model of each power generation units in the system. It also utilizes the two-parameter Weibull distribution to artificially generate wind speed and the quadratic speed power conversion formula to evaluate wind power. The proposed reliability evaluation method has the following advantages:

1. It has the advantages of SMCS which considers the time sequence of the power system and the change of load to accurately simulate the actual running of power system. Hence, this reliability evaluation method can be used to calculate reliability indices such as failure frequency, time of failure duration.

2. This method is easy to apply to th evaluation of the reliability of different proposed power systems. It is only necessary s to modify the power generation unit parameters and load demand parameters in the system according to the required systems. Moreover, the reliability of the proposed power system with different dispatch ratios of WP-HPS cooperation method can be evaluated, and the judgment basis for the Independent System Operator (ISO) to determine the optimal value of the dispatch ratio for reliable operation can be set.

In Chapter 4, the IEEE-30 Bus Test System is taken as an example to analyze the reliability of the power system with different wind penetration levels. Taking one wind farm as an example, when the wind penetration level increases from 0% to 20%, the system reliability index LOLE increases from 3.96 hours/year to 25.06 hours/year. Simulation studies on the output characteristics of wind power showed that the available output of the system fluctuates greatly after the wind power was integrated. The Operating Reserve (OR) provided by CGUs was unable to meet the needs of the power system and the power system reliability was greatly reduced. To reduce the influence of wind power characteristics on power system, HPS is utilized to increase the capacity of OR and improve the reliability of the system.

Contribution 2: propose a new wind power and HPS control strategy to reduce the impact of wind power integration

To reduce the influence of wind power characteristic on the power system, the proposed WP-HPS cooperation method was proposed. The dispatch limitation is introduced in the WP-HPS cooperation method, which is to limit the wind power that can be absorbed by the system to a certain value, if the available wind power output is larger than this value, a portion of the wind power output needs to be curtailed, in order to achieve adequate and dynamic control in the system. The HPS stores excess wind power and discharges when the system is insufficient to improve system reliability.

In this cooperation of the porposed generation system, there are two possible operation strategies when the output of CGUs is insufficient; strategy 1: supply only by HPS with wind power supplying basic load, strategy 2: in addition to HPS, if the available generation output of wind power is greater than the dispatch limitation, the additional wind power can also supply the load.

The two operational strategies were then modelled and compared the ability to improve system reliability in the IEEE 30 Bus Test System. The simulation results in Chapter 5 show that when the wind penetration level is 10%, in order to maintain the reliability of the system, the optimal dispatch ratio that the WP-HPS cooperation (strategy 1) method can accept is 4%, and the corresponding HPS capacity is (21.6 MW, 230.4 MWh), the optimal dispatch ratio WP-HPS cooperation (strategy 2) method can accept is 5%, and the corresponding HPS capacity is (14.4 MW, 288.0 MWh). In comparison, Strategy 2 improves the reliability of the system more effectively and adopts a higher dispatch ratio of wind power to meet the requirements of system reliability, thereby improving the utilization of wind power. Therefore, strategy 2 is utilized as the

cooperation model in the proposed WP-HPS cooperation method. The main advantages of WP-HPS cooperation (strategy 2) method are:

1. Applying the dispatch ratio to the proposed power generation system. The dispatch ratio is proposed to limit the wind energy directly absorbed by the power system to a fixed percentage of the load demand and the remaining load is supplied by the CGUs. Owing to the effect of the dispatch ratio, the fluctuation of the wind power output actually absorbed by the system is much smaller than the available wind power output, which can effectively alleviate the peaking and valley-filling pressure of the CGUs.

2. The pumping–generating cycle of HPS is based on reliability. This operating cycle of the HPS is different to previous fixed cycle (storing water at night when the load is small and discharging during the daytime) and free cycle (storing water when the electricity price is low and discharging otherwise). This operating cycle is based on a supply and demand relationship to store excess wind power and provide power when the wind generation on the system is insufficient, can reduce the occurrence of insufficient power supply and effectively improve the reliability of the system.

This thesis then applied the WP-HPS cooperation (strategy 2) method to two test systems: 1) the IEEE 118-Bus Test System for analyzing the WP-HPS cooperation (strategy 2) method for the long-term planning and daily operation of each wind penetration level system. 2) an actual power system for solving the problem of

reliability reduction caused by an increase in wind penetration level. The results of the assessment are briefly summarized as follows:

1）To test the applicability of the WP-HPS cooperation (strategy 2) method for long-term planning and daily operation, this method was applied to the 118 Bus Test System. In long-term planning, the proposed method was applied in the power systems with 6 different wind penetration levels from low to high. The results proved that WP-HPS cooperation (strategy 2) method makes a significant contribution to alleviating the impact of wind power volatility. The proposed method can improve the reliability of the power system with a wind penetration level not exceeding 40% to the original level. When the wind penetration level reaches 50%, the proposed method cannot meet the reliability requirements, and the total installed capacity of the generation system needs to be increased. the operation of daily load cycle of four different wind penetration level were analyzed for power flow. Taking 30% wind penetration level as an example, the daily network energy loss of the WP-HPS cooperation (strategy 2) method is only 30.18% higher than without wind power, while the daily network energy loss without using the proposed method is 69.08%. The simulation results show that the proposed method can effectively reduce the network energy losses caused by wind power integration and smooth the fluctuation of network power losses.

2) The WP-HPS cooperation (strategy 2) method was applied to the actual power system of the West Inner Mongolia Power Grid (WIMPG) to analyze the proposed cooperation method for improving the reliability of the existing system. The evaluation results show that the cooperation between wind power and HPS in the planned construction not only can meet the requirements of system reliability but also can

reduce the wind curtailment rate to the level required.. In order to achieve the value of the Curtailment Rate (CR) less than 15%, and to ensure that the system reliability is at the required level in 2020, the Scheme 4 (Hohhot HPS, Xilinhot HPS, Wuhai HPS, and Baotou HPS) could meet that requirements, and the corresponding dispatch ratio is 8.5% and the reliability index LOLE is 22.42 hours/year. Therefore, the proposed method proves feasible in the WIMPG, and provides advice for the future planning of the system.

Contribution 3: develop the reliability cost-benefit analysis to quantify the improvement of the WP-HPS cooperation ***method in system reliability as economic indicators***

In past publications many RCBA methods for determining the operating reserve capacity were proposed. The key to this method is to assess the costs and benefits of OR in reliability and provide a basis for determining optimal OR capacity. In this thesis, the RCBA method was modified according to the proposed WP-HPS cooperation method to determine the optimal capacity of HPS. The main advantages of the proposed RCBA method are:

1. The benefits of HPS for system reliability are quantified as economic indicators. It is difficult to estimate the reliability benefit produced by HPS under a certain power supply reliability level. Hence, the reliability benefit in this method consists of reduced CIC after integrating HPS and the coal benefits resulting from savings in the use of wind power.

2. It can quickly evaluate the TB that HPS brings to system reliability for different capacity scenarios, provide a basis for ISO to select the optimal capacity scenario of HPS from the planning capacity scenarios that meets the system reliability requirements.

The RCBA method and reliability assessment method are used together in three test systems. The test results are summarized as follows:

1. The case study in IEEE 30 Bus system shows that compared with the WP-HPS cooperation (strategy 1), the WP-HPS cooperation (strategy 2) method requires a smaller capacity installation of HPS to improve system reliability to the original level, saving more reliability costs and having higher total benefits. Therefore, from the RCBA perspective, the WP-HPS cooperation (strategy 2) method is also better than the WP-HPS cooperation (strategy 1) method.

2. The case study in IEEE 118 Bus system shows that when the wind penetration level reaches 40%, the WP-HPS cooperation (strategy 2) method can meet the reliability requirements, but due to the expensive reliability cost, it has a negative value of TB. Hence, WP-HPS cooperation (strategy 2) method is suitable for this power system with the wind penetration level of 30% or less from the perspective of RCBA and probability-based simulation reliability assessment method.

3. The case study in WIMPG shows that to alleviate the impact of increased installed wind power capacity on system reliability, the Scheme 3 (Hohhot HPS, Xilinhot HPS, Baotou HPS) need to be put into operation in 2020 to obtain the maximum TB from the perspective of RCBA. Although in order to reduce CR to below 15%, the Scheme

4 (Hohhot HPS, Xilinhot HPS, Wuhai HPS, and Baotou HPS) should be adopted, which is also economically feasible from the perspective of RCBA.

8.2 Future work

This thesis contributes to alleviating the impact of wind power fluctuations on the power system with the increase in wind penetration level and proposes the WP-HPS cooperation (strategy 2) method to maintain system reliability, smooth CGUs output, and reduce wind curtailment ratio. However, possible extensions and improvements may be applied to the methods and concepts presented in this thesis in the following specific aspects:

- The reliability evaluation of the power generation system in this thesis is to assess whether the system output can meet the load requirements; it does not consider the limitation of transmission power loss and fault in the transmission network nor does it consider the voltage and power constraints. In future research, it is necessary to consider the impact of the above factors for a more comprehensive reliability assessment.

- This thesis considers the output of CGUs as a whole, without considering the limitation of the ramping speed of each generator, considering that the ramping speed limits the peaking ability of CGUs. Therefore, it is necessary to consider the speed of generator ramping in future work.

- Due to the lack of actual industrial data, the reliability evaluation method cannot be tested in real systems. The Monte Carlo Simulation is based on powerful

software that generates random numbers and is tested repeatedly over a long period of time. The simulation results are close to real data, and although the accuracy and validity of the evaluation have been proven through case studies, it is best to test the proposed method using real industry data.

- With the vigorous development of energy storage technology, an increasing number of different types of energy storage equipment is being applied to power systems, which can effectively improve the peaking ability of the power system. Therefore, it is necessary to consider the working characteristics of other type energy storage devices in the system planning in future work.

- In many areas, the development of renewable energy includes wind power as well as solar power. Future work can consider planning the operating reserve capacity according to the latest research on solar power generation or a combination of both wind and solar power.

Reference

[1] D. G. Lee, “Renewable energy: power for a sustainable future,” *Australas. J. Environ. Manag.*, 2017.

[2] Y. Takashima, T. Koizumi, and N. Wada, “Renewable energy,” *Hitachi Rev.*, 2014.

[3] I. E. A. International and E. Agency, “World Energy Investment 2017.”

[4] B. C. Ummels, M. Gibescu, E. Pelgrum, W. L. Kling, and A. J. Brand, “Impacts of wind power on thermal generation unit commitment and dispatch,” *IEEE Trans. Energy Convers.*, 2007.

[5] J. Fletcher, “Normal distribution,” *BMJ*, 2009.

[6] I. Y. F. Lun and J. C. Lam, “A study of Weibull parameters using long-term wind observations,” *Renew. Energy*, 2000.

[7] D. Villanueva, J. L. Pazos, and A. Feijóo, “Probabilistic load flow including wind power generation,” *IEEE Trans. Power Syst.*, 2011.

[8] F. Castro Sayas and R. N. N. Allan, “Generation availability assessment of wind farms,” in *Generation, Transmission and Distribution, IEE Proceedings-*, 1996.

[9] A. Boone, “Simulation of short-term wind speed forecast errors using a multi-variate ARMA (1, 1) time-series model,” *Power*, 2005.

[10] R. Billinton and W. Li, *Reliability Assessment of Electric Power Systems Using Monte Carlo Methods*, vol. 49, no. 0. 1994.

[11] P. Pinson, H. Madsen, H. A. Nielsen, G. Papaefthymiou, and B. Klöckl, "From probabilistic forecasts to statistical scenarios of short-term wind power production," *Wind Energy*, 2009.

[12] X. Y. Ma, Y. Z. Sun, and H. L. Fang, "Scenario generation of wind power based on statistical uncertainty and variability," *IEEE Trans. Sustain. Energy*, 2013.

[13] G. Papaefthymiou, P. H. Schavemaker, L. van der Sluis, W. L. Kling, D. Kurowicka, and R. M. Cooke, "Integration of stochastic generation in power systems," *Int. J. Electr. Power Energy Syst.*, 2006.

[14] B. M. G. Lauby *et al.*, "Balancing Act," *IEEE Power Energy Mag.*, vol. 6, no. 9, pp. 75–85, 2011.

[15] J. Wen, Y. Zheng, and F. Donghan, "A review on reliability assessment for wind power," *Renewable and Sustainable Energy Reviews*. 2009.

[16] European Wind Energy Association, "Large Scale Integration of Wind Energy in the European Power Supply: Analysis Issues and Recommendations," 2005.

[17] National Energy Administration, "The Situation of Wind Power integrated Power System." [Online]. Available: http://www.nea.gov.cn/2017-01/26/c_136014615.htm. [Accessed: 20-Feb-2019].

[18] P. S. Georgilakis, "Technical challenges associated with the integration of wind power into power systems," *Renewable and Sustainable Energy Reviews*. 2008.

[19] G. Yan *et al.*, “Optimization of energy storage system capacity for relaxing peak load regulation bottlenecks,” *Proc. CSEE*, vol. 32, no. 28, pp. 27–35, 2012.

[20] J. Zou, S. Rahman, and X. Lai, “Mitigation of wind output curtailment by coordinating with pumped storage and increasing transmission capacity,” in *IEEE Power and Energy Society General Meeting*, 2015.

[21] B. A. I. Jian-hua, X. Song-xu, J. I. A. De-xiang, and C. Lu, “Study of Major Questions of Wind Power Digestion and Transmission in China,” *Power Syst. clean energy*, vol. 26, no. 1, pp. 14–17, 2010.

[22] H. Zhao, Q. Wu, S. Hu, H. Xu, and C. N. Rasmussen, “Review of energy storage system for wind power integration support,” *Appl. Energy*, 2015.

[23] S. Rehman, L. M. Al-Hadhrami, and M. M. Alam, “Pumped hydro energy storage system: A technological review,” *Renew. Sustain. Energy Rev.*, 2015.

[24] J. Hetzer, D. C. Yu, and K. Bhattarai, “An economic dispatch model incorporating wind power,” *IEEE Trans. Energy Convers.*, 2008.

[25] A. Tuohy and M. O’Malley, “Impact of pumped storage on power systems with increasing wind penetration,” in *2009 IEEE Power and Energy Society General Meeting, PES ’09*, 2009.

[26] U. Raudsaar, I. Drovtar, and A. Rosin, “Overview - Pumped-hydro energy storage for balancing wind energy forecast errors,” in *9th International: 2014 Electric Power Quality and Supply Reliability Conference, PQ 2014 - Proceedings*, 2014.

[27] M. A. Hozouri, A. Abbaspour, M. Fotuhi-Firuzabad, and M. Moeini-Aghtaie, "On the use of pumped storage for wind energy maximization in transmission-constrained power systems," *IEEE Trans. Power Syst.*, 2015.

[28] R. Jiang, J. Wang, and Y. Guan, "Robust unit commitment with wind power and pumped storage hydro," *IEEE Trans. Power Syst.*, 2012.

[29] E. D. Castronuovo and J. A. P. Lopes, "Optimal operation and hydro storage sizing of a wind-hydro power plant," *Int. J. Electr. Power Energy Syst.*, 2004.

[30] J. García-González, R. M. R. de la Muela, L. M. Santos, and A. M. Gonzalez, "Stochastic joint optimization of wind generation and pumped-storage units in an electricity market," *IEEE Trans. Power Syst.*, 2008.

[31] J. Matevosyan and L. Söder, "Optimal daily planning for hydro power system coordinated with wind power in areas with limited export capability," in *2006 9th International Conference on Probabilistic Methods Applied to Power Systems, PMAPS*, 2006.

[32] R. Billinton, *Reliability Evaluation of Power Systems*. 1996.

[33] L. T. Anstine, R. E. Burke, J. E. Casey, R. Holgate, R. S. John, and H. G. Stewart, "Application of Probability Methods to the Determination of Spinning Reserve Requirements for the Pennsylvania-New Jersey-Maryland Interconnection," *IEEE Trans. Power Appar. Syst.*, 1963.

[34] R. Billinton and R. N. Allan, *Reliability evaluation of power systems*. 1996.

[35] H. B. Gooi, "Optimal scheduling of spinning reserve," *IEEE Trans. Power Syst.*, 1999.

[36] D. Chattopadhyay and R. Baldick, “Unit commitment with probabilistic reserve,” *2002 IEEE Power Eng. Soc. Winter Meet. Conf. Proc. (Cat. No.02CH37309)*, 2002.

[37] R. Doherty and M. O'Malley, “A new approach to quantify reserve demand in systems with significant installed wind capacity,” *IEEE Trans. Power Syst.*, 2005.

[38] R. Billinton, B. Karki, R. Karki, and G. Ramakrishna, “Unit commitment risk analysis of wind integrated power systems,” *IEEE Trans. Power Syst.*, 2009.

[39] E. M. Gouveia and M. A. Matos, “Operational reserve of a power system with a large amount of wind power,” *Proc. 8th Int. Conf. Prob. Methods Appl. to Power Syst.*, pp. 717–722, 2004.

[40] R. Doherty and M. O’Malley, “Quantifying reserve demands due to increasing wind power penetration,” in *2003 IEEE Bologna PowerTech - Conference Proceedings*, 2003.

[41] J. Wang, X. Wang, and Y. Wu, “Operating reserve model in the power market,” *IEEE Trans. Power Syst.*, 2005.

[42] M. A. Ortega-Vazquez and D. S. Kirschen, “Estimating the spinning reserve requirements in systems with significant wind power generation penetration,” *IEEE Trans. Power Syst.*, 2009.

[43] C. W. Yu, X. S. Zhao, F. S. Wen, C. Y. Chung, T. S. Chung, and M. X. Huang, “Pricing and procurement of operating reserves in competitive pool-based electricity markets,” *Electr. Power Syst. Res.*, 2005.

[44] L. X. SU Peng, LIU Tianqi, “Determination of Optimal Spinning Reserve of Power Grid Containing Wind,” *Power Syst. Technol.*, vol. 34, no. 12, pp. 158–162, 2010.

[45] R. Castellanos, M. Ramirez, G. Calderon, and A. R. Messina, “Impact studies of the effect of large-scale wind integration in the Mexican power grid,” *2017 IEEE PES Innov. Smart Grid Technol. Conf. Eur. ISGT-Europe 2017 - Proc.*, vol. 2018-Janua, pp. 1–5, 2018.

[46] S. Zhu, Y. Zhang, and A. A. Chowdhury, “Capacity Credit of Wind Generation Based on Minimum Resource Adequacy Procurement,” vol. 48, no. 2, pp. 730–735, 2012.

[47] “Global Wind Statitics 2017,” *Global Wind Energy Council (GWEC)*, 2018. .

[48] O. Edenhofer *et al., Renewable energy sources and climate change mitigation: Special report of the intergovernmental panel on climate change*. 2011.

[49] N. I. Meyer, “Learning from wind energy policy in the EU: Lessons from Denmark, Sweden, and Spain,” *Eur. Environ.*, 2007.

[50] J. Nordensvärd and F. Urban, “The stuttering energy transition in Germany: Wind energy policy and feed-in tariff lock-in,” *Energy Policy*, 2015.

[51] E. Ryland, “Danish wind power policy: Domestic and international forces,” *Env. Polit.*, 2010.

[52] N. I. Meyer, “Renewable energy policy in Denmark,” *Energy Sustain. Dev.*, 2004.

[53] G. Iglesias, P. Del Río, and J. Á. Dopico, “Policy analysis of authorisation procedures for wind energy deployment in Spain,” *Energy Policy*, 2011.

[54] P. del Río González, “Ten years of renewable electricity policies in Spain: An analysis of successive feed-in tariff reforms,” *Energy Policy*, 2008.

[55] C. Nolden, “Governing community energy-Feed-in tariffs and the development of community wind energy schemes in the United Kingdom and Germany,” *Energy Policy*, 2013.

[56] D. J. Ward and O. R. Inderwildi, “Global and local impacts of UK renewable energy policy,” *Energy Environ. Sci.*, 2013.

[57] S. Zhao and C. Singh, “Reliability study of onshore and offshore wind generation and impact of location,” *IEEE Power Energy Soc. Gen. Meet.*, vol. 2014-Octob, no. October, pp. 1–5, 2014.

[58] T. Ackermann and L. Söder, “Wind energy technology and current status: a review,” *Renew. Sustain. Energy Rev.*, 2000.

[59] G. M. Joselin Herbert, S. Iniyan, E. Sreevalsan, and S. Rajapandian, “A review of wind energy technologies,” *Renewable and Sustainable Energy Reviews*. 2007.

[60] M. E. H. Al-kharbosy, “Enhancement Protection and Operation of The Doubly Fed Induction Generator During Grid,” 2012.

[61] S. Soter and R. Wegener, “Development of induction machines in wind power technology,” in *Proceedings of IEEE International Electric Machines and Drives Conference, IEMDC 2007*, 2007.

[62] R. C. Bansal, “Three-phase self-excited induction generators: An overview,” *IEEE Transactions on Energy Conversion*. 2005.

[63] G. Tapia and A. Tapia, “Wind generation optimisation algorithm for a doubly fed induction generator,” *IEE Proc. - Gener. Transm. Distrib.*, 2005.

[64] Z. Chen and H. Li, “Overview of different wind generator systems and their comparisons,” *IET Renew. Power Gener.*, 2008.

[65] T. P. Chang, “Performance comparison of six numerical methods in estimating Weibull parameters for wind energy application,” *Appl. Energy*, vol. 88, no. 1, pp. 272–282, 2011.

[66] J. V. Seguro and T. W. Lambert, “Modern estimation of the parameters of the Weibull wind speed distribution for wind energy analysis,” *J. Wind Eng. Ind. Aerodyn.*, vol. 85, no. 1, pp. 75–84, 2000.

[67] S. Akpinar and E. K. Akpinar, “Estimation of wind energy potential using finite mixture distribution models,” *Energy Convers. Manag.*, 2009.

[68] J. A. Carta and P. Ramírez, “Use of finite mixture distribution models in the analysis of wind energy in the Canarian Archipelago,” *Energy Convers. Manag.*, vol. 48, no. 1, pp. 281–291, 2007.

[69] J. A. Carta, P. Ramírez, and S. Velázquez, “A review of wind speed probability distributions used in wind energy analysis. Case studies in the Canary Islands,” *Renewable and Sustainable Energy Reviews*. 2009.

[70] A. N. Celik, A. Makkawi, and T. Muneer, “Critical evaluation of wind speed frequency distribution functions,” *J. Renew. Sustain. Energy*, 2010.

[71] A. Garcia, J. L. Torres, E. Prieto, and A. De Francisco, “Fitting wind speed distributions: A case study,” *Sol. Energy*, 1998.

[72] R. E. Luna and H. W. Church, “Estimation of Long-term Concentrations Using a ‘Universal’ Wind Speed Distribution,” *Journa*, 1974.

[73] I. Bogardi and I. Matyasovszky, “Estimating daily wind speed under climate change,” *Sol. Energy*, 1996.

[74] P. Wais, “Two and three-parameter Weibull distribution in available wind power analysis,” *Renew. Energy*, 2017.

[75] I. Fyrippis, P. J. Axaopoulos, and G. Panayiotou, “Wind energy potential assessment in Naxos Island, Greece,” *Appl. Energy*, vol. 87, no. 2, pp. 577–586, 2010.

[76] F. A. L. Jowder, “Weibull and Rayleigh Distribution Functions of Wind Speeds in Kingdom of Bahrain,” *Wind Eng.*, 2006.

[77] A. Ucar and F. Balo, “Investigation of wind characteristics and assessment of wind-generation potentiality in Uludağ-Bursa, Turkey,” *Appl. Energy*, vol. 86, no. 3, pp. 333–339, 2009.

[78] B. Safari and J. Gasore, “A statistical investigation of wind characteristics and wind energy potential based on the Weibull and Rayleigh models in Rwanda,” *Renew. Energy*, vol. 35, no. 12, pp. 2874–2880, 2010.

[79] A. N. Celik, “A statistical analysis of wind power density based on the Weibull and Rayleigh models at the southern region of Turkey,” *Renew. Energy*, 2004.

[80] K. Xie and R. Billinton, “Energy and reliability benefits of wind energy conversion systems,” *Renew. Energy,* 2011.

[81] T. P. Chang, “Estimation of wind energy potential using different probability density functions,” *Appl. Energy,* vol. 88, no. 5, pp. 1848–1856, 2011.

[82] M. Blanchard and G. Desrochers, “Generation of autocorrelated wind speeds for wind energy conversion system studies,” *Sol. Energy,* 1984.

[83] R. Billinton, H. Chen, and R. Ghajar, “Time-series models for reliability evaluation of power systems including wind energy,” *Microelectron. Reliab.*, 1996.

[84] E. Erdem and J. Shi, “ARMA based approaches for forecasting the tuple of wind speed and direction,” *Appl. Energy*, 2011.

[85] P. Chen, T. Pedersen, B. Bak-Jensen, and Z. Chen, “ARIMA-based time series model of stochastic wind power generation,” *IEEE Trans. Power Syst.*, 2010.

[86] R. Karki, P. Hu, and R. Billinton, “A simplified wind power generation model for reliability evaluation,” *IEEE Trans. Energy Convers.*, 2006.

[87] F. Vallee, J. Lobry, and O. Deblecker, “Impact of the wind geographical correlation level for reliability studies,” *IEEE Trans. Power Syst.*, 2007.

[88] P. F. Correia and J. M. Ferreira de Jesus, “Simulation of correlated wind speed and power variates in wind parks,” *Electr. Power Syst. Res.*, 2010.

[89] S. Wang, S. Shi, K. Lo, and J. Lu, “An Approach to Calculate the Capacity of Pump-Hydro Combined Energy Storage with Wind Power Integration,” *World J. Eng. Technol.*, vol. 04, no. 03, pp. 43–49, 2016.

[90] P. Ye *et al.*, “Research on flexible self starting strategy of wind storage isolated network system,” *2017 3rd IEEE Int. Conf. Control Sci. Syst. Eng. ICCSSE 2017*, pp. 443–447, 2017.

[91] A. M. O. Haruni, A. Gargoom, M. E. Haque, and M. Negnevitsky, “Dynamic operation and control of a hybrid wind-diesel stand alone power systems,” in *Conference Proceedings - IEEE Applied Power Electronics Conference and Exposition - APEC*, 2010.

[92] A. Wright, “Wind Turbine Control Systems,” in *Wind Turbine Technology: Fundamental Concepts in Wind Turbine Engineering, Second Edition*, 2010.

[93] W. Long, “Research on site selection of pumpe storage power station and combined optimizaiton operation of wind power,” 2017.

[94] Y. Y. Hong, H. L. Chang, and C. S. Chiu, “Hour-ahead wind power and speed forecasting using simultaneous perturbation stochastic approximation (SPSA) algorithm and neural network with fuzzy inputs,” *Energy*, 2010.

[95] G. Sideratos and N. D. Hatziargyriou, “An advanced statistical method for wind power forecasting,” *IEEE Trans. Power Syst.*, 2007.

[96] W.-Y. Chang, “A Literature Review of Wind Forecasting Methods,” *J. Power Energy Eng.*, 2014.

[97] I. R. Young, S. Zieger, and A. V. Babanin, “Global Trends in Wind Speed,” *Science (80-.).*, 2011.

[98] S. Rong, Z. Li, and W. Li, “Investigation of the promotion of wind power consumption using the thermal-electric decoupling techniques,” *Energies*, 2015.

[99] R. B. and G. Bai, “Generating Capacity Adequacy Associated With Wind Energy,” *IEEE Trans. Energy Convers.*, vol. 19, no. 3, pp. 641–646, 2004.

[100] S. Shi and P. Systems, “Operation and Assessment of Wind Energy on Power System Reliability Evaluation Declaration of Author ’ s Right,” 2014.

[101] C. Bueno and J. A. Carta, “Technical-economic analysis of wind-powered pumped hydrostorage systems. Part I: Model development,” *Sol. Energy*, 2005.

[102] C. Bueno and J. A. Carta, “Technical-economic analysis of wind-powered pumped hydrostorage systems. Part II: Model application to the island of El Hierro,” *Sol. Energy,* 2005.

[103] J. G. Slootweg, S. W. H. De Haan, H. Polinder, and W. L. Kling, “General Model for Representing Variable-Speed Wind Turbines in Power System Dynamics Simulations,” *IEEE Power Engineering Review*. 2002.

[104] E. Barbour, I. A. G. Wilson, J. Radcliffe, Y. Ding, and Y. Li, “A review of pumped hydro energy storage development in significant international electricity markets,” *Renewable and Sustainable Energy Reviews*. 2016.

[105] D. O. Akinyele and R. K. Rayudu, “Review of energy storage technologies for sustainable power networks,” *Sustain. Energy Technol. Assessments*, 2014.

[106] G. de Oliveira e Silva and P. Hendrick, “Pumped hydro energy storage in buildings,” *Appl. Energy,* 2016.

[107] S. Hameer and J. L. van Niekerk, “A review of large-scale electrical energy storage,” *International Journal of Energy Research*. 2015.

[108] A. M. Foley, P. G. Leahy, K. Li, E. J. McKeogh, and A. P. Morrison, “A long-term analysis of pumped hydro storage to firm wind power,” *Appl. Energy*, 2015.

[109] J. P. Deane, B. P. Ó Gallachóir, and E. J. McKeogh, “Techno-economic review of existing and new pumped hydro energy storage plant,” *Renewable and Sustainable Energy Reviews*. 2010.

[110] J. S. Anagnostopoulos and D. E. Papantonis, “Pumping station design for a pumped-storage wind-hydro power plant,” *Energy Convers. Manag.,* 2007.

[111] C. Crampes and M. Moreaux, “Pumped storage and cost saving,” *Energy Econ.,* 2010.

[112] M. Black and G. Strbac, “Value of storage in providing balancing services for electricity generation systems with high wind penetration,” *J. Power Sources,* 2006.

[113] D. Raslter, “Electricity Energy Storage Technology Options: A White Paper Primer on Applications, Costs, and Benefits,” 2010.

[114] A. A. Chowdhury, L. Bertling, B. P. Glover, and E. Haringa, “A Monte Carlo simulation model for multi-area generation reliability evaluation,” in *2006 9th*

International Conference on Probabilistic Methods Applied to Power Systems, PMAPS, 2006.

[115] R. Billinton and W. Li, "Reliability Assessment of Electric Power Systems Using Monte Carlo Methods," vol. 49, no. 0, p. 6221, 1994.

[116] O. A. Mousavi, G. B. Gharehpetian, and ..., "Estimating risk of cascading blackout using probabilistic methods," *Electr. Power and …*, 2009.

[117] A. M. Rei, M. Armando, L. Da Suva, J. L. Jardim, and J. C. O. De Mello, "Static and dynamic aspects in bulk power system reliability evaluations," *IEEE Trans. Power Syst.*, 2000.

[118] V. A. Levi, J. M. Nahman, and D. P. Nedic, "Security modeling for power system reliability evaluation," *IEEE Trans. Power Syst.*, 2001.

[119] E. Vaahedi, W. Li, T. Chia, and H. Dommel, "Large scale probabilistic transient stability assessment using B.C. Hydro's on-line tool," *IEEE Trans. Power Syst.*, 2000.

[120] L. A. Lightfoot, "Reliability Evaluation of Power Systems," *Electron. Power*, 1984.

[121] W. Li, *Risk Assessment Of Power Systems: Models, Methods, and Applications*. 2005.

[122] R. Billinton and R. N. Allan, *Chapter 2: Generating Capacity-Basic Probability Methods, in Reliability Evaluation of Power Systems*, Second edi. 1996.

[123] C. F. Desieno and L. L. Stine, “A Probability Method for Determining the Reliability of Electric Power Systems,” *IEEE Trans. Power Appar. Syst.*, vol. 83, no. 2, pp. 174–181, 1964.

[124] A. Hanson and L. Grigsby, “Power system analysis,” in *Systems, Controls, Embedded Systems, Energy, and Machines*, 2017.

[125] J. F. Prada, “The Value of Reliability in Power Systems: Pricing Operating Reserves,” *Mit El 99-005 Wp*, 1999.

[126] P. P. Williamson, “Mathematical Statistics With Applications,” *J. Am. Stat. Assoc.*, 2006.

[127] I. D. Margaris, S. A. Papathanassiou, N. D. Hatziargyriou, A. D. Hansen, and P. Sorensen, “Frequency Control in Autonomous Power Systems with High Wind Power Penetration,” *IEEE Trans. Sustain. Energy*, 2012.

[128] R. Allan and R. Billinton, “Probabilistic assessment of power systems,” *Proc. IEEE*, 2000.

[129] A. Ahmadi-Khatir, M. Bozorg, and R. Cherkaoui, “Probabilistic spinning reserve provision model in multi-control zone power system,” *IEEE Trans. Power Syst.*, 2013.

[130] R. Billinton, *Reliability Evaluation of Engineering Systems: Concepts and Techniques*, Second Edi. New York and London, 1992.

[131] A. K. Chattopadhyay and T. Chattopadhyay, “Monte Carlo simulation,” in *Springer Series in Astrostatistics*, 2014.

[132] A. Naess, B. J. Leira, and O. Batsevych, “System reliability analysis by enhanced Monte Carlo simulation,” *Struct. Saf.*, 2009.

[133] E. Distribution, “Exponential Distribution,” *J. Stat. Plan. Inference*, 1966.

[134] K. Conradsen, L. B. Nielsen, and L. P. Prahm, “Review of Weibull Statistics for Estimation of Wind Speed Distributions,” *J. Clim. Appl. Meteorol.*, 1984.

[135] R. Billinton and L. Gan, “Use Of Monte Carlo Simulation In Teaching Generating Capacity Adequacy Assessment,” *IEEE Trans. Power Syst.*, 1991.

[136] A. M. Leite Da Silva *et al.*, “Application of Monte Carlo simulation to generating system well-being analysis considering renewable sources,” *Eur. Trans. Electr. Power*, 2007.

[137] A. Sankarakrishnan and R. Billinton, “Sequential Monte Carlo Simulation For Composite Power Reliablity Analysis with time varying loads,” *IEEE Trans. Power Syst.*, 1995.

[138] L. Goel, X. Liang, and Y. Ou, “Monte Carlo simulation-based customer service reliability assessment,” *Electr. Power Syst. Res.*, 1999.

[139] PJM, “PJM Generation Adequacy Analysis : Technical Methods Capacity Adequacy Planning Department,” *October*, no. October, 2003.

[140] D. Razzouk, “Cost-benefit analysis,” in *Mental Health Economics: The Costs and Benefits of Psychiatric Care*, 2017.

[141] O. Dzobo, C. T. Gaunt, and R. Herman, “Investigating the use of probability distribution functions in reliability-worth analysis of electric power systems,” *Int. J. Electr. Power Energy Syst.*, 2012.

[142] R. N. Allan, R. Billinton, I. Sjarief, L. Goel, and K. S. So, “A Reliability Test System For Educational Purposes - Basic Distribution System Data and Results,” *IEEE Trans. Power Syst.*, 1991.

[143] DECC, “Department of Energy & Climate Change Annex C: Rliability Standard Methodology,” no. July, pp. 1–12, 2013.

[144] J. P. Hennessey, “Some Aspects of Wind Power Statistics,” *J. Appl. Meteorol.*, 1977.

[145] C. G. Justus, W. R. Hargraves, A. Mikhail, and D. Graber, “Methods for Estimating Wind Speed Frequency Distributions,” *J. Appl. Meteorol.*, 1978.

[146] K. C. Chou and R. B. Corotis, “Simulation of hourly wind speed and array wind power,” *Sol. Energy*, 1981.

[147] R. I. Harris and N. J. Cook, “The parent wind speed distribution: Why Weibull?,” *J. Wind Eng. Ind. Aerodyn.*, 2014.

[148] M. Bollen and F. Hassan, *Integration of Distributed Generation in the Power System*. 2011.

[149] S. Ahmad, W. H. W. M. a, M. a Bawadi, and M. S. S. a, “Analysis of Wind Speed Variations and Estimation of Weibull Parameters for Wind Power Generation in Malavsia,” *October*, 2006.

[150] National Meteorological Information Center, “Hourly data from surface meteorological stations in China,” 2019. [Online]. Available: http://data.cma.cn/en/?r=data/detail&dataCode=A.0012.0001.

[151] M. Shahidehpour and Y. Wang, *Communication and Control in Electric Power Systems*. 2003.

[152] S. A. Papathanassiou and N. G. Boulaxis, “Power limitations and energy yield evaluation for wind farms operating in island systems,” *Renew. Energy*, vol. 31, no. 4, pp. 457–479, 2006.

[153] H. Holttinen and J. Pedersen, “The effect of large scale wind power on a thermal system operation,” *Proc. 4th Int. Work. Large-Scale Integr. Wind Power Transm. Networks Offshore Wind Farms*, pp. 1–7, 2003.

[154] D. Connolly, H. Lund, B. V. Mathiesen, and M. Leahy, “Modelling the existing Irish energy-system to identify future energy costs and the maximum wind penetration feasible,” *Energy*, 2010.

[155] A. Tuohy and M. O’Malley, “Impact of pumped storage on power systems with increasing wind penetration,” *2009 IEEE Power Energy Soc. Gen. Meet. PES ’09*, 2009.

[156] J. P. Deane, E. J. McKeogh, and B. P. . Gallachoir, “Derivation of intertemporal targets for large pumped hydro energy storage with stochastic optimization,” *IEEE Trans. Power Syst.*, 2013.

[157] S. V. Papaefthymiou, E. G. Karamanou, S. A. Papathanassiou, and M. P. Papadopoulos, “A wind-hydro-pumped storage station leading to high RES penetration in the autonomous island system of Ikaria,” *IEEE Trans. Sustain. Energy*, 2010.

[158] Z. Y. Gao, P. Wang, L. Bertling, and J. H. Wang, “Sizing of energy storage for power systems with wind farms based on reliability cost and wroth analysis,” *IEEE Power Energy Soc. Gen. Meet.*, 2011.

[159] J. S. Anagnostopoulos and D. E. Papantonis, “Simulation and size optimization of a pumped-storage power plant for the recovery of wind-farms rejected energy,” *Renew. Energy*, 2008.

[160] B. A. Antal, “Pumped Storage Hydropower: A Technical Review,” *Dep. Civ. Eng. -Univ.of Color. Denver*, 2014.

[161] Y. Fu, M. Shahidehpour, and Z. Li, “Long-term security-constrained unit commitment: Hybrid Dantzig-Wolfe decomposition and subgradient approach,” *IEEE Trans. Power Syst.*, 2005.

[162] China NERI, “China Wind Power Development Outlook for 2030,” p. 82, 2010.

[163] C. Yu, “China power yearbook,” 2017.

[164] S. Sun, F. Liu, S. Xue, M. Zeng, and F. Zeng, “Review on wind power development in China: Current situation and improvement strategies to realize future development,” *Renew. Sustain. Energy Rev.*, vol. 45, pp. 589–599, 2015.

[165] X. Bai, “Study on Wind Power Heating System in Western Inner Mogolia,” 2017.

[166] G. Qi, J. Zhibin, H. Chenhui, and G. Zhengnan, “Analysis of Experience on Constructing of Wind Power Dispatching Mode in West Inner Mongolia Power Grid,” 2013.

[167] J. Li, S. Pengfei, and H. Gao, *China Wind Power Outlook*. 2012.

[168] NDRC, “13th Five Year Plan development plan for renewable energy,” 2016.

[169] C. Zhang, L. Zhong, S. Liang, K. T. Sanders, J. Wang, and M. Xu, “Virtual scarce water embodied in inter-provincial electricity transmission in China,” *Appl. Energy*, vol. 187, pp. 438–448, 2017.

[170] Inner Mongolia energy development bureau, “Inner Mongolia ‘13th five-year’ Wind Power Development and Access Grid Rules,” 2015.

[171] Inner Mongolia energy development bureau, “Inner Mongolia ‘12th five-year’ Wind Power Development and Access Grid Rules,” 2010.

[172] L. K. LI Ping-jun, GAO Zheng-nan, WANG Hai-li, YANG Tao, ZHANG Zhong, WANG Meng, “Construction of West Inner Mongolia Power Market system to promote new energy consumption,” *China Electr. Eng. Soc. Power Mark. Spec. Comm.*, 2018.

[173] China Energy Administration, “Clean Energy Dissipation Action Plan（2018-2020）,” 2018.

Appendix

Appendix 1: Various load scenarios and corresponding wind power conditions of IEEE 118 Bus Test System

Case 1: 10% wind penetration level

Maximum Load demand (7780 MW)	Maximum wind power output	350 MW
	Average wind power output	175 MW
	Minimum wind power output	0 MW
Average load demand (5087 MW)	Maximum wind power output	229 MW
	Average wind power output	114 MW
	Minimum wind power output	0 MW
Minimum load demand (2460 MW)	Maximum wind power output	111 MW
	Average wind power output	55 MW
	Minimum wind power output	0 MW

Case 2: 15% wind penetration level

Maximum Load demand (7780 MW)	Maximum wind power output	506 MW
	Average wind power output	253 MW
	Minimum wind power output	0 MW
Average load demand (5087 MW)	Maximum wind power output	331 MW
	Average wind power output	165 MW
	Minimum wind power output	0 MW
Minimum load demand (2460 MW)	Maximum wind power output	160 MW
	Average wind power output	80 MW
	Minimum wind power output	0 MW

Case 3: 20% wind penetration level

Maximum Load demand (7780 MW)	Maximum wind power output	661 MW
	Average wind power output	331 MW
	Minimum wind power output	0 MW
Average load demand (5087 MW)	Maximum wind power output	432 MW
	Average wind power output	216 MW
	Minimum wind power output	0 MW
Minimum load demand (2460 MW)	Maximum wind power output	209 MW
	Average wind power output	105 MW
	Minimum wind power output	0 MW

Case 4: 30% wind penetration level

Maximum Load demand (7780 MW)	Maximum wind power output	778 MW
	Average wind power output	389 MW
	Minimum wind power output	0 MW
Average load demand (5087 MW)	Maximum wind power output	509 MW
	Average wind power output	254 MW
	Minimum wind power output	0 MW
Minimum load demand (2460 MW)	Maximum wind power output	246 MW
	Average wind power output	123 MW
	Minimum wind power output	0 MW

Appendix 2: Daily network power losses for power system with wind power

Time interval	Network power losses (MW)			
	10% penetration	15% penetration	20% penetration	30% penetration
0:00~0:30	90.89	93.36	97.83	110.19
0:30~1:00	87.22	88.44	88.24	90.44
1:00~1:30	98.83	108.24	118.43	149.28
1:30~2:00	104.00	113.48	128.95	172.39
2:00~2:30	105.43	124.33	146.40	220.23
2:30~3:00	93.13	104.64	118.86	163.95
3:00~3:30	78.55	79.29	79.62	79.00
3:30~4:00	75.32	76.62	77.15	81.53
4:00~4:30	78.98	88.93	100.60	133.59
4:30~5:00	70.73	75.34	80.19	95.76
5:00~5:30	71.32	77.92	85.02	108.54
5:30~6:00	68.24	71.14	75.61	88.59
6:00~6:30	64.87	64.92	66.09	67.44
6:30~7:00	73.40	83.60	95.74	130.04
7:00~7:30	117.00	179.90	250.63	382.27
7:30~8:00	70.34	70.97	71.00	73.97
8:00~8:30	85.31	101.49	123.49	186.85
8:30~9:00	84.97	100.73	122.22	184.16
9:00~9:30	80.69	89.37	97.55	124.81
9:30~~10:00	84.42	90.13	96.30	114.59
10:00~10:30	91.30	93.03	94.17	102.47
10:30~11:00	104.91	114.63	130.21	168.58

11:00~11:30	143.07	104.57	106.41	107.67
11:30~12:00	125.96	117.80	120.19	130.97
12:00~12:30	142.71	169.15	207.29	110.91
12:30~13:00	144.15	126.70	129.38	132.90
13:00~13:30	145.58	158.54	185.00	259.16
13:30~14:00	148.66	160.33	183.30	246.57
14:00~14:30	136.05	159.30	178.17	233.41
14:30~15:00	171.85	172.10	201.47	292.08
15:00~15:30	136.26	142.95	155.26	180.72
15:30~16:00	151.68	218.76	294.95	405.96
16:00~16:30	160.87	139.36	143.62	156.89
16:30~17:00	171.07	165.95	185.59	246.54
17:00~17:30	178.40	166.28	176.87	200.25
17:30~18:00	171.49	173.71	177.82	190.30
18:00~18:30	167.04	190.98	205.42	248.41
18:30~19:00	154.49	177.74	185.89	214.21
19:00~19:30	155.42	178.51	192.30	232.15
19:30~20:00	147.29	156.48	160.60	166.75
20:00~20:30	132.74	167.76	184.07	233.90
20:30~21:00	126.18	156.39	170.31	208.63
21:00~21:30	132.51	132.60	135.67	142.54
21:30~22:00	111.38	131.08	136.12	151.94
22:00~22:30	122.11	145.41	168.01	233.16
22:30~23:00	115.22	113.57	117.18	128.39
23:00~23:30	143.07	147.28	183.85	261.81
23:30~0:00	125.96	138.77	174.47	280.60

Appendix 3: Daily network power losses for wind power cooperated with HPS

Time interval	Network power losses (MW)			
	10% penetration	15% penetration	20% penetration	30% penetration
0:00~0:30	87.89	90.90	96.98	103.10
0:30~1:00	79.89	78.93	77.17	78.40
1:00~1:30	104.64	117.41	131.06	175.40
1:30~2:00	111.39	128.45	153.50	111.66
2:00~2:30	123.21	152.63	169.49	107.44
2:30~3:00	103.19	97.28	93.74	99.08
3:00~3:30	71.99	69.60	68.38	68.02
3:30~4:00	72.30	71.20	71.64	75.86
4:00~4:30	86.38	98.87	119.72	178.19
4:30~5:00	72.39	77.79	86.07	84.24
5:00~5:30	76.42	85.81	97.19	78.35
5:30~6:00	68.48	74.28	78.26	76.34
6:00~6:30	60.29	58.31	58.00	59.15
6:30~7:00	83.05	98.72	114.31	119.75
7:00~7:30	90.89	77.63	78.24	79.79
7:30~8:00	65.68	64.19	63.77	64.95
8:00~8:30	88.77	104.80	119.62	123.75
8:30~9:00	75.14	77.64	80.70	84.31
9:00~9:30	78.55	80.70	85.96	90.66
9:30~~10:00	85.28	87.94	93.32	95.84
10:00~10:30	86.43	87.42	88.41	96.49
10:30~11:00	111.95	121.75	135.19	125.79
11:00~11:30	96.65	93.92	92.32	93.05

11:30~12:00	110.19	110.92	113.62	126.82
12:00~12:30	168.14	205.77	252.73	238.32
12:30~13:00	116.64	114.94	113.32	118.38
13:00~13:30	159.92	180.21	208.54	216.08
13:30~14:00	135.53	139.66	147.73	153.76
14:00~14:30	136.84	143.01	150.60	157.94
14:30~15:00	136.96	143.39	148.54	157.20
15:00~15:30	134.83	140.39	148.20	153.84
15:30~16:00	134.44	139.71	147.78	153.80
16:00~16:30	129.80	133.36	136.77	156.89
16:30~17:00	157.68	167.09	183.17	166.33
17:00~17:30	158.54	165.83	172.64	185.50
17:30~18:00	163.09	162.69	163.67	163.70
18:00~18:30	183.07	200.84	218.34	179.77
18:30~19:00	169.09	176.91	185.89	177.78
19:00~19:30	171.62	186.98	202.07	207.74
19:30~20:00	146.54	144.24	143.86	152.93
20:00~20:30	163.52	182.15	207.29	283.89
20:30~21:00	150.86	164.15	182.61	241.79
21:00~21:30	124.39	123.38	122.94	129.64
21:30~22:00	125.23	128.10	133.10	158.80
22:00~22:30	144.45	171.08	203.56	181.09
22:30~23:00	107.26	109.14	112.17	128.02
23:00~23:30	141.82	138.17	133.50	118.37
23:30~0:00	96.05	99.56	103.98	109.11

Appendix4: Daily network power losses for HPS injection point on daily network energy losses

HPS injection node	Daily network energy losses (MWh)			
	10% penetration	10% penetration	10% penetration	10% penetration
1	5794.62	6088.63	6480.18	6667.04
2	6046.29	6333.28	6716.55	6898.62
3	6104.32	6394.53	6781.59	6970.91
4	5342.34	5610.51	5975.63	6178.14
5	5803.98	6074.99	6442.52	6650.05
6	5515.97	5783.42	6147.21	6338.57
7	5918.21	6184.85	6546.91	6733.68
8	5226.28	5490.76	5852.20	6059.97
9	5185.87	5458.41	5828.71	6041.87
10	5232.02	5512.55	5891.47	6109.08
11	6103.76	6370.99	6733.05	6918.94
12	5581.29	5826.28	6164.54	6342.18
13	6009.05	6308.59	6705.92	6890.22
14	5968.87	6257.15	6642.55	6824.48
15	5744.06	6034.09	6422.48	6619.91
16	5824.23	6106.82	6486.52	6671.65
17	5912.28	6190.79	6567.37	6779.73
18	5641.19	5935.72	6329.22	6531.80

19	5744.77	6040.39	6434.84	6633.42
20	5842.59	6147.82	6552.57	6744.90
21	5747.40	6052.73	6457.68	6650.68
22	5638.31	5940.31	6341.78	6537.15
23	5431.88	5712.55	6091.06	6297.37
24	5322.63	5589.97	5953.95	6146.17
25	5036.09	5322.29	5707.35	5936.31
26	5039.02	5324.37	5708.48	5938.78
27	5564.53	5867.31	6269.42	6472.17
28	5895.12	6204.10	6612.79	6807.53
29	6237.13	6547.80	6958.24	7148.91
30	5301.13	5574.30	5944.92	6162.67
31	5738.96	6046.26	6453.24	6649.88
32	5570.67	5870.75	6270.01	6472.58
33	6146.79	6458.47	6870.18	7053.50
34	5734.20	6036.65	6438.31	6642.04
35	6426.28	6732.58	7138.53	7335.13
36	5806.63	6113.70	6520.49	6718.94
37	6455.46	6751.09	7145.61	7350.84
38	5489.19	5781.08	6171.06	6386.80
39	6309.63	6631.59	7054.38	7244.84
40	6027.50	6361.02	6795.52	6999.08
41	6458.32	6786.89	7216.45	7404.99

42	6043.50	6377.98	6813.20	7011.15
43	5956.63	6274.35	6692.71	6873.90
44	5808.93	6128.30	6548.67	6725.28
45	5772.06	6090.75	6510.58	6682.55
46	5634.09	5953.81	6374.73	6555.04
47	5625.41	5945.22	6366.08	6546.70
48	5634.65	5953.58	6373.81	6553.57
49	5588.98	5905.77	6322.51	6501.62
50	5633.38	5951.53	6371.23	6548.42
51	5658.79	5974.46	6391.74	6560.21
52	5621.26	5937.38	6355.08	6527.50
53	5621.33	5936.70	6353.40	6526.26
54	5586.76	5898.73	6311.91	6469.44
55	5600.07	5912.79	6326.87	6488.61
56	5598.59	5910.49	6323.65	6480.90
57	5677.43	5993.54	6411.40	6584.28
58	5693.12	6008.21	6425.04	6594.02
59	5497.88	5813.50	6230.12	6407.77
60	5810.72	6130.63	6551.92	6746.79
61	5547.30	5867.82	6289.69	6487.11
62	5547.48	5867.46	6288.71	6483.93
63	5541.43	5858.95	6277.00	6460.76
64	5577.60	5893.69	6309.78	6500.72

65	5506.80	5813.65	6218.52	6426.15
66	5565.83	5879.71	6292.60	6497.55
67	5560.45	5879.93	6300.41	6496.63
68	5764.74	6066.91	6466.53	6673.21
69	5554.82	5855.27	6254.03	6462.25
70	5432.78	5688.04	6031.59	6206.40
71	5403.84	5622.78	5922.46	6068.15
72	5444.64	5716.46	6083.55	6261.04
73	5408.89	5651.03	5979.46	6138.22
74	5599.24	5913.00	6324.14	6514.13
75	6070.86	6387.42	6800.69	6988.81
76	5600.38	5924.71	6348.99	6538.15
77	5530.05	5840.84	6250.00	6445.26
78	5779.46	6094.34	6508.16	6698.98
79	5598.74	5913.08	6326.62	6519.72
80	5537.16	5841.75	6244.45	6446.74
81	5556.38	5859.74	6260.65	6464.44
82	5685.54	6000.46	6415.24	6613.31
83	5675.77	5991.77	6408.20	6611.45
84	5715.57	6036.14	6458.26	6668.90
85	5378.80	5697.98	6117.85	6350.45
86	4986.31	5330.38	5775.52	6027.98
87	4543.86	4904.49	5365.70	5633.38

88	5635.71	5949.60	6364.01	6588.61
89	5684.53	5993.94	6403.64	6637.31
90	5510.97	5828.04	6245.49	6464.72
91	5490.16	5807.18	6224.91	6445.12
92	5483.57	5790.41	6197.26	6423.72
93	5587.30	5896.72	6306.44	6519.18
94	5582.51	5884.83	6286.22	6497.48
95	5582.87	5892.98	6302.75	6506.19
96	5624.14	5933.89	6342.74	6543.85
97	5545.88	5857.74	6269.17	6469.51
98	5498.24	5806.13	6213.70	6419.04
99	5357.73	5655.92	6053.37	6266.11
100	5145.69	5420.81	5793.72	6015.74
101	5435.39	5737.49	6139.36	6354.17
102	5546.26	5852.92	6259.67	6478.37
103	4838.81	5082.09	5421.77	5627.87
104	5055.60	5303.39	5646.93	5839.23
105	5026.78	5258.63	5584.66	5767.14
106	5503.25	5766.13	6125.14	6315.04
107	5401.26	5685.58	6068.16	6258.27
108	5117.40	5245.56	5456.86	5562.35